

A11102 145937

NAT'L INST OF STANDARDS & TECH R.I.C.



A1102145937

Janz, George J/Section 1. Electricity of
QC100 .U573 V28:2:1969 C.1 NBS-PUB-C 196

NSRDS-NBS 28



NBS
PUBLICATIONS

Molten Salts: Volume 2,

1. Electrochemistry---

Gibbs Free Energies and Excess Free Energies
From Equilibrium-Type Cells

2. Surface Tension Data

U.S. DEPARTMENT OF COMMERCE

NATIONAL BUREAU OF STANDARDS



QC

100

.U573

No.28

v.2.

1969

NBS

Copy 2

UNITED STATES DEPARTMENT OF COMMERCE

MAURICE H. STANS, *Secretary*

U.S., NATIONAL BUREAU OF STANDARDS • A. V. ASTIN, *Director*

...

Molten Salts: Volume 2

Section 1. Electrochemistry of Molten Salts: Gibbs Free Energies and Excess Free Energies From Equilibrium-Type Cells

G. J. Janz* and Chr. G. M. Dijkhuis*

Section 2. Surface Tension Data

G. J. Janz,* G. R. Lakshminarayanan,*

R. P. T. Tomkins,* and J. Wong*

*This report was prepared under contract at the Molten Salts Data Center,
Rensselaer Polytechnic Institute, Troy, N.Y. 12180



NSRDS-NBS 28

Nat. Stand. Ref. Data Ser., Nat. Bur. Stand. (U.S.), 28, 116 pages (August 1969)
CODEN: NSRDA

Issued August 1969

JAN 12 1970

146208

QC 100

.U573

NO. 28 V. 2

1969

Copy 2

Library of Congress Catalog Number: 68-60051

Foreword

The National Standard Reference Data System is a Government-wide effort to provide for the technical community of the United States effective access to the quantitative data of physical science, critically evaluated and compiled for convenience, and readily accessible through a variety of distribution channels. The System was established in 1963 by action of the President's Office of Science and Technology and the Federal Council for Science and Technology.

The responsibility to administer the System was assigned to the National Bureau of Standards and an Office of Standard Reference Data was set up at the Bureau for this purpose. Since 1963, this Office has developed systematic plans for meeting high-priority needs for reliable reference data. It has undertaken to coordinate and integrate existing data evaluation and compilation activities (primarily those under sponsorship of Federal agencies) into a comprehensive program, supplementing and expanding technical coverage when necessary, establishing and maintaining standards for the output of the participating groups, and providing mechanisms for the dissemination of the output as required.

The System now comprises a complex of data centers and other activities, carried on in Government agencies, academic institutions, and nongovernmental laboratories. The independent operational status of existing critical data projects is maintained and encouraged. Data centers that are components of the NSRDS produce compilations of critically evaluated data, critical reviews of the state of quantitative knowledge in specialized areas, and computations of useful functions derived from standard reference data. In addition, the centers and projects establish criteria for evaluation and compilation of data and make recommendations on needed modifications or extensions of experimental techniques.

Data publications of the NSRDS take a variety of physical forms, including books, pamphlets, loose-leaf sheets and computer tapes. While most of the compilations have been issued by the Government Printing Office, several have appeared in scientific journals. Under some circumstances, private publishing houses are regarded as appropriate primary dissemination mechanisms.

The technical scope of the NSRDS is indicated by the principal categories of data compilation projects now active or being planned: nuclear properties, atomic and molecular properties, solid state properties, thermodynamic and transport properties, chemical kinetics, colloid and surface properties, and mechanical properties.

An important aspect of the NSRDS is the advice and planning assistance which the National Research Council of the National Academy of Sciences-National Academy of Engineering provides. These services are organized under an overall Review Committee which considers the program as a whole and makes recommendations on policy, long-term planning, and international collaboration. Advisory Panels, each concerned with a single technical area, meet regularly to examine major portions of the program, assign relative priorities, and identify specific key problems in need of further attention. For selected specific topics, the Advisory Panels sponsor subpanels which make detailed studies of users' needs, the present state of knowledge, and existing data resources as a basis for recommending one or more data compilation activities. This assembly of advisory services contributes greatly to the guidance of NSRDS activities.

The NSRDS-NBS series of publications is intended primarily to include evaluated reference data and critical reviews of long-term interest to the scientific and technical community.

A. V. ASTIN, *Director.*

Abstract

This book consists of two sections as follows:

Section 1

The critical evaluation of excess free energies of binary molten salt mixtures with a common ion from equilibrium-type electrochemical cells is described in this report. For this purpose calculations using the original emf data were systematically undertaken to establish comparisons of free energy values of various workers that would be significant. The reversibility of electrodes is investigated by comparing the electromotive force of cells with a single molten salt as liquid electrolyte with thermochemical data.

Section 2

Data on the surface tensions of single salt melts have been systematically collected and evaluated. Results are given for 106 inorganic compounds over a range of temperatures where available.

Key words: Critically evaluated data; equilibrium electrochemical cells; excess entropies; excess Gibbs free energies; Gibbs free energies; molten salt mixtures; molten salts; surface tension; thermodynamics of molten salts.

Acknowledgments

The participation of T. G. Coker, F. W. Dampier, P. K. Lorenz, H. Siegenthaler, and A. Timidei in various stages of this work at Rensselaer is acknowledged with pleasure.

Contents

	Page
Section 1. Electrochemistry of molten salts: Gibbs free energies and excess free energies from equilibrium-type cells.....	1
G. J. Janz and Chr. G. M. Dijkhuis.	
Section 2. Surface tension data.....	49
G. J. Janz, G. R. Lakshminarayanan, R. P. T. Tomkins, and J. Wong.	

Molten Salts: Volume 2

Section 1. Electrochemistry of Molten Salts: Gibbs Free Energies and Excess Free Energies from Equilibrium-Type Cells

G. J. Janz* and Chr. G. M. Dijkhuis*

The critical evaluation of excess free energies of binary molten salt mixtures with a common ion from equilibrium-type electrochemical cells is described in this report. For this purpose calculations using the original emf data were systematically undertaken to establish comparisons of free energy values of various workers that would be significant. The reversibility of electrodes is investigated by comparing the electromotive force of cells with a single molten salt as liquid electrolyte with thermochemical data.

Key words: Critically evaluated data; equilibrium electrochemical cells; excess entropies; excess Gibbs free energies; Gibbs free energies; molten salt mixtures; molten salts; thermodynamics of molten salts.

Contents

	Page
1. Introduction.....	1
2. Units, fundamental constants, and symbols.....	1
3. Theoretical principles and method of calculation.....	2
3.1. Statistical Analysis of Data.....	3
4. Uncertainties.....	3
5. Discussion.....	3
5.1. Cells.....	3
5.2. Individual mixtures.....	6
6. Cumulative table of excess free energies.....	27
7. Tables of E° values and excess properties for individual mixtures.....	28
8. References.....	47
9. Compound index.....	48

1. Introduction

Thermodynamic data of molten salts can be gained by various experimental techniques, e.g., heats of mixing calorimetry [1], vapor pressure measurements [2], cryometry [3], and electrochemical cells [4].¹ Next to high temperature heats of mixing calorimetry, the measurement of the electromotive force of electrochemical cells is possibly the method capable of greatest precision and accuracy, providing due attention is directed to certain features of the experimental work [5]. The calculation of excess free energies of molten salt mixtures from concentration cell data is well understood [3, 4, 5, 6], and while a considerable amount of literature in this area exists [5, 6], it is difficult to obtain meaningful results since the liquid junction potential is generally unknown; this makes the derived thermodynamic results uncertain. This uncertainty does not arise in the calculation of free energies and excess free energies from emf data of

equilibrium-type cells, i.e. cells with two different electrodes. The critical evaluation of excess free energies of binary molten salt mixtures with a common ion from equilibrium-type cells is described in this report. The following aspects are considered: units, fundamental constants and symbols; theoretical principles and method of calculation; uncertainties and discussion of some cells; and the guide-lines for the critical evaluation of each contribution.

2. Units,* Fundamental Constants, and Symbols

The fundamental constants are those adopted by the National Bureau of Standards (NBS Technical News Bulletin, October 1963). All energy values are expressed in terms of the thermochemical calorie or in terms of the millivolt.

*The NBS Office of Standard Reference Data, as administrator of the National Standard Reference Data System, has officially adopted the use of SI units for all NSRDS publications, in accordance with NBS practice. This publication does not use SI units because contractual commitments with the author predate establishment of a firm policy on their use by NBS. Appropriate conversion factors are found above. The NBS urges that specialists and other users of data in this field accustom themselves to SI units as rapidly as possible.

*Molten Salts Data Center, Rensselaer Polytechnic Institute, Troy, N.Y. 12180.

¹ Figures in brackets indicate the literature references on page 47.

Fundamental Constants

Symbol	Name	Value
N	Avogadro Constant	$6.02252 \times 10^{23} \pm 0.00028 \times 10^{23}/\text{mol}$
F	Faraday Constant	$96,487.0 \pm 1.6 \text{ C/mol}$ ($23,060.9 \pm 0.4 \text{ cal/V equiv}$)
T	Temperature in °K	
t	Temperature in °C	$0^\circ\text{C} = 273.15^\circ\text{K}$
e	Electronic Charge	$1.60210 \times 10^{-19} \text{ C}$
R	Gas Constant	$8.3143 \pm 0.0012 \text{ J/K mol}$ $1.98716 \pm 0.00029 \text{ cal/deg mol}$
cal	Thermochemical calorie	4.1840 J

Symbols and Terminology

G	= Molar Gibbs free energy
G^E	= Excess molar Gibbs free energy
H^E	= Molar heat of mixing
S^E	= Excess molar entropy of mixing
μ_{AX}^E	= Excess chemical potential of component AX ; Partial excess molar Gibbs free energy of mixing of component AX
h_{AX}^E	= Partial excess heat of mixing of component AX
s_{AX}^E	= Partial excess molar entropy of mixing of component AX
x_{AX}	= Mole fraction of component AX . In a binary mixture $AX(x)$, $BX(1-x)$ the mole fraction of AX is $N_{AX}/(N_{AX} + N_{BX})$
E	= Cell emf
z	= Number of equivalents

3. Theoretical Principles and Method of Calculation

The following are the basic principles and concepts used for the evaluation of excess free energies and excess entropies from emf values of equilibrium-type cells [7]. The excess molar Gibbs free energy of mixing (G^E) of a molten binary mixture $AX(1-x)$, $BX(x)$ may be expressed by the equation:

$$G^E = x(1-x)(a + bx + cx^2) \quad (1)$$

The expressions for the excess chemical potentials of the components AX and BX (μ_{AX}^E and μ_{BX}^E) follow readily from eq 1 and the Gibbs-Duhem relation, i.e.

$$\mu_{AX}^E = [a - b + 2(b - c)x + 3cx^2]x^2 \quad (2a)$$

and

$$\mu_{BX}^E = (a + 2bx + 3cx^2)(1-x)^2 \quad (2b)$$

The values of the constants a , b , and c may be obtained from a graphical analysis of μ_{AX}^E/x^2 or $\mu_{BX}^E/(1-x)^2$ as a function of the mole fraction, i.e.:

$$\mu_{AX}^E/x^2 = a - b + 2(b - c)x + 3cx^2 \quad (3a)$$

and

$$\mu_{BX}^E/(1-x)^2 = a + 2bx + 3cx^2 \quad (3b)$$

By expressing the excess entropy (S^E) according to the equation:

$$S^E = x(1-x)(a' + b'x + c'x^2) \quad (4)$$

it follows similarly that:

$$s_{AX}^E/x^2 = a' - b' + 2(b' - c')x + 3c'x^2 \quad (5a)$$

and

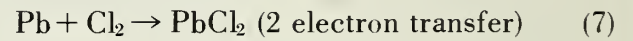
$$s_{BX}^E/(1-x)^2 = a' + 2b'x + 3c'x^2 \quad (5b)$$

The parameters a' , b' , and c' in eq 5 may be determined from an analysis of s_{AX}^E/x^2 or $s_{BX}^E/(1-x)^2$ as a function of x .

The excess chemical potentials (eq 3a and eq 3b) and the excess entropies (eq 5a and eq 5b) can be determined from experimental emf data. Consider the cell:



The cell reaction is:



from which it follows:

$$-2EF = \mu_{\text{PbCl}_2} - \mu_{\text{Pb}} - \mu_{\text{Cl}_2} \quad (8)$$

If one now defines ideal solution behaviour by means of the Temkin relation [8]

$$\mu_{\text{PbCl}_2} = \mu_{\text{PbCl}_2}^\circ + RT \ln(1-x) + \mu_{\text{PbCl}_2}^E \quad (9)$$

it can be shown from eqs 8 and 9 that

$$-2EF = \mu_{\text{PbCl}_2}^\circ + RT \ln(1-x) + \mu_{\text{PbCl}_2}^E - \mu_{\text{Pb}} - \mu_{\text{Cl}_2} \quad (10)$$

For the case where the electrolyte is pure PbCl_2 (i.e. $x = 0$), the emf of this cell is given by:

$$-2E^\circ F = \mu_{\text{PbCl}_2}^\circ - \mu_{\text{Pb}} - \mu_{\text{Cl}_2} \quad (11)$$

Combining eqs 10 and 11 gives:

$$-2(E - E^\circ)F = RT \ln(1-x) + \mu_{\text{PbCl}_2}^E \quad (12)$$

When E and μ are expressed in mV, the result is:

$$-\mu_{\text{PbCl}_2}^E = 2(E - E^\circ)F + 0.19845T \log(1-x) \quad (13)$$

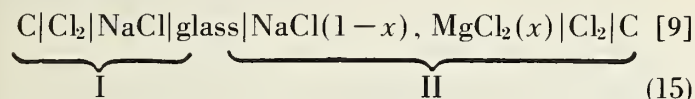
Thus it follows that from a knowledge of E , E° , and x , a measure of the excess free energies can be gained by this method.

The partial excess entropy can be gained from the temperature dependence of the E values, i.e.

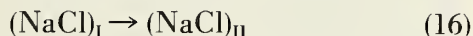
$$\begin{aligned} s_{\text{PbCl}_2}^E &= -(\delta\mu_{\text{PbCl}_2}^E/\delta t)_x \\ &= 2(\delta E^\circ/\delta t)_x - 2(\delta E/\delta t)_x - 0.19845 \log(1-x) \end{aligned} \quad (14)$$

Thus $s_{\text{pbCl}_2}^E$ may be gained from the temperature dependence of E° and E or from the temperature dependence of $\mu_{\text{pbCl}_2}^E$ (eq 13), whereas the parameters a' , b' , and c' in eq 4 may be obtained from an analysis of $s_{\text{pbCl}_2}^E/x^2$ as a function of x (eq 5).

Thermodynamic properties of molten salts have also been determined from cells in which glass functions as a cation selective membrane. Consider the cell



The cell reaction was found to be [9, 10]



from which it follows that

$$-EF = (\mu_{\text{NaCl}})_{\text{II}} - (\mu_{\text{NaCl}})_{\text{I}} \quad (17)$$

Again defining ideal mixing behaviour by means of the Temkin relation [8] and expressing E and μ in mV it follows that

$$\mu_{\text{NaCl}}^E = E + 0.19845 T \log (1-x) \quad (18)$$

Excess free energies and excess entropies can now be calculated from the experimental emf of cell (15) analogous to the procedure for cell (6).

The values of E and E° (eq 13) are generally large when compared to the difference quantity $(E - E^\circ)$, so that the excess free energy by this method rests heavily on the determination of relatively small values from the difference of two relatively much larger numbers. The calculation of the $(E - E^\circ)$ values has generally been by a graphical method. While the graphical analysis provides a ready assessment of the data, inspection showed that the difference quantity $(E - E^\circ)$ should be evaluated by a linear and a quadratic least squares analysis if reliable precisions are to be gained. The latter procedure was adopted in the present work. It was also found that it was worthwhile to recalculate the free energies and the excess free energies from the literature emf data. These recalculations were undertaken by following the guidelines and principles discussed in this section to establish a self-consistent set of results, with reliable precision estimates, as required for meaningful intercomparison.

3.1. Statistical Analysis of Data

Linear and quadratic equations of emf-temperature relationship were fitted to available sets of experimental data by the method of least squares. All calculations were with the digital computer facilities at Rensselaer Polytechnic Institute and double precision Fortran IV programs. The criterion for choosing a linear or quadratic equation of best

fit for a set of emf-temperature data is the standard deviation computed from the residuals and is defined by:

$$s = \sqrt{\frac{\sum_{e=1}^n (X_e - X_c)^2}{n - q}}$$

where X_e = the experimental emf value at each temperature, X_c = the value calculated from the least squares equation at the same temperature as X_e , n = number of experimental data points, and q = number of coefficients in the least squares equation (2 for linear and 3 for quadratic). The standard deviation s is used as the precision estimate.

4. Uncertainties

The cell emfs and the $(E - E^\circ)$ values (eq 12) have been recalculated at various temperatures by means of a linear and a quadratic least-squares analysis of the literature data. The standard deviation in the temperature dependence of the emf data was also calculated. Excess entropies have been derived from "best fit" linear or quadratic equations.

Experimental considerations and standard deviation in the temperature dependence of emfs were taken into account for the evaluation of the parameters in the equation for the excess free energy (eq 1) and in the equation for the excess entropy (eq 4). An exact mathematical analysis was considered; however, it was found that the statistical treatment was unsatisfactory since it was difficult to give sufficient weight to factors arising in experimental procedures. The problem of systematic errors in various investigations is considered in section 5.1. The intercomparison of various emf studies with the same salt as the liquid electrolyte, and the comparison of these values with thermochemical data [11,12,13] are used for this purpose. Such comparisons establish the guide-lines for the discussions in section 5.2 of the individual mixtures.

5. Discussion

5.1. Cells

5.1.1. Ag|AgCl|Cl₂|C.

[11, 16, 19, 20, 21, 22, 23, 24, 25, 26, 27]

The reported E° values of this cell are compared in table 1. Mixed potentials at the Ag electrode have been reported and discussed [14, 15]. Although Senderoff and Brenner [15] do not give a thermodynamically sound argument for the absence of mixed potentials at the Ag electrode, it seems most likely that differences in E° values between various authors are mostly due to a nonequilibrium behaviour of the Cl₂|C electrode [16, 17, 18]. Small differences might also be due to different corrections for the thermal emf of the Ag|C couple.

The investigation of Senderoff and Mellors [16] appears to be the most thorough. The C electrode was pretreated in a Cl_2 atmosphere for two hours at 2300 °C. During the studies, the Cl_2 pressure was controlled and electrolysis was used to attain equilibrium rapidly. The Ag electrode was protected from chlorine gas by a quartz tube envelope having a porous quartz disk at the bottom.

Table 1 shows that the E° values of Panish, Newton, Grimes, and Blankenship [19, 20] are in perfect agreement with the E° data of Senderoff and Mellors [16] up to 900 °C; the values of Leonardi and Brenet [21], Murgulescu and Sternberg [22] and Salstrom [23] show a maximum departure of 10 mV at 900 °C. The Stern [24, 25] values differ from Senderoff and Mellors [16] by 23 mV at 900 °C. Panish, Newton, Grimes, and Blankenship [19, 20] use an experimental procedure similar to that of Senderoff and Mellors.

Stern [24, 25] did not apply a correction for the thermoelectric effect. Other factors, such as imperfect pretreatment of the $\text{Cl}_2|\text{C}$ electrode may also contribute in part to the difference of 23 mV. The unstable potentials in the dilute AgCl mixtures could be due to oxide impurities and dissolved oxygen in the Ag wire. This would also explain in part the difference in $(\delta E^\circ/\delta T)$ between Stern [24, 25] and Senderoff and Mellors [16].

While the experimental procedures of Leonardi and Brenet [21], Murgulescu and Sternberg [22], and Salstrom [23] differ somewhat from Senderoff and Mellors [16] it is apparent from table 1 that the measurements are of a high quality.

5.1.2. $\text{Be}|\text{BeCl}_2|\text{Cl}_2|\text{C}$. [11, 13, 28, 29, 30, 31, 32]

The cell $\text{Be}|\text{BeCl}_2|\text{Cl}_2|\text{C}$ can not be measured experimentally due to electronic conductivity of the melt (Be metal dissolves in molten BeCl_2) and because of the high volatility of molten BeCl_2 .

Kuroda and Matsumoto [28] have measured cells such as $\text{Be}|\text{BeCl}_2$, $\text{NaCl}|\text{Cl}_2|\text{C}$ and have determined the E° value of this cell by an extrapolation method. The extrapolation is unsatisfactory and while uncertainties are introduced by combining thermochemical E° values and experimental emfs, this latter approach is recommended. The thermochemical data are unsatisfactory. Thus at 500 °C, for example, the JANAF tables [13] list a value for E° as 1974 mV, while Sethi and Jindal [29] calculated 1844 mV, and Hamer, Malmberg, and Rubin [11] reported 2144 mV. Owing to the uncertainties in E° the excess properties of BeCl_2 containing mixtures are not calculated in the present work.

5.1.3. $\text{Cd}|\text{CdCl}_2|\text{Cl}_2|\text{C}$. [11, 33, 34, 35, 36]

A complication in this system is the significant solubility of Cd metal in molten CdCl_2 . This influences the emf of the cell and may also give rise to a junction potential. Electronic conductivity of

this cell has, however, not been reported; this may be because the reaction of Cd metal with Cl_2 near the $\text{Cl}_2|\text{C}$ electrode completely depletes the melt near this electrode of dissolved Cd metal.

A reaction involving CdCl_2 , Cl_2 , and graphite has been reported [33, 34] so that the selection of the graphite for the $\text{Cl}_2|\text{C}$ electrode in CdCl_2 containing melts must be made with care in order to minimize this problem.

Lorenz and Velde [35] found an E° value which is in good agreement with values reported by Lantratov and Alabyshev [36] (table 3).

Lantratov and Alabyshev [36] pretreated the C electrode in a Cl_2 atmosphere and separated the molten Cd as much as possible from the bulk of the melt. Their E° value at 600 °C is 1338 mV and the thermochemical value [11] at 600 °C is 1331 mV; the difference may be due, in part, to thermoelectric effects.

5.1.4. $(\text{Ce}, \text{Sn})|\text{CeCl}_3|\text{Cl}_2|\text{C}$. [37, 39] $(\text{Ce}, \text{Bi})|\text{CeCl}_3|\text{Cl}_2|\text{C}$. [38]

Cerium metal has a significant solubility in molten CeCl_3 . The cells: $(\text{Ce}, \text{Sn})|\text{CeCl}_3(1-x), \text{KCl}(x)|\text{Cl}_2|\text{C}$ and $\text{Ce}|\text{CeCl}_3(1-x), \text{KCl}(x)|\text{Cl}_2|\text{C}$ where $x \ll 1$, have been investigated by Senderoff, Mellors and Bretz [37]. Whereas the emfs of the former were stable, the emf data for the latter showed a continuous drift. The requirements for a suitable alloy electrode, according to these investigators [37] are as follows. The diluent metal of the alloy should be very noble compared with cerium. The alloy should consist of two phases over a considerable range of composition to assure constant activity of Ce in the heterogeneous alloy. The activity of cerium in the alloy should be sufficiently low. The alloy must behave electrochemically as a reversible $\text{Ce}^{3+}|\text{Ce}^\circ$ electrode. Senderoff, Mellors and Bretz [37] found that these requirements were met in the cell $(\text{Ce}, \text{Sn})|\text{CeCl}_3|\text{Cl}_2|\text{C}$.

The cell $(\text{Ce}, \text{Bi})|\text{CeCl}_3|\text{Cl}_2|\text{C}$ has been investigated by Neil [38]. The composition of the alloy was determined after each experiment in order to calculate the activity of Ce in the Ce.Bi alloy.

5.1.5. $\text{Mg}|\text{MgCl}_2|\text{Cl}_2|\text{C}$. [35, 40, 11, 13] $(\text{Mg}, \text{Bi})|\text{MgCl}_2|\text{Cl}_2|\text{C}$. [38, 41]

The cell $\text{Mg}|\text{MgCl}_2|\text{Cl}_2|\text{C}$ has been measured by means of the decomposition potential method by Lorenz and Velde [35] and by Markov, Delimarskii and Panchenko [40]. It should be noted that this method does not assure equilibrium conditions; a comparison of thermochemical values and the "decomposition-potential E° " for the present system shows that the two values differ significantly (table 4). The appreciable solubility of Mg metal in molten MgCl_2 presents a further difficulty for meaningful interpretations of the E° values.

The difficulties involved in the $\text{Mg}|\text{MgCl}_2|\text{Cl}_2|\text{C}$ cell were bypassed by Neil, Clark, and Wiswall

[38, 41] through the use of a magnesium alloy electrode, e.g., (Mg, Bi)|MgCl₂|Cl₂|C; thermodynamic reversibility of the Cl₂|C electrode was also investigated in this study. Varying alloy compositions were used and the $\mu_{\text{MgCl}_2}^E$ was calculated from the measured cell emf and the activity of Mg in the alloy (from the alloy composition data).

5.1.6. Mn|MnCl₂|Cl₂|C. [11, 42, 43]

The cells Mn|MnCl₂, NaCl|Cl₂|C and Mn|MnCl₂, KCl|Cl₂|C have been studied by Bruneaux, Ziolkiewicz and Morand [42, 43]. The E° of the systems with $x_{\text{MnCl}_2}=1.0$ was gained by extrapolation of the data for the preceding cells for a range of compositions. While this "extrapolated E° " is in good agreement with the thermochemical value [11], more information is needed before a reliable E° value can be recommended. The use of Mn containing alloy electrodes should be considered in further studies (c.f. Ce, Sn; Mg, Bi).

5.1.7. Pb|PbCl₂|Cl₂|C. [11, 13, 35, 38, 44, 45, 46, 47, 48, 49, 50, 51, 52]

A comparison of the emf data for this cell reported by various investigators is in table 5. The recent work of Hagemark and Hengstenberg [44] is probably the most accurate investigation. Up to 600 °C the Lantratov and Alabyshev [45] values are in reasonable agreement with the Hagemark and Hengstenberg [44] data. The difference between these two authors could be due to thermoelectric effects up to 600 °C. Hagemark and Hengstenberg [44] using a Cl₂|C electrode, nearly identical to that of Senderoff and Mellors [16], took care to minimize thermal emfs by using a graphite electrode for the electrical contact with the molten lead and investigated the influence of electrolysis on the emf. The purities of PbCl₂ and Pb were also checked and the observed emf values were corrected for fluctuations in the Cl₂ pressure (the latter corrections were less than 0.8 mV).

5.1.8. Pu|PuCl₃|Cl₂|C. [53, 54]

Benz [53] and Benz and Leary [54] have studied the cells: Pu|PuCl₃, KCl|Cl₂|C [53] and Pu|PuCl₃, NaCl|Cl₂|C [54]. The E° was calculated by assuming regular solution theory for the binary mixtures; this approach is not satisfactory. Unfortunately the properties of PuCl₃, e.g., the high melting point of PuCl₃, its volatility, and the marked solubility of Pu metal in PuCl₃ make a direct measurement of E° virtually impossible. The alloy electrode technique should be explored in further investigation of PuCl₃ mixtures.

5.1.9. Zn|ZnCl₂|Cl₂|C. [11, 35, 50, 56, 57, 58, 59, 60, 61, 62]

A comparison of literature values for this cell is in table 6. Delimarskii and Markov [55] noted that the finite vapor pressure of ZnCl₂ decreases the effective Cl₂ pressure and that this results in values of the emf that are too low. The Lorenz and Velde values [35] were corrected accordingly by Delimarskii and Markov [55].

The most thorough investigation of this cell is that of Takahashi [56] in which the Cl₂ pressure corrections were undertaken on the assumption that ZnCl₂ and Cl₂ do not interact in the vapor phase. In this investigation ZnCl₂, which is extremely hygroscopic, was dried and freed from oxide impurities, and finally electrolysed to remove traces of moisture before the emf measurement. The results of Takahashi [56] are the only ones which are in good agreement with the thermochemical values [11]. Takahashi [56] did not report a correction for the thermal emf of the Zn|C couple; this correction is undoubtedly small compared with the differences between the various reported emfs.

5.1.10. Ag|AgBr|Br₂|C. [12, 63, 64, 65, 66, 67, 68]

Inspection of table 7 shows that the experimental values of Salstrom and Hildebrand [63] and Murgulescu and Marchidan [64] are in good agreement with the thermochemical data published by Hamer, Malmberg and Rubin [12].

Salstrom and Hildebrand [63] used carefully dried AgBr and established that electrolysis did not change the cell emf. Corrections for variations of the Br₂ pressure and for thermoelectric effects were also made in this study. Murgulescu and Marchidan [64] pretreated the C electrode in a Br₂ atmosphere and by pre-electrolysis in molten AgBr. Most likely the differences between reported values (table 7) are due to thermoelectric effects.

5.1.11. Cd|CdBr₂|Br₂|C. [12, 69, 70]

There is only one investigation of this cell (Lantratov and Shevlyakova [69]) and the results have been reported in the form of an equation. The uncertainties in this cell are the same as for the cell Cd|CdCl₂|Cl₂|C. Salstrom [70] was unable to study this cell Cd|CdBr₂|Br₂|C due to metal fog formation.

The difference between the experimental emf [69] and the thermochemical values [12] (41 mV at 600 °C) makes further investigations of this cell desirable.

5.1.12. Pb|PbBr₂|Br₂|C. [12, 13, 70, 71, 72, 73]

Inspection of table 9 shows that there is an appreciable difference between the thermochemical data for this cell [12, 13].

The most recent experimental investigation of this cell is by Lantratov and Shevlyakova [71]. A thin-walled graphite tube was used as the Br_2 electrode, and this was saturated with Br_2 and was heated for 1.5 hr between 700 °C and 750 °C. The E° values differ appreciably from the thermochemical values [12, 13] and from other experimental values [70, 72].

Salstrom [70] and Salstrom and Hildebrand [72] reported that equilibrium at the Br_2 electrode was established in 1 to 2 hr if the C rod electrode was preheated in Br_2 at several atmospheres pressure and then heated in an oxygen flame. Without this pretreatment, 18 to 20 hr were required before a stable emf was observed. These investigators [70, 72] corrected for the thermoelectric emf using an empirically established factor. The difference between the E° and the thermochemical value may be, in part, due to this factor.

5.1.13. $\text{Ag}|\text{AgI}|\text{I}_2|\text{C}$. [12, 74, 75, 76]

The only investigations on this system are those of Sternberg, Adorian, and Galasiu [74, 75, 76]. The attainment of a reversible iodine electrode was gained by keeping iodine in a gaseous state from the moment of its generation up to its removal from the cell. It was noted that the graphite had to be in contact with iodine for 20 hr to establish stable potentials; this period could be reduced to 5 to 6 hr by electrolysis. The reported E° values are corrected for the thermoelectric effect at the $\text{Ag}|\text{C}$ couple.

Table 10 shows that the agreement with thermochemical values is satisfactory.

5.1.14. $\text{Ag}|\text{AgNO}_3|\text{NO}_2, \text{O}_2|\text{Pt}$. [4, 77, 78, 79, 80, 81]

The only investigation of this cell is that reported by Ketelaar and Dammers-de Klerk [4, 77]. A three-phase contact between the $(\text{NO}_2, \text{O}_2)$ mixture, the liquid nitrate, and platinum was found to be essential for measurements of thermodynamic significance. The results are in complete agreement with the E° as calculated by the authors [77] from thermochemical data [78, 79, 80, 81].

5.1.15. Cells with Glass as Cation Selective Membranes. [9, 10, 33, 34, 82, 83, 84]

The most complete investigations with this kind of cell are those of Ostvold and Forland [9, 10, 82, 83]. Well defined types of glass were investigated for cation-selective properties by transport measurements. It was also shown from theoretical considerations that thermodynamic results are possible from such cells if the transport numbers through the glass are known. Dijkhuis and Ketelaar [33, 34, 85] and Sternberg and Herdlicka [84], from indirect evidence, established that the electrical contact through such glass membranes is by one kind of ion only.

Thermochemical data of some "undercooled" alkali halides are given in table 11; these are of interest for cells with cation-selective glass membranes.

5.2. Discussion of Individual Mixtures

- | | | | |
|-----------------|----------------------------|----------------------------|-----------------|
| 1. (Ag, Li)Cl; | 15. (Mg, Rb)Cl; | 29. (Pu, Na)Cl; (Pu, K)Cl; | 43. (Pb, K)Br; |
| 2. (Ag, Na)Cl; | 16. (Mn, Na)Cl, (Mn, K)Cl; | 30. (Zn, Li)Cl; | 44. (Pb, Zn)Br; |
| 3. (Ag, K)Cl; | 17. (Ca, Na)Cl; | 31. (Zn, Na)Cl; | 45. (Ag, K)I; |
| 4. (Ag, Pb)Cl; | 18. (Sr, Na)Cl; | 32. (Zn, K)Cl; | 46. (Cd, Na)I; |
| 5. (Be, Na)Cl; | 19. (Ba, Na)Cl; | 33. (Zn, Rb)Cl; | 47. (Pb, Na)I; |
| 6. (Cd, Na)Cl; | 20. (Pb, Li)Cl; | 34. (Zn, Cs)Cl; | 48. Ag(Br, Cl); |
| 7. (Cd, K)Cl; | 21. (Pb, Na)Cl; | 35. (Zn, Ba)Cl; | 49. Ag(I, Cl); |
| 8. (Cd, Ba)Cl; | 22. (Pb, K)Cl; | 36. (Ag, Li)Br; | 50. Ag(I, Br); |
| 9. (Ce, Na)Cl; | 23. (Pb, Rb)Cl; | 37. (Ag, Na)Br; | 51. K(Br, Cl); |
| 10. (Ce, K)Cl; | 24. (Pb, Cs)Cl; | 38. (Ag, K)Br; | 52. Na(Br, Cl); |
| 11. (Ce, Ca)Cl; | 25. (Pb, Ca)Cl; | 39. (Ag, Rb)Br; | 53. Pb(Br, Cl) |
| 12. (Mg, Li)Cl; | 26. (Pb, Sr)Cl; | 40. (Ag, Pb)Br; | |
| 13. (Mg, Na)Cl; | 27. (Pb, Ba)Cl; | 41. (Cd, K)Br; | |
| 14. (Mg, K)Cl; | 28. (Pb, Zn)Cl; | 42. (Pb, Na)Br; | |

5.2.1. $\text{AgCl}(1-x), \text{LiCl}(x)$.

Cells: $\text{Ag}|\text{AgCl}, \text{LiCl}|\text{Cl}_2|\text{C}$. [20, 26]
Tables: 1, 12
Figure: 1a

Parameters for the excess free energy:

$$\begin{aligned} a &= 2.1 \text{ kcal/mol} \\ b &= 0.0 \text{ kcal/mol} \\ c &= 0.0 \text{ kcal/mol} \end{aligned}$$

Estimated uncertainty in $4G^E(x=0.5)$: 0.2 kcal/mol

Parameters for the excess entropy:

$$\begin{aligned} a' &= 0.0 \text{ e.u.} \\ b' &= 0.0 \text{ e.u.} \\ c' &= 0.0 \text{ e.u.} \end{aligned}$$

Estimated uncertainty in $4S^E(x=0.5)$: 0.5 e.u.

A comparison of the E° values of both authors with the Senderoff and Mellors [16] values indicates

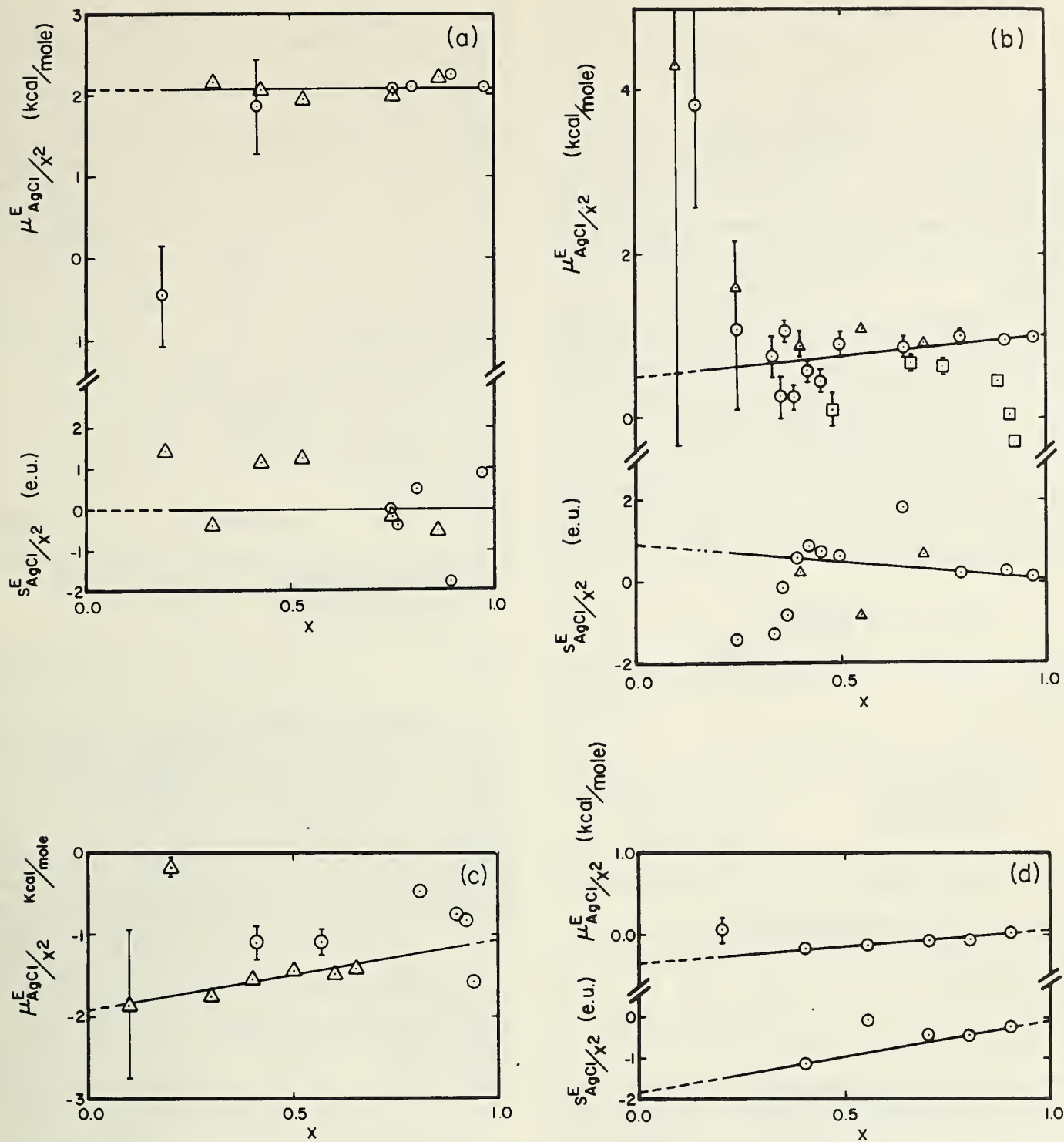


FIGURE 1. Experimental values of μ_{AgCl}^E/x^2 and s_{AgCl}^E/x^2 in molten binary chloride mixtures. The limits of uncertainty and the solid lines are the result of the present analysis.

- a. AgCl, LiCl
 - Panish, Newton, Grimes, Blankenship [20], 800 °C
 - △ Salstrom, Kew, Powell [26], 600 °C
- b. AgCl, NaCl
 - Panish, Blankenship, Grimes, Newton [19], 800 °C
 - Stern [25], 800 °C
 - △ Sternberg and Gheorghiu [27], 800 °C
- c. AgCl, KCl
 - △ Murgulescu and Sternberg [22], 650 °C
 - Stern [24], 700 °C
- d. AgCl, PbCl₂
 - Salstrom [23], 550 °C

a temperature limit of 800 °C for the Salstrom, Kew and Powell [26] measurements, whereas the Panish, Newton, Grimes, and Blankenship [20] values are accurate even up to 900 °C. However, the fact that extrapolated E° values are accurate does not mean that the same holds for extrapolated emfs of mixtures, especially when only a small temperature range is investigated e.g. $x=0.864$ [26]. Panish, Newton, Grimes, and Blankenship [20] have covered the concentration range $0 \leq x \leq 0.9714$, whereas Salstrom, Kew, and Powell [26] investigated only lower melting mixtures ($0 \leq x \leq 0.864$).

Most experimental points reported by Salstrom, Kew, and Powell [26] are included at 600 °C, whereas the Panish, Newton, Grimes, and Blankenship data [20] have a "best temperature range" from 650 to 800 °C. Although the values of Panish, Newton, Grimes, and Blankenship [20] suggest some asymmetry ($a=1.75$ kcal/mol, $b=0.60$ kcal/mol, $a'=-1.6$ e.u., $b'=2.6$ e.u.) the recommended values are gained from a combination of the data of Panish, Newton, Grimes, and Blankenship [20] and Salstrom, Kew, and Powell [26].

5.2.2. AgCl(1-x), NaCl(x).

Cells: Ag|AgCl(1-x), NaCl(x)|Cl₂|C. [19, 27, 25]
Tables: 1, 13
Figure: 1b

Parameters for the excess free energy:

$$\begin{aligned} a &= 0.8 \text{ kcal/mol} \\ b &= 0.0 \text{ kcal/mol} \\ c &= 0.0 \text{ kcal/mol} \end{aligned}$$

Estimated uncertainty in $4G^E(x=0.5)$: 0.2 kcal/mol

Parameters for the excess entropy:

$$\begin{aligned} a' &= 0.5 \text{ e.u.} \\ b' &= 0.0 \text{ e.u.} \\ c' &= 0.0 \text{ e.u.} \end{aligned}$$

Estimated uncertainty in $4S^E(x=0.5)$: 0.2 e.u.

The experimental difficulties for measuring cells Ag|AgCl, NaCl|Cl₂|C are about the same as for cells Ag|AgCl, LiCl|Cl₂|C (section 5.2.1). However, it is easier to prepare a water-free AgCl, NaCl mixture than it is to make AgCl, LiCl water-free. It was found in section 5.1.1 that the E° values of Panish, Blankenship, Grimes, and Newton [19, 20] agree with the Senderoff and Mellors values [16]. The Sternberg and Gheorghiu [27] E° value is slightly different from the Senderoff and Mellors values [16] which could partly be due to a different correction for the thermoelectric effect of the Ag|C couple. The Stern values [25] have appreciable systematic errors.

Panish, Blankenship, Grimes, and Newton [19] investigated the concentration range $0 \leq x \leq 0.9687$ and have a "best-temperature range" from 750 to

800 °C. Sternberg and Gheorghiu [27] covered the range $0 \leq x \leq 0.7$ and have a "best-temperature" of 800 °C.

Inspection of figure 1b shows that there is a difference between values of Panish, Blankenship, Grimes, and Newton [19] and Sternberg and Gheorghiu [27] for small x , whereas the data of Stern [25] deviate strongly from the other two sets of data. The work of Panish, Blankenship, Grimes, and Newton [19] indicates asymmetry in G^E and S^E ($a=0.78$ kcal/mol, $b=0.27$ kcal/mol, $c=0.0$ kcal/mol, $a'=0.50$ e.u., $b'=-0.40$ e.u., $c'=0.0$ e.u.). However the recommended G^E and S^E values are an "average" of data reported by Panish, Blankenship, Grimes, and Newton [19] and Sternberg and Gheorghiu [27].

5.2.3. AgCl(1-x), KCl(x).

Cells: Ag|AgCl, KCl|Cl₂|C.

Tables: 1, 14

Figure: 1c

[24, 22]

Parameters for the excess free energy (650 °C):

$$\begin{aligned} a &= -1.5 \text{ kcal/mol} \\ b &= 0.4 \text{ kcal/mol} \\ c &= 0.0 \text{ kcal/mol} \end{aligned}$$

Estimated uncertainty in $4G^E(x=0.5)$: 0.2 kcal/mol

From an experimental point of view the cell Ag|AgCl, KCl|Cl₂|C is about the same as the cell Ag|AgCl, NaCl|Cl₂|C (section 5.2.2). For reasons outlined in section 5.2.2 the recommended excess values have been derived from emf data as published by Murgulescu and Sternberg [22]. These authors have only covered the concentration range $0 \leq x \leq 0.65$. The values nevertheless indicate an asymmetrical G^E (fig. 1c). The s_{AgCl}^E/x^2 values are too scattered to enable an estimate of S^E .

5.2.4. AgCl(1-x), PbCl₂(x)

Cells: Ag|AgCl, PbCl₂|Cl₂|C.

Tables: 1, 15

Figure: 1d

[23]

Parameters for the excess free energy (550 °C):

$$\begin{aligned} a &= -0.15 \text{ kcal/mol} \\ b &= 0.20 \text{ kcal/mol} \\ c &= 0.00 \text{ kcal/mol} \end{aligned}$$

Estimated uncertainty in $4G^E(x=0.5)$: 0.05 kcal/mol

Parameters for the excess entropy (550 °C):

$$\begin{aligned} a' &= -0.9 \text{ e.u.} \\ b' &= 0.8 \text{ e.u.} \\ c' &= 0.0 \text{ e.u.} \end{aligned}$$

Estimated uncertainty in $4S^E(x=0.5)$: 0.1 e.u.

From an intercomparison of E° values (section 5.1.1) it follows that there are no systematic errors

involved in the E° values of Salstrom [23, 26].

Salstrom [23] freed the mixture from moisture and oxidation and hydrolysis products by bubbling dry hydrogen chloride through the melt. He covered the concentration range $0 \leq x \leq 0.9$. Inspection of figure 1d shows that it is most likely that the reaction $2\text{Ag} + \text{Pb}^{2+} \rightarrow 2\text{Ag}^+ + \text{Pb}$ has not influenced the cell emf.

5.2.5. $\text{BeCl}_2(1-x), \text{NaCl}(x)$.

Cells: $\text{Be}|\text{BeCl}_2, \text{NaCl}|\text{Cl}_2|\text{C}$.

Table: 2 [29, 28, 30, 31, 32]

It was pointed out in section 5.1.2 that although the cells $\text{Be}|\text{BeCl}_2, \text{NaCl}|\text{Cl}_2|\text{C}$ have been measured under equilibrium conditions, G^E values will not be reported due to difficulties involved in obtaining reliable E° values.

5.2.6. $\text{CdCl}_2(1-x), \text{NaCl}(x)$.

Cells: $\text{Cd}|\text{CdCl}_2(1-x), \text{NaCl}(x)|\text{Cl}_2|\text{C}$. [36]
 $\text{W}|\text{Cd}|\text{CdCl}_2, \text{NaCl}|\text{glass}|\text{CdCl}_2, \text{NaCl}|\text{Cd}|\text{W}$
 $(1-x) \quad (x) \quad (0.6) \quad (0.4)$
 [33, 34]

Tables: 3, 16

Figure: 2a

Parameters for the excess free energy (600 °C):

$$\begin{aligned} a &= -4.45 \text{ kcal/mol} \\ b &= -3.85 \text{ kcal/mol} \\ c &= 0.00 \text{ kcal/mol} \end{aligned}$$

Estimated uncertainty in $4G^E(x=0.5)$ 0.1 kcal/mol

The excess free energy as determined from cell $\text{Cd}|\text{CdCl}_2|\text{Cl}_2|\text{C}$ has an uncertainty due to Cd metal solubility in the melt (section 5.1.3). It can be seen from figure 2a that according to Lantratov and Alabyshev [36] the G^E of $\text{CdCl}_2, \text{NaCl}$ mixtures has a high value for the parameter c which is not very probable when one compares the mixture $\text{CdCl}_2, \text{NaCl}$ with the mixture $\text{CdCl}_2, \text{KCl}$ (section 5.2.7). Lantratov and Alabyshev [36] find extremely negative and extremely asymmetrical values for the excess entropy (table 16).

Knowledge of E° values is not required for the calculation of the excess properties from cells in which glass functions as a cation-selective membrane [33, 34]. Dijkhuis and Ketelaar [33, 34] give indirect evidence that electrical transport through glass in the cell $\text{W}|\text{Cd}|\text{CdCl}_2, \text{NaCl}|\text{glass}|\text{CdCl}_2, \text{NaCl}|\text{Cd}|\text{W}$ is only by sodium ions, and calculate the excess properties accordingly.

5.2.7. $\text{CdCl}_2(1-x), \text{KCl}(x)$.

Cells: $\text{Cd}|\text{CdCl}_2(1-x), \text{KCl}(x)|\text{Cl}_2|\text{C}$. [36]
 Tables: 3, 17
 Figure: 2b

Parameters for the excess free energy (600 °C):

$$\begin{aligned} a &= -7.5 \text{ kcal/mol} \\ b &= -10.7 \text{ kcal/mol} \\ c &= 0.0 \text{ kcal/mol} \end{aligned}$$

Estimated uncertainty in $4G^E(x=0.5)$ 0.5 kcal/mol

The uncertainties involved in deriving excess properties from cells $\text{Cd}|\text{CdCl}_2, \text{NaCl}|\text{Cl}_2|\text{C}$ have been discussed in sections 5.1.3 and 5.2.6; cells $\text{Cd}|\text{CdCl}_2, \text{KCl}|\text{Cl}_2|\text{C}$ have been studied by Lantratov and Alabyshev [36]. However, while $\mu_{\text{CdCl}_2}^E/x^2$ versus x values derived from cells $\text{Cd}|\text{CdCl}_2, \text{NaCl}|\text{Cl}_2|\text{C}$ show appreciable curvature, the $\mu_{\text{CdCl}_2}^E/x^2$ versus x plot as derived from cells $\text{Cd}|\text{CdCl}_2, \text{KCl}|\text{Cl}_2|\text{C}$ gives a straight line relationship. This could be due to the fact that the absolute value of G^E is higher for the mixture $\text{CdCl}_2, \text{KCl}$ than for the mixture $\text{CdCl}_2, \text{NaCl}$ which means that experimental errors have a relatively smaller influence for the former mixture. However, the excess entropies as determined from cells $\text{Cd}|\text{CdCl}_2, \text{KCl}|\text{Cl}_2|\text{C}$ seem to be too high ($a' = -10$ e.u., $b' = 0$ e.u., $c' = 0$ e.u., estimated uncertainty in $4S^E(x=0.5) = 5$ e.u.).

5.2.8. $\text{CdCl}_2(1-x), \text{BaCl}_2(x)$.

Cells: $\text{Cd}|\text{CdCl}_2, \text{BaCl}_2|\text{Cl}_2|\text{C}$. [36]
 Tables: 3, 18
 Figure: 2c

Parameters for the excess free energy (600 °C):

$$\begin{aligned} a &= -1.0 \text{ kcal/mol} \\ b &= -8.8 \text{ kcal/mol} \\ c &= 0.0 \text{ kcal/mol} \end{aligned}$$

Estimated uncertainty in $4G^E(x=0.5)$: 0.5 kcal/mol

Some uncertainties involved in CdCl_2 containing formation cells have been outlined in sections 5.1.3, 5.2.6, and 5.2.7. Special difficulties resulting from properties of BaCl_2 have not been reported by Lantratov and Alabyshev [36]. Inspection of figure 2c shows a straight line relationship between $\mu_{\text{CdCl}_2}^E/x^2$ versus x and $s_{\text{CdCl}_2}^E/x^2$ versus x . This gives some indication about the S^E values ($a' = -9.0$ e.u., $b' = -8.5$ e.u.; estimated uncertainty in $4S^E(x=0.5)$: 1.0 e.u.).

5.2.9. $\text{CeCl}_3(1-x), \text{NaCl}(x)$.

Cells: $(\text{Ce}, \text{Sn})|\text{CeCl}_3(1-x), \text{NaCl}(x)|\text{Cl}_2|\text{C}$. [37]
 Table: 19
 Figure: 3a

Parameters for the excess free energy (800 °C):

$$\begin{aligned} a &= -2.7 \text{ kcal/mol} \\ b &= -13.6 \text{ kcal/mol} \\ c &= 9.3 \text{ kcal/mol} \end{aligned}$$

Estimated uncertainty in $4G^E(x=0.5)$: 0.4 kcal/mol

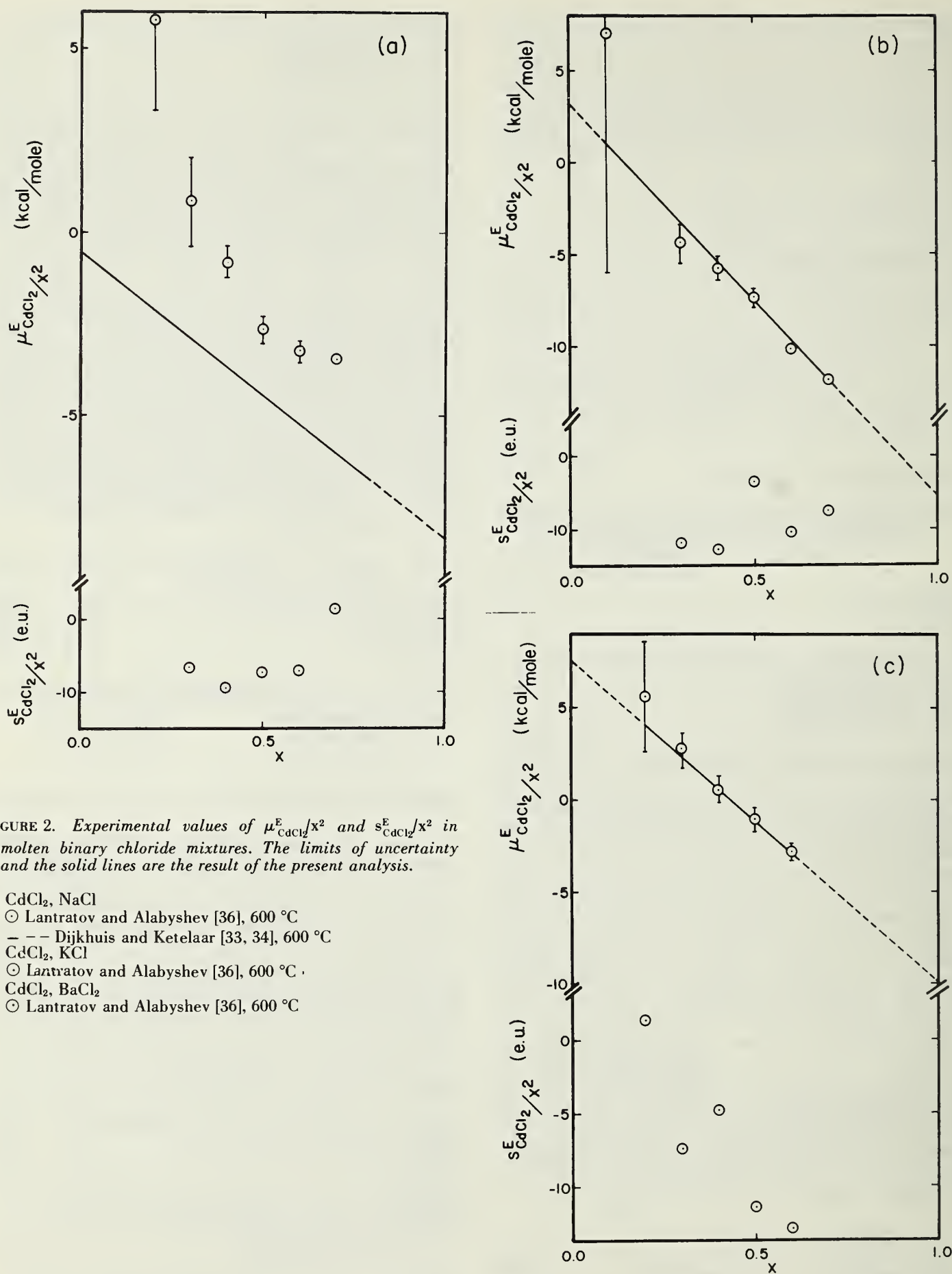


FIGURE 2. Experimental values of $\mu^E_{\text{CdCl}_2}/x^2$ and $s^E_{\text{CdCl}_2}/x^2$ in molten binary chloride mixtures. The limits of uncertainty and the solid lines are the result of the present analysis.

- a. CdCl_2 , NaCl
 \odot Lantratov and Alabyshev [36], 600 °C
 --- Dijkhuis and Ketelaar [33, 34], 600 °C
- b. CdCl_2 , KCl
 \odot Lantratov and Alabyshev [36], 600 °C
- c. CdCl_2 , BaCl_2
 \odot Lantratov and Alabyshev [36], 600 °C

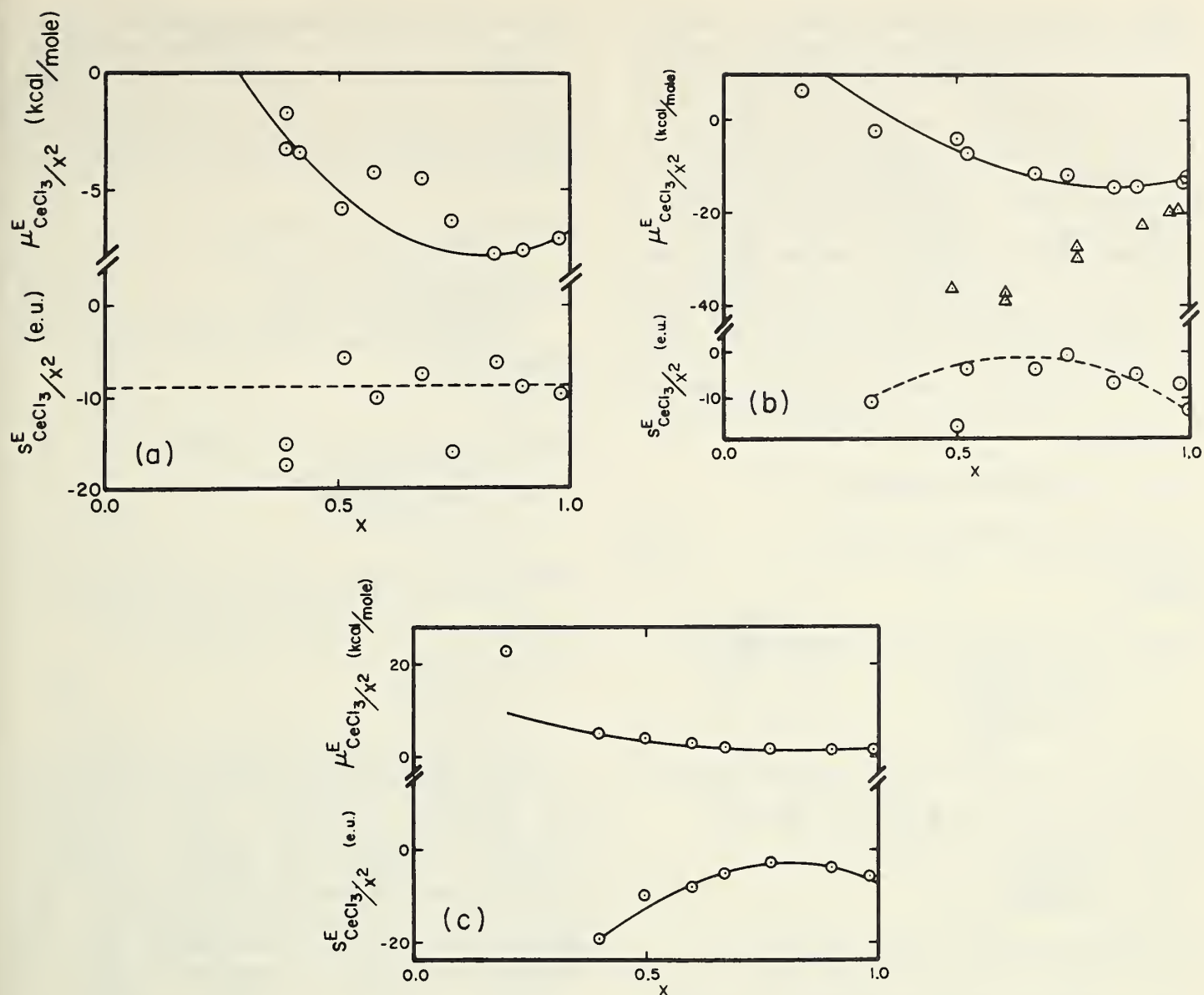


FIGURE 3. Experimental values of $\mu_{\text{CeCl}_3}^E/x^2$ and $S_{\text{CeCl}_3}^E/x^2$ in molten binary chloride mixtures. The solid lines are the results of the present analysis.

- a. CeCl_3 , NaCl
 | \circ Senderoff, Mellors, Bretz [37], 800 °C
 b. CeCl_3 , KCl
 \circ Senderoff, Mellors, Bretz [37], 850 °C
 \triangle Neil [38], 850 °C
 c. CeCl_3 , CaCl_2
 \circ Senderoff, Mellors, Bretz [39], 850 °C

It was outlined in section 5.1.4 that Senderoff, Mellors, and Bretz [37] investigated the reversibility of this cell. Emf data have only been reported at three temperatures (800 °C, 850 °C, and 900 °C). This means that random errors could not be calculated.

The $\mu_{\text{CeCl}_3}^E/x^2$ versus x plot (fig. 3a) shows a curvature which indicates that the parameter c has an appreciable value when compared with the parameters a and b .

The $S_{\text{CeCl}_3}^E/x^2$ versus x plot also suggests some curvature; however, the scatter of the data allows only a rough estimate of S^E ($a' = -8$ e.u., $b' = 0$ e.u. and $c' = 0$ e.u.).

5.2.10. $\text{CeCl}_3(1-x)$, $\text{KCl}(x)$.

Cells: $(\text{Ce}, \text{Sn})|\text{CeCl}_3, \text{KCl}|\text{Cl}_2|\text{C}$. [37]
 $(\text{Ce}, \text{Bi})|\text{CeCl}_3, \text{KCl}|\text{Cl}_2|\text{C}$. [38]

Table: 20
 Figure: 3b

Parameters for the excess free energy (850 °C):

$$\begin{aligned} a &= -1.87 \text{ kcal/mol} \\ b &= -31.75 \text{ kcal/mol} \\ c &= 20.48 \text{ kcal/mol} \end{aligned}$$

Estimated uncertainty in $4G^E(x=0.5)$: 0.4 kcal/mol

The comparison of excess properties as derived from the two cells provides a means of comparing the alloy electrodes. Table 20 and figure 3b show clearly that the values from the (Ce, Bi) electrode deviate strongly from those derived from the (Ce, Sn) electrode. Neil [38] has calculated the activity of Ce in the alloy from the alloy composition, whereas Senderoff, Mellors, and Bretz [37] worked with a constant alloy composition. For this reason the Senderoff, Mellors, and Bretz values are recommended. The plot of $s_{\text{CeCl}_3}^E/x^2$ versus x as derived from measurements of Senderoff, Mellors, and Bretz [37] suggests asymmetry. However, S^E values can only be estimated ($a' = -10.8$ e.u., $b' = 28.4$ e.u., $c' = -29.6$ e.u.; estimated uncertainty in $4S^E(x=0.5)$: 2 e.u.) due to the scatter of the experimental points.

5.2.11. $\text{CeCl}_3(1-x)$, $\text{CaCl}_2(x)$.

Cells: (Ce, Sn)| CeCl_3 , CaCl_2 | Cl_2 |C. [39]
Table: 21
Figure: 3c

Parameters for the excess free energy (850 °C):

$$\begin{aligned}a &= 4.80 \text{ kcal/mol} \\b &= -8.79 \text{ kcal/mol} \\c &= 5.37 \text{ kcal/mol}\end{aligned}$$

Estimated uncertainty in $4G^E(x=0.5)$: 0.5 kcal/mol

Parameters for the excess entropy (850 °C):

$$\begin{aligned}a' &= -20.6 \text{ e.u.} \\b' &= 43.8 \text{ e.u.} \\c' &= -29.2 \text{ e.u.}\end{aligned}$$

Estimated uncertainty in $4S^E(x=0.5)$: 2 e.u.

The experimental arrangement was the same as for cells containing CeCl_3 , NaCl (section 5.2.9) and CeCl_3 , KCl (section 5.2.10). Special care was taken to avoid impurities in the CaCl_2 .

Figure 3c shows clearly that both G^E and S^E are asymmetrical in normal mole fractions. The continuity in plots of $\mu_{\text{CeCl}_3}^E/x^2$ versus x and $s_{\text{CeCl}_3}^E/x^2$ versus x indicates small random errors.

5.2.12. $\text{MgCl}_2(1-x)$, $\text{LiCl}(x)$.

Cells: $\text{Mg}|\text{MgCl}_2(1-x)$, $\text{LiCl}(x)|\text{Cl}_2$ |C. [40]
Tables: 4, 22
Figure: 4a

Parameters for the excess free energy (700 °C):

$$\begin{aligned}a &= 3.95 \text{ kcal/mol} \\b &= -5.75 \text{ kcal/mol} \\c &= 0.00 \text{ kcal/mol}\end{aligned}$$

Estimated uncertainty in $4G^E(x=0.5)$: 0.5 kcal/mol

The recommended values might have an even higher systematic error than is indicated above, due

to the fact that the decomposition-potential method ($i-V$) was used. This is not an equilibrium measurement. The excess entropy of this mixture ($a' = 26.5$ e.u., $b' = -17.5$ e.u., $c' = 0.0$ e.u.) seems to be too high. This could indicate that appreciable systematic errors are involved in the Markov, Delimarskii, and Panchenko data [40].

5.2.13. $\text{MgCl}_2(1-x)$, $\text{NaCl}(x)$.

Cells: $\text{Mg}|\text{MgCl}_2$, $\text{NaCl}|\text{Cl}_2$ |C. [40]
(Mg, Bi)| MgCl_2 , $\text{NaCl}|\text{Cl}_2$ |C. [38, 41]
 $\text{C}|\text{Cl}_2|\text{NaCl}|\text{glass}|\text{MgCl}_2$, $\text{NaCl}|\text{Cl}_2$ |C. [9]
Tables: 4, 23
Figures: 4b, 4b'

Parameters for the excess free energy:

$$\begin{aligned}a &= -4.80 \text{ kcal/mol} \\b &= -9.39 \text{ kcal/mol} \\c &= 7.08 \text{ kcal/mol}\end{aligned}$$

Estimated uncertainty in $4G^E(x=0.5)$: 0.5 kcal/mol

Parameters for the excess entropy (850 °C):

$$\begin{aligned}a' &= -1.2 \text{ e.u.} \\b' &= 0.0 \text{ e.u.} \\c' &= 0.0 \text{ e.u.}\end{aligned}$$

The $\mu_{\text{MgCl}_2}^E$ values of the mixture can be calculated from the cells $\text{Mg}|\text{MgCl}_2$, $\text{NaCl}|\text{Cl}_2$ |C [40] and (Mg, Bi)| MgCl_2 , $\text{NaCl}|\text{Cl}_2$ |C [38, 41] whereas μ_{NaCl}^E values are measured in cells $\text{C}|\text{Cl}_2|\text{NaCl}|\text{glass}|\text{MgCl}_2$, $\text{NaCl}|\text{Cl}_2$ |C [9]. Markov, Delimarskii, and Panchenko [40] used a nonequilibrium type cell (section 5.2.12) whereas the cell with the alloy electrode (Neil, Clark and Wiswall [38, 41]) is in principle an equilibrium measurement.

Inspection of figure 4b shows a curvature in $\mu_{\text{MgCl}_2}^E/x^2$ versus x according to Neil, Clark and Wiswall [41]. ($a = -4.15$ kcal/mol, $b = -14.18$ kcal/mol, $c = 11.09$ kcal/mol.) In this study data have been determined at 825 °C only. This means that excess entropies cannot be calculated from the temperature dependence of these emf data.

Ostfold [9] has determined μ_{NaCl}^E values by means of emf measurements on cells in which glass functions as a sodium ion selective membrane (section 5.1.15). These values are presented in figure 4b'. Although this plot shows a curvature ($a = -2.58$ kcal/mol, $b = -13.26$ kcal/mol, $c = 9.13$ kcal/mol), the scatter of points around the composition $x = 0.5$ makes a quantitative estimate uncertain.

From experimental consideration it follows that the Ostfold values [9] are most accurate on the NaCl side of the system, whereas the Neil, Clark, and Wiswall values [41] are most accurate on the MgCl_2 side. The recommended values were determined by appropriate weighing of the two sets of data.

Figure 4b' shows that the excess entropy, as determined by Ostfold [9], has an appreciable random error. These data are suitable for an estimate

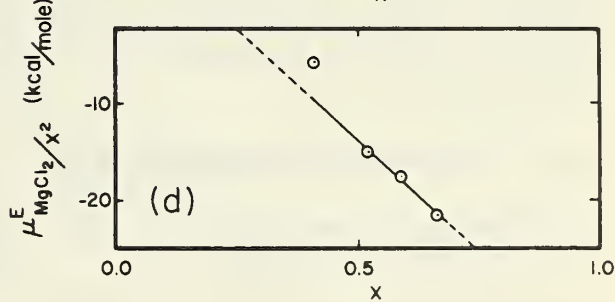
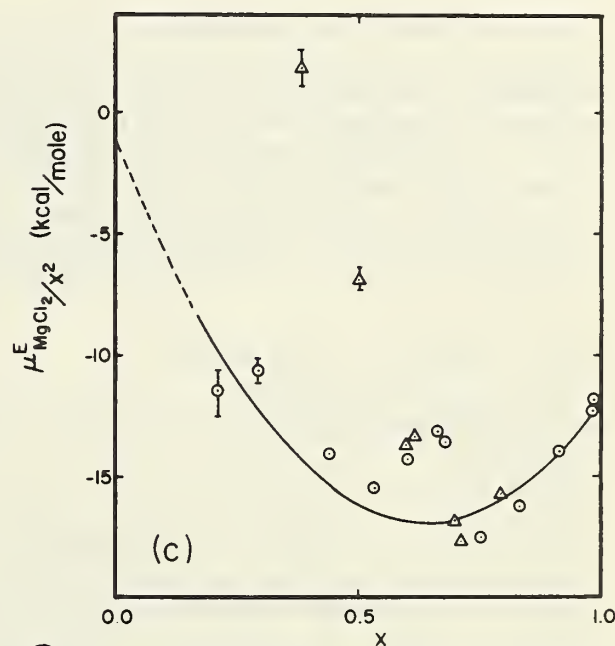
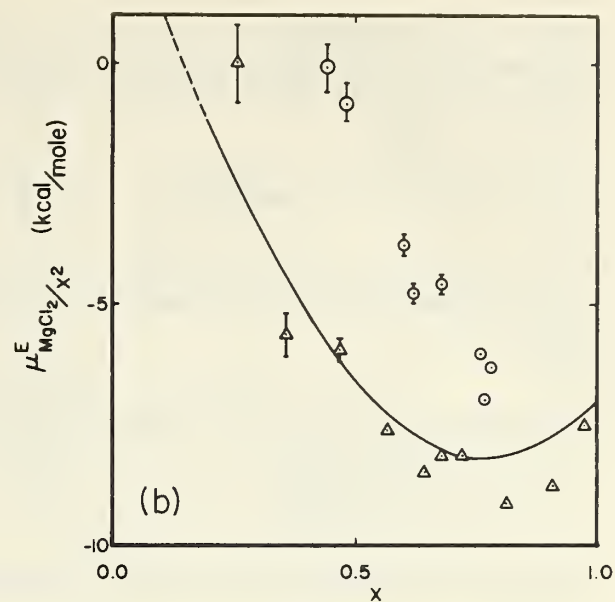
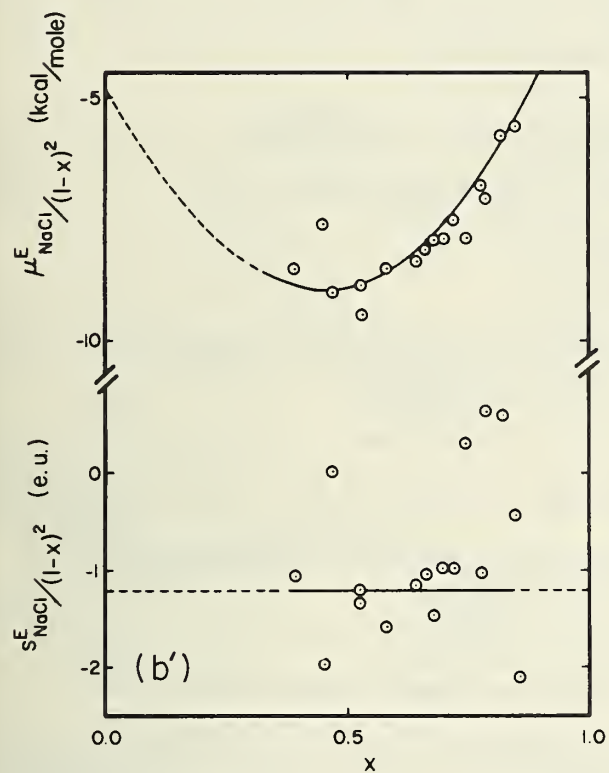
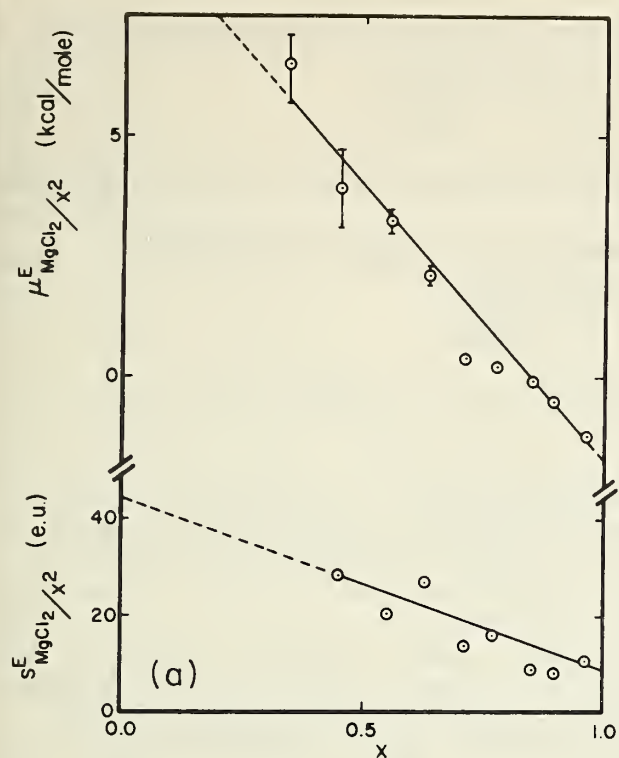


FIGURE 4. Experimental values of $\mu_{\text{MgCl}_2}^E/x^2$ (or $\mu_{\text{NaCl}}^E/(1-x)^2$) and $S_{\text{MgCl}_2}^E/x^2$ (or $S_{\text{NaCl}}^E/(1-x)^2$) in molten binary chloride mixtures containing MgCl_2 . The limits of uncertainty and the solid lines are the result of the present analysis.

- a. MgCl_2 , LiCl
 \circ Markov, Delimarskii and Panchenko [40], 700 °C
- b. MgCl_2 , NaCl
 \circ Markov, Delimarskii, Panchenko [40], 700 °C
 \triangle Neil, Clark, Wiswall [41], 825 °C
- b'. MgCl_2 , NaCl
 \circ Ostvold [9], 850 °C
- c. MgCl_2 , KCl
 \triangle Markov, Delimarskii, Panchenko [40], 700 °C
 \circ Neil, Clark, Wiswall [41], 800 °C
- d. MgCl_2 , RbCl
 \circ Markov, Delimarskii, and Panchenko [40], 700 °C

of the excess entropy ($a' = -1$ e.u., $b' = c' = 0$ e.u.). It is seen that the excess entropy of the mixture MgCl_2 , NaCl has a small influence on the total excess free energy.

5.2.14. $\text{MgCl}_2(1-x)$, $\text{KCl}(x)$.

Cells: $\text{Mg}|\text{MgCl}_2(1-x), \text{KCl}(x)|\text{Cl}_2|\text{C}$. [40]
 $(\text{Mg}, \text{Bi})|\text{MgCl}_2(1-x), \text{KCl}(x)|\text{Cl}_2|\text{C}$. [38, 41]

Tables: 4, 24

Figure: 4c

Parameters for the excess free energy (800 °C):

$$\begin{aligned} a &= -12.84 \text{ kcal/mol} \\ b &= -11.88 \text{ kcal/mol} \\ c &= 12.96 \text{ kcal/mol} \end{aligned}$$

Estimated uncertainty in $4G^E$ ($x=0.5$): 0.9 kcal/mol

The cells have been discussed in section 5.2.13. It was pointed out in that section that due to non-equilibrium conditions unacceptable uncertainties are involved in the kind of cell investigated by Markov, Delimarskii, and Panchenko [40]. The recommended values were calculated from the cell of Neil, Clark, and Wiswall [41]. The latter authors published their values at one temperature only and the excess entropies can therefore not be calculated.

5.2.15. $\text{MgCl}_2(1-x)$, $\text{RbCl}(x)$.

Cells: $\text{Mg}|\text{MgCl}_2, \text{RbCl}|\text{Cl}_2|\text{C}$. [40]

Table: 25

Figure: 4d

This mixture has been investigated by a non-equilibrium method. One can expect to get only some order of magnitude for the excess free energy from this kind of cell: $a = -11.5$ kcal/mol, $b = -20.5$ kcal/mol. The cell used by Markov, Delimarskii, and Panchenko [40] was discussed in section 5.2.13.

5.2.16. MnCl_2 , NaCl and MnCl_2 , KCl .

Cells: $\text{Mn}|\text{MnCl}_2, \text{NaCl}|\text{Cl}_2|\text{C}$. [42, 43]
 $\text{Mn}|\text{MnCl}_2, \text{KCl}|\text{Cl}_2|\text{C}$. [42, 43]

These cells have been discussed in section 5.1.6. As the E° value of this cell is uncertain it was decided not to recommend excess properties for these mixtures.

5.2.17. $\text{CaCl}_2(1-x)$, $\text{NaCl}(x)$.

Cells: $\text{C}|\text{Cl}_2|\text{NaCl}|\text{glass}|\text{CaCl}_2(1-x), \text{NaCl}(x)|\text{Cl}_2|\text{C}$. [9]

Table: 26

Figure: 5a

Parameters for the excess free energy (850 °C):

$$\begin{aligned} a &= -2.45 \text{ kcal/mol} \\ b &= -0.45 \text{ kcal/mol} \\ c &= 0.0 \text{ kcal/mol} \end{aligned}$$

Estimated uncertainty in $4G^E$ ($x=0.5$): 0.5 kcal/mol

Parameters for the excess entropy (850 °C):

$$\begin{aligned} a' &= -1.75 \text{ e.u.} \\ b' &= 3.39 \text{ e.u.} \\ c' &= -3.68 \text{ e.u.} \end{aligned}$$

Estimated uncertainty in $4S^E$ ($x=0.5$): 0.4 e.u.

The use of glass as a cation-selective membrane is discussed in section 5.1.15. Ostvold [9] found that electrical transport through glass was by means of sodium ions only. This author bubbled dry hydrogen chloride through the melt for 2 to 5 hr in order to remove hydroxides.

Inspection of figure 5a shows a curvature in the $\mu_{\text{NaCl}}^E/(1-x)^2$ versus x plot. However, this curvature depends strongly on mixtures dilute in NaCl or mixtures dilute in CaCl_2 . A straight line relationship is recommended. The $s_{\text{NaCl}}^E/(1-x)^2$ versus x plot shows a curvature and the S^E values are recommended accordingly.

5.2.18. $\text{SrCl}_2(1-x)$, $\text{NaCl}(x)$.

Cells: $\text{C}|\text{Cl}_2|\text{NaCl}|\text{glass}|\text{SrCl}_2(1-x), \text{NaCl}(x)|\text{Cl}_2|\text{C}$. [9]

Table: 27

Figure: 5b

Parameters for the excess free energy (850 °C):

$$\begin{aligned} a &= -0.02 \text{ kcal/mol} \\ b &= -1.92 \text{ kcal/mol} \\ c &= 1.03 \text{ kcal/mol} \end{aligned}$$

Estimated uncertainty in $4G^E$ ($x=0.5$): 0.5 kcal/mol

Parameters for the excess entropy (850 °C):

$$\begin{aligned} a' &= -0.81 \text{ e.u.} \\ b' &= 2.08 \text{ e.u.} \\ c' &= -1.73 \text{ e.u.} \end{aligned}$$

Estimated uncertainty in $4S^E$ ($x=0.5$): 0.4 e.u.

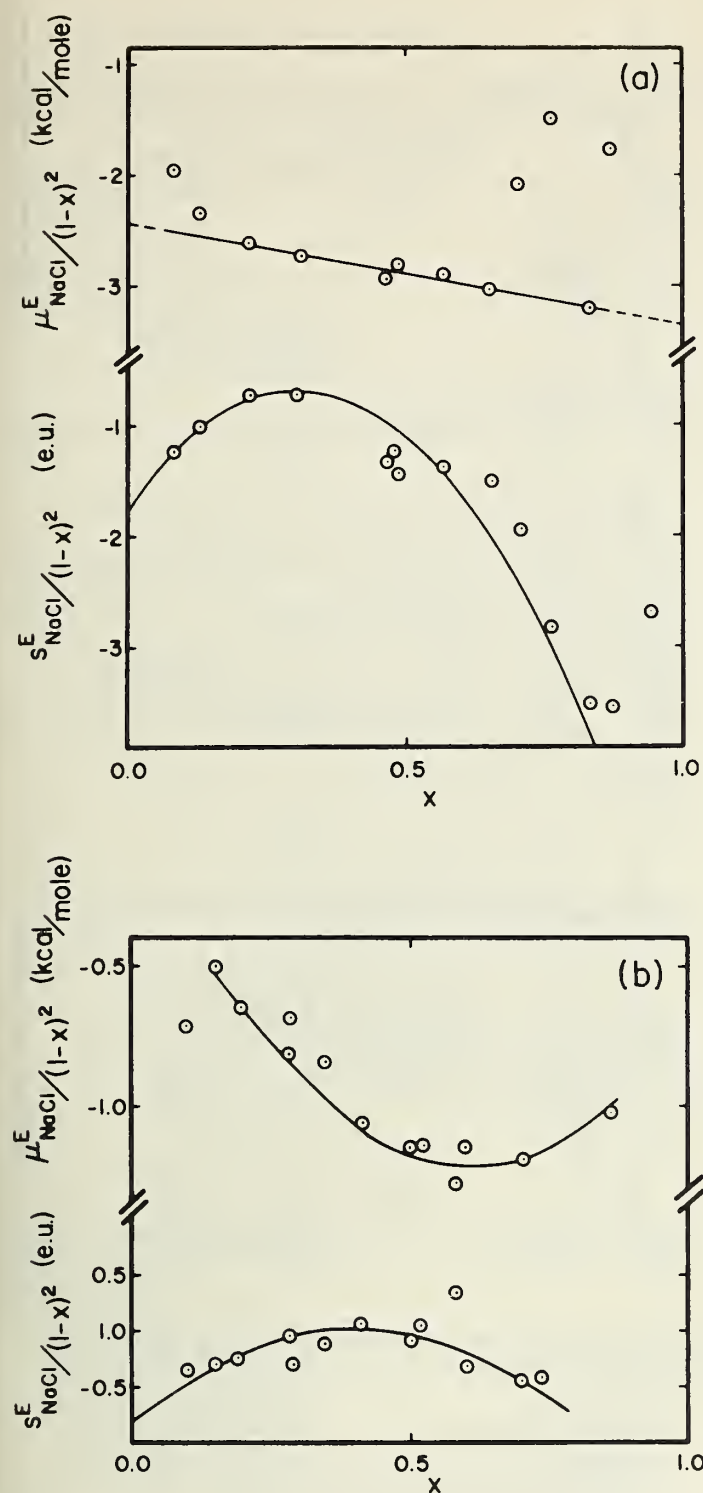
The experimental procedure was the same as for the mixture CaCl_2 , NaCl (section 5.2.17). Inspection of figure 5b shows clearly a curvature in both the $\mu_{\text{NaCl}}^E/(1-x)^2$ versus x and $s_{\text{NaCl}}^E/(1-x)^2$ versus x plot. The parameters for the excess free energy and for the excess entropy have been calculated, accordingly, from the Ostvold data [9].

5.2.19. $\text{BaCl}_2(1-x)$, $\text{NaCl}(x)$.

Cells: $\text{C}|\text{Cl}_2|\text{NaCl}|\text{glass}|\text{BaCl}_2(1-x), \text{NaCl}(x)|\text{Cl}_2|\text{C}$. [9]

Table: 28

Figure: 5c



Parameters for the excess free energy (850 °C):

$$\begin{aligned} a &= 0.08 \text{ kcal/mol} \\ b &= -0.04 \text{ kcal/mol} \\ c &= 0.00 \text{ kcal/mol} \end{aligned}$$

Estimated uncertainty in $4G^E(x=0.5)$: 0.1 kcal/mol

Parameters for the excess entropy (850 °C):

$$\begin{aligned} a' &= 0.14 \text{ e.u.} \\ b' &= 0.07 \text{ e.u.} \\ c' &= 0.00 \text{ e.u.} \end{aligned}$$

Estimated uncertainty in $4S^E(x=0.5)$: 0.05 e.u.

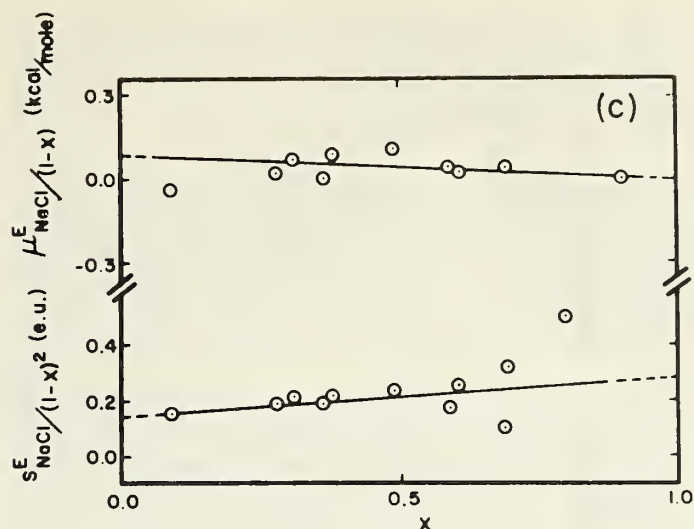


FIGURE 5. Experimental values for $\mu_{\text{NaCl}}^E/(1-x)^2$ and $s_{\text{NaCl}}^E/(1-x)^2$ in binary alkaline earth chloride-sodium chloride mixtures. The solid lines are the result of the present analysis.

- a. CaCl_2 , NaCl
 ○ Ostvold [9], 850 °C
 b. SrCl_2 , NaCl
 ○ Ostvold [9], 850 °C
 c. BaCl_2 , NaCl
 ○ Ostvold [9], 850 °C

The cell has been discussed in section 5.2.17. Inspection of figure 5c suggests curvature for both $\mu_{\text{NaCl}}^E/(1-x)^2$ versus x and $s_{\text{NaCl}}^E/(1-x)^2$ versus x . However, it was decided that the curvature was not pronounced enough and straight line relationships are recommended.

5.2.20. $\text{PbCl}_2(1-x)$, $\text{LiCl}(x)$.

Cells: $\text{Pb}|\text{PbCl}_2, \text{LiCl}|\text{Cl}_2|\text{C}$.

[45, 46]

Tables: 5, 29

Figure: 6a

Parameters for the excess free energy (600 °C):

$$\begin{aligned} a &= 0.45 \text{ kcal/mol} \\ b &= -0.55 \text{ kcal/mol} \\ c &= 0.00 \text{ kcal/mol} \end{aligned}$$

Estimated uncertainty in $4G^E(x=0.5)$: 0.2 kcal/mol

Lantratov and Alabyshev [45] have investigated the cell under equilibrium conditions. Inspection of table 7.1.7a shows at 600 °C a difference of 5 mV between the E° values of Hagemark and Hengstenberg [44] and Lantratov and Alabyshev [45]. This difference could be due to thermoelectric effects. Lantratov and Alabyshev [45] do not report special precautions in handling LiCl .

Markov, Delimarskii and Panchenko [46] have used the decomposition potential method. For this

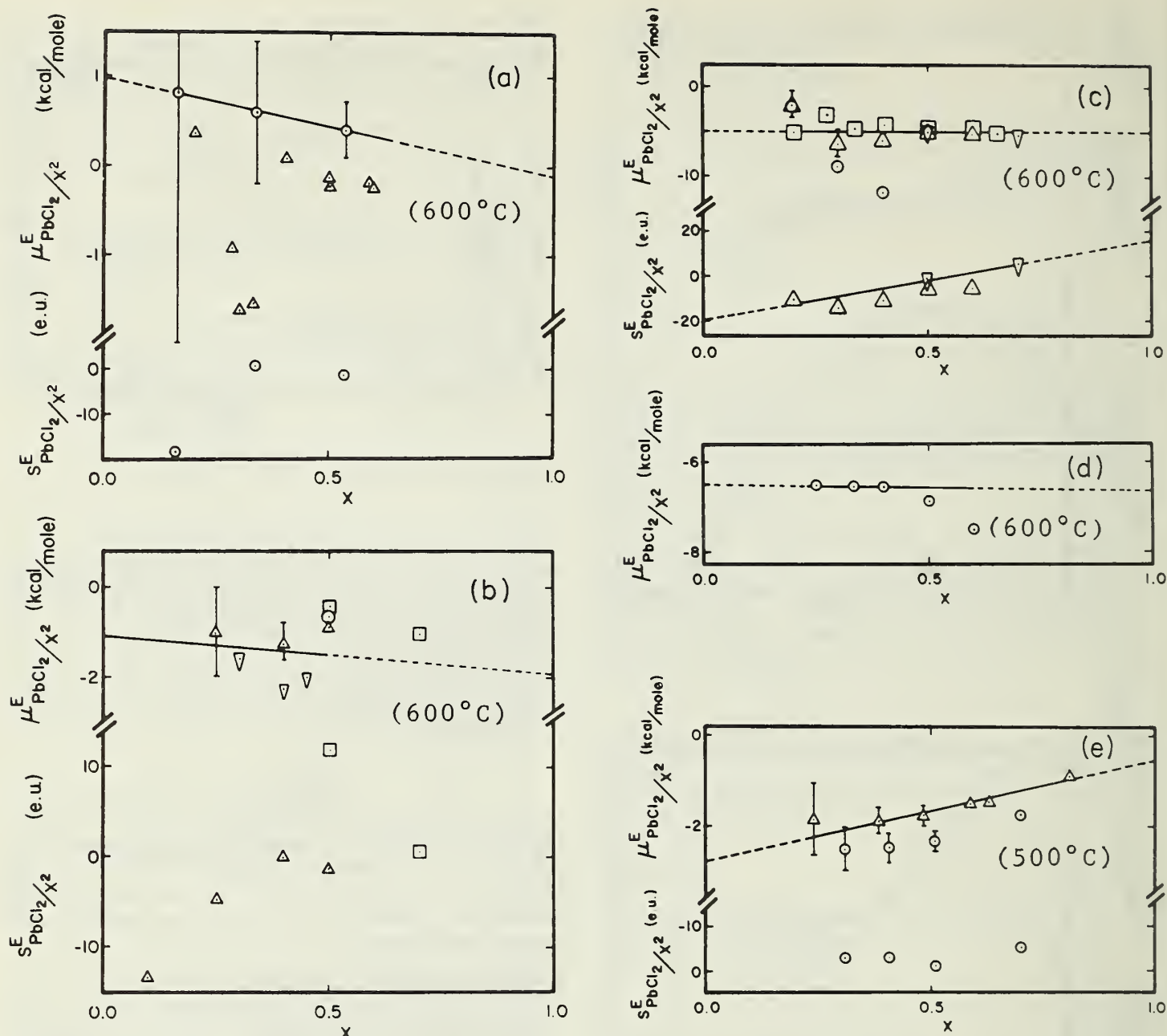


FIGURE 6. Experimental values for $\mu_{\text{PbCl}_2}^E/x^2$ and $S_{\text{PbCl}_2}^E/x^2$ in binary chloride mixtures. The limits of uncertainty and the solid lines are the result of the present analysis.

- a. PbCl_2 , LiCl
 - △ Markov, Delimarskii, Panchenko [46], 600 °C
 - Lantratov, Alabyshev [45], 600 °C
- b. PbCl_2 , NaCl
 - ▽ Markov, Delimarskii, Panchenko [46], 600 °C
 - △ Lantratov, Alabyshev [45], 600 °C
 - Suskii [48], 600 °C
 - Hagemark, Hengstenberg [44], 600 °C
 - Dijkhuis, Ketelaar [33, 34], 600 °C
- c. PbCl_2 , KCl
 - Hildebrand and Ruhle [49], 600 °C
 - △ Lantratov and Alabyshev [45], 600 °C
 - Markov, Delimarskii, Panchenko [46], 600 °C
 - ▽ Hagemark and Hengstenberg [44], 600 °C

- d. PbCl_2 , RbCl
 - Markov, Delimarskii, Panchenko [46], 600 °C
- e. PbCl_2 , ZnCl_2
 - Wachter, Hildebrand [50], 500 °C
 - △ Nakamura and Brenet [51], 500 °C

reason the recommended free energy data have been calculated from the Lantratov and Alabyshev [45] equilibrium data. The three points (fig. 6a) give a perfect linear relation between $\mu_{\text{PbCl}_2}^E/x^2$ and x . Although the random error in these measurements

is quite high, an asymmetrical excess free energy is recommended. The temperature dependence of data reported by Lantratov and Alabyshev [45] does not give much information about the excess entropy of this mixture.

5.2.21. $\text{PbCl}_2(1-x), \text{NaCl}(x)$.

Cells: $\text{Pb}|\text{PbCl}_2, \text{NaCl}|\text{Cl}_2|\text{C}$. [44, 45, 46, 48]
 $\text{W}|\text{Pb}|\text{PbCl}_2, \text{NaCl}|\text{glass}|\text{PbCl}_2(x=0.6),$
 $\text{NaCl}(x=0.4)|\text{Pb}|\text{W}$. [33, 34]

Tables: 5, 30

Figure: 6b

Parameters for the excess free energy (600 °C):

$$a = -1.52 \text{ kcal/mol}$$

$$b = -0.39 \text{ kcal/mol}$$

$$c = 0.00 \text{ kcal/mol}$$

Estimated uncertainty in $4G^E$ ($x=0.5$): 0.2 kcal/mol

The $\mu_{\text{PbCl}_2}^E/x^2$ versus x data, as determined by various authors are presented in figure 6b. Equilibrium cells; e.g., $\text{Pb}|\text{PbCl}_2, \text{NaCl}|\text{Cl}_2|\text{C}$ have been investigated by Lantratov and Alabyshev [45] and by Hagemark and Hengstenberg [44]. By combining these two sets of data the mixture $\text{PbCl}_2, \text{NaCl}$ turns out to be regular with a value of the a parameter of $-1 \text{ kcal/mol} \pm 0.5 \text{ kcal/mol}$.

Dijkhuis and Ketelaar [33, 34] used a cell in which glass functions as a cation-selective membrane (section 5.1.15). As these authors did not have to subtract large quantities in order to find a small difference these values are recommended.

Inspection of figure 6b shows that the Markov, Delimarskii and Panchenko values [46], which were determined by a nonequilibrium technique, do not agree with the equilibrium values.

The $s_{\text{PbCl}_2}^E/x^2$ values as determined from the temperature dependence of emfs of equilibrium cells have too much scatter to allow the derivation of excess entropies (table 30).

5.2.22. $\text{PbCl}_2(1-x), \text{KCl}(x)$.

Cells: $\text{Pb}|\text{PbCl}_2, \text{KCl}|\text{Cl}_2|\text{C}$. [44, 45, 46, 49]

Tables: 5, 31

Figure: 6c

Parameters for the excess free energy (600 °C):

$$a = -5.0 \text{ kcal/mol}$$

$$b = 0.0 \text{ kcal/mol}$$

$$c = 0.0 \text{ kcal/mol}$$

Estimated uncertainty in $4G^E$ ($x=0.5$): 1.0 kcal/mol

Parameters for the excess entropy (600 °C):

$$a' = -2.0 \text{ e.u.}$$

$$b' = 18.0 \text{ e.u.}$$

$$c' = 0.0 \text{ e.u.}$$

Estimated uncertainty in $4S^E$ ($x=0.5$): 1.0 e.u.

The $\mu_{\text{PbCl}_2}^E/x^2$ data of this mixture as determined by various authors have been plotted versus x in figure 6c. Hildebrand and Ruhle [49] used a nonequilibrium technique and find values that deviate strongly from the data determined by means of

equilibrium measurements. However, it is remarkable that Markov, Delimarskii, and Panchenko [46] who also used a nonequilibrium method find values that are in good agreement with the equilibrium data.

The data of Hagemark and Hengstenberg [44] suggest some asymmetry in the excess free energy. However, the recommended values for the excess free energy were determined by combining the equilibrium data reported by Hagemark and Hengstenberg [44] and by Lantratov and Alabyshev [45].

The temperature dependence of the emfs of formation cells gives rise to a strongly asymmetrical excess entropy. This asymmetry follows from the data of Lantratov and Alabyshev [45] and Hagemark and Hengstenberg [44] (see fig. 6c).

5.2.23. $\text{PbCl}_2(1-x), \text{RbCl}(x)$.

Cells: $\text{Pb}|\text{PbCl}_2, \text{RbCl}|\text{Cl}_2|\text{C}$. [46]

Tables: 5, 32

Figure: 6d

Parameters for the excess free energy (600 °C):

$$a = -6.5 \text{ kcal/mol}$$

$$b = -0.1 \text{ kcal/mol}$$

$$c = 0.0 \text{ kcal/mol}$$

Estimated uncertainty in $4G^E$ ($x=0.5$): 1.0 kcal/mol

This mixture has only been investigated by means of the nonequilibrium technique of Markov, Delimarskii, and Panchenko [46]. The recommended values have to be considered as an order of magnitude.

5.2.24 $\text{PbCl}_2(1-x), \text{CsCl}(x)$.

Cells: $\text{Pb}|\text{PbCl}_2, \text{CsCl}|\text{Cl}_2|\text{C}$. [44]

Tables: 5, 33

Parameters for the excess free energy (650 °C):

$$a = -7.3 \text{ kcal/mol}$$

$$b = -5.2 \text{ kcal/mol}$$

$$c = 0.0 \text{ kcal/mol}$$

Estimated uncertainty in $4G^E$ ($x=0.5$): 0.5 kcal/mol

This mixture was investigated by an equilibrium method. However, Hagemark and Hengstenberg [44] only investigated two compositions. The recommended values have been derived under the assumption that the parameter c is zero.

The excess entropies determined by Hagemark and Hengstenberg [44] seem to be too high. It is interesting to note that according to Hagemark and Hengstenberg [44] the excess entropy is given by $a' = 10.8 \text{ e.u.}$, $b' = -12.3 \text{ e.u.}$, $c' = 0.0 \text{ e.u.}$; this implies that the excess entropy is positive at the PbCl_2 side of the system, and becomes negative at the CsCl side.

5.2.25. $\text{PbCl}_2(1-x)$, $\text{CaCl}_2(x)$.

Cells: $\text{Pb}|\text{PbCl}_2, \text{CaCl}_2|\text{Cl}_2|\text{C}$. [45]
Tables: 5, 34

Parameters for the excess free energy (650 °C):

$$\begin{aligned}a &= 0.6 \text{ kcal/mol} \\b &= -2.8 \text{ kcal/mol} \\c &= 0.0 \text{ kcal/mol}\end{aligned}$$

Estimated uncertainty in $4G^E$ ($x=0.5$): 0.5 kcal/mol

Lantratov and Alabyshev [45] used an equilibrium method for the investigation of this mixture. Only two compositions were studied. The recommended parameters have been determined with the assumption that the parameter c is zero.

5.2.26. $\text{PbCl}_2(1-x)$, $\text{SrCl}_2(x)$.

Cells: $\text{Pb}|\text{PbCl}_2, \text{SrCl}_2|\text{Cl}_2|\text{C}$. [45]
Tables: 5, 35

Parameters for the excess free energy (650 °C):

$$\begin{aligned}a &= 1.3 \text{ kcal/mol} \\b &= -1.6 \text{ kcal/mol} \\c &= 0.0 \text{ kcal/mol}\end{aligned}$$

Estimated uncertainty in $4G^E$ ($x=0.5$): 0.4 kcal/mol

Lantratov and Alabyshev [45] used an equilibrium method for the investigation of this mixture; only two compositions were studied. The recommended parameters have been determined with the assumption that the parameter c is zero.

5.2.27. $\text{PbCl}_2(1-x)$, $\text{BaCl}_2(x)$.

Cells: $\text{Pb}|\text{PbCl}_2, \text{BaCl}_2|\text{Cl}_2|\text{C}$. [45]
Tables: 5, 36

Parameters for the excess free energy (650 °C):

$$\begin{aligned}a &= -0.7 \text{ kcal/mol} \\b &= -3.0 \text{ kcal/mol} \\c &= 0.0 \text{ kcal/mol}\end{aligned}$$

Estimated uncertainty in $4G^E$ ($x=0.5$): 0.2 kcal/mol

Lantratov and Alabyshev [45] used an equilibrium cell for the investigation of this mixture; only two compositions were studied. The recommended values have been determined with the assumption that the parameter c is zero.

5.2.28 $\text{PbCl}_2(1-x)$, $\text{ZnCl}_2(x)$.

Cells: $\text{Pb}|\text{PbCl}_2, \text{ZnCl}_2|\text{Cl}_2|\text{C}$. [50]
 $\text{C}|\text{Cl}_2|\text{PbCl}_2|\text{Pb}|\text{PbCl}_2(1-x),$
 $\text{ZnCl}_2(x)|\text{Cl}_2|\text{C}$. [51]
Tables: 5, 37
Figure: 6e

Parameters for the excess free energy:

$$\begin{aligned}a &= -1.65 \text{ kcal/mol} \\b &= 1.15 \text{ kcal/mol} \\c &= 0.00 \text{ kcal/mol}\end{aligned}$$

Estimated uncertainty in $4G^E$ ($x=0.5$) 0.2 kcal/mol

Wachter and Hildebrand [50] and Nakamura and Brenet [51] have worked with equilibrium cells. The two cells are essentially the same. However, the cell of Nakamura and Brenet [51] has the advantage that E° and E are already subtracted in the actual measurement and the recommended values for the excess free energy were determined from the data of this study accordingly. The values of Wachter and Hildebrand [50] differ slightly from these values (fig. 6e).

The excess entropy has been estimated from the data of Wachter and Hildebrand [50]. The data in the $s_{\text{PbCl}_2}^E/x^2$ versus x plot are scattered. A reasonable estimate for the excess entropy of this mixture is $a'=1.5$ e.u. and $b'=c'=0.0$ e.u., with an uncertainty estimate of 0.5 e.u.

5.2.29. $\text{PuCl}_3(1-x)$, $\text{NaCl}(x)$, and $\text{PuCl}_3(1-x)$, $\text{KCl}(x)$.

Cells: $\text{Pu}|\text{PuCl}_3, \text{NaCl}|\text{Cl}_2|\text{C}$. [54]
 $\text{Pu}|\text{PuCl}_3, \text{KCl}|\text{Cl}_2|\text{C}$. [53]

These cells have been measured by Benz and Leary [54] and by Benz [53]. Due to the high melting point of PuCl_3 the cell $\text{Pu}|\text{PuCl}_3|\text{Cl}_2|\text{C}$ could not be measured and the method used by Benz and Leary [54] and by Benz [53] for the determination of the E° is questionable. Excess properties for the mixtures mentioned above have therefore not been calculated.

5.2.30. $\text{ZnCl}_2(1-x)$, $\text{LiCl}(x)$.

Cells: $\text{Zn}|\text{ZnCl}_2, \text{LiCl}|\text{Cl}_2|\text{C}$. [58]
Tables: 6, 38
Figure: 7a

Parameters for the excess free energy (550 °C):

$$\begin{aligned}a &= 2.9 \text{ kcal/mol} \\b &= -1.3 \text{ kcal/mol} \\c &= 0.0 \text{ kcal/mol}\end{aligned}$$

Estimated uncertainty in $4G^E$ ($x=0.5$): 1.5 kcal/mol

Markov and Volkov [58] have measured this cell by means of the decomposition potential method (nonequilibrium method). Table 6 shows that their E° values deviate strongly from the E° values obtained by equilibrium methods.

The excess free energy of the mixture ZnCl_2 , LiCl has been determined from the Markov and Volkov [58] data under the assumption that cancellation errors is most probable at the ZnCl_2 side of the

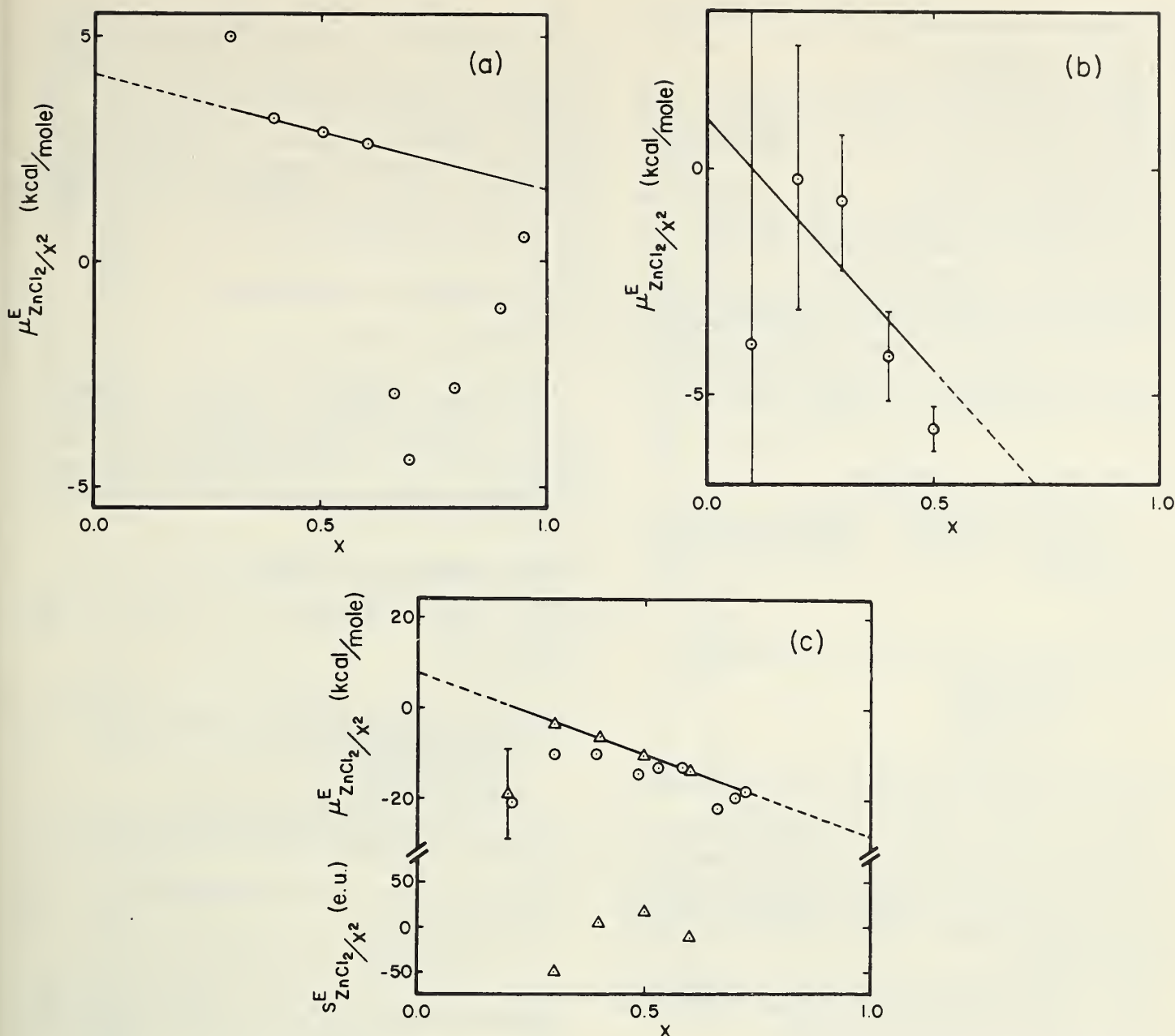


FIGURE 7. Experimental values of $\mu_{\text{ZnCl}_2}^E/x^2$ and $s_{\text{ZnCl}_2}^E/x^2$ in molten binary chloride mixtures. The limits of uncertainty and the solid lines are the result of the present analysis.

- a. ZnCl_2 , LiCl
 \odot Markov and Volkov [58], 550 °C
b. ZnCl_2 , NaCl
 \odot Lantratov, Alabyshev [59]
— — — Dijkhuis, Ketelaar [85]
c. ZnCl_2 , KCl
 \odot Markov, Volkov [60].
 \triangle Lantratov, Alabyshev [59]

system. The recommended data are no better than an order of magnitude.

5.2.31. $\text{ZnCl}_2(1-x)$, $\text{NaCl}(x)$.

Cells: $\text{Zn}|\text{ZnCl}_2, \text{NaCl}|\text{Cl}_2|\text{C}$. [59]
 $\text{W}|\text{Zn}|\text{ZnCl}_2, \text{NaCl}|\text{glass}|\text{ZnCl}_2(x=0.6),$
 $\text{NaCl}(x=0.4)|\text{Zn}|\text{W}$. [85]

Tables: 6, 39

Figure: 7b

Parameters for the excess free energy (600 °C):

$$a = -4.37 \text{ kcal/mol}$$

$$b = -5.54 \text{ kcal/mol}$$

$$c = 0.00 \text{ kcal/mol}$$

Estimated uncertainty in $4G^E$ ($x=0.5$): 0.4 kcal/mol

Difficulties involved in measuring the equilibrium cell $\text{Zn}|\text{ZnCl}_2|\text{Cl}_2|\text{C}$ have been discussed in section 5.1.9. It has to be concluded from this discussion

that appreciable systematic errors are involved in the excess properties as derived from the Lantratov and Alabyshev [59] data.

Dijkhuis and Ketelaar [85] have bypassed some of the experimental difficulties involved in ZnCl_2 formation cells by using glass as a cation selective membrane (sec. 5.1.15).

In such cells the mixture was completely closed to the atmosphere; the use of the $\text{Cl}_2|\text{C}$ electrode was unnecessary so that the vapor pressure of the mixtures did not influence the emfs.

Inspection of figure 7b shows that the values determined from the formation cells [59] and those from cells with glass as a cation selective membrane are in good agreement. It would appear that some fortunate cancellations of errors occurs in the studies with the formation cells [59].

5.2.32. $\text{ZnCl}_2(1-x)$, $\text{KCl}(x)$.

Cells: $\text{Zn}|\text{ZnCl}_2, \text{KCl}|\text{Cl}_2|\text{C}$. [60] Nonequilibrium
 $\text{Zn}|\text{ZnCl}_2, \text{KCl}|\text{Cl}_2|\text{C}$. [59] Equilibrium.

Tables: 6, 40

Figure: 7c

Parameters for the excess free energy (550 °C):

$$a = -10 \text{ kcal/mol}$$

$$b = -18 \text{ kcal/mol}$$

$$c = 0 \text{ kcal/mol}$$

Estimated uncertainty in $4G^E$ ($x=0.5$): 2 kcal/mol

The two kinds of cells have already been discussed in sections 5.2.30 and 5.2.31. It was noted that while appreciable systematic errors are present in these studies, the excess properties, derived from these two different kinds of cells are in reasonable agreement.

The recommended values for the excess free energy have been calculated from the equilibrium data of Lantratov and Alabyshev [59].

5.2.33. $\text{ZnCl}_2(1-x)$, $\text{RbCl}(x)$.

Cells: $\text{Zn}|\text{ZnCl}_2, \text{RbCl}|\text{Cl}_2|\text{C}$. [60, 61]
 Tables: 6, 41

These systems have been studied only by a nonequilibrium technique (Markov and Volkov [60] and Markov [61]). The excess free energy has been estimated from the most recent data [60]. The results, graphed as $\mu_{\text{ZnCl}_2}^E/x^2$ versus x , are quite scattered. The estimated values of the parameters a and b are at 550 °C: $a = -19$ kcal/mol; $b = -9$ kcal/mol, $c = 0$ kcal/mol. The uncertainty in these parameters may be as high as 5 kcal/mol.

5.2.34. $\text{ZnCl}_2(1-x)$, $\text{CsCl}(x)$.

Cells: $\text{Zn}|\text{ZnCl}_2, \text{CsCl}|\text{Cl}_2|\text{C}$. [62]
 Tables: 6, 42

Markov and Volkov [62] investigated this mixture by a nonequilibrium technique. The errors involved are appreciable in this method and have been discussed in preceding sections (5.2.32, 5.2.33). The results, in the $\mu_{\text{ZnCl}_2}^E/x^2$ versus x plot, are too scattered to enable an accurate determination of the excess free energy. By assuming regular solution behavior, the order of magnitude of the excess free energy is approximated as: $a = -15$ kcal/mol and $b = c = 0$ kcal/mol.

5.2.35. $\text{ZnCl}_2(1-x)$, $\text{BaCl}_2(x)$.

Cells: $\text{Zn}|\text{ZnCl}_2, \text{BaCl}_2|\text{Cl}_2|\text{C}$. [59]

Lantratov and Alabyshev [59] have studied this system under equilibrium conditions. Systematic errors are present in their measurement. It is reported [59] that the excess free energy of the mixture is negative, and less negative than for the mixture $\text{ZnCl}_2, \text{NaCl}$ (sec. 5.2.31).

5.2.36. $\text{AgBr}(1-x)$, $\text{LiBr}(x)$.

Cells: $\text{Ag}|\text{AgBr}, \text{LiBr}|\text{Br}_2|\text{C}$. [63]

Tables: 7, 43

Figure: 8a

Parameters for the excess free energy (550 °C):

$$a = 1.8 \text{ kcal/mol}$$

$$b = 0.0 \text{ kcal/mol}$$

$$c = 0.0 \text{ kcal/mol}$$

Estimated uncertainty in $4G^E$ ($x=0.5$): 0.15 kcal/mol

Parameters for the excess entropy (550 °C):

$$a' = -0.45 \text{ e.u.}$$

$$b' = 0.45 \text{ e.u.}$$

$$c' = 0.00 \text{ e.u.}$$

Estimated uncertainty in $4S^E$ ($x=0.5$): 0.15 e.u.

Salstrom and Hildebrand [63] used an equilibrium cell for this system. Air and hydrolysis products were removed with a stream of dry hydrogen bromide in the pretreatment of the salts in the molten state. As already noted (sec. 5.1.10) the results of this study are of high quality.

One composition, $x=0.89$, was not included for the excess entropy calculations since the investigation of this composition was restricted to a relatively small temperature range.

5.2.37. $\text{AgBr}(1-x)$, $\text{NaBr}(x)$.

Cells: $\text{Ag}|\text{AgBr}, \text{NaBr}|\text{Br}_2|\text{C}$. [67]

Tables: 7, 44

Figure: 8b

Parameters for the excess free energy (600 °C):

$$a = 1.05 \text{ kcal/mol}$$

$$b = 0.00 \text{ kcal/mol}$$

$$c = 0.00 \text{ kcal/mol}$$

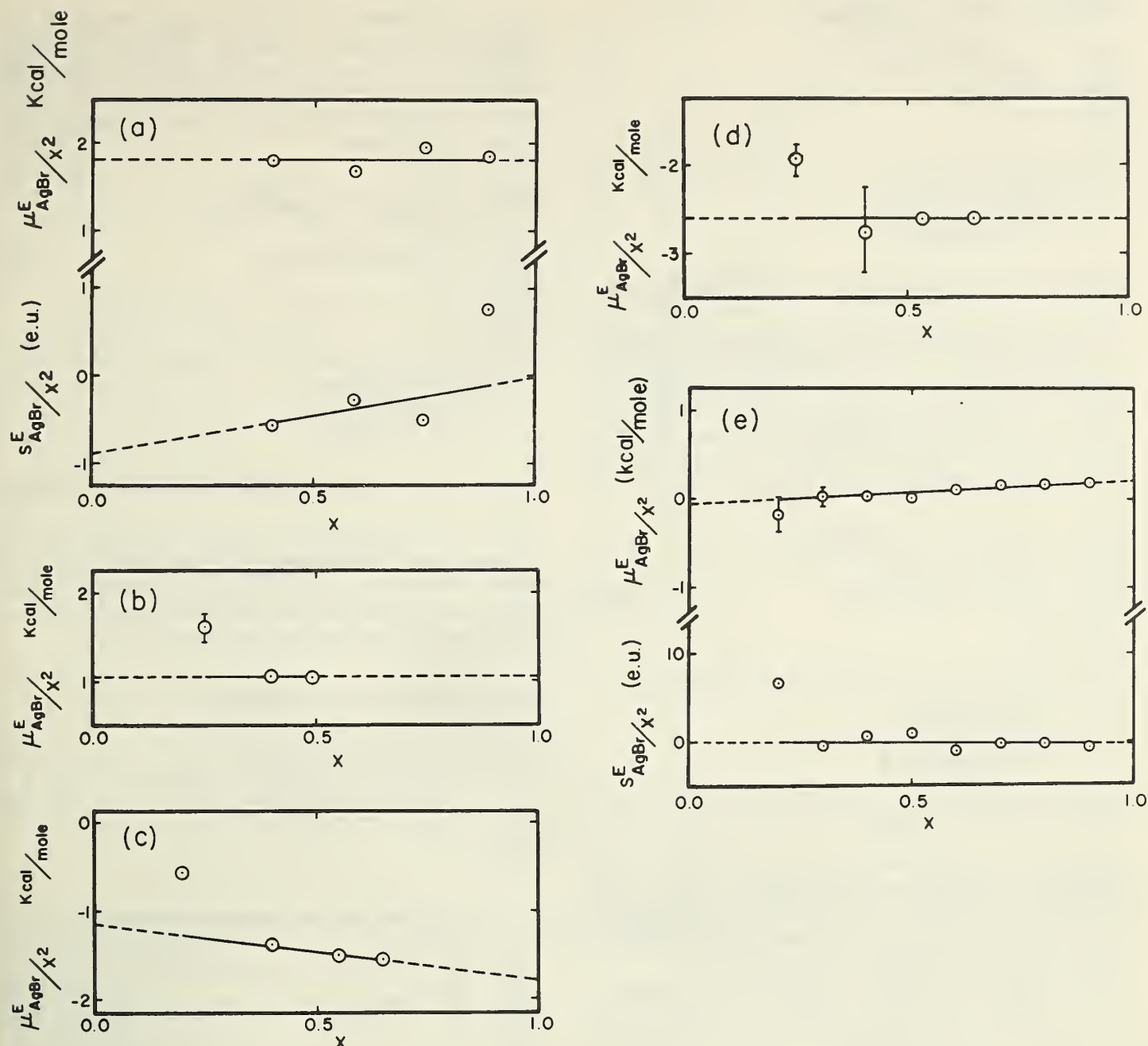


FIGURE 8. Experimental values of μ_{AgBr}^E/x^2 and S_{AgBr}^E/x^2 in molten binary bromide mixtures. The limits of uncertainty and the solid lines are the result of the present analysis.

- a. AgBr, LiBr
 ○ Salstrom and Hildebrand [63], 550 °C
- b. AgBr, NaBr
 ○ Salstrom [67], 600 °C
- c. AgBr, KBr
 ○ Salstrom [68], 600 °C
- d. AgBr, RbBr
 ○ Salstrom [65], 550 °C
- e. AgBr, PbBr₂
 ○ Salstrom [65], 550 °C

Estimated uncertainty in $4G^E$ ($x=0.5$): 0.1 kcal/mol

Salstrom [67] used the same experimental procedure for these cells as for the cells Ag|AgBr, LiBr|Br₂|C (sec. 5.2.36). As noted in section 5.1.10, this formation cell has been studied under equilib-

rium conditions.

Inspection of table 44 shows that the reported data only allow an estimate for the excess entropy. The values thus approximated are: $a'=1.8$ e.u., $b'=c'=0.0$ e.u., with an uncertainty in $4S^E$ ($x=0.5$) of 0.5 e.u.

5.2.38. AgBr(1-x), KBr(x).

Cells: Ag|AgBr, KBr|Br₂|C. [68]
Tables: 7, 45
Figure: 8c

Parameters for the excess free energy (600 °C):

$$\begin{aligned}a &= -1.45 \text{ kcal/mol} \\b &= -0.30 \text{ kcal/mol} \\c &= 0.00 \text{ kcal/mol}\end{aligned}$$

Estimated uncertainty in $4G^E(x=0.5)$: 0.10 kcal/mol

The above mentioned cell has been investigated by Salstrom [68]. The experimental procedures, essentially, were the same as in the studies of the related systems: Ag|AgBr, LiBr|Br₂|C [63] (sec. 5.2.36) and Ag|AgBr, NaBr|Br₂|C [67] (sec. 5.2.37).

Inspection of table 45 shows that the excess entropy of this mixture is nearly zero.

5.2.39. AgBr(1-x), RbBr(x).

Cells: Ag|AgBr, RbBr|Br₂|C. [65]
Tables: 7, 46
Figure: 8d

Parameters for the excess free energy (550 °C):

$$\begin{aligned}a &= -2.6 \text{ kcal/mol} \\b &= 0.0 \text{ kcal/mol} \\c &= 0.0 \text{ kcal/mol}\end{aligned}$$

Estimated uncertainty in $4G^E(x=0.5)$: 0.2 kcal/mol

The cell was studied by Salstrom [65], using equilibrium techniques. Inspection of figure 8d suggests an asymmetrical free energy of mixing but the range of compositions studied was insufficient to determine the asymmetry quantitatively.

The excess entropy data suggest a small negative excess entropy for this mixture ($a' = -0.5$ e.u., $b' = c' = 0.0$ e.u.); the data are rather scattered and the result is at best qualitative.

5.2.40. AgBr(1-x), PbBr₂(x).

Cells: Ag|AgBr, PbBr₂|Br₂|C. [61]
Tables: 7, 47
Figure: 8e

Parameters for the excess free energy (550 °C)

$$\begin{aligned}a &= 0.05 \text{ kcal/mol} \\b &= 0.15 \text{ kcal/mol} \\c &= 0.00 \text{ kcal/mol}\end{aligned}$$

Estimated uncertainty in $4G^E(x=0.5)$: 0.05 kcal/mol

Parameters for the excess entropy (500 °C):
 $a' = b' = c' = 0$ e.u.

Estimated uncertainty in $4S^E(x=0.5)$: 0.5 e.u.

The equilibrium properties of this cell have been discussed in section 5.1.10. The Salstrom emf data [61] show near ideality for this mixture. Although the entropy data (table 47 and figure 8e) are scattered, it is evident that the excess entropy of this system is about zero.

5.2.41. CdBr₂(1-x), KBr(x).

Cells: Cd|CdBr₂, KBr|Br₂|C. [69]
Table: 48
Figure: 9

Parameters for the excess free energy (597.5 °C):

$$\begin{aligned}a &= -8.3 \text{ kcal/mol} \\b &= -6.6 \text{ kcal/mol} \\c &= 0.0 \text{ kcal/mol}\end{aligned}$$

Estimated uncertainty in $4G^E(x=0.5)$: 1.0 kcal/mol

The cell Cd|CdBr₂|Br₂|C was investigated by Lantratov and Shevlyakova [69] and has been discussed in section 5.1.11. As noted, further studies of the cell appear desirable. The parameters for the excess free energy are estimates only.

5.2.42. PbBr₂(1-x), NaBr(x).

Cells: Pb|PbBr₂, NaBr|Br₂|C. [73]
W|Pb|PbBr₂, NaBr|glass|PbBr₂($x=0.6$).
NaBr($x=0.4$)|Br₂|C. [33, 34]
Table: 9, 49
Figure: 10a

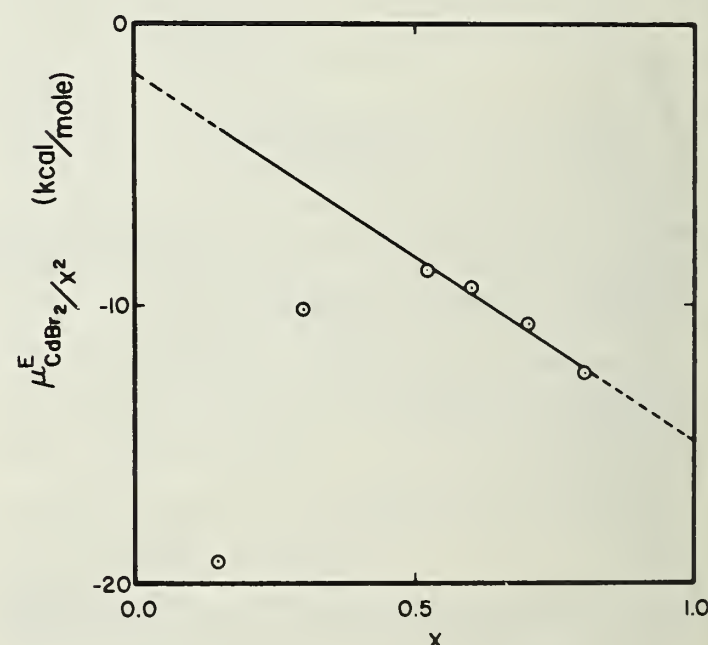


FIGURE 9. Experimental values of $\mu_{\text{CdBr}_2}^E/x^2$ in the molten binary mixture CdBr₂, KBr(x). The solid line is the result of the present analysis.

○ Lantratov and Shevlyakova [69], 597.5 °C

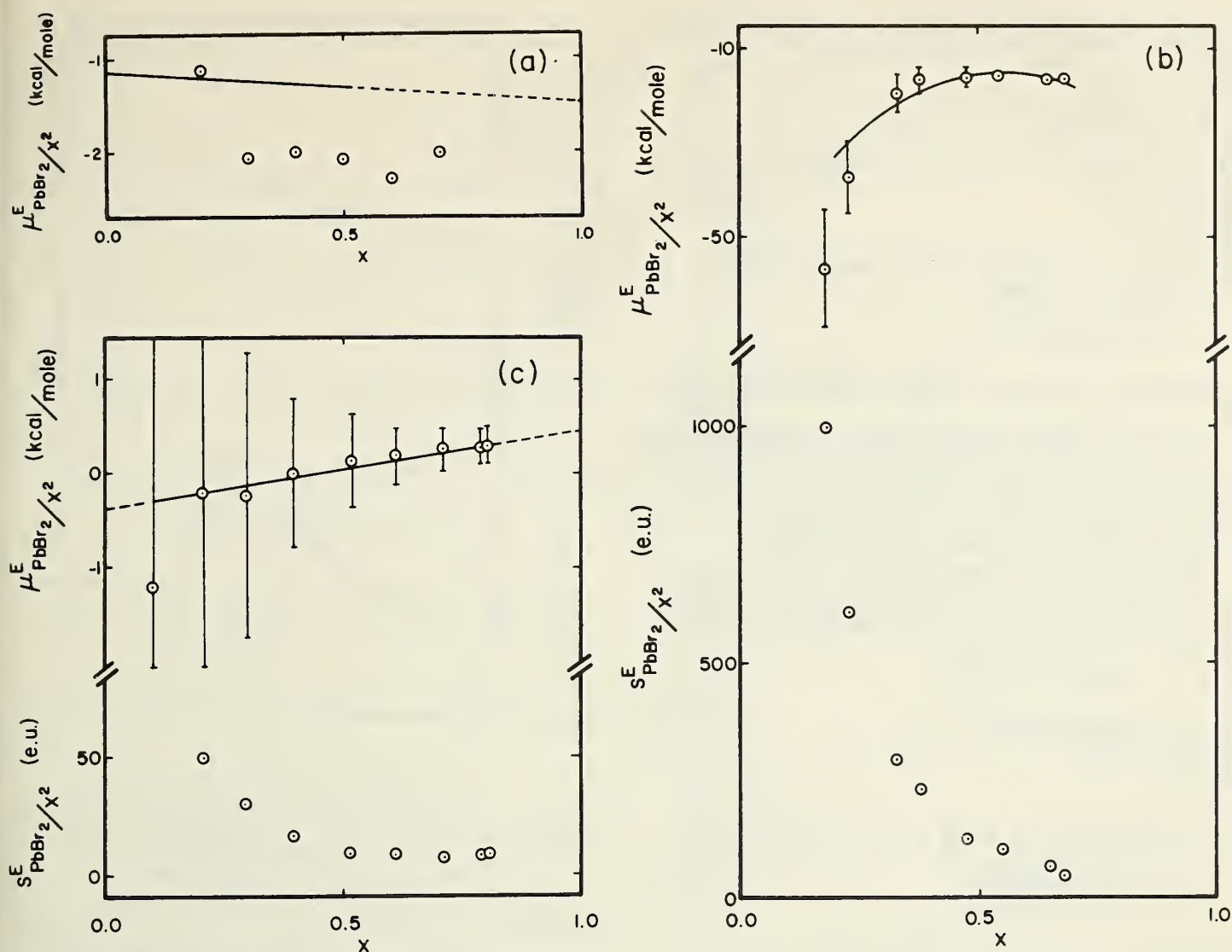


FIGURE 10. Experimental values of $\mu_{\text{PbBr}_2}^E/x^2$ and $S_{\text{PbBr}_2}^E/x^2$ in molten binary bromide mixtures. The limits of uncertainty and the solid lines are the result of the present analysis.

- a. PbBr_2 , NaBr
 ○ Lantratov and Shevlyakova [73], 589 °C
 b. PbBr_2 , KBr
 ○ Lantratov and Shevlyakova [71], 550 °C
 c. PbBr_2 , ZnBr_2
 ○ Salstrom [70], 500 °C

Parameters for the excess free energy (589 °C):

$$\begin{aligned} a &= -1.31 \text{ kcal/mol} \\ b &= -0.16 \text{ kcal/mol} \\ c &= 0.00 \text{ kcal/mol} \end{aligned}$$

Estimated uncertainty in $G^E(x=0.5)$: 0.2 kcal/mol

The cell $\text{Pb}|\text{PbBr}_2|\text{Br}_2|\text{C}$ was discussed in section 5.1.12. Inspection of table 9 shows that there is an appreciable difference between the E° values of Lantratov and Shevlyakova [73] and from the other investigations.

Dijkhuis and Ketelaar [33, 34] determined the excess free energy of this mixture with a cell in which glass functions as a cation selective membrane. Taking due cognizance of the uncertainties in the E° value of the formation cell [73], the results

of these two investigations are in surprisingly good accord.

5.2.43. $\text{PbBr}_2(1-x)$, $\text{KBr}(x)$.

Cells: $\text{Pb}|\text{PbBr}_2, \text{KBr}|\text{Br}_2|\text{C}$.

Tables: 9, 50

Figure: 10b

[71]

Parameters for the excess free energy (550 °C):

$$\begin{aligned} a &= -27.5 \text{ kcal/mol} \\ b &= 32.5 \text{ kcal/mol} \\ c &= -50.0 \text{ kcal/mol} \end{aligned}$$

Estimated uncertainty in $4G^E(x=0.5)$: 0.7 kcal/mol

The experimental uncertainties involved in the

cell of Lantratov and Shevlyakova [71] have been discussed in sections 5.1.12 and 5.2.42.

5.2.44. $\text{PbBr}_2(1-x), \text{ZnBr}_2(x)$.

Cells: $\text{Pb}|\text{PbBr}_2(1-x), \text{ZnBr}_2(x)|\text{Br}_2|\text{C}$. [70]

Tables: 9, 51

Figure: 10c

Parameters for the excess free energy (500 °C):

$$a = 0.05 \text{ kcal/mol}$$

$$b = 0.40 \text{ kcal/mol}$$

$$c = 0.00 \text{ kcal/mol}$$

Estimated uncertainty in $4G^E(x=0.5)$: 0.2 kcal/mol

As seen in table 9, the E° values of Salstrom [70] for cells such as $\text{Pb}|\text{PbBr}_2|\text{Br}_2|\text{C}$ are in good agreement with the results from thermochemical data. This is support for the recommendation of the excess free energy as an accurate result.

The temperature dependence of the Salstrom E° values does not agree with the thermochemical data, so that the excess entropies may be too high.

5.2.45. $\text{AgI}(1-x), \text{KI}(x)$.

Cells: $\text{Ag}|\text{AgI}, \text{KI}|\text{I}_2|\text{C}$. [75]

Tables: 10, 52

Figure: 11

Parameters for the excess free energy (600 °C):

$$a = -1.95 \text{ kcal/mol}$$

$$b = 1.20 \text{ kcal/mol}$$

$$c = 0.1 \text{ kcal/mol}$$

Estimated uncertainty in $4G^E(x=0.5)$: 0.2 kcal/mol

Parameters for the excess entropy (600 °C):

$$a' = 0.0 \text{ e.u.}$$

$$b' = 3.7 \text{ e.u.}$$

$$c' = 0.0 \text{ e.u.}$$

Estimated uncertainty in $4S^E(x=0.5)$: 0.2 e.u.

Sternberg, Adorian, and Galasiu [74, 75, 76] devised a reversible iodine electrode (sec. 5.1.13). The E° value agrees well with the thermochemical value, so that the excess properties may be accepted as quite reliable.

The excess entropies were calculated from the equations for the temperature dependence of the emf data as published by these investigators [75].

5.2.46. $\text{CdI}_2(1-x), \text{NaI}(x)$.

Cells: $\text{W}|\text{Cd}|\text{CdI}_2, \text{NaI}|\text{glass}|\text{CdI}_2(x=0.5), \text{NaI}(x=0.5)|\text{Cd}|\text{W}$. [33, 34]

Parameters for the excess free energy (600 °C):

$$a = -2.28 \text{ kcal/mol}$$

$$b = -1.89 \text{ kcal/mol}$$

$$c = 0.00 \text{ kcal/mol}$$

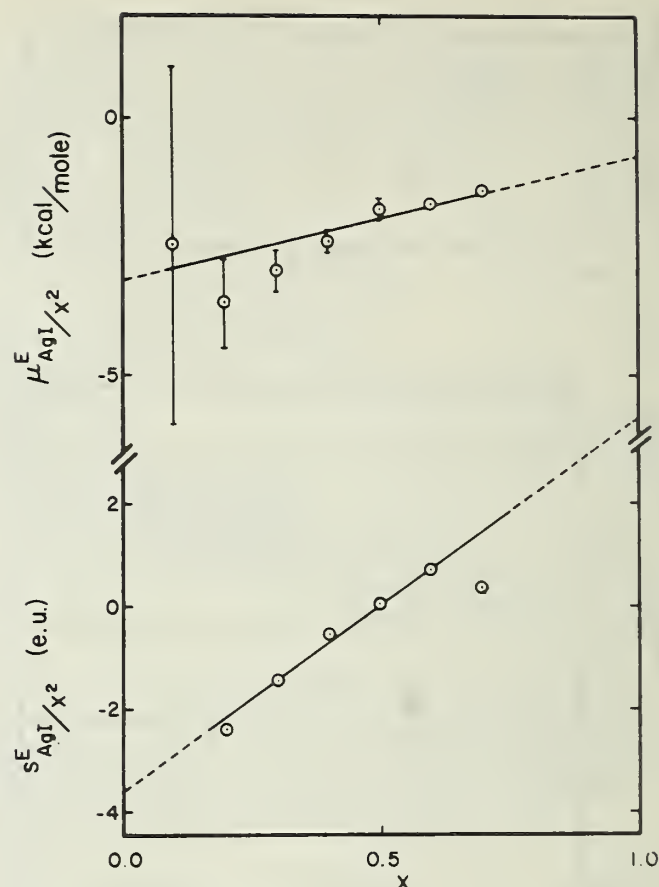


FIGURE 11. Experimental values of μ_{AgI}^E/x^2 in the molten binary mixture $\text{AgI}, \text{KI}(x)$. The solid line and the limits of uncertainty are the result of the present analysis.

⊙ Sternberg, Adorian, Galasiu [75], 600 °C

Estimated uncertainty in $4G^E(x=0.5)$: 0.5 kcal/mol

Dijkhuis and Ketelaar [33, 34] have studied this mixture with cells having glass as cation-selective membranes (sec. 5.1.15). The technique is discussed in section 5.1.15.

5.2.47. $\text{PbI}_2(1-x), \text{NaI}(x)$.

Cells: $\text{W}|\text{Pb}|\text{PbI}_2, \text{NaI}|\text{glass}|\text{PbI}_2(x=0.6), \text{NaI}(x=0.4)|\text{Pb}|\text{W}$. [33, 34]

Parameters for the excess free energy (600 °C):

$$a = -0.46 \text{ kcal/mol}$$

$$b = -0.14 \text{ kcal/mol}$$

$$c = 0.00 \text{ kcal/mol}$$

Estimated uncertainty in $4G^E(x=0.5)$: 0.2 kcal/mol

Dijkhuis and Ketelaar [33, 34] have studied this mixture with cells having glass as a cation-selective membrane (sec. 5.1.15).

5.2.48. $\text{AgBr}(1-x), \text{AgCl}(x)$.

Cells: $\text{Ag}|\text{AgBr}, \text{AgCl}|\text{Br}_2|\text{C}$. [64]

Tables: 7, 53

Figure: 12

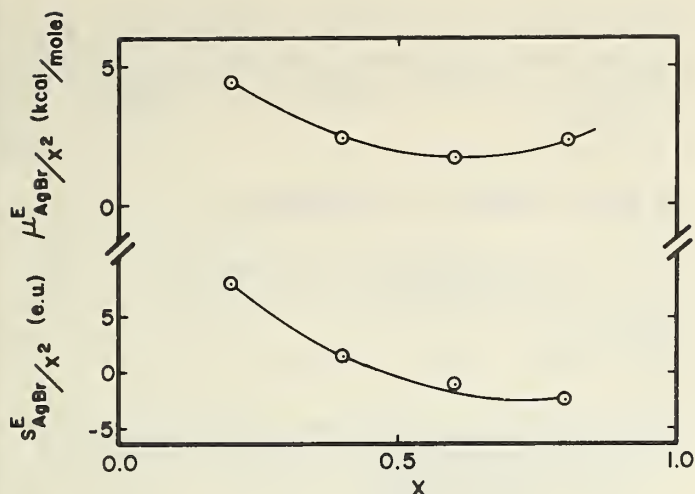


FIGURE 12. Experimental values of μ_{AgBr}^E/x^2 and S_{AgBr}^E/x^2 in the molten binary mixture AgBr, AgCl(x). The solid lines are the result of the present analysis.

○ Murgulescu, Marchidan [64], 600 °C

Parameters for the excess free energy (600 °C):

$$\begin{aligned} a &= 3.25 \text{ kcal/mol} \\ b &= -4.43 \text{ kcal/mol} \\ c &= 5.22 \text{ kcal/mol} \end{aligned}$$

Estimated uncertainty in $4G^E$ ($x=0.5$): 0.1 kcal/mol

Parameters for the excess entropy (600 °C):

$$\begin{aligned} a' &= 2.63 \text{ e.u.} \\ b' &= -15.06 \text{ e.u.} \\ c' &= 13.07 \text{ e.u.} \end{aligned}$$

Estimated uncertainty in $4S^E$ ($x=0.5$): 0.2 e.u.

Murgulescu and Marchidan [64] used equilibrium techniques (sec. 5.1.10) and the E° value is in excellent agreement with thermochemical data (sec. 5.1.10); the random error is low. It therefore appears that the curvatures in the μ_{AgBr}^E/x^2 versus x graph and the corresponding excess entropy plot are physically significant.

5.2.49. AgI(1-x), AgCl(x).

Cells: Ag|AgI, AgCl|I₂|C.

Table: 54

Figure: 13a

Parameters for the excess free energy (600 °C):

$$\begin{aligned} a &= 0.45 \text{ kcal/mol} \\ b &= 0.00 \text{ kcal/mol} \\ c &= 0.00 \text{ kcal/mol} \end{aligned}$$

Estimated uncertainty in $4G^E$ ($x=0.5$): 0.15 kcal/mol

Parameters for the excess entropy (600 °C):

$$\begin{aligned} a' &= -0.57 \text{ e.u.} \\ b' &= 3.07 \text{ e.u.} \\ c' &= 0.00 \text{ e.u.} \end{aligned}$$

Estimated uncertainty in $4S^E$ ($x=0.5$): 0.2 e.u.

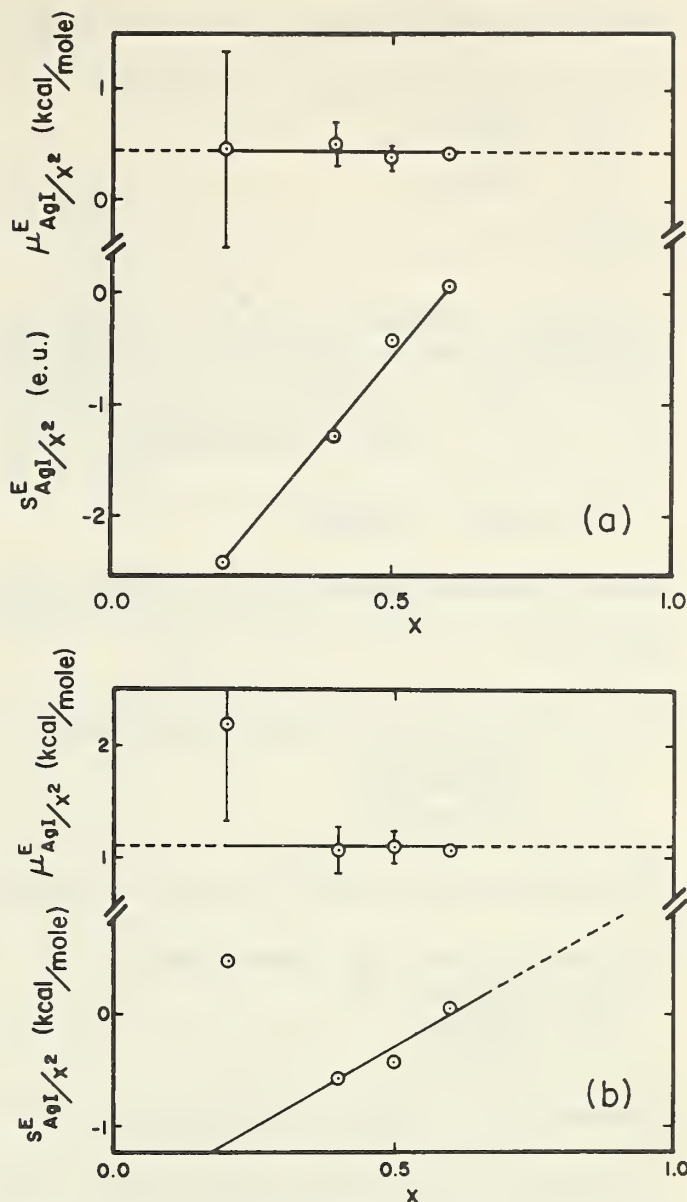


FIGURE 13. Experimental values of μ_{AgI}^E/x^2 and S_{AgI}^E/x^2 in molten binary mixtures. The solid lines are the result of the present analysis.

a. AgI, AgCl

○ Sternberg, Adorian, Galasiu [76], 600 °C

b. AgI, AgBr

○ Sternberg, Adorian, Galasiu [76], 600 °C

Sternberg, Adorian and Galasiu [76] studied this mixture using the conventional silver electrode and a reversible iodine electrode of their design (sec. 5.1.13). The correspondence between the experimental E° value and the thermochemical values is good.

5.2.50 AgI(1-x), AgBr(x).

Cells: Ag|AgI, AgBr|I₂|C.

Table: 55

Figure 13b

Parameters for the excess free energy (600 °C):

$$\begin{aligned} a &= 1.10 \text{ kcal/mol} \\ b &= 0.00 \text{ kcal/mol} \\ c &= 0.00 \text{ kcal/mol} \end{aligned}$$

Estimated uncertainty in $4G^E$ ($x=0.5$): 0.2 kcal/mol

Parameters for the excess entropy (600 °C):

$$\begin{aligned} a' &= -0.30 \text{ e.u.} \\ b' &= 1.45 \text{ e.u.} \\ c' &= 0.00 \text{ e.u.} \end{aligned}$$

Estimated uncertainty in $4S^E$ ($x=0.5$): 0.2 e.u.

Sternberg, Adorian and Galasiu [76] investigated this mixture using the same technique as for the AgI, KI (sec. 5.2.45) and AgI, AgCl (sec. 5.2.49) mixtures. As already noted (sec. 5.1.13) these results are clearly of high quality.

5.2.51. KBr(1-x), KCl(x).

Cells: C|Br₂|KBr|glass|KBr(1-x), KCl(x)|Br₂|C.

Table: 56

Figure: 14

Parameters for the excess free energy (800 °C):

$$\begin{aligned} a &= 0.50 \text{ kcal/mol} \\ b &= -0.55 \text{ kcal/mol} \\ c &= 0.00 \text{ kcal/mol} \end{aligned}$$

Estimated uncertainty in $4G^E$ ($x=0.5$): 0.1 kcal/mol

Parameters for the excess entropy (800 °C):

$$\begin{aligned} a' &= -0.89 \text{ e.u.} \\ b' &= 1.20 \text{ e.u.} \\ c' &= -2.33 \text{ e.u.} \end{aligned}$$

Estimated uncertainty in $4S^E$ ($x=0.5$): 0.2 e.u.

Ostvold [9] used a glass cation selective membrane for the determination of the excess properties of mixtures KBr, KCl. While the results

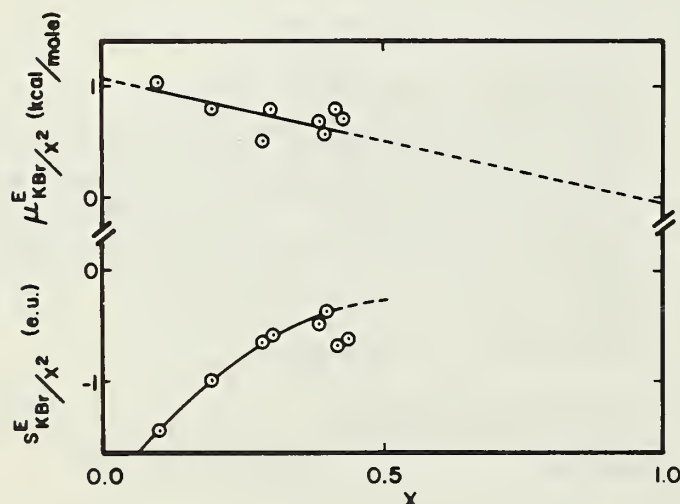


FIGURE 14. Experimental values of μ_{KBr}^E/x^2 and S_{KBr}^E/x^2 in the molten binary mixture KBr(1-x), KCl(x).
○ Ostvold [9], 800 °C

indicate that there is some curvature in the μ_{KBr}^E/x^2 versus x plot, the scatter in the data is such that the assumption of the straight line relationship seems justified.

5.2.52. NaBr(1-x), NaCl(x).

Cells: C|Br₂|NaBr|glass|NaBr(1-x), NaCl(x)|Br₂|C.

[9, 84]

Table: 57

Figure: 15

Parameters for the excess free energy (800 °C):

$$\begin{aligned} a &= 0.40 \text{ kcal/mol} \\ b &= -0.10 \text{ kcal/mol} \\ c &= 0.00 \text{ kcal/mol} \end{aligned}$$

Estimated uncertainty in $4G^E$ ($x=0.5$): 0.1 kcal/mol

Parameters for the excess entropy (800 °C):

$$\begin{aligned} a' &= -0.39 \text{ e.u.} \\ b' &= 0.33 \text{ e.u.} \\ c' &= -0.67 \text{ e.u.} \end{aligned}$$

Estimated uncertainty in $4S^E$ ($x=0.5$): 0.1 e.u.

Ostvold [9] and Sternberg and Herdlicka [84] both used glass cation-selective membranes for the investigations of this system. It is seen from figure 15 that the two investigations are in excellent accord. The Ostvold [9] data show a somewhat smaller scatter and were used for the determination of the parameters for the excess free energy.

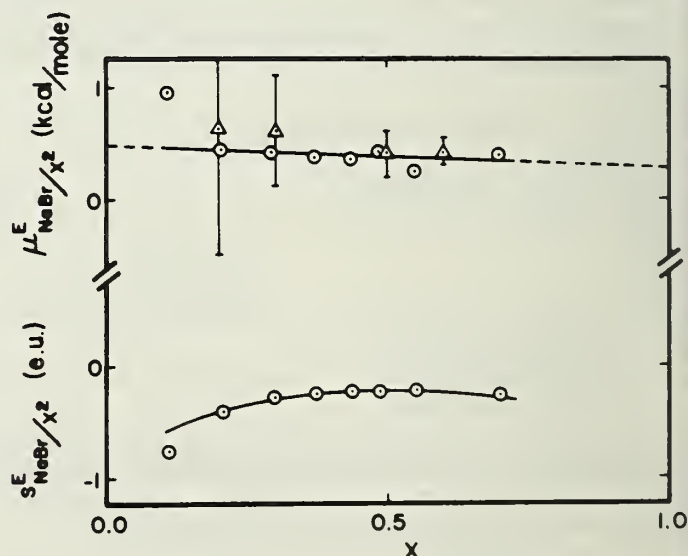


FIGURE 15. Experimental values of μ_{NaBr}^E/x^2 and S_{NaBr}^E/x^2 in the binary mixture NaBr(1-x), NaCl(x).
○ Ostvold [9], 800 °C
△ Sternberg, Herdlicka [84] 800 °C

5.2.53. $\text{PbBr}_2(1-x), \text{PbCl}_2(x)$.

Cells: $\text{Pb}|\text{PbBr}_2(1-x), \text{PbCl}_2(x)|\text{Br}_2|\text{C}$. [72]
Tables: 9, 58
Figure: 16

Parameters for the excess free energy (500 °C):
 $a = -2.6 \text{ kcal/mol}$
 $b = 0.0 \text{ kcal/mol}$
 $c = 0.0 \text{ kcal/mol}$

Estimated uncertainty in $4G^E(x=0.5)$: 0.5 kcal/mol

As noted elsewhere (table 9) the E° values of Salstrom and Hildebrand [72] are in accord with those of Hamer, Malmberg and Rubin [12] calculated from thermochemical data. The temperature-dependence observed by Salstrom and Hildebrand seems to be questionable. The $\mu_{\text{PbBr}_2}^E/x^2$ values are quite scattered and the excess free energy of this mixture seems to be appreciably negative.

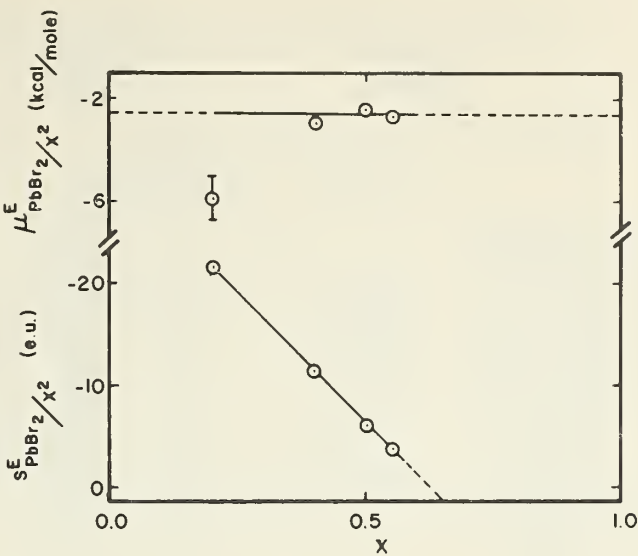


FIGURE 16. Experimental values of $\mu_{\text{PbBr}_2}^E/x^2$ and $s_{\text{PbBr}_2}^E/x^2$ in the molten binary mixture $\text{PbBr}_2(1-x), \text{PbCl}_2(x)$.
⊙ Salstrom, Hildebrand [72], 500 °C

6. Cumulative Table of Excess Free Energies

According to the previous analysis the parameters a , b , and c in the equation for the excess free energy of mixing,

$$G^E = x(1-x) (a + bx + cx^2),$$

have the following values:

Mixture	Temperature	Reference	$G^E = x(1-x) (a + bx + cx^2)$		
			a	b	c
	(°C)		kcal/mol	kcal/mol	kcal/mol
AgCl, LiCl(x).....		[20, 26]	2.1	0	0
AgCl, NaCl(x).....		[19, 25, 27]	0.8	0	0
AgCl, KCl(x).....	650	[22, 24]	-1.5	0.4	0
AgCl, PbCl ₂ (x).....	550	[23]	-0.15	.2	0
CdCl ₂ , NaCl(x).....	600	[33, 34, 36]	-4.45	-3.85	0
CdCl ₂ , KCl(x).....	600	[36]	-7.5	-10.7	0
CdCl ₂ , BaCl ₂ (x).....	600	[36]	-1.0	-8.8	0
CeCl ₃ , NaCl(x).....	800	[37]	-2.7	-13.6	9.3
CeCl ₃ , KCl(x).....	850	[37, 38]	-1.87	-31.75	20.48
CeCl ₃ , CaCl ₂ (x).....	850	[39]	4.80	-8.79	5.37
MgCl ₂ , LiCl(x).....	700	[40]	3.95	-5.75	0
MgCl ₂ , NaCl(x).....		[9, 38, 40, 41]	-4.80	-9.39	7.08
MgCl ₂ , KCl(x).....	800	[38, 40, 41]	-12.84	-11.88	12.96
CaCl ₂ , NaCl(x).....	850	[9]	-2.45	-0.45	0
SrCl ₂ , NaCl(x).....	850	[9]	-0.02	-1.92	1.03
BaCl ₂ , NaCl(x).....	850	[9]	.08	-0.04	0
PbCl ₂ , LiCl(x).....	600	[45, 46]	.45	-.55	0
PbCl ₂ , NaCl(x).....	600	[33, 34, 44,] [45, 46, 48]	-1.52	-.39	0
PbCl ₂ , KCl(x).....	600	[44, 45, 46, 49]	-5.0	.0	0

Mixture	Temperature	Reference	$G^E = x(1-x) (a + bx + cx^2)$		
			a	b	c
	(°C)		kcal/mol	kcal/mol	kcal/mol
PbCl ₂ , RbCl(x).....	600	[46]	-6.5	0	0
PbCl ₂ , CsCl(x).....	650	[44]	-7.3	-5.2	0
PbCl ₂ , CaCl ₂ (x).....	650	[45]	0.6	-2.8	0
PbCl ₂ , SrCl ₂ (x).....	650	[45]	1.3	-1.6	0
PbCl ₂ , BaCl ₂ (x).....	650	[45]	-0.7	-3.0	0
PbCl ₂ , ZnCl ₂ (x).....	500	[50, 51]	-1.65	1.15	0
ZnCl ₂ , LiCl(x).....	550	[58]	2.9	-1.3	0
ZnCl ₂ , NaCl(x).....	600	[59, 85]	-4.37	-5.54	0
ZnCl ₂ , KCl(x).....	550	[59, 60]	-10	-18	0
ZnCl ₂ , BaCl ₂		[59]	$0 \geq a \geq -4$		
AgBr, LiBr(x).....	550	[63]	1.8	0	0
AgBr, NaBr(x).....	600	[67]	1.05	0	0
AgBr, KBr(x).....	600	[68]	-1.45	-0.30	0
AgBr, RbBr(x).....	550	[65]	-2.6	0	0
AgBr, PbBr ₂ (x).....	550	[66]	0.05	.15	0
CdBr ₂ , KBr(x).....	597.5	[69]	-8.3	-6.6	0
PbBr ₂ , NaBr(x).....	589	[73]	-1.31	-0.16	0
PbBr ₂ , KBr(x).....	550	[71]	-27.5	32.5	-50.0
PbBr ₂ , ZnBr ₂ (x).....	500	[70]	0.05	0.40	0
AgI, KI(x).....	600	[75]	-1.95	1.20	.1
CdI ₂ , NaI.....	600	[33, 34]	-2.28	-1.89	0
PbI ₂ , NaI.....	600	[33, 34]	-0.46	-0.14	0
AgBr, AgCl(x).....	600	[64]	3.25	-4.43	5.22
AgI, AgCl(x).....	600	[76]	0.45	0	0
AgI, AgBr(x).....	600	[76]	1.15	0	0
KBr, KCl(x).....	800	[9]	0.50	-.55	0
NaBr, NaCl(x).....	800	[9, 84]	.40	-.10	0
PbBr ₂ , PbCl ₂ (x).....	500	[72]	-2.6	0	0

7. Tables of E° Values and Excess Properties for Individual Mixtures

TABLE 1a. $E^\circ(mV) = a + bt + ct^2$ for the cell $Ag|AgCl|Cl_2|C$
The parameters a , b , and c have been generated from literature values by a linear and a quadratic least-squares analysis.

a	$b \times 10^3$	$c \times 10^6$	Standard deviation (mV)	Temperature range (°C)	Reference
1026.5	-263.0	0	max. 2.0	530-920	[16]
1093.0	-484.9	173.2	0.5	455-900	[21]
1066.6	-372.8	72.4	.9	482-800	[19, 20]
1028.6	-275.4	0	.1	480-638	[22, 27]
1064.2	-330.7	0	1.5	476-628	[24, 25]
1042.6	-285.8	0	0.4	498-600	[23]
*1087.7	*-485.3	*204.7	.3	500-600	[11]

*Thermochemical data.

TABLE 1b. E° (mV) of the cell $\text{Ag}|\text{AgCl}|\text{Cl}_2|\text{C}$ at various temperatures ($^\circ\text{C}$) according to table 1a
(Extrapolated values are included.)

500°	550°	600°	700°	800°	900°	Standard deviation (mV)	Temperature range ($^\circ\text{C}$)	Reference
895.0	881.5	868.4	842.1	815.8	789.5	max. 2.0	530–920	[16]
893.9	878.7	864.5	838.5	816.0	796.9	0.5	455–900	[21]
898.3	883.4	869.0	841.1	814.7	789.8	.9	482–800	[19, 20]
890.9	877.2	863.4	835.9	808.3	780.7	.1	480–638	[22, 27]
898.8	882.3	865.8	832.7	799.7	766.6	1.5	476–628	[24, 25]
899.7	885.4	871.1	842.5	814.0	785.4	0.4	498–600	[23]
*896.0	*883.0	*870.0	*848.0	*826.0	*805.0	.3	500–600	[11]

*Thermochemical data.

TABLE 2a. E° (mV) = $a + bt + ct^2$ for the cell $\text{Be}|\text{BeCl}_2|\text{Cl}_2|\text{C}$
The parameters a , b and c have been generated from literature values by a linear and a quadratic least-squares analysis.

a	$b \times 10^3$	$c \times 10^6$	Standard deviation (mV)	Temperature range ($^\circ\text{C}$)	Reference
2264.0	–850.0	0	0	400–500	[28]
2170.5	–652.6	0	.6	410–550	[29]
*2369.3	*–450.0	*0	.4	450–550	[11]
*2324.8	*–804.7	*206.4	.1	326–626	[13]

*Thermochemical data.

TABLE 2b. E° (mV) of the cell $\text{Be}|\text{BeCl}_2|\text{Cl}_2|\text{C}$ at various temperatures ($^\circ\text{C}$) according to table 2a
(An extrapolated value is included).

450°	500°	550°	Standard deviation (mV)	Temperature range ($^\circ\text{C}$)	Reference
1881	1839	1796	0	400–500	[28]
1877	1844	1812	.6	410–550	[29]
*2167	*2144	*2122	.4	450–550	[11]
*2004.5	*1974.1	*1944.6	.1	326–626	[13]

*Thermochemical data.

TABLE 3a. $E^\circ (mV) = a + bt + ct^2$ for the cell $Cd|CdCl_2|Cl_2|C$
The parameters a , b , and c have been generated from literature values by a linear and a quadratic least-squares analysis.

a	$b \times 10^3$	$c \times 10^6$	Standard deviation (mV)	Temperature range ($^\circ C$)	Reference
1556.6	-148.8	-353.4	1.5	600-771	[35]
1669.6	-553.3	0	1.2	578-687	[36]

TABLE 3b. $E^\circ (mV)$ of the cell $Cd|CdCl_2|Cl_2|C$ at various temperatures ($^\circ C$) according to table 3a
(Extrapolated values are included)

600 $^\circ$	650 $^\circ$	700 $^\circ$	750 $^\circ$	Standard deviation (mV)	Temperature range ($^\circ C$)	Reference
1340.1	1310.6	1279.2	1246.2	1.5	600-771	[35]
1338	1310	1282	1255	1.2	578-687	[36]
*1331						

*Thermochemical data

TABLE 4a. $E^\circ (mV) = a + bt + ct^2$ for the cell $Mg|MgCl_2|Cl_2|C$
The parameters a , b , and c have been generated from literature values by a linear and a quadratic least-squares analysis.

a	$b \times 10^3$	$c \times 10^6$	Standard deviation (mV)	Temperature range ($^\circ C$)	Reference
4673.5	-5165.2	2980.0	2.8	704-799	[35]
3750.2	-2650.0	1325.2	1.5	718-770	[40]
2955.7	-658.7	44.9	0.0	726-1026	[13]

TABLE 4b. $E^\circ (mV)$ of the cell $Mg|MgCl_2|Cl_2|C$ at various temperatures ($^\circ C$) according to table 4a
(Extrapolated values are included.)

750 $^\circ$	800 $^\circ$	850 $^\circ$	900 $^\circ$	Standard deviation (mV)	Temperature range ($^\circ C$)	Reference
2475.8	2448.5	2436.1	2438.6	2.8	704-799	[35]
2508	2478	2455	2439	1.5	718-770	[40]
*2487.0	*2457.0	*2428.2	*2399.0	0.0	726-1026	[13]
.....	*2460					[11]

*Thermochemical data.

TABLE 5a. E° (mV) = $a + bt + ct^2$ for the cell $\text{Pb}|\text{PbCl}_2|\text{Cl}_2|\text{C}$
The parameters a , b , and c have been generated from literature values by a linear and a quadratic least-squares analysis.

a	$b \times 10^3$	$c \times 10^6$	Standard deviation (mV)	Temperature range (°C)	Reference
1578.2	-602.0	0	not reported	500-620	[44]
1524.8	-411.3	-177.8	1.7	553-809	[35]
1538.3	-527.7	0	1.0	532-681	[45]
1538.3	-527.7	0	1.0	550-600	[46, 47]
1635.7	-730.5	0	0.8	501-607	[49]
1581.5	-617.6	0	.7	499-582	[50]
1563.0	-533.5	0	not reported	not reported	[51]
1537.0	-533.5	0	1.0	527-634	[38]
*1551.0	*-560.0	*0	0	500-600	[11]
*1590.3	*-681.3	*102.0	.1	526-826	[13]

*Thermochemical data.

TABLE 5b. E° (mV) of the cell $\text{Pb}|\text{PbCl}_2|\text{Cl}_2|\text{C}$ at various temperatures (°C) according to table 5a
(Extrapolated values are included)

550°	600°	650°	700°	Standard deviation (mV)	Temperature range (°C)	Reference
1247	1217	1187	1157	not reported	500-600	[44]
1244.8	1214.0	1182.4	1149.8	1.7	553-809	[35]
1248	1222	1195	1169	1.0	532-681	[45]
1248	1218	1195	1169	1.0	550-600	[46, 47]
1234	1197	1161	1124	0.8	501-607	[49]
1242	1211	1180	1149	.7	499-582	[50]
1242	1213	1183	1154	not reported	not reported	[51]
1243.6	1216.9	1190.2	1163.6	1.0	527-634	[38]
*1243	*1215	0	500-600	[11]
*1246.5	*1218.2	*1190.6	*1163.4	.1	526-826	[13]

*Thermochemical data

TABLE 6a. E° (mV) = $a + bt + ct^2$ for the cell $\text{Zn}|\text{ZnCl}_2|\text{Cl}_2|\text{C}$
The parameters a , b , and c have been generated from literature values by a linear and a quadratic least-squares analysis.

a	$b \times 10^3$	$c \times 10^6$	Standard deviation (mV)	Temperature range ($^\circ\text{C}$)	Reference
1866	-530	0	not reported	not reported	[56]
1568.8	565.0	-1137.1	4.1	418-699	[35]
1909.9	-673.3	0	0.2	440-530	[57]
1919.1	-693.7	0	.5	501-575	[50]
1919	-711	0	not reported	550-600	[58]
1904.6	-681.9	0	2.0	441-570	[59]
*1860.3	*-514.3	*0	0.3	300-600	[11]

*Thermochemical data

TABLE 6b. E° (mV) of the cell $\text{Zn}|\text{ZnCl}_2|\text{Cl}_2|\text{C}$ at various temperatures ($^\circ\text{C}$) according to table 6a
(Extrapolated values are included)

450 $^\circ$	500 $^\circ$	550 $^\circ$	600 $^\circ$	Standard deviation (mV)	Temperature range ($^\circ\text{C}$)	Reference
1627	1601	1574	1548	not reported	not reported	[56]
1592.8	1567.0	1535.6	1498.4	4.1	418-699	[35]
1606.9	1573.2	1539.6	1505.9	0.2	440-530	[57]
1606.9	1572.3	1537.6	1502.9	.5	501-575	[50]
1599	1563	1529	1493	not reported	550-600	[58]
1598	1564	1530	1495	2.0	441-570	[59]
	1588.5	1553.0		not reported	not reported	[61]
*1629	*1603	*1577	*1552	0.3	300-600	[11]

*Thermochemical data

TABLE 7a. E° (mV) = $a + bt + ct^2$ for the cell $\text{Ag}|\text{AgBr}|\text{Br}_2|\text{C}$
The parameters a , b , and c have been generated from literature values according to a linear and a quadratic least-squares analysis.

a	$b \times 10^3$	$c \times 10^6$	Standard deviation (mV)	Temperature range ($^\circ\text{C}$)	Reference
930.0	-287.3	0	0.25	442-565	[63]
928.9	-289.1	0	.3	510-600	[64]

TABLE 7b. E° (mV) of the cell $\text{Ag}|\text{AgBr}|\text{Br}_2|\text{C}$ at various temperatures ($^\circ\text{C}$) according to table 7a

(Extrapolated values are included)

450°	500°	550°	600°	Standard deviation (mV)	Temperature range ($^\circ\text{C}$)	Reference
800.7	786.4	772.0	757.6	0.25	442–565	[63]
798.8	784.4	769.9	755.5	.3	510–600	[64]
*795	*781	*767	*754	[12]

*Thermochemical data

TABLE 8a. E° (mV) = $a + bt + ct^2$ for the cell $\text{Cd}|\text{CdBr}_2|\text{Br}_2|\text{C}$

The parameters a , b , and c have been generated from literature values according to a linear and a quadratic least-squares analysis.

a	$b \times 10^3$	$c \times 10^6$	Standard deviation (mV)	Temperature range ($^\circ\text{C}$)	Reference
1425.3	–498.9	0	[69]

TABLE 8b. E° (mV) of the cell $\text{Cd}|\text{CdBr}_2|\text{Br}_2|\text{C}$ at various temperatures ($^\circ\text{C}$) according to table 8a

600°	650°	Standard deviation (mV)	Temperature range ($^\circ\text{C}$)	Reference
1126.0	1101	[69]
*1085	[12]

*Thermochemical data

TABLE 9a. E° (mV) = $a + bt + ct^2$ for the cell $\text{Pb}|\text{PbBr}_2|\text{Br}_2|\text{C}$

The parameters a , b , and c have been generated from literature values according to a linear and a quadratic least-squares analysis.

a	$b \times 10^3$	$c \times 10^6$	Standard deviation (mV)	Temperature range ($^\circ\text{C}$)	Reference
883.9	1815.5	–2984.9	8.9	321–568	[71]
1216.5	–89.2	–561.7	2.4	423–532	[70]
1335.1	–606.6	0	0.4	438–576	[72]
1429.0	–1000.1	409.0	0	500–600	[12]
*1340.7	*–679.5	*150.1	.06	426–726	[13]

*Thermochemical data.

TABLE 9b. E° (mV) of the cell $\text{Pb}|\text{PbBr}_2|\text{Br}_2|\text{C}$ at various temperatures ($^\circ\text{C}$) according to table 9a
(Extrapolated values are included)

400°	450°	500°	550°	600°	Standard deviation (mV)	Temperature range ($^\circ\text{C}$)	Reference
1133	1096	1045	979.5	898.6	8.9	321–568	[71]
1091	1063	1031	997.5	960.8	2.4	423–532	[70]
1092.5	1062	1032	1001	971.1	0.4	438–576	[72]
*1094	*1062	*1031	*1003	*976	0	500–600	[12]
*1093	*1065.3	*1038	*1012.4	*987.1	.06	426–726	[13]

*Thermochemical data

TABLE 10a. E° (mV) / $a + bt + ct^2$ for the cell $\text{Ag}|\text{AgI}|\text{I}_2|\text{C}$
The parameters a , b , and c have been generated from literature values according to a linear and a quadratic least-squares analysis.

a	$b \times 10^3$	$c \times 10^6$	Standard deviation (mV)	Temperature range ($^\circ\text{C}$)	Reference
700	–250	0	1.5	[74]

TABLE 10b. E° (mV) of the cell $\text{Ag}|\text{AgI}|\text{I}_2|\text{C}$ at various temperatures ($^\circ\text{C}$) according to table 10a

600°	650°	700°	Standard deviation (mV)	Temperature range ($^\circ\text{C}$)	Reference
550	537.5	525	1.5	[74]
*563	[12]

*Thermochemical data

TABLE 11. $E^\circ (mV) = a + bt + ct^2$ for the cells *Alkali Metal|Alkali Halide|Halide|C*

The parameters a , b , and c have been generated from thermochemical literature values [13] by a linear and a quadratic least-squares analysis.

	a	$b \times 10^3$	$c \times 10^6$	Standard deviation (mV)	Temperature range ($^\circ\text{C}$)
Li LiF F ₂ C.....	5890.1	-830.4	64.0	0.05	926-1226
Li LiCl Cl ₂ C.....	3830.9	-573.3	0	7.4	626-926
Li LiBr Br ₂ C.....	3469.0	-668.8	91.1	0.1	626-926
Li LiI I ₂ C.....	2829.0	-626.2	88.5	.03	526-826
Na NaF F ₂ C.....	6206.5	-1809.2	113.8	0.03	1026-1326
Na NaCl Cl ₂ C.....	2830.4	1746.1	-1536.2	14.7	826-1126
Na NaBr Br ₂ C.....	2497.6	1803.8	-1559.7	14.7	826-1126
Na NaI I ₂ C.....	1553.3	2725.8	-2061.8	10.3	726-1026
K KF F ₂ C.....	6015.5	-1707.9	106.0	0.07	926-1226
K KCl Cl ₂ C.....	4708.6	-1680.8	141.6	.1	826-1126
K KBr Br ₂ C.....	5085.7	-3106.5	922.4	7.1	826-1126
K KI I ₂ C.....	3188.6	68.6	-744.0	7.7	726-1026

TABLE 12. *Excess properties of mixtures*

AgCl(1-x), LiCl(x)

(The numbers following the \pm in column 2 are precision estimates.)

x	μ_{AgCl}^E/x^2 (kcal/mol)	s_{AgCl}^E/x^2 (e. u.)
<i>Reference [20], 800 $^\circ\text{C}$</i>		
0.0950	9.455 ± 8.687	8.432
.1850	-0.473 ± 0.606	-80.663
.4150	1.861 ± 0.577	-3.107
.7480	2.043 ± 0.067	-0.012
.7620	2.009 ± 0.037	-.409
.8090	2.108 ± 0.055	.504
.8950	2.221 ± 0.051	-1.791
.9714	2.122 ± 0.032	0.833
x	μ_{AgCl}^E/x^2 (kcal/mol)	s_{AgCl}^E/x^2 (e. u.)
<i>Reference [26], 600 $^\circ\text{C}$</i>		
0.1960	3.482 ± 0.420	1.380
.3100	2.161 ± 0.120	-0.408
.4270	2.062 ± 0.062	1.177
.5310	1.972 ± 0.048	1.268
.7480	2.015 ± 0.025	-0.161
.8640	2.205 ± 0.018	-.516

TABLE 13. *Excess properties of mixtures*

AgCl(1-x), NaCl(x)

(The numbers following the \pm in column 2 are precision estimates.)

x	μ_{AgCl}^E/x^2 (kcal/mol)	s_{AgCl}^E/x^2 (e.u.)
<i>Reference [19], 800 °C</i>		
0.1500	3.791 ± 1.229	-6.356
.2450	1.077 ± 0.962	-1.460
.3330	0.749 ± 0.228	-1.310
.3540	$.221 \pm 0.277$	-0.184
.3650	1.038 ± 0.157	-.848
.3850	0.249 ± 0.187	.545
.4190	$.579 \pm 0.145$.854
.4500	$.434 \pm 0.182$.718
.4950	$.895 \pm 0.131$.621
.6490	$.844 \pm 0.104$	1.796
.7910	$.999 \pm 0.044$	0.184
.9022	$.959 \pm 0.025$.246
.9687	$.989 \pm 0.025$.093

x	μ_{AgCl}^E/x^2 (kcal/mol)	s_{AgCl}^E/x^2 (e.u.)
<i>Reference [27], 800 °C</i>		
0.100	4.312 ± 4.658	-136.750
.250	1.564 ± 0.572	-5.718
.400	0.886 ± 0.155	0.245
.550	1.112 ± 0.037	-.839
.700	0.922 ± 0.012	.706

x	μ_{AgCl}^E/x^2 (kcal/mol)	s_{AgCl}^E/x^2 (e.u.)
<i>Reference [25], Stern, 800 °C</i>		
0.4740	0.083 ± 0.196	9.011
.6669	$.669 \pm 0.099$	3.179
.7470	$.613 \pm 0.078$	3.182
.8767	$.438 \pm 0.044$	3.327
.9109	$.055 \pm 0.042$	11.629
.9225	$-.279 \pm 0.042$	4.365

TABLE 14. *Excess properties of mixtures*

AgCl(1-x), KCl(x)

(The numbers following the \pm in column 2 are precision estimates.)

x	μ_{AgCl}^E/x^2 (kcal/mol)	s_{AgCl}^E/x^2 (e.u.)
<i>Reference [24], 700 °C</i>		
0.4091	-1.116 ± 0.221	7.108
.5734	-1.086 ± 0.148	2.770
.8093	-0.473 ± 0.053	3.102
.9018	$-.766 \pm 0.042$	4.001
.9201	$-.807 \pm 0.058$	3.260
.9353	-1.605 ± 0.051	0.801

x	μ_{AgCl}^E/x^2 (kcal/mol)	s_{AgCl}^E/x^2 (e.u.)
<i>Reference [22], 650 °C</i>		
0.100	-1.845 ± 0.922	4.84
.200	-0.173 ± 0.115	121.925
.300	-1.741 ± 0.051	-0.794
.400	-1.543 ± 0.071	-4.828
.500	-1.430 ± 0.009	138.132
.600	-1.485 ± 0.014	782.303
.650	-1.453 ± 0.012	-1.223

TABLE 15. *Excess properties of mixtures*AgCl(1-x), PbCl₂(x)(The numbers following the \pm in column 2 are precision estimates.)

x	μ_{AgCl}^E/x^2 (kcal/mol)	s_{AgCl}^E/x^2 (e.u.)
<i>Reference [23], 550 °C</i>		
0.200	0.058 ± 0.288	-3.345
.400	$-.173 \pm 0.071$	-1.168
.550	$-.122 \pm 0.039$	-0.084
.700	$-.095 \pm 0.028$	-.452
.800	$-.053 \pm 0.018$	-.483
.900	$.039 \pm 0.021$	-.253

TABLE 16. *Excess properties of mixtures*CdCl₂(1-x), NaCl(x)(The numbers following the \pm in column 2 are precision estimates.)

x	$\mu_{\text{CdCl}_2}^E/x^2$ (kcal/mol)	$s_{\text{CdCl}_2}^E/x^2$ (e.u.)
<i>Reference [36], 600 °C</i>		
0.200	5.765 \pm 2.421	-46.005
.300	0.821 \pm 1.128	-6.790
.400	-.835 \pm 0.431	-9.484
.500	-2.693 \pm 0.351	-7.628
.600	-3.300 \pm 0.270	-7.149
.700	-3.531 \pm 0.168	1.158

TABLE 17. *Excess properties of mixtures*CdCl₂(1-x), KCl(x)(The numbers following the \pm in column 2 are precision estimates.)

x	$\mu_{\text{CdCl}_2}^E/x^2$ (kcal/mol)	$s_{\text{CdCl}_2}^E/x^2$ (e.u.)
<i>Reference [36], 600 °C</i>		
0.100	7.149 \pm 13.375	68.950
.300	-4.561 \pm 1.229	-11.710
.400	-5.880 \pm 0.662	-12.712
.500	-7.306 \pm 0.461	-3.846
.600	-10.370 \pm 0.295	-10.621
.700	-11.897 \pm 0.180	-7.313

TABLE 18. *Excess properties of mixtures*CdCl₂(1-x), BaCl₂(x)

x	$\mu_{\text{CdCl}_2}^E/x^2$ (kcal/mol)	$s_{\text{CdCl}_2}^E/x^2$ (e.u.)
<i>Reference [36], 600 °C</i>		
0.200	5.650 \pm 2.998	1.267
.300	2.767 \pm 0.922	-7.404
.400	0.519 \pm 0.692	-4.901
.500	-1.144 \pm 0.627	-11.632
.600	-2.786 \pm 0.295	-13.067

TABLE 19. *Excess properties of mixtures*CeCl₃(1-x), NaCl(x)

x	$\mu_{\text{CeCl}_3}^E/x^2$ (kcal/mol)	$s_{\text{CeCl}_3}^E/x^2$ (e.u.)
<i>Reference [37], 800 °C</i>		
0.3883	-1.760	-15.109
.3901	-3.302	-17.591
.4159	-3.371	-43.882
.5102	-5.848	-5.555
.5780	-4.328	-10.208
.6781	-4.524	-7.307
.7441	-6.372	-15.689
.8393	-7.919	-6.220
.9042	-7.718	-8.680
.9828	-7.190	-9.737

TABLE 20. *Excess properties of mixtures*CeCl₃(1-X), KCl(x)

x	$\mu_{\text{CeCl}_3}^E/x^2$ (kcal/mol)	$s_{\text{CeCl}_3}^E/x^2$ (e.u.)
<i>Reference [37], 850 °C</i>		
0.1754	6.148	-57.867
.3204	-2.719	-10.926
.5007	-4.167	-16.578
.5203	-7.871	-4.115
.6695	-11.539	-4.152
.7340	-11.657	-1.045
.8422	-14.351	-7.142
.8889	-14.360	-5.099
.9343	-13.338	-6.741
.9985	-13.287	-12.607

x	$\mu_{\text{CeCl}_3}^E/x^2$ (kcal/mol)
<i>Reference [38], 850 °C</i>	
0.251	-74.598
.487	-36.685
.605	-37.702
.606	-38.938
.758	-27.502
.761	-29.183
.900	-22.839
.956	-19.913
.976	-19.737

TABLE 21. *Excess properties of mixtures*
CeCl₃(1-x), CaCl₂(x)

x	$\mu_{\text{CeCl}_3}^E/x^2$ (kcal/mol)	$s_{\text{CeCl}_3}^E/x^2$ (e.u.)
<i>Reference [39], 850 °C</i>		
0.0947	61.495	52.556
.1980	22.590	-64.464
.3988	4.887	-19.509
.4936	3.625	-9.865
.5987	2.560	-7.977
.6677	1.914	-5.736
.7669	1.328	-3.180
.8989	1.005	-3.950
.9899	1.273	-6.157

TABLE 22. *Excess properties of mixtures*
MgCl₂(1-x), LiCl(x)

(The numbers following the \pm in column 2 are precision estimates.)

x	$\mu_{\text{MgCl}_2}^E/x^2$ (kcal/mol)	$s_{\text{MgCl}_2}^E/x^2$ (e.u.)
<i>Reference [40], 700 °C</i>		
0.334	6.473 ± 0.745	144.484
.447	$3.913 \pm .784$	28.428
.553	$3.249 \pm .332$	20.301
.634	$2.082 \pm .208$	26.992
.707	$0.332 \pm .148$	13.417
.773	$.201 \pm .208$	15.762
.852	$-.115 \pm .115$	8.764
.896	$-.512 \pm .115$	7.747
.960	$-1.321 \pm .106$	10.534

TABLE 23. *Excess properties of mixtures* MgCl₂(1-x), NaCl(x)

(The numbers following the \pm in column 2 are precision estimates.)

x	$\mu_{\text{MgCl}_2}^E/x^2$ (kcal/mol)	$s_{\text{MgCl}_2}^E/x^2$ (e.u.)
<i>Reference [40] 700 °C</i>		
0.441	-0.048 ± 0.521	49.381
.479	$-.814 \pm 0.422$	30.157
.597	-3.780 ± 0.233	14.733
.621	-4.771 ± 0.240	24.639
.677	-4.568 ± 0.251	18.245
.758	-6.035 ± 0.161	11.281
.778	-6.362 ± 0.198	9.879
.764	-7.045 ± 0.127	11.512
x	$\mu_{\text{MgCl}_2}^E/x^2$ (kcal/mol)	
<i>Reference [41], 825 °C</i>		
0.256	0.000 ± 0.775	
.353	-5.627 ± 0.408	
.467	-5.963 ± 0.233	
.562	-7.601 ± 0.161	
.641	-8.519 ± 0.125	
.675	-8.124 ± 0.111	
.719	-8.122 ± 0.099	
.811	-9.123 ± 0.076	
.908	-8.731 ± 0.062	
.975	-7.469 ± 0.053	
x	$\mu_{\text{NaCl}}^E/(1-x)^2$ (kcal/mol)	$s_{\text{NaCl}}^E/(1-x)^2$ (e.u.)
<i>Reference [9], 850 °C</i>		
0.862	-1.579	-2.105
.853	-5.556	-0.463
.819	-5.793	.610
.784	-7.066	.642
.780	-6.818	-1.033
.744	-7.939	0.305
.720	-7.526	-1.020
.698	-7.895	-0.987
.681	-7.859	-1.473
.663	-8.099	-1.056
.638	-8.397	-1.145
.581	-8.542	-1.595
.526	-8.856	-1.335
.527	-9.522	-1.207
.448	-7.581	-1.969
.469	-9.043	-0.035
.387	-8.515	-1.064

TABLE 24. *Excess properties of Mixtures* $\text{MgCl}_2(1-x)$, $\text{KCl}(x)$

(The numbers following the \pm in column 2 are precision estimates.)

x	$\mu_{\text{MgCl}_2}^E/x^2$ (kcal/mol)
<i>Reference [38, 41], 800 °C</i>	
0.208	-11.566 ± 1.061
.290	-10.694 ± 0.553
.437	-14.140 ± 0.231
.531	-15.605 ± 0.161
.602	-14.349 ± 0.138
.657	-13.207 ± 0.115
.675	-13.610 ± 0.092
.748	-17.517 ± 0.092
.832	-16.180 ± 0.069
.912	-13.946 ± 0.046
.980	-12.287 ± 0.046
.985	-11.853 ± 0.046
x	$\mu_{\text{MgCl}_2}^E/x^2$ (kcal/mol) $s_{\text{MgCl}_2}^E/x^2$ (e.u.)

TABLE 25. *Excess properties of mixtures* $\text{MgCl}_2(1-x)$, $\text{RbCl}(x)$

(The numbers following the \pm in column 2 are precision estimates.)

x	$\mu_{\text{MgCl}_2}^E/x^2$ (kcal/mol)	$s_{\text{MgCl}_2}^E/x^2$ (e.u.)
<i>Reference [40], 700 °C</i>		
0.410	-6.049 ± 0.493	36.093
.523	-15.151 ± 0.304	34.806
.590	-17.450 ± 0.291	24.326
.657	-21.592 ± 0.203	21.148

TABLE 26. *Excess properties of mixtures* $\text{CaCl}_2(1-x)$, $\text{NaCl}(x)$

x	$\mu_{\text{NaCl}}^E/(1-x)^2$ (kcal/mol)	$s_{\text{NaCl}}^E/(1-x)^2$ (e.u.)
<i>Reference [9], 850 °C</i>		
0.981	0	-27.778
.939	0	-2.703
.870	-1.775	-3.550
.831	-3.217	-3.496
.761	-1.471	-2.802
.706	-2.083	-1.968
.656	-3.043	-1.522
.566	-2.919	-1.380
.484	-2.816	-1.427
.483	-2.881	-1.235
.465	-2.935	-1.328
.307	-2.728	-0.729
.222	-2.577	-.760
.133	-2.328	-1.011
.082	-1.958	-1.246

TABLE 27. *Excess properties of mixtures* $\text{SrCl}_2(1-x)$, $\text{NaCl}(x)$

x	$\mu_{\text{NaCl}}^E/(1-x)^2$ (kcal/mol)	$s_{\text{NaCl}}^E/(1-x)^2$ (e.u.)
<i>Reference [9], 850 °C</i>		
0.860	-1.020	2.551
.735	-0.114	-0.427
.700	-1.189	-.444
.597	-1.145	-.308
.583	-1.271	.345
.515	-1.139	.043
.500	-1.148	-.080
.412	-1.059	.058
.346	-0.844	-.117
.285	-.683	-.293
.278	-.815	-.038
.193	-.654	-.246
.152	-.501	-.306
.097	-.724	-.343

TABLE 28. *Excess properties of mixtures*
BaCl₂(1-x), NaCl(x)

x	$\mu_{\text{NaCl}}^E/(1-x)^2$ (kcal/mol)	$s_{\text{NaCl}}^E/(1-x)^2$ (e.u.)
<i>Reference [9], 850 °C</i>		
0.903	0	1.064
.801	-.379	.505
.696	.043	.325
.691	.052	.105
.605	.032	.256
.587	.035	.176
.490	.115	.231
.381	.091	.209
.365	-.002	.198
.312	.070	.211
.277	.023	.191
.092	-.044	.146

TABLE 29. *Excess properties of mixtures*
PbCl₂(1-x), LiCl(x)
(The numbers following the \pm in column 2 are precision estimates.)

x	$\mu_{\text{PbCl}_2}^E/x^2$ (kcal/mol)	$s_{\text{Cl}_2}^E/x^2$ (e.u.)
<i>Reference [45], 600 °C</i>		
0.1600	0.812 ± 3.964	-18.555
.3375	$.606 \pm 0.809$.668
.5340	$.413 \pm 0.291$	-1.310
x	$\mu_{\text{PbCl}_2}^E/x^2$ (kcal/mol)	
<i>Reference [46], 600 °C</i>		
0.2030	0.375	
.2840	-.930	
.2990	-1.615	
.3270	-1.508	
.4030	.116	
.4970	-.138	
.4980	-.235	
.5920	-.140	
.5950	-.232	

TABLE 30. *Excess properties of mixtures* PbCl₂(1-x), NaCl(x)

(The numbers following the \pm in column 2 are precision estimates.)

x	$\mu_{\text{PbCl}_2}^E/x^2$ (kcal/mol)	
<i>Reference [48], 600 °C</i>		
0.500	-0.722	
x	$\mu_{\text{PbCl}_2}^E/x^2$ (kcal/mol)	$s_{\text{PbCl}_2}^E/x^2$ (e.u.)
<i>Reference [45], 600 °C</i>		
0.100	8.532 ± 8.302	-13.610
.250	-1.033 ± 1.033	-4.870
.400	-1.211 ± 0.461	-0.029
.500	-0.830 ± 0.442	-2.721
x	$\mu_{\text{PbCl}_2}^E/x^2$ (kcal/mol)	
<i>Reference [46], 600 °C</i>		
0.3030	-1.615	
.3970	-2.331	
.4490	-2.052	
x	$\mu_{\text{PbCl}_2}^E/x^2$ (kcal/mol)	$s_{\text{PbCl}_2}^E/x^2$ (e.u.)
<i>Reference [44], 600 °C</i>		
0.500	-0.517 ± 0.166	13.568
.700	$-.978 \pm 0.018$	1.016

TABLE 31. *Excess properties of mixtures* $\text{PbCl}_2(1-x)$, $\text{KCl}(x)$ (The numbers following the \pm in column 2 are precision estimates.)

x	$\mu_{\text{PbCl}_2}^E/x^2$ (kcal/mol)	$s_{\text{PbCl}_2}^E/x^2$ (e.u.)
<i>Reference [49], 600 °C</i>		
0.050	-54.423 ± 14.759	-254.600
.100	-22.830 ± 5.535	-87.860
.200	-2.191 ± 0.922	-125.795
.300	-9.173 ± 0.666	-50.759
.400	-11.819 ± 0.231	-38.482

x	$\mu_{\text{PbCl}_2}^E/x^2$ (kcal/mol)	$s_{\text{PbCl}_2}^E/x^2$ (e.u.)
<i>Reference [45], 600 °C</i>		
0.200	-2.191 ± 2.191	-10.837
.300	-6.355 ± 1.485	-14.323
.400	-5.592 ± 0.777	-11.299
.500	-5.350 ± 0.369	-5.359
.600	-5.541 ± 0.256	-4.458

x	$\mu_{\text{PbCl}_2}^E/x^2$ (kcal/mol)
<i>Reference [46], 600 °C</i>	
0.2030	-5.222
.2710	-2.956
.3350	-4.789
.4000	-4.403
.5010	-5.116
.5060	-4.912
.5940	-5.318
.6560	-5.365

x	$\mu_{\text{PbCl}_2}^E/x^2$ (kcal/mol)	$s_{\text{PbCl}_2}^E/x^2$ (e.u.)
<i>Reference [44], 600 °C</i>		
0.500	-5.202 ± 0.129	-1.392
.700	-5.601 ± 0.113	6.392

TABLE 32. *Excess properties of mixtures* $\text{PbCl}_2(1-x)$, $\text{RbCl}(x)$

x	$\mu_{\text{PbCl}_2}^E/x^2$ (kcal/mol)
<i>Reference [46], 600 °C</i>	
0.2000	-10.614
.2510	-6.534
.3330	-6.554
.3980	-6.553
.4980	-6.894
.5970	-7.506

TABLE 33. *Excess properties of mixtures* $\text{PbCl}_2(1-x)$, $\text{CsCl}(x)$
(The numbers following the \pm in column 2 are precision estimates.)

x	$\mu_{\text{PbCl}_2}^E/x^2$ (kcal/mol)	$s_{\text{PbCl}_2}^E/x^2$ (e.u.)
<i>Reference [44], 650 °C</i>		
0.500	-7.315 ± 0.055	10.856
.700	-9.393 ± 0.046	5.704

TABLE 34. *Excess properties of mixtures* $\text{PbCl}_2(1-x)$, $\text{CaCl}_2(x)$

x	$\mu_{\text{PbCl}_2}^E/x^2$ (kcal/mol)
<i>Reference [45], 650 °C</i>	
0.200	2.191
.400	1.123

TABLE 35. *Excess properties of mixtures* $\text{PbCl}_2(1-x)$, $\text{SrCl}_2(x)$

x	$\mu_{\text{PbCl}_2}^E/x^2$ (kcal/mol)
<i>Reference [45], 650 °C</i>	
0.200	2.191
.400	1.543

TABLE 36. *Excess properties of mixtures*
PbCl₂(1-x), BaCl₂(x)

x	$\mu_{\text{PbCl}_2}^E/x^2$ (kcal/mol)
<i>Reference [45], 650 °C</i>	
0.200	1.038
.400	-.187

TABLE 37. *Excess properties of mixtures*
PbCl₂(1-x), ZnCl₂(x)
(The numbers following the \pm in column 2 are precision estimates.)

x	$\mu_{\text{PbCl}_2}^E/x^2$ (kcal/mol)	$s_{\text{PbCl}_2}^E/x^2$ (e.u.)
<i>Reference [50], 500 °C</i>		
0.145	-5.710 ± 2.195	-55.233
.312	-2.537 ± 0.475	2.560
.405	-2.502 ± 0.337	3.079
.510	-2.350 ± 0.178	1.126
.699	-1.746 ± 0.085	5.149

x	$\mu_{\text{PbCl}_2}^E/x^2$ (kcal/mol)
<i>Reference [51], 500 °C</i>	
0.242	-1.865 ± 0.786
.385	-1.931 ± 0.311
.486	-1.763 ± 0.196
.586	-1.520 ± 0.134
.632	-1.500 ± 0.115
.809	$-.870 \pm 0.071$

TABLE 38. *Excess properties of mixtures* ZnCl₂(1-x),
LiCl(x)

x	$\mu_{\text{ZnCl}_2}^E/x^2$ (kcal/mol)
<i>Reference [58], 550 °C</i>	
0.2990	4.953
.4030	3.210
.5040	2.887
.6050	2.634
.6590	-2.959
.7000	-4.453
.7990	-2.820
.8940	-1.058
.9530	0.533

TABLE 39. *Excess properties of mixtures* ZnCl₂(1-x),
NaCl(x)
(The numbers following the \pm in column 2 are precision estimates.)

x	$\mu_{\text{ZnCl}_2}^E/x^2$ (kcal/mol)	$s_{\text{ZnCl}_2}^E/x^2$ (e.u.)
<i>Reference [59], 550 °C</i>		
0.100	-3.920 ± 11.991	-147.36
.200	-0.231 ± 2.883	-31.822
.300	$-.743 \pm 1.485$	-36.153
.400	-4.151 ± 0.980	-6.140
.500	-5.756 ± 0.498	+2.758

TABLE 40. *Excess properties of mixtures ZnCl₂(1 - x), KCl(x)*(The numbers following the \pm in column 2 are precision estimates.)

x	$\mu_{\text{ZnCl}_2}^E/x^2$ (kcal/mol)	
<i>Reference [60], 550 °C</i>		
0.102	-49.446	
.204	-20.955	
.300	-10.428	
.395	-10.407	
.487	-15.035	
.528	-12.969	
.591	-13.112	
.660	-21.778	
.700	-19.417	
.720	-18.492	
x	$\mu_{\text{ZnCl}_2}^E/x^2$ (kcal/mol)	$s_{\text{ZnCl}_2}^E/x^2$ (e.u.)
<i>Reference [59], 550 °C</i>		
0.100	33.438 ± 23.522	-2097.81
.200	-19.025 ± 10.031	560.485
.300	-3.561 ± 1.333	-47.940
.400	-6.745 ± 0.749	4.583
.500	-10.516 ± 0.480	14.786
.600	-14.157 ± 0.743	-9.698

TABLE 41. *Excess properties of mixtures ZnCl₂(1 - x), RbCl(x)*(The numbers following the \pm in column 2 are precision estimates.)

x	$\mu_{\text{ZnCl}_2}^E/x^2$ (kcal/mol)	
<i>Reference [60], 550 °C</i>		
0.105	-71.697	
.209	-31.293	
.313	-15.404	
.400	-25.034	
.500	-19.814	
.610	-27.963	
.688	-22.671	
x	$\mu_{\text{ZnCl}_2}^E/x^2$ (kcal/mol)	$s_{\text{ZnCl}_2}^E/x^2$ (e.u.)
<i>Reference [61], 550 °C</i>		
0.211	-2.020 ± 0.623	34.928
.264	-4.135 ± 0.397	16.808
.315	-4.790 ± 0.233	28.918
.366	-6.040 ± 0.207	18.741
.392	-7.548 ± 0.270	16.429
.453	-9.102 ± 0.090	21.173
.526	-13.251	

TABLE 42. *Excess properties of mixtures*
ZnCl₂(1-x), CsCl(x)

x	$\mu_{\text{ZnCl}_2}^E/x^2$ (kcal/mol)
<i>Reference [62], 600 °C</i>	
0.216	-31.969
.300	-22.574
.409	-13.440
.418	-18.520
.432	-20.070
.490	-16.348
.588	-11.094
.650	-37.333
.685	-41.972
.700	-58.375
.740	-165.650
.750	-166.801

TABLE 43. *Excess properties of mixtures*
AgBr(1-x), LiBr(x)
(The numbers following the \pm in column 2 are precision estimates.)

x	μ_{AgBr}^E/x^2 (kcal/mol)	s_{AgBr}^E/x^2 (e.u.)
<i>Reference [63], 550 °C</i>		
0.4063	1.801 ± 0.055	-0.587
.5914	1.667 ± 0.039	-.310
.7452	1.965 ± 0.030	-.507
.8900	1.861 ± 0.012	-.748

TABLE 44. *Excess properties of mixtures*
AgBr(1-x), NaBr(x)
(The numbers following the \pm in column 2 are precision estimates.)

x	μ_{AgBr}^E/x^2 (kcal/mol)	s_{AgBr}^E/x^2 (e.u.)
<i>Reference [67], 600 °C</i>		
0.2514	1.605 ± 0.145	2.737
.3995	1.061 ± 0.060	1.784
.4870	1.040 ± 0.039	10.470

TABLE 45. *Excess properties of mixtures* AgBr(1-x),
KBr(x)

x	μ_{AgBr}^E/x^2 (kcal/mol)	s_{AgBr}^E/x^2 (e.u.)
<i>Reference [68], 600 °C</i>		
0.2000	-0.577	11.300
.3995	-1.372	0.058
.5498	-1.480	.099
.6462	-1.540	1.353

TABLE 46. *Excess properties of mixtures* AgBr(1-x),
RbBr(x)
(The numbers following the \pm in column 2 are precision estimates.)

x	μ_{AgBr}^E/x^2 (kcal/mol)	s_{AgBr}^E/x^2 (e.u.)
<i>Reference [65], 550 °C</i>		
0.2530	-1.946 ± 0.180	0.180
.4040	-2.783 ± 0.510	-3.561
.5330	-2.606 ± 0.032	-0.787
.6480	-2.608 ± 0.028	-.533

TABLE 47. *Excess properties of mixtures* AgBr(1-x),
PbBr₂(x)
(The numbers following the \pm in column 2 are precision estimates.)

x	μ_{AgBr}^E/x^2 (kcal/mol)	s_{AgBr}^E/x^2 (e.u.)
<i>Reference [66], 550 °C</i>		
0.200	-0.173 ± 0.231	6.572
.300	$.025 \pm 0.101$	-0.589
.400	$.028 \pm 0.058$.404
.500	$.009 \pm 0.037$.738
.600	$.090 \pm 0.032$	-.974
.700	$.141 \pm 0.018$	-.783
.800	$.159 \pm 0.018$	-.267
.900	$.168 \pm 0.014$	-.649

TABLE 48. *Excess properties of mixtures CdBr₂(1-x), KBr(x)*

x	$\mu_{\text{CdBr}_2}^E/x^2$ (kcal/mol)
<i>Reference [69], 597.5 °C</i>	
0.150	-19.269
.300	-10.197
.523	-8.777
.600	-9.409
.700	-10.698
.800	-12.423

TABLE 49. *Excess properties of mixtures PbBr₂(1-x), NaBr(x)*

x	$\mu_{\text{PbBr}_2}^E/x^2$ (kcal/mol)
<i>Reference [73], 589 °C</i>	
0.200	-1.153
.300	-2.075
.400	-2.018
.500	-2.075
.600	-2.299
.700	-2.029

TABLE 50. *Excess properties of mixtures PbBr₂(1-x), KBr(x)*

The numbers following the \pm in column 2 are precision estimates.)

x	$\mu_{\text{PbBr}_2}^E/x^2$ (kcal/mol)	$s_{\text{PbBr}_2}^E/x^2$ (e.u.)
<i>Reference [71], 550 °C</i>		
0.1800	-57.082 \pm 12.669	995.525
.2300	-37.402 \pm 7.760	607.372
.3300	-19.885 \pm 3.770	292.498
.3800	-17.136 \pm 2.843	232.299
.4800	-16.274 \pm 1.783	124.049
.5500	-16.299 \pm 1.356	102.684
.6500	-16.620 \pm 0.971	65.787
.6800	-16.387 \pm .888	43.767

TABLE 51. *Excess properties of mixtures PbBr₂(1-x), ZnBr₂(x)*
(The numbers following the \pm in column 2 are precision estimates.)

x	$\mu_{\text{PbBr}_2}^E/x^2$ (kcal/mol)	$s_{\text{PbBr}_2}^E/x^2$ (e.u.)
<i>Reference [70], 500 °C</i>		
0.0980	-1.201 \pm 12.492	240.937
.2060	-.217 \pm 2.827	49.656
.2960	-.263 \pm 1.474	30.115
.3960	-.030 \pm 0.823	16.281
.5140	.131 \pm .489	9.671
.6080	.175 \pm .325	8.552
.7120	.267 \pm .238	7.866
.7900	.274 \pm .208	8.510
.8000	.288 \pm .194	8.219

TABLE 52. *Excess properties of mixtures AgI(1-x), KI(x)*
(The numbers following the \pm in column 2 are precision estimates.)

x	μ_{AgI}^E/x^2 (kcal/mol)	s_{AgI}^E/x^2 (e.u.)
<i>Reference [75], 600 °C</i>		
0.1	-2.444 \pm 3.459	-9.45
.2	-3.580 \pm 0.876	-2.423
.3	-2.988 \pm 0.392	-1.460
.4	-2.385 \pm 0.219	-0.576
.5	-1.830 \pm 0.138	.028
.6	-1.669 \pm 0.092	.705
.7	-1.477 \pm 0.069	.292

TABLE 53. *Excess properties of mixtures AgBr(1-x), AgCl(x)*

x	μ_{AgBr}^E/x^2 (kcal/mol)	s_{AgBr}^E/x^2 (e.u.)
<i>Reference [64], 600 °C</i>		
0.200	4.439 \pm 0.173	8.012
.400	2.391 \pm 0.044	1.456
.600	1.730 \pm 0.018	-1.019
.800	2.262 \pm 0.012	-2.220

TABLE 54. *Excess properties of mixtures* AgI(1-x), AgCl(x)

(The numbers following the \pm in column 2 are precision estimates.)

x	μ_{AgI}^E/x^2 (kcal/mol)	s_{AgI}^E/x^2 (e.u.)
<i>Reference [76], 600 °C</i>		
0.200	0.455 ± 0.876	-2.423
.400	$.497 \pm 0.219$	-1.297
.500	$.384 \pm 0.138$	-0.434
.600	$.404 \pm 0.092$.064

TABLE 55. *Excess properties of mixtures* AgI(1-x), AgBr(x)

x	μ_{AgI}^E/x^2 (kcal/mol)	s_{AgI}^E/x^2 (e.u.)
<i>Reference [76], 600 °C</i>		
0.200	2.185 ± 0.876	0.460
.400	1.074 ± 0.219	-.576
.500	1.122 ± 0.138	-.434
.600	1.086 ± 0.092	.064

TABLE 56. *Excess properties of mixtures* KBr(1-x), KCl(x)

x	μ_{KBr}^E/x^2 (kcal/mol)	s_{KBr}^E/x^2 (e.u.)
<i>Reference [9], 800 °C</i>		
0.098	1.042	-1.458
.193	0.806	-0.995
.284	.496	-.645
.298	.811	-.586
.384	.678	-.508
.396	.574	-.478
.414	.817	-.694
.427	.713	-.653

TABLE 57. *Excess properties of mixtures* NaBr(1-x), NaCl(x)

x	μ_{NaBr}^E/x^2 (kcal/mol)	s_{NaBr}^E/x^2 (e.u.)
<i>Reference [9], 800 °C</i>		
0.103	0.943	-0.755
.204	.433	-.385
.295	.402	-.276
.371	.363	-.262
.435	.365	-.243
.483	.429	-.244
.55	.231	-.221
.7	.408	-.286

(The numbers following the \pm in column 2 are precision estimates.)

x	μ_{NaBr}^E/x^2 (kcal/mol)	
<i>Reference [84], 800 °C</i>		
0.200	0.657 ± 1.153	
.300	$.612 \pm 0.507$	
.500	$.424 \pm 0.184$	
.600	$.438 \pm 0.138$	

TABLE 58. *Excess properties of mixtures* PbBr₂(1-x), PbCl₂(x)
(The numbers following the \pm in column 2 are precision estimates.)

x	$\mu_{\text{PbBr}_2}^E/x^2$ (kcal/mol)	$s_{\text{PbBr}_2}^E/x^2$ (e.u.)
<i>Reference [72], 500 °C</i>		
0.200	-5.938 ± 0.807	21.562
.400	-2.998 ± 0.173	11.415
.500	-2.527 ± 0.092	6.190
.550	-2.790 ± 0.122	3.812

8. References

- [1] Kleppa, O. J., The solution chemistry of simple fused salts *Ann. Rev. Phys. Chem.* **16**, 187 (1965).
- [2] Bloom, H., *J. Pure Appl. Chem.* **7**, 389 (1963).
- [3] Forland, T., in *Fused Salts*, ed. B. R. Sundheim, McGraw-Hill Book Co., N.Y. (1964).
- [4] Ketelaar, J. A. A., and Dammers-de Klerk, Mrs. A. A., *Proc. Koninkl. Ned. Akad. Wetenschap.* **68B**, 169 (1965).
- [5] Laity, R. W., in *Reference Electrodes*, ed. D. J. G. Ives and G. J. Janz (Academic Press, New York and London, 1961).
- [6] Blander, M., in *Molten Salt Chemistry*, ed. M. Blander, Interscience Publishers, N.Y. (1963).
- [7] Dijkhuis, Chr. G. M., Dijkhuis, Ria, and Janz, G. J., *Chem. Rev.*, **68**, 253 (1968).
- [8] Temkin, M., *Acta Physicochim.*, U.S.S.R., **20**, 411 (1945).
- [9] Ostvold, T., On the Application of Glass Membranes as Alkali Electrodes at Elevated Temperatures, Thesis, Institute for Physical Chemistry, Trondheim, Norway, (1966).
- [10] Ostvold, T., *Acta. Chem. Scand.* **20**, 2187 (1966).
- [11] Hamer, W. J., Malmberg, M. S., and Rubin, B., *J. Electrochem. Soc.* **103**, 8 (1956).
- [12] Hamer, W. J., Malmberg, M. S., and Rubin, B., *J. Electrochem. Soc.* **112**, 750 (1965).
- [13] JANAF Thermochemical Tables, Clearinghouse for Federal Scientific and Technical Information, The Dow Chemical Company, Midland, Michigan, 48640, U.S.A.
- [14] Discussion of T. Forland and C. G. M. Dijkhuis, *Discussions Faraday Soc.* **32**, 161 (1961).
- [15] Senderoff, S., and Brenner, A., *J. Electrochem. Soc.* **101**, 31 (1954).
- [16] Senderoff, S., and Mellors, G. W., *Rev. Sci. Instr.* **29**, 151 (1958).
- [17] Drossbach, P., *J. Electrochem. Soc.* **103**, 700 (1956).
- [18] Murgulescu, I. G., Sternberg, S., and Bejan, L., *Rev. Roumaine Chim.* **11**, 447 (1966).
- [19] Panish, M. B., Blankenship, F. F., Grimes, W. R., and Newton, R. F., *J. Phys. Chem.* **62**, 1325 (1958).
- [20] Panish, M. B., Newton, R. F., Grimes, W. R., and Blankenship, F. F., *J. Phys. Chem.* **63**, 668 (1959).
- [21] Leonardi, J., and Brenet, J., *Compt. Rend.* **261**, 116 (1965).
- [22] Murgulescu, G., and Sternberg, S., *Rev. Chim., Acad. Rep. Populaire Roumaine*, **2**, 251 (1957).
- [23] Salstrom, E. J., *J. Am. Chem. Soc.* **56**, 1272 (1934).
- [24] Stern, K. H., *J. Phys. Chem.* **60**, 679 (1956).
- [25] Stern, K. H., *J. Phys. Chem.* **62**, 385 (1958).
- [26] Salstrom, E. J., Kew, T. J., and Powell, T. M., *J. Am. Chem. Soc.* **58**, 1848 (1936).
- [27] Sternberg, S., and Gheorghiu, S., *Studii si Cercet de Chimie, Acad. Rep. Populaire Roumaine* **7**, 107 (1959).
- [28] Kuroda, T., and Matsumoto, O., *J. Electrochem. Soc. Japan* **33**, 29 (1965).
- [29] Sethi, R. S., and Jindal, H. L., *Current Sci. (India)* **34**, 284 (1965).
- [30] Delimarskii, Yu.K., and Skobets, E. M. S., *J. Phys. Chem. (U.S.S.R.)* **20**, 1005 (1946).
- [31] Sheiko, I. N., and Delimarskii, Yu.K., *Ukr. Khim. Zh.* **25**, 295 (1959).
- [32] Markov, B. F., and Delimarskii, Yu.K., *Zh. Fiz. Khim.* **31**, 2589 (1957).
- [33] Dijkhuis, C. G. M., An Investigation of Molten Cadmium Halide-Alkali Halide mixtures by emf measurements, Thesis, University of Amsterdam (1964).
- [34] Dijkhuis, C. G. M., and Ketelaar, J. A. A., *Electrochim. Acta* **11**, 1607 (1966).
- [35] Lorenz, R., and Velde, H., *Z. Anorg. Allgem. Chem.* **183**, 81 (1929).
- [36] Lantratov, M. F., and Alabyshev, A. F., *J. Appl. Chem. (U.S.S.R.)* **26**, 321 (1953).
- [37] Senderoff, S., Mellors, G. E., and Bretz, R. I., *N.Y. Acad. Sci.* **79**, 878 (1960).
- [38] Neil, D. E., Thermodynamic Properties of Molten Chloride Solutions, Thesis, Rensselaer Polytechnic Institute, Troy, N.Y. (1959). *Dissertation Abstr.* **20**, 2591 (1960).
- [39] Senderoff, S., Mellors, G. W., and Bretz, R. I., *J. Electrochem. Soc.* **108**, 93 (1961).
- [40] Markov, B. F., Delimarskii, Yu. K., and Panchenko, I. D., *Zh. Fiz. Khim.* **29**, 51 (1955).
- [41] Neil, D. E., Clark, H. M., and Wiswall, R. H. Jr., *J. Chem. and Eng. Data* **10**, 21 (1965).
- [42] Bruneaux, M., Ziolkiewicz, S., and Morand, G., *Compt. Rend.* **257**, 3591 (1963).
- [43] Bruneaux, M., Ziolkiewicz, S., and Morand, G., *J. Chim. Phys.* **61**, 1215 (1964).
- [44] Hagemark, K., and Hengstenberg, D., *J. Chem. and Eng. Data* **11**, 596 (1966).
- [45] Lantratov, M. F., and Alabyshev, A. F., *Zh. Prikl. Khim.* **26**, 263 (1953). *Eng. Transl.: J. Appl. Chem. (U.S.S.R.)* **26**, 235 (1953).
- [46] Markov, B. F., Delimarskii, Yu. K., and Panchenko, I. D., *Zh. Fiz. Khim.* **28**, 1987 (1954).
- [47] Markov, B. F., Delimarskii, Yu. K., and Panchenko, I. D., *J. Polymer Sci.* **31**, 263 (1958).
- [48] Suskii, L., *Zh. Fiz. Khim.* **30**, 1855 (1956).
- [49] Hildebrand, J. H., and Ruhle, G. C., *J. Am. Chem. Soc.* **49**, 722 (1927).
- [50] Wachter, A., and Hildebrand, J. H., *J. Am. Chem. Soc.* **52**, 4655 (1930).
- [51] Nakamura, Y., and Brenet, J., *Compt. Rend.* **262C**, 673 (1966).
- [52] Alabyshev, A. F., Lantratov, M. F., and Morachevskii, A. G., *Izvest. V.U.Z.M.V.O.S.S.S.R., Khim Tekhnol.* **3**, 649 (1960).
- [53] Benz, R., *J. Phys. Chem.* **65**, 81 (1961).
- [54] Benz, R., and Leary, J. A., *J. Phys. Chem.* **65**, 1056 (1961).
- [55] Delimarskii, Yu. K., and Markov, B. F., *Electrochemistry of Fused Salts* (R. E. Wood, transl.), The Sigma Press, Washington, D.C., U.S.A. (1961).
- [56] Takahashi, M., *J. Electrochem. Soc. Japan* **28**, E-117 (1960).
- [57] Marsland, D. B., *Dissertation Abstr.* **19**, 1222 (1958).
- [58] Markov, B. F., and Volkov, S. V., *Ukr. Khim. Zh.* **30**, 341 (1964).
- [59] Lantratov, M. F., and Alabyshev, A. F., *Zh. Prikl. Khim.* **27**, 722 (1954). *Engl. Transl.: J. App. Chem. (U.S.S.R.)*, **27**, 685 (1954).
- [60] Markov, B. F., and Volkov, S. V., *Ukr. Khim. Zh.* **30**, 545 (1964).
- [61] Markov, B. F., *Zh. Fiz. Khim.* **31**, 2288 (1957).
- [62] Markov, B. F., and Volkov, S. V., *Ukr. Khim. Zh.* **30**, 906 (1964).
- [63] Salstrom, E. J., and Hildebrand, J. H., *J. Am. Chem. Soc.* **52**, 4650 (1930).
- [64] Murgulescu, I. G., and Marchidan, D. I., *Rev. Chim. Acad. Rep. Populaire Roumaine* **3**, 47 (1958).
- [65] Salstrom, E. J., *J. Am. Chem. Soc.* **54**, 4252 (1932).
- [66] Salstrom, E. J., *J. Am. Chem. Soc.* **54**, 2653 (1932).
- [67] Salstrom, E. J., *J. Am. Chem. Soc.* **53**, 1794 (1931).
- [68] Salstrom, E. J., *J. Am. Chem. Soc.* **53**, 3385 (1931).
- [69] Lantratov, M. F., and Shevlyakova, T. N., *Zh. Prikl. Khim.* **4**, 1065 (1961).
- [70] Salstrom, E. J., *J. Am. Chem. Soc.* **55**, 1029 (1933).
- [71] Lantratov, M. F., and Shevlyakova, T. N., *Zh. Neorgan. Khim.* **4**, 1153 (1959).
- [72] Salstrom, E. J., and Hildebrand, J. H., *J. Am. Chem. Soc.* **52**, 4641 (1930).
- [73] Lantratov, M. F., and Shevlyakova, T. N., *Zh. Neorgan. Khim.* **6**, 192 (1961).
- [74] Sternberg, S., Adorian, I., and Galasiu, I., *J. Chim. Phys.* **62**, 63 (1965).
- [75] Sternberg, S., Adorian, I., and Galasiu, I., *Electrochim. Acta* **11**, 385 (1966).
- [76] Sternberg, S., Adorian, I., and Galasiu, I., *Rev. Roumaine Chim.* **11**, 581 (1966).
- [77] Ketelaar, J. A. A., and Dammers-de Klerk, Mrs. A. A., *Rec. Trav. Chim.* **83**, 322 (1964).
- [78] NBS Circular 500, Selected Values of Chemical Thermodynamic Properties, United States Government Printing Office, Washington, D.C. (1952).

- [79] Landolt-Börnstein, Zahlenwerke und Funktionen, Vol. 2, Part 4, Springer Verlag Berlin (1961).
- [80] Kelley, K. K., Contributions to the Data on Theoretical Metallurgy, Vol. 10, Bureau of Mines, United States Government Printing Office, Washington, D.C. (1949).
- [81] Altshuller, A. P., J. Phys. Chem. **61**, 251 (1957).
- [82] Forland, T., and Ostvold, T., Acta Chem. Scand. **20**, 2086 (1966).
- [83] Ostvold, T., Acta Chem. Scand. **20**, 2320 (1966).
- [84] Sternberg, S., and Herdlicka, C., Rev. Roumaine Chim., **11**, 29 (1966).
- [85] Dijkhuis, Chr. G. M., and Ketelaar, J. A. A., Electrochim. Acta, **12**, 795 (1967).

9. Compound Index

	Page		Page
AgBr.....	5, 6, 30	LiI.....	35
– AgCl.....	6, 24, 25, 28, 45	MgCl ₂	4, 5, 30
– KBr.....	6, 21, 22, 28, 44	– KCl.....	6, 13, 14, 27, 39
– LiBr.....	6, 20, 21, 22, 28, 44	– LiCl.....	6, 12, 13, 27, 38
– NaBr.....	6, 21, 22, 28, 44	– NaCl.....	6, 12, 13, 27, 38
– PbBr ₂	6, 21, 22, 28, 44	– RbCl.....	6, 13, 14, 39
– RbBr.....	6, 21, 22, 28, 44	MnCl ₂	5
AgCl.....	3, 4, 28, 29	– KCl.....	6, 14
– KCl.....	6, 7, 8, 27, 36	– NaCl.....	6, 14
– LiCl.....	6, 7, 8, 27, 35	NaBr.....	26, 35
– NaCl.....	6, 7, 8, 27, 36	– NaCl.....	6, 25, 28, 46
– PbCl ₂	6, 7, 8, 27, 36	NaCl.....	3, 12, 14, 35
AgI.....	6, 34	– MgCl ₂	3
– AgBr.....	6, 25, 28, 46	NaF.....	35
– AgCl.....	6, 25, 28, 46	NaI.....	35
– KI.....	6, 24, 26, 28, 45	PbBr ₂	5, 6, 22, 23, 34
AgNO ₃	6	– KBr.....	6, 23, 28, 45
BaCl ₂ –NaCl.....	6, 14, 15, 27, 40	– NaBr.....	6, 22, 23, 27, 45
BeCl ₂	4, 29	– PbCl ₂	6, 27, 28, 46
– NaCl.....	4, 6, 9	– ZnBr ₂	6, 23, 24, 28, 45
CaCl ₂ –NaCl.....	6, 14, 15, 27, 39	PbCl ₂	5, 18, 31
CdBr ₂	5, 22, 33	– BaCl ₂	6, 18, 28, 42
– KBr.....	6, 22, 28, 45	– CaCl ₂	6, 18, 28, 41
CdCl ₂	4, 5, 9, 30	– CsCl.....	6, 17, 28, 41
– BaCl ₂	6, 9, 10, 27, 37	– KCl.....	6, 16, 17, 27, 41
– KCl.....	6, 9, 10, 27, 37	– LiCl.....	6, 15, 16, 27, 40, 42
– NaCl.....	6, 9, 10, 27, 37	– NaCl.....	2, 6, 16, 17, 27, 40
CdI ₂ –NaI.....	6, 24, 28	– RbCl.....	6, 16, 17, 28, 41
CeCl ₃	4	– SrCl ₂	6, 18, 28, 41
– CaCl ₂	6, 11, 12, 27	– ZnCl ₂	6, 16, 18, 28, 42
– KCl.....	4, 6, 11, 12, 27, 37	PbI ₂ –NaI.....	6, 24, 28
– NaCl.....	6, 9, 11, 12, 27, 38	PuCl ₃	5, 18
KBr.....	26, 35	– KCl.....	5, 6, 18
– KCl.....	6, 26, 28, 46	– NaCl.....	5, 6, 18
KCl.....	35	SrCl ₂ –NaCl.....	6, 14, 15, 27, 39
KF.....	35	ZnCl ₂	5, 19, 32
KI.....	35	– BaCl ₂	6, 20, 28
LiBr.....	35	– CsCl.....	6, 20, 42
LiCl.....	35	– KCl.....	6, 19, 20, 28, 42
LiF.....	35	– LiCl.....	6, 18, 19, 28
		– NaCl.....	6, 19, 20, 28, 42
		– RbCl.....	6, 20, 42

Molten Salts: Volume 2

Section 2. Surface Tension Data

G. J. Janz,* G. R. Lakshminarayanan,*
R. P. T. Tomkins,* and J. Wong*

Data on the surface tensions of single salt melts have been systematically collected and evaluated. Results are given for 107 inorganic compounds over a range of temperatures where available.

Key words: Critically evaluated data; molten salts; surface tension.

Contents

	Page		Page
1. Introduction.....	49	Carbonates.....	66
2. Symbols and units.....	50	Nitrates.....	67
3. Theory and practice.....	50	Nitrites.....	70
3.1. Introduction.....	50	Silicates.....	70
3.2. Maximum Bubble pressure method.....	50	Metaphosphates.....	71
3.3. Detachment methods.....	51	Sulfates.....	72
a. Wilhelmy slide plate method.....	51	Molybdates.....	74
b. Pin method.....	51	Tungstates.....	74
c. Maximum pull on cylinder method.....	52	Miscellaneous.....	74
d. Ring method.....	52	6. Numerical values of surface tension.....	78
3.4. Capillary rise method.....	52	Fluorides.....	78
3.5. Methods based on the shape of static drops on bubbles.....	53	Chlorides.....	80
a. Sessile bubble method.....	53	Bromides.....	85
b. Pendent drop method.....	53	Iodides.....	87
3.6. Summary.....	54	Oxides.....	90
4. Treatment of surface tension data.....	54	Sulfides.....	91
4.1. Statistical analysis of data.....	54	Metaborates.....	92
4.2. Selection of the best values.....	54	Carbonates.....	92
4.3. Estimation of uncertainty.....	55	Nitrates.....	93
4.4. Preparation of the tables.....	55	Nitrites.....	95
5. Discussion.....	55	Silicates.....	96
Fluorides.....	55	Metaphosphates.....	97
Chlorides.....	57	Sulfates.....	99
Bromides.....	62	Molybdates.....	101
Iodides.....	64	Tungstates.....	102
Oxides.....	65	Miscellaneous.....	102
Sulfides.....	66	7. Cumulative table of temperature dependent equations...	104
Metaborates.....	66	8. References.....	109
		9. Compound index.....	110

1. Introduction

This work was undertaken to meet the need for the critical assessment of the surface tension data of inorganic compounds as single-salt melts. Results are given for some 107 compounds for which data were published before December 31, 1966.

The order of listing the salts in this compilation follows a classification by anions, i.e. *monatomic anions*: Fluorides (9), Chlorides (22), Bromides (12),

Iodides (7), Oxides (8), Sulfides (2); *polyatomic anions*: Metaborates (3), Carbonates (3), Nitrates (11), Nitrites (2), Silicates (5), Metaphosphates (7), Sulfates (5), Molybdates (4), Tungstates (2). Additional salts are given as Miscellaneous. The number of salts is indicated in parentheses after each anionic group. The order within an anionic group is given in an index list which precedes the tables of numerical values for each group. In the bibliography, those references having data of molten salt mixtures are marked with an asterisk.

*Molten Salts Data Center, Rensselaer Polytechnic Institute, Troy, N.Y. 12180.

2. Symbols and Units

The temperature dependence of the surface tension has been expressed by linear or quadratic equations:

$$\gamma = a + bt$$

$$\gamma = a + bt + ct^2$$

where a , b , and c are constants. Unless otherwise stated, the units in this compilation are:

Temperature t , °C; 0 °C = 273.15 °K [22]

Surface Tension γ , dyne cm⁻¹ a, b

3. Theory and Practice

3.1. Introduction

Some 200 surface tension determinations have been made on 107 single-component salt melts using eight experimental techniques. The most versatile method, and one that is applicable to these molten systems at elevated temperatures, is the method of maximum bubble pressure; 75 percent of the total determinations on the 107 molten salts have been made by this technique. Other methods, in descending percentages of application are: Wilhelmy slide plate, capillary rise, maximum pull on cylinder, pin, pendant drop, ring, and sessile bubble. The percent application, tabulated in table 1, summarizes the fraction of the total determinations made by each technique.

TABLE 1. *Classification of the molten salt surface tension techniques by the fraction of the total determinations made by each technique as percent application*

Method	Percent application	Method	Percent application
Maximum bubble pressure.....	74.6	Pin method.....	3.2
Wilhelmy slide plate.....	7.2	Pendant drop.....	2.5
Capillary rise.....	5.7	Ring method.....	2.0
Maximum pull on cylinder.....	4.2	Sessile bubble.....	0.6

3.2. Maximum Bubble Pressure Method

The maximum bubble pressure method of determining the surface tension of a liquid, suggested by Simon [81]** in 1851, was first applied to molten salt systems in 1917, by Jaeger [46]. It involves the very slow formation of a bubble at the tip of a capillary immersed in the melt and the subsequent determination of the maximum pressure in the bubble at the very instant it bursts. Cantor [55] discussed the theory of bubble formation; his equation for the maximum bubble pressure [55, 56] is:

$$\gamma = \frac{pr}{2} \left[1 - \frac{2r}{3h} - \frac{1}{6} \left(\frac{r}{h} \right)^2 \cdot \cdot \cdot \right] \quad (1)$$

where γ = surface tension of the melt (dyne cm⁻¹),

^a When γ is treated as a free energy per unit area, it is given the unit, erg cm⁻²; this is dimensionally identical to dyne cm⁻¹.

^b For conversion to the SI system:*

$$1 \text{ dyne cm}^{-1} = 1 \times 10^{-3} \text{ Nm}^{-1}$$

*The NBS Office of Standard Reference Data, as administrator of the National Standard Reference Data System, has officially adopted the use of SI units for all NSRDS publications, in accordance with NBS practice. This publication does not use SI Units because contractual commitments with the author predate establishment of a firm policy on their use by NBS. The appropriate conversion factor is found above for γ . The NBS urges that specialists and other users of data in this field accustom themselves to SI Units as rapidly as possible.

**Figures in brackets indicate the literature references on page 109.

r = radius of the capillary (cm), p = maximum pressure difference between the inside and outside of the bubble at the level of the end of the tip (dyne cm⁻²), $h = \frac{p}{g(\rho - \rho')}$, the height (cm) of a column of the melt equivalent to pressure p , ρ = density of the melt being measured (gcm⁻³), ρ' = density of the gas (gcm⁻³), and g = acceleration of gravity.

Sugden [52a] showed that the Schrödinger approximation [56] is valid for values of $\sqrt{\frac{r}{h}} < 0.2$. For $\sqrt{\frac{r}{h}} > 0.2$, the method of successive approximations and the Sugden tables should be used. The thorough investigations of Hoffman [82] and Tripp [83] showed that the mathematical theory is in accord with experiment only if the bubbles are formed slowly (one bubble per 30 or 60 s). When the rate of bubble formation is high, the situation is more complex and not readily amenable to theoretical treatment.

The most extensive series of studies by this method are those of Jaeger [46] (51 salts) and Ellis et al. [34-39] (20 salts). The method is well suited for molten salts with surface tensions from 50 to

150 dyne cm⁻¹, and for measurements from room temperature to 1600 °C.

This method does not lend itself well for studies of viscous melts (e.g. ZnCl₂) or molten salts having high vapor pressures [31a]. The formation of bubbles may be erratic in such melts. If a series of smaller bubbles is formed on the "burst", the pressure drop will be stepwise in the system. Again, the bubble may not burst even though pressure is increased and decreased; another possible occurrence is that response to the bubble burst is slow and abnormally small in melts of this type.

Some of the experimental features that distinguish the high-temperature application of this technique from the ambient-temperature applications are as follows:

(a) Certain melts may be quite corrosive. The radius of the capillary tip should be checked, preferably after each experiment. The time and area of contact of the melt with various components of the surface tension assembly also should be minimized.

(b) Visual observations of the melt are frequently not possible. The contact of the capillary tip with the surface of the melt may have to be detected by indirect techniques (e.g. electrical contact).

(c) There may be a cooling effect at the surface of the melt during the formation and release of the bubbles from the capillary tip. Preheating of the inert bubbling gas to the temperature of the measurement has been recommended by Jaeger [46] and Semenchenko and Shikhobalova [4]. For slow bubbling rates, Dahl and Duke [31a] found this precaution unnecessary.

3.3. Detachment Methods

A "detachment method" is any method in which the force required to detach an object from the surface of the liquid is measured. The maximum pull just before the object is detached from the surface is equated to the weight of the object plus γL , where L is the total perimeter introduced into the melt. The weight of the liquid which has been raised above the liquid surface, at the moment of detachment, is thus given by the total tension that its surface will support if the contact angle is zero. The following four methods are molten salt surface tension detachment methods.

(a) Wilhelmy Slide Plate Method

In the Wilhelmy application [84] of the above principle, the maximum pulling force is determined for the detachment of a thin platinum plate from the liquid surface. For a straight edge, this force is proportional to the surface tension of the liquid. The plate is suspended from one arm of a balance and is dipped into the liquid; the melt container is then lowered until detachment occurs. The "pull" on the balance arm is noted at the instant detachment

occurs. The surface tension is calculated by the expression:

$$W_{\text{tot}} = W_{\text{plate}} + 2\gamma(L + x) \quad (2)$$

where L = width of the slide, x = thickness of the slide, and W_{tot} , W_{plate} = observed weights at the moment of detachment and before dipping into liquid, respectively. End effects are assumed negligible. This technique has been estimated to be accurate to within ± 0.1 percent for room temperature measurements of aqueous and organic liquids [57]. Bertozzi [26, 45] has applied this technique to molten alkali metal nitrates (300–600 °C) and halides (600–900 °C) with an uncertainty of ± 0.6 percent.

(b) Pin Method

This was introduced by Janz and Lorenz [48, 49] to measure simultaneously the surface tensions and densities of molten alkali nitrates and carbonates; it has also been used by Morris, McNair and Koops [24] for the molten molybdates. The surface tension detachment pin is part of an Archimedean density bob. The weight is noted at room temperature and again at the working temperature after temperature equilibrium has been reached, so as to correct for the change in the buoyant force of air at higher temperatures. The crucible with the melt is then raised until the pin just contacts the melt; at this point the contact weight (W_c) and the relative crucible height are noted. The crucible is now lowered and the maximum "pull" at the moment of detachment is measured. The break-point weight (W_b) and the final rest weight (W_r) are noted.

The surface tension pull of the bob is $2\pi r\gamma$ dynes, where r and γ have their conventional significance; this is equal to the difference between the break and the rest weights, i.e. $gW_d = g(W_b - W_r)$ assuming zero angle of contact at the break-point. It follows that the surface tension is given by:

$$\gamma = \frac{gW_d}{2\pi r} = AW_d \quad (3)$$

where the constant A is a characteristic of the pin dimensions. If the radius of the pin at any temperature t °C is expressed as:

$$r = r_0(1 + \alpha\Delta t) \quad (4)$$

where r_0 = radius of the pin at the calibration temperature (t_0), α = the coefficient of linear expansion of the pin material, and $\Delta t = (t - t_0)$, eq (3) becomes:

$$\gamma = \frac{A_0 W_d}{1 + \alpha\Delta t} \quad (5)$$

where the constant $A_0 = \frac{g}{2\pi r_0}$. The value of A_0 can

be gained if r_0 is known or by the use of calibration liquids of accurately known surface tensions. Densities can be gained as part of the same experiment in the conventional manner by complete immersion of the Archimedean bob when the surface tension measurements have been completed.

(c) Maximum Pull on Cylinder Method

This is a modification of the ring method, the ring being replaced by a vertical hollow cylinder. It has been widely used at ambient and high temperatures. An equation similar to that developed by Harkins, Young and Cheng [65] for the ring method is used to calculate the surface tension, i.e.:

$$\gamma = \frac{Mg}{4\pi R} F \quad (6)$$

where R = the mean radius of the cylinder (cm), F = a dimensionless factor depending on R^3/V and $R/xV = (M/\rho_l)$ is the volume of liquid held up by the cylinder (cm^3), and x = the thickness of the cylinder wall (cm).

In using this method for determining the surface tensions of silicate slags, King found [58] that the values of the F factors for a cylinder were not the same as for a ring. Liquids of known surface tensions were used to gain correction factors and thus the calibration curve applicable to the cylinder ($R = \frac{1}{4}$ in) was found. Bradbury and Maddocks [27a, 27b], using a cylinder also with $R = \frac{1}{4}$ in, reported a somewhat different calibration curve for $F(R^3/V)$. No explanation was advanced for the difference in the two calibration curves. The difference may be attributed, in part, to the neglect of the dimensionless variable R/x in the preceding calibration; differences in the thickness of the walls of the cylinders used by King [58] and by Bradbury et al. [27a, 27b] would also contribute but the information is insufficient to assess this further.

The effect of the contact angle, θ , on the maximum pull on the cylinder was investigated by King; it was negligible unless $\theta > 40^\circ$.

(d) Ring Method

A thorough discussion of the theory and experimental aspects of this method at ambient temperature is given by Harkins elsewhere [51]. The principles of this method were developed largely in two papers by Harkins, Young and Cheng [65], and Harkins and Jordan [66]. Callis, van Wazer, and Metcalf used this technique for sodium metaphosphate and mixtures of Na_2O and P_2O_5 at high temperatures, with due cognizance of the factors [66] necessary for the calculation of surface tensions. A comparison of the surface tension data for sodium metaphosphate by this method [28, 88] and two other techniques, i.e., the maximum pull on cylinder [27] and the maximum bubble

pressure method [9, 46] is given in figure 1. (Percent departure is defined on p. 55). The percent departures are calculated relative to the data of Owens and Mayer [88] as the reference.

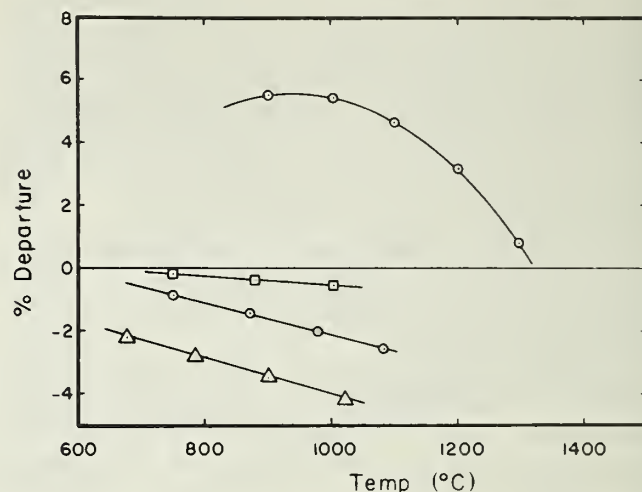


FIGURE 1. Comparison of percent departure of the data for NaPO_3 .

- Owens and Mayer (1964) [88]
- Jaeger (1917) [46]
- Callis, van Wazer and Metcalf (1955) [28]
- Bradbury and Maddocks (1959) [27b]
- △ Sokolova and Voskresenskaya (1963) [9]

3.4. Capillary Rise Method

The capillary rise method is the simplest for closed systems (a requirement for low-melting salts of high volatility, e.g., UF_6 [50], ZnCl_2 [38] GaCl_3 [42–44]); it is best suited for systems where visual observation of the melt is possible. The principles of this method are well established. For the single capillary technique, Harkins [51] gives:

$$\gamma = \frac{1}{2} r h g (\rho - \rho') \quad (7)$$

where γ = surface tension (dyne cm^{-1}), r = radius of capillary (cm), h = height of meniscus from immersed end of capillary (cm), g = acceleration of gravity, ρ = density of liquid measured (g cm^{-3}) and ρ' = density of vapor (g cm^{-3}). If a double capillary assembly is used, the Sugden relation [52] applies:

$$\gamma = \frac{1}{2} H (\rho - \rho') g \left(\frac{1}{b_1} - \frac{1}{b_2} \right)^{-1} \quad (8)$$

where γ , g , ρ , ρ' , carry the conventional significance and H is the vertical distance between the lowest points of the menisci in the two vertical tubes of radius r_1 and r_2 (cm), and b_1 and b_2 are the radii of curvature at these points (cm).

The derivations of eqs (7) and (8) assume a zero contact angle. This has been confirmed experimentally for water and some organic liquids in contact with glass by Richards and Carver [53]; the assumption has been carried over to molten salt surface tension assemblies, apparently without

TABLE 2. Molten salt surface tension techniques: Theory and practice

Method	Temperature range (°C)	Surface tension range (dyne cm ⁻¹)	Equations
Maximum bubble pressure..	ambient-1600	50-150	$\gamma = \frac{pr}{2} \left[1 - \frac{2r}{3h} - \frac{1}{6} \left(\frac{r}{h} \right)^2 \dots \right]$
Capillary rise.....	ambient- 200	10- 50	Single cap. $\gamma = \frac{1}{2} rhg(\rho - \rho')$ Double cap. $\gamma = \frac{1}{2} rHg(\rho - \rho') \left(\frac{1}{b_1} - \frac{1}{b_2} \right)^{-1}$
Plate.....	300- 900	50-150	$W_{\text{tot}} = W_{\text{plate}} + 2\gamma(L + x)$
Pin.....	350-1100	150-250	$\gamma = \frac{A_0 W_d}{1 + \alpha \Delta t}; A_0 = \frac{g}{2\pi r_0}$
Pendant drop.....	100-2000	150-700	Apply $\frac{d_s}{d_m}$, d_m , ρ to tables [56]
Cylinder.....	800-1400	50-150	$\gamma = \frac{Mg}{4\pi R} F_{\text{cyl}}$
Ring.....	650- 950	50-150	$\gamma = \frac{Mg}{4\pi R} F_{\text{ring}}$
Sessile bubble.....	350- 500	10- 50	Use Bashforth and Adams tables

independent verification for such high temperature systems.

3.5. Methods Based on the Shape of Static Drops on Bubbles

The general procedure for this class of methods is to form a liquid drop or a gas bubble in the liquid studied under conditions such that it is not subject to disturbance, and then to make certain measurements of its dimensions. These methods favor the observations of long term changes in surface tensions (i.e., under conditions when slow time effects are involved).

(a) Sessile Bubble Method*

This technique consists of forming a gas bubble (inert gas) at the tip of a vertically mounted square-ended tube immersed in the liquid which is contained in a spectrometer cuvette; microphoto-

graphic techniques are generally used to gain the dimensions while the bubble is stationary. The equatorial diameter and height of the bubble are thus gained (travelling microscope). The magnification factor can be checked readily by measuring the diameter of the tube. Only one molten salt system, ZnCl_2 [39] has been investigated by this technique. The Bashforth and Adams Tables [62] were used to evaluate the surface tensions from the dimensions of the bubbles. Because of difficulties in measuring the pertinent dimensions the results are of low precision.

(b) Pendant Drop Method

In this technique, the salt is melted and contacted with a rod of material that is inert to attack by the melt. By withdrawing the rod a drop hangs pendant on the end of the rod. Surface tension can be calculated from measurements of the absolute diameter of the pendant drop and a shape factor fixed by a "selected" diameter, d_s , defined as the diameter normal to the drop axis at a distance from the base of the drop equal to the maximum diameter, d_m of the drop. The surface tension is related to the liquid density, the absolute value of d_m , and the ratio $\frac{d_s}{d_m}$ as given by Adamson [56] elsewhere.

*The application of the sessile drop method apparently has not been considered for fused salts in the open literature. However, the method has been found useful for some molten fluoride mixtures [93]. If the purities of the cover gas, the substrate, and the fused salt are scrupulously maintained it is possible to obtain a precision better than 3 percent. It is estimated that the absolute accuracy of this very straight-forward method may be as good as the precision.

The surface tensions of the oxide systems, Al_2O_3 , B_2O_3 , GeO_2 , SiO_2 and P_2O_5 have been gained by this method; the overall uncertainty is estimated to be about ± 7 percent.

3.6. Summary

Some of the preceding observations are presented in a summary form in table 2. The ranges of surface tensions and temperatures relative to the applicability of each method are illustrated in a bar graph form in figure 2.

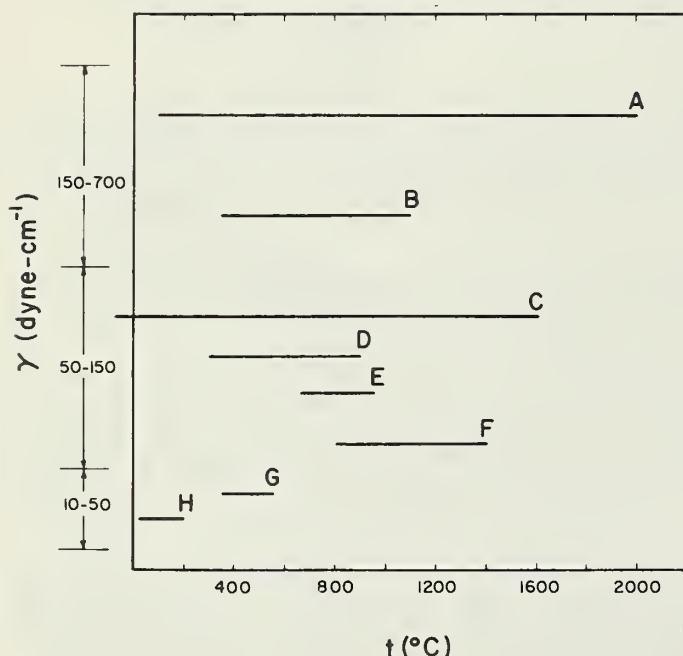


FIGURE 2. Surface tension range and temperature range for the various surface tension techniques.

A. Pendent drop; B. pin method; C. maximum bubble pressure; D. Wilhelmy slide plate; E. ring method; F. maximum pull on cylinder; G. sessile bubble; H. capillary rise. The vertical axis denotes the surface tension range in which the technique has been applied.

4. Treatment of Surface Tension Data

4.1. Statistical Analysis of Data

Linear and quadratic equations of surface tension-temperature relationship were fitted to available sets of experimental data by the method of least squares. The calculations were made on the digital computer facilities at Rensselaer Polytechnic Institute using double precision Fortran IV language. The criterion for choosing a linear or quadratic equation of best fit for a set of surface

tension-temperature data is the standard deviation computed from the residuals and is defined by:

$$s = \sqrt{\frac{\sum_{i=1}^n (\gamma_e - \gamma_c)^2}{n - q}}$$

where γ_e = the experimental surface tension value at each temperature, γ_c = the value calculated from the least squares equation at the same temperature as γ_e , n = number of experimental data points, and q = number of coefficients in the least squares equation (2 for linear and 3 for quadratic).

For most of the data, linear temperature-dependent equations proved the best fits; where there was a large scatter of experimental points over a wide temperature range, coupled with volatilizations and/or with possible partial decomposition of the melt, the quadratic equations were favored. If s -values of approximately the same magnitude were found for both linear and quadratic equations, the linear equation was chosen.

4.2. Selection of the Best Values

The data were classified into three general groups as follows:

Group A—More than one set of experimental data available

The surface tension investigations for each compound were assessed from the following viewpoints to select the most thorough study: experimental technique with emphasis on the preparation and purity of the salt concerned; number of measurements; temperature range of the measurements and chemical stability of the salt in this range; the standard error of estimate, s , of the data. Where possible, the uncertainty and precision of related molten salt results from each center were also taken into consideration. Departure graphs are used to illustrate the data status for compounds in this group.

Group B—One set of experimental data reported

For about two-thirds of the compounds in this group, the results are from one laboratory; a selection of "best value" is not feasible for these results. Estimates of precision, s , were obtained by least squares regression analyses of the experimental data, and uncertainties were estimated from a knowledge of the quantitative aspects of the experi-

mental procedures of the investigators. The remainder of the compounds were investigated in more than one center and frequently by more than one technique. Comparisons of values obtained from different laboratories and/or by different experimental methods thus make possible a selection of the best values for these salts. The final selection was always guided by details of the experimental work as well.

Group C—No experimental data points reported

The results for compounds in this group (MgCl_2 and $\text{Ca}(\text{PO}_3)_2$ excepted) were reported from one laboratory in the form of temperature-dependent equations only. The selection of "best values" is not feasible for such systems; the surface tension values in section 6 were gained from the equations; the estimates of uncertainty and precision in the temperature ranges within which the determinations were carried out are cited where possible.

As a subdivision within this group, salts were included for which one or two experimental points have been reported, e.g. UF_6 , CuCl , HgCl_2 , HgBr_2 , Al_2O_3 , PbO , FeO , and Cu_2S .

4.3. Estimation of Uncertainty

The departures of the results of individual investigations from the recommended values were used to firm up the estimates of uncertainty. Where this was not feasible (e.g., salts in Group B and C) more qualitative factors such as experimental techniques and previous investigations of the authors were used as a guide for uncertainty estimates. The precision of the data was an important consideration throughout. Such considerations lead to values for the relative estimates of uncertainties as low as ± 0.1 percent; however, it should be recognized that the absolute accuracy is not likely to be better than ± 2 percent. While it is generally accepted that impurities have minor effects on the surface tension of molten salts, the methods, dependent on contact angle, trace impurities (H_2O , FeO), may lead to significant errors. For FeO it has been estimated [90] that an error of about 0.5 percent in composition affects the surface tension values up to 2 percent.

For a comparison of the results from various laboratories with the numerical values of this compilation (sec. 6), the percent departure has been calculated as follows:

$$\text{Percent departure} = \left[\frac{\text{compared value} - \text{tabulated value}}{\text{tabulated value}} \right] \times 100$$

It should be noted that both the compared value and the tabulated value are the numerical values derived from the respective least squares equations. Percent departure graphs are given where possible to illustrate the results.

4.4. Preparation of the Tables

The surface tension values were computed for each salt at 10°C intervals from the corresponding "best" equation for the same temperature range for which the investigation was carried out. The melting point of the salt, the "best" equation, the precision estimate and the literature sources for both the surface tension and melting point are given in each table (sec. 6). The underscored literature reference indicates the source selected for the best values.

5. Discussion

In this section the following information is given for each compound; for the data used to gain the best equation such details as experimental technique, number of data points, temperature range are given; the precision, estimates of uncertainty, and where possible, percent departure values and graphs are also given; for many investigations the preparation, purification, and stability of the salt and other salient experimental features are discussed.

Lithium Fluoride, Rubidium Fluoride, Cesium Fluoride, and Lithium Chloride

[Classification: Group A, see tables 3, 6, 7, and 10, pp. 78 and 79 for numerical values]

The surface tensions of these four halides have been measured by Jaeger [46] and Ellis [37] (maximum bubble pressure method). The data of Ellis for all four halides, LiF (34 points, 895 to 1095°C), RbF (38 points, 795 to 945°C), CsF (36 points, 775 to 920°C), and LiCl (19 points, 645 to 865°C) are recommended as the "best" values. Jaeger's data show departures of 7.1 to 6.8 percent for LiF , 1.9 percent to -1.3 percent for RbF , 0.8 to 1.0 percent for CsF , and 6.8 to 5.0 percent for LiCl in the same temperature ranges, respectively. The departures are illustrated in figure 3 (a-d), respectively.

Some of the experimental aspects of Ellis' investigation [37] are as follows: the precautions outlined in section 3.2 for the maximum bubble pressure technique were taken into consideration; the surface tension assembly was in a dry box under

anhydrous conditions and nitrogen, the bubbling gas, was passed through NaK before it entered the capillary system.

The uncertainty estimates for these salts are: LiF, ± 3.0 percent; RbF, ± 1.0 percent; CsF, ± 1.0 percent, and LiCl, ± 3.0 percent.

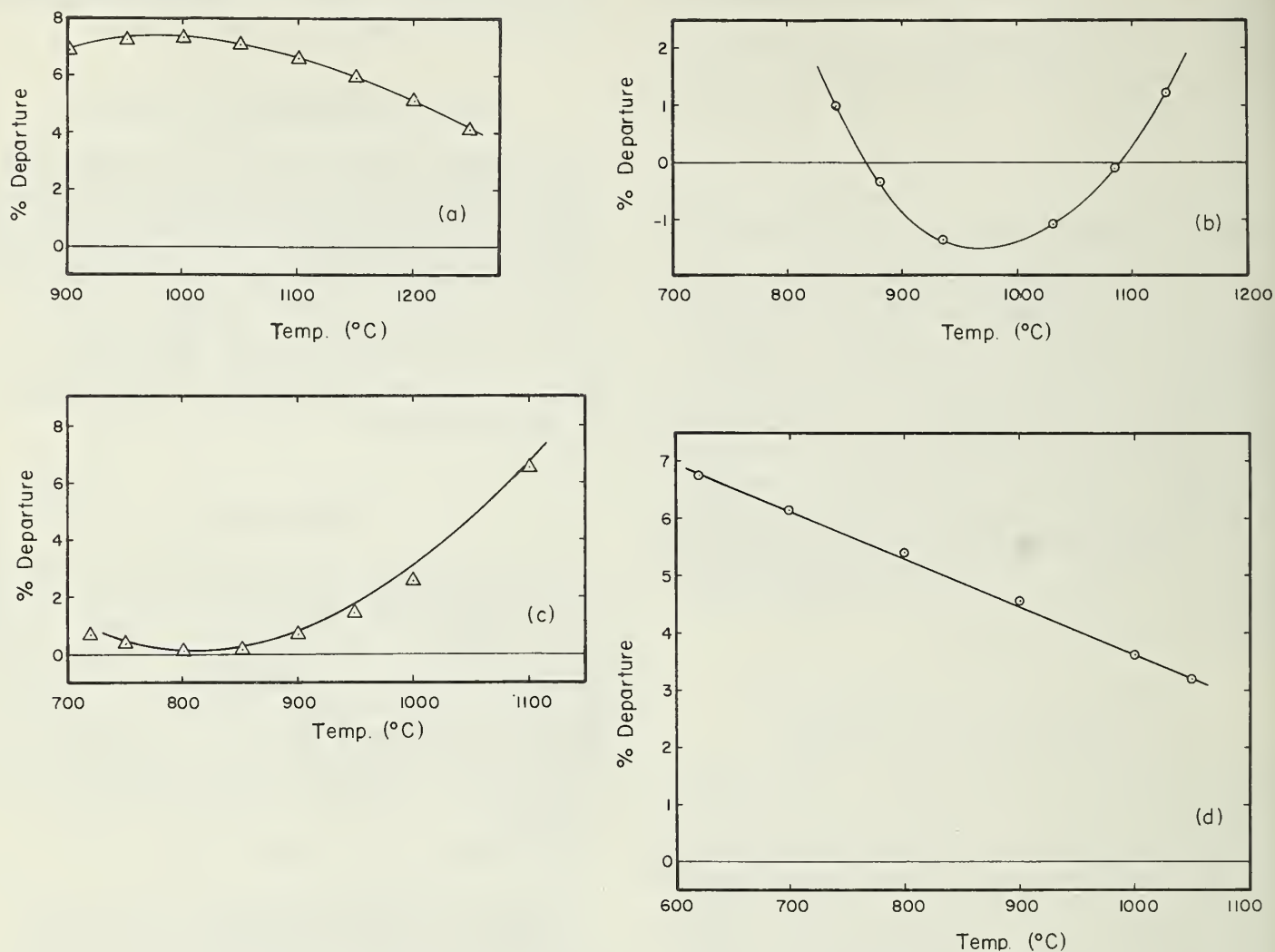


FIGURE 3. Comparison of percent departures for the data for LiF, RbF, CsF, and LiCl.

- a. LiF
 - Ellis (1961) [37]
 - Δ Jaeger (1917) [46]
- b. RbF
 - Ellis (1961) [37]
 - \odot Jaeger (1917) [46]
- c. CsF
 - Ellis (1961) [37]
 - Δ Jaeger (1917) [46]
- d. LiCl
 - Ellis (1961) [37]
 - \odot Jaeger (1917) [46]

Sodium Fluoride

[Classification: Group A; see table 4, p. 78 for numerical values]

The maximum bubble pressure technique has been used by three groups, [32, 37, 46] to establish the surface tension of molten NaF. The data of Bloom and Burrows [32] are recommended as the "best" values in the range 1000 to 1080 °C. Compared to the data of Bloom and Burrows, the results of Ellis [37] and Jaeger [46] show considerable departures (e.g., -13 percent and 9.8 percent, respectively, at 1050 °C). This comparison is illustrated in figure 4.

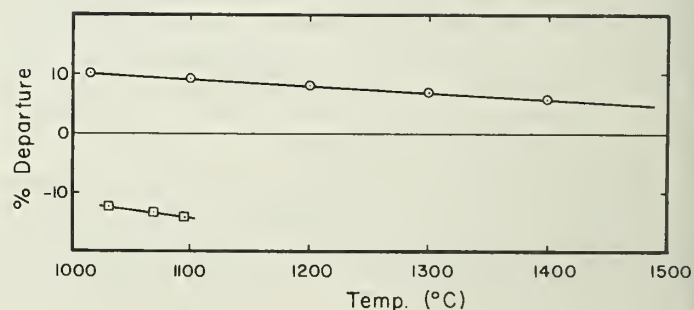


FIGURE 4. Comparison of percent departure of the data for NaF.

- Bloom and Burrows (1960) [32]
- \odot Jaeger (1917) [46]
- \square Ellis (1961) [37]

Some of the experimental aspects of the investigation of Bloom and Burrows [32] are as follows: analytical reagent sodium fluoride (98% NaF) was used; dry argon was used to form bubbles in the melt.

The uncertainty is estimated to be no better than ± 8.0 percent.

Potassium Fluoride

[Classification: Group B; see table 5, p. 78 for numerical values]

The surface tension of KF has been studied by Jaeger [46] (maximum bubble pressure technique). The data (12 points, 912 to 1310 °C) can be expressed by a quadratic equation ($\gamma = 176.2 - 0.108t - 0.333 \times 10^{-4}t^2$, $s = 0.3$ dyne cm^{-1}). The hygroscopic nature of KF and the wide temperature range undoubtedly contribute, in part, to the preference of a quadratic equation over a linear equation.

Some of the experimental aspects of Jaeger's work are as follows: platinum capillaries of radii 0.04935 to 0.05025 cm were used; nitrogen, the bubbling gas, obtained by heating aqueous solutions of NaNO_2 and NH_4Cl , was purified by passing respectively through alkaline-pyrogallol solution, concentrated H_2SO_4 and P_2O_5 ; it was preheated to the melt temperature before passing through the capillary system.

An accuracy estimate is not possible owing to insufficient information.

Rubidium Fluoride

(see under LiF, p. 55)

Cesium Fluoride

(see under LiF, p. 55)

Thorium Tetrafluoride and Uranium Tetrafluoride

[Classification: Group C; see tables 8 and 9, p. 79 for numerical values]

The surface tensions of molten ThF_4 and UF_4 have been determined by Kirshenbaum and Cahill [70] (maximum bubble pressure technique). About 25 experimental determinations were made over the whole liquidus temperature range of each salt, i.e., ThF_4 1110 °C (m.p.), 1680 °C (b.p.) and UF_4 1036 °C (m.p.), 1450 °C (b.p.). Argon, the bubbling gas, was passed through titanium flakes at 400 °C to remove traces of nitrogen, oxygen, and water vapor. The capillary tips were inspected after each run and mechanically treated prior to use. The main impurities in UF_4 and ThF_4 were UO_2F_2 and ThO_2 respectively. X-ray diffraction patterns re-

vealed that the concentration of ThO_2 in ThF_4 melt was less than 1 wt percent. Analysis of UF_4 melt at the end of the experiment indicated the presence of 0.5 to 1.0 wt percent UO_2F_2 , while the starting material contained 0.2 wt percent UO_2F_2 .

The uncertainty estimates for both salts are ± 3.0 percent.

Uranium Hexafluoride

[Classification: Group C; see table 10, p. 79 for numerical values]

Two surface tension values have been reported by Priest [50]: $\gamma = 17.66 \pm 0.51$ and 16.48 ± 0.06 dyne cm^{-1} at 65 °C and 72.5 °C, respectively. The capillary rise method was used and all measurements were under vacuum. Pyrex glass (outgassed and shown to be inert to attack by UF_6) was used for the experimental assembly. Uranium hexafluoride was purified by successive sublimations over anhydrous KF and distilled into the cell. The radius of the capillary was obtained by calibration with chloroform and benzene. An accuracy estimate is difficult due to lack of information.

Cryolite

[Classification: Group C; see table 11, p. 79 for numerical values]

The surface tension of molten Na_3AlF_6 has been determined by Bloom and Burrows [32] (maximum bubble pressure technique). The tabulated values for the range, 1000 to 1080 °C, were calculated from the equation reported by the authors [32] ($\gamma = 262.0 - 0.128t$, $s = 1.9$ dyne cm^{-1}). High-purity natural cryolite (99.6% Na_3AlF_6) was used in this investigation, the inert bubbling gas being dry argon. An estimate of accuracy is difficult since the experimental points were not reported and experimental detail is minimal.

Lithium Chloride

(see under LiF, p. 55)

Sodium Chloride

[Classification: Group A; see table 13, p. 80 for numerical values]

Three different techniques have been used to measure the surface tension of molten NaCl by eight groups of investigators; the method of maximum bubble pressure was employed in six studies [1, 4, 7, 13, 46, 60], the ring and Wilhelmy slide plate techniques in the other two [10, 45]. The results of Sokolova and Voskresenskaya [13] are recommended as the "best" values. The percent departures of the values of the other investigators from those of Sokolova are illustrated in figure 5.

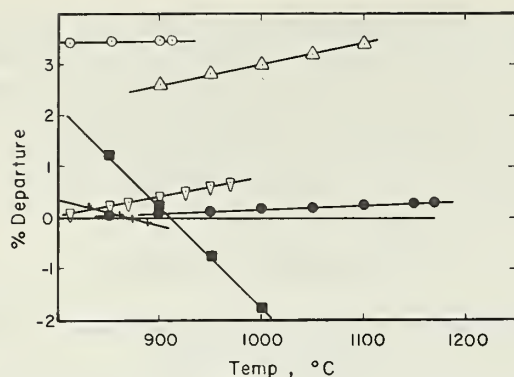


FIGURE 5. Comparison of percent departures of the data for NaCl.

- Sokolova and Voskresenskaya (1962) [13]
- Bertozzi (1965) [45]
- △ Semenchenko and Shikhobalova (1947) [4]
- Bloom, Davis and James (1960) [1]
- ▽ Desyatnikov (1956) [60]
- + Lantratov (1961) [7]
- Jaeger (1917) [46]

Some of the experimental aspects of Sokolova's investigation are as follows: NaCl was recrystallized twice, dried at 250 °C and stored in a desiccator over sulfuric acid until required for use; the temperature gradient in the region of the specimen was less than 0.5 deg cm⁻¹ for a distance of 2.5 to 3 cm; argon, used as the bubbling gas, was passed through pyrogallol solution, dried with concentrated H₂SO₄ and further with P₂O₅ supported on glass wool; a slow bubbling rate (one bubble per minute) was used for the surface tension measurement.

The uncertainty is estimated to be ± 0.1 percent.

Potassium Chloride

[Classification: Group A; see table 14, p. 80 for numerical values]

Two different techniques have been used to measure the surface tension of molten KCl by 10 groups; in nine [1, 4, 6, 12, 29, 31, 40, 46, 60] the maximum bubble pressure method was used, while the Wilhelmy slide plate technique was used in the remaining study [45]. The values of Dahl and Duke [31] ($s=0.4$ dyne cm⁻¹) in the range 810 to 880 °C are recommended as the "best" values. The departures of the values of other investigators from those of Dahl and Duke are illustrated in figure 6.

Some of the experimental aspects of the investigation of Dahl and Duke are discussed on p. 61. The accuracy is estimated to be ± 0.5 percent.

Rubidium Chloride

[Classification: Group A; see table 14, p. 80 for numerical values]

Two different techniques have been used to measure the surface tension of molten RbCl by

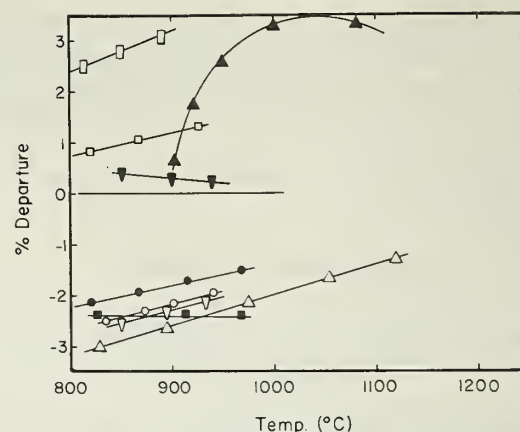


FIGURE 6. Comparison of percent departures of the data for KCl.

- Dahl and Duke (1957) [31a]
- ▲ Semenchenko and Shikhobalova (1947) [4]
- Bertozzi (1965) [45]
- ▼ Lehman (1959) [29]
- Bloom, Davis, and James (1960) [1]
- Peake and Bothwell (1954) [12]
- ▽ Neithamer and Peake (1961) [6]
- Desyatnikov (1956) [60]
- △ Jaeger (1917) [46]
- Reding (1966) [40]

three groups; the maximum bubble pressure method [4, 46], and the Wilhelmy slide plate method [45]. The values of Jaeger [46] are recommended as the "best" values in the range 750 to 1150 °C. Compared to the data of Jaeger, the results of Semenchenko and Shikhobalova [4] and Bertozzi [45] show departures of 0.1 percent (900 to 1000 °C) and -2.0 to -0.6 percent (730 to 860 °C) respectively. Figure 7 illustrates this comparison.

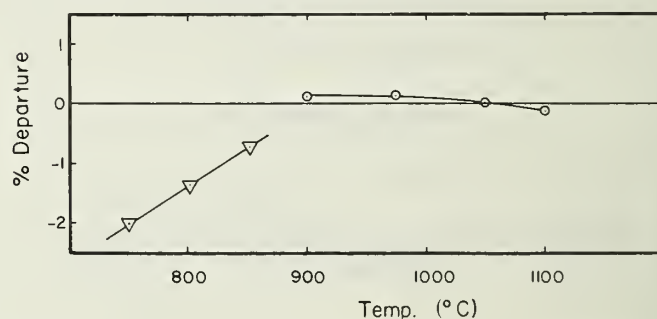


FIGURE 7. Comparison of percent departures of the data for RbCl.

- Jaeger (1917) [46]
- Semenchenko and Shikhobalova (1947) [4]
- ▽ Bertozzi (1965) [45]

Some of the experimental aspects of Jaeger's work are discussed on p. 57. The uncertainty is estimated to be ± 0.1 percent.

Cesium Chloride

[Classification: Group A; see table 16, p. 81 for numerical values]

Two different techniques have been used for the surface tension studies of molten CsCl by four

groups; in three [4, 29, 46] the maximum bubble pressure was used, while the Wilhelmy slide plate method was used in the other [45]. The values of Jaeger [46] are recommended as the "best" values in the range 663 to 1083 °C. Compared to the data of Jaeger, the results of Bertozzi [45], Semenchenko and Shikhobalova [4] and Lehman [29] show departures of -0.2 percent (700 to 800 °C), -0.2 to 0.4 percent (900 to 1080 °C), and -2.9 to -1.0 percent (750 to 880 °C) respectively; this is illustrated in figure 8.

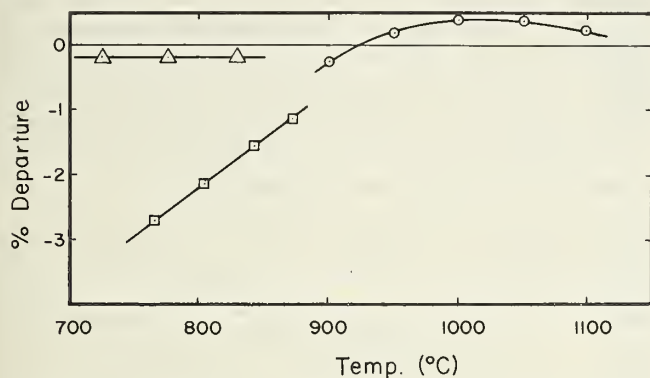


FIGURE 8. Comparison of percent departures of the data for CsCl.

- Jaeger (1917) [46]
- Semenchenko and Shikhobalova (1947) [4]
- △ Bertozzi (1965) [45]
- Lehman (1959) [29]

Some of the experimental aspects of Jaeger's [46] work are discussed on p. 57. The uncertainty is estimated to be +0.2 percent.

Cuprous Chloride and Cuprous Sulfide

[Classification: Group C; see table 17, p. 81 for numerical values]

One experimental point for each compound, reported by Boni and Derge [92], appear to be the only values established to date. The melts were contained in alumina crucibles and the surface tensions were measured by the maximum bubble pressure technique, with argon as the bubbling gas.

The information is insufficient for an accuracy estimate.

Silver Chloride, Silver Bromide, and Silver Iodide*

[Classification: Group C; see tables 18 and 26, pp. 81 and 83 for numerical values]

The surface tension of molten AgCl and AgBr have been determined by Boardman, Palmer, and Heymann [14] (maximum bubble pressure tech-

*Silver iodide was also studied by the same authors [14] over the temperature range 560 to 620 °C, but no values were reported. Above 620 °C, AgI decomposes and reproducible surface tension results are not possible.

nique). No thermal decomposition was observed in the temperature ranges investigated, i.e., AgCl (460 to 700 °C) and AgBr (460 to 620 °C).

The capillaries were drawn from British-Thomson-Houston C46 glass tubing and were calibrated with tap water. Nitrogen was used as bubbling gas; details of purification were not given. Contact of the capillary tip with the melt surface was determined visually. Mechanical checks and recalibration of the capillaries were done after each experiment.

The uncertainty of the data for both salts is estimated to be ± 1.0 percent.

Magnesium Chloride

[Classification: Group C; see table 19, p. 81 for numerical values]

Two different techniques have been used to measure the surface tension of molten MgCl_2 ; the maximum bubble pressure method [40, 60] and the ring method [10]. The values of Desyatnikov [60] are recommended as the "best" values in the temperature range of 720 to 930 °C. The results of Barzakovskii [10] and Reding [40] showed departures of ± 0.1 percent and 8.5 to 7.5 percent respectively in the same temperature range; these are illustrated in figure 9.

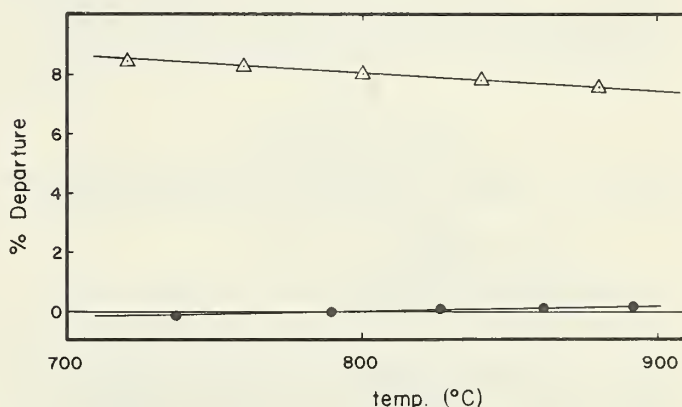


FIGURE 9. Comparison of percent departures of the data for MgCl_2 .

- Desyatnikov (1956) [60]
- △ Reding (1966) [40]
- Barzakovskii (1940) [10]

Some details of the Desyatnikov investigation are as follows: anhydrous MgCl_2 was melted under a stream of dry hydrogen chloride over a period of 6 to 8 hr to prevent hydrolysis; analysis for SO_4 and Fe indicated that these constituents did not exceed 0.005 percent, while the MgO content was found to be about 0.2 to 0.4 percent; CO_2 was used as the bubbling gas and was bubbled through the melt for 20 to 30 min prior to the surface tension measurements; due cognizance of the precautions outlined in section 3.2 was taken; the capillary tips were refinished before each experiment, and the bubbling rate was 2 to 3 bubbles per minute; measurements

at each temperature were carried out consecutively with three capillaries, each of a different diameter.

The uncertainty is estimated to be ± 0.8 percent.

Calcium Chloride

[Classification: Group A; see table 20, p. 82 for numerical values]

The surface tension of molten CaCl_2 has been determined by three groups [7, 29, 37] (maximum bubble pressure method). The values of Ellis [37] in the range 840 to 920 °C are recommended as the "best" values. The departures of the values of the other investigators from those of Ellis are: Lantratov [7], -0.5 to $+0.5$ percent in the range 720 to 870 °C and Lehman [29], 2.0 to 5.5 percent in the range 796 to 914 °C. These are shown in figure 10.

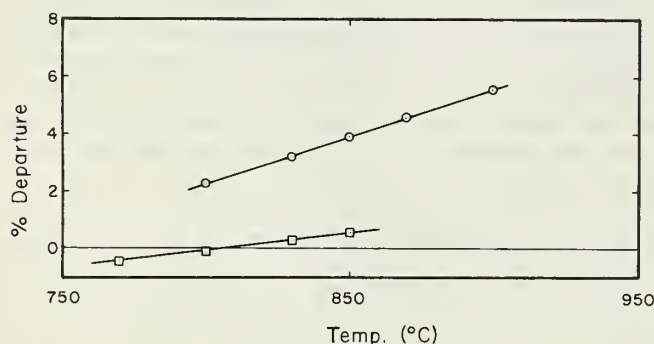


FIGURE 10. Comparison of percent departures of the data for CaCl_2 .

— Ellis (1961) [37]
 ○ Lehman (1959) [29]
 □ Lantratov (1961) [7]

Some of the experimental aspects of Ellis' investigation are discussed on p. 55. CaCl_2 was prepared by the action of HCl on CaCO_3 . The crystallized product was dried under vacuum (0.3 mm Hg) at about 300 °C over a period of 48 hr. The product was then transferred to a Vycor flask* attached to a high vacuum system, (25 μm or better) and fused. The temperature was increased gradually over a period of 3 to 4 days, after which the salt was kept molten for several hours. The vacuum was broken with dry N_2 , followed by bubbling the melt with anhydrous HCl . The salt was then cooled in an atmosphere of HCl , the sample was transferred to a mason jar for storage (Cl, 35.69% by analysis; 35.82% theoretical.)

The uncertainty is estimated to be ± 0.5 percent.

*Certain commercial products and instruments are identified in order to specify adequately the experimental procedure. In no case does such identification imply recommendation or endorsement by the National Bureau of Standards, nor does it imply that the product or equipment identified are necessarily the best available for the purpose.

Strontium Chloride

(see under CaI_2 , p. 65)

Barium Chloride

[Classification: Group A; see table 22, p. 82 for numerical values]

The surface tension of molten BaCl_2 has been determined by two groups [12, 13] (maximum bubble pressure technique). The results of Peake and Bothwell [12] (8 points, 981–1041 °C) are recommended as the "best" values. Compared to the values of Peake and Bothwell, the data of Sokolova and Voskresenskaya [13] show departures of 2.4 to 3.2 percent in the same temperature range; this comparison is illustrated in figure 11.

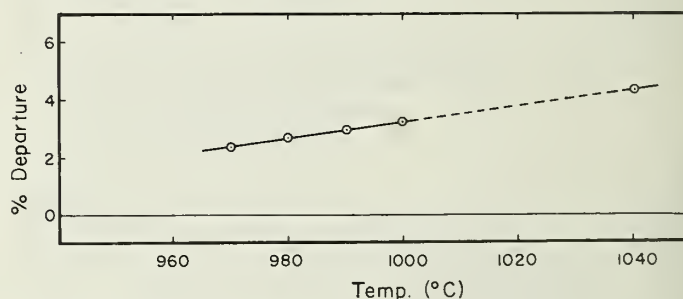


FIGURE 11. Comparison of percent departures of the data for BaCl_2 .

— Peake and Bothwell (1954) [12]
 ○ Sokolova and Voskresenskaya (1962) [13]

Some of the experimental details of the work of Peake and Bothwell are discussed on p. 73. The uncertainty is estimated to be ± 1.0 percent.

Zinc Chloride and Zinc Bromide

[Classification: Group C; see tables 23 and 40, pp. 82 and 87 respectively for numerical values]

The surface tensions of these two zinc halides have been determined by Ellis [39] using the sessile bubble technique. Results showed that the temperature coefficients of surface tension for both of these salts were not constant over the ranges of temperature of investigation (ZnCl_2 , 300 to 720 °C and ZnBr_2 , 500 to 670 °C).

Some of the experimental aspects of Ellis' investigation are as follows: N.F. grade zinc halides were dehydrated by heating gently under vacuum up to their melting points, sparging the melt with the corresponding anhydrous hydrogen halide up to 700 °C and then purging the melt with purified and dried argon or helium.

The uncertainties are estimated to be ± 3.0 percent (in the range 300 to 550 °C for ZnCl_2 and 500 to 600 °C for ZnBr_2) and ± 1.5 percent (in the range 550 to 700 °C for ZnCl_2 and 600 to 700 °C for ZnBr_2).

Cadmium Chloride, Cadmium Bromide, Calcium Bromide, and Barium Iodide

[Classification: Group B; see tables 24, 41, 35, and 49, pp. 83, 85, 87, and 89 respectively for numerical values]

The surface tensions of these four Group II metal halides have been determined by Ellis [35, 37] (maximum bubble pressure technique). The data for CdCl_2 (14 points, 580 to 921 °C) and CdBr_2 (38 points, 635 to 775 °C) are better represented by quadratic equations ($s=0.3$ dyne cm^{-1} and $s=1.0$ dyne cm^{-1} respectively), while those for CaBr_2 (3 points, 774 to 809 °C) and BaI_2 (9 points, 826 to 958 °C) are represented by linear equations ($s=0.3$ dyne cm^{-1} and $s=0.4$ dyne cm^{-1} respectively).

The precautions outlined in section 3.2 for the maximum bubble pressure technique were taken into consideration. The surface tension assembly was in a dry box under anhydrous conditions and nitrogen, the bubbling gas, was passed through NaK before it entered the capillary system.

The anhydrous salts were prepared and purified as follows: CdCl_2 —Reagent-grade CdCl_2 was vacuum dried at 200° C for 2 days; CdBr_2 —Reagent-grade CdBr_2 was vacuum dried at 200 °C for 2 days; CaBr_2 — $\text{CaBr}_2 \cdot n\text{H}_2\text{O}$ was first predried under vacuum (0.3 mm Hg) at 300 °C; it was then transferred to a Vycor flask attached to a high vacuum system (25 μm or better) and fused; the temperature was increased gradually over a period of 3 to 4 days, after which the salt was kept molten for several hours; the vacuum was broken in dry nitrogen atmosphere followed by bubbling the melt for several hours with anhydrous HBr ; the salt was then cooled in an atmosphere of HBr and transferred to a mason jar for storage (Br, 79.79% by analysis; 79.95%, theoretical); BaI_2 —Barium Iodide (obtained from John Harrison Laboratory, University of Pennsylvania) was used without further purification.

The uncertainty of the surface tension data for the above salts is estimated to be ± 1.0 percent.

Stannous Chloride

[Classification: Group A; see table 25, p. 83 for numerical values]

The surface tension of molten SnCl_2 has been measured by Jaeger [46] and Ellis [35] (maximum bubble pressure method). The data of Ellis (8 points, 280 to 480 °C) are recommended as the "best" values. Comparison of percentage departure of Jaeger's results is illustrated in figure 12.

Some of the experimental aspects of Ellis' investigation are discussed on p. 55. SnCl_2 was prepared by fusing commercial anhydrous stannous chloride under vacuum, sparging with anhydrous HCl and finally filtering under vacuum through a sintered Pyrex disk.

The uncertainty is estimated to be ± 1.0 percent.

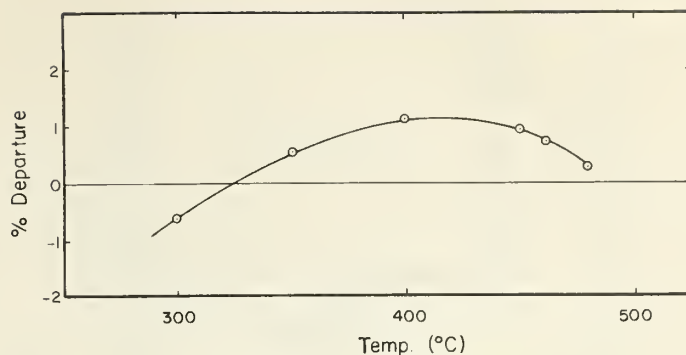


FIGURE 12. Comparison of percent departures of the data for SnCl_2 .

— Ellis (1958) [35]
○ Jaeger (1917) [46]

Mercuric Chloride and Mercuric Bromide

[Classification: Group C; see table 26, p. 83 for numerical values]

The surface tensions of molten HgCl_2 and HgBr_2 have been determined by Prideaux and Jarratt [59] (maximum bubble pressure method). Very few experimental details were given by the investigators. Mercuric chloride and mercuric bromide exhibit narrow liquidus temperature ranges [69] (277 to 304 °C and 241 to 319 °C respectively).

An accuracy estimate is not possible owing to insufficient information.

Lead Chloride

[Classification: Group B; see table 27, p. 83 for numerical values]

Two different techniques have been used to measure the surface tension of molten PbCl_2 by three groups; the maximum bubble pressure method [1, 31] and the ring method [10]. The values of Dahl and Duke [31] in the temperature range 520 to 580 °C are recommended as the "best" values. Compared to the data of Dahl and Duke, the results of Bloom, Davis, and James [1] and Barzakovskii [10] show departures of ± 0.3 percent and 5 to 10 percent respectively. The volatility of the melt partially accounts for the high percent departure of the values by the ring method. Comparison of percent departure of the data of Bloom et al. is illustrated in figure 13. Some of the experimental aspects of the investigation of Dahl and Duke [31] are as follows: The precautions outlined in section 3.2 for the maximum bubble pressure technique were taken into consideration. PbCl_2 (Baker and Adamson) was heated to a temperature just above its melting point (498 °C), cooled, powdered, and stored in a drying oven at 110 °C until used. The system was under an atmosphere of helium during surface tension measurement.

The uncertainty is estimated to be ± 1.0 percent.

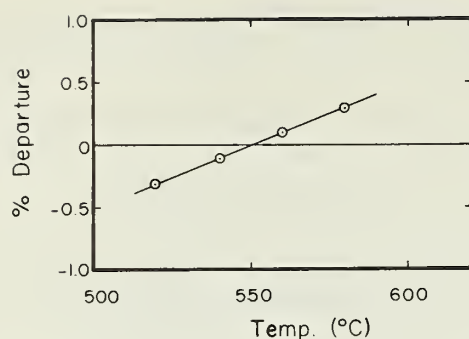


FIGURE 13. Comparison of percent departures of the data for PbCl_2 .
 — Dahl and Duke (1958) [31]
 ○ Bloom, Davis and James (1960) [1]

Aluminum Chloride

[Classification: Group B; see table 28, p. 84 for numerical values]

The surface tension of molten AlCl_3 has been determined by Nisel'son and Sokolova [61] (200 to 320 °C, capillary rise technique). The anhydrous salt was prepared by doubly distilling analytical reagent grade AlCl_3 in evacuated glass ampules with a few aluminum turnings to reduce any impurity of iron to the divalent form (less volatile). Capillaries made of borosilicate glass (readily wetted by liquid AlCl_3) were used.

An estimate of accuracy is not possible owing to insufficient information.

Gallium Trichloride

[Classification: Group A; see table 29, p. 84 for numerical values]

The surface tension of molten GaCl_3 has been determined by two groups [44, 61] (capillary rise technique). The data of Greenwood and Wade [44] (15 points, 80 to 140 °C) are recommended as the "best" values. The results of Nisel'son and Sokolova [61] show departure of -4.8 to -5.7 percent in the same temperature range. This comparison is illustrated in figure 14.

The uncertainty for the surface tension values is estimated to be ± 3.0 percent.

Gallium Trichloride Monopiperidine, Gallium Trichloride Dipiperidine, and Gallium Trichloride Pyridine Complex

[Classification: Group C; see table 30, p. 84 for numerical values]

The surface tension for these organic complex compounds of GaCl_3 were investigated by Greenwood and Wade [42, 43] (120 to 160 °C; double-capillary rise method). The thermal stability for this series of compounds was confirmed as part of this investigation through the related physical

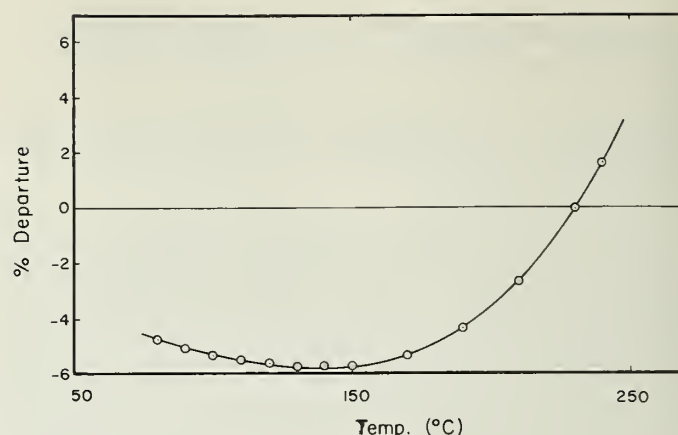


FIGURE 14. Comparison of percent departures of the data for GaCl_3 .
 — Greenwood and Wade (1957) [44]
 ○ Nisel'son and Sokolova (1965) [61].

property measurements, e.g., conductivity, viscosity, density, and vapor pressure. Although the experimental details for the surface tension measurements were insufficient to warrant an accuracy estimate, the data appear to be of good quality.

Bismuth Trichloride and Bismuth Tribromide

[Classification: Group B; see tables 31 and 42, pp. 84 and 87 respectively]

The surface tensions of molten BiCl_3 and BiBr_3 have been determined by Jaeger [46] (maximum bubble pressure technique). The data for both BiCl_3 (5 points, 271 to 382 °C) and BiBr_3 (9 points, 250 to 442 °C) are better represented by quadratic equations ($s = 0.1 \text{ dyne cm}^{-1}$ and $s = 0.1 \text{ dyne cm}^{-1}$ respectively).

The experimental technique and the uncertainty of the data of Jaeger are discussed on p. 73.

Bismuth trichloride and bismuth tribromide are thermally stable up to their boiling points 441 °C and 461 °C respectively [69].

Sodium Bromide

[Classification: Group A; see table 32, p. 85 for numerical values]

Two different techniques have been used to measure the surface tension of molten NaBr by four groups; the maximum bubble pressure method [1, 13, 46] and the Wilhelmy slide plate method [45]. The results of Sokolova and Voskresenskaya [13] (10 points, 750 to 800 °C) are recommended as the "best" values. The values of Bloom, Davis, and James [1], Bertozzi [45], and Jaeger [46] show departures of -5 to -3 percent (750 to 850 °C), -0.5 to 0.5 percent (750 to 850 °C) and 2.0 to 2.5 percent (700 to 800 °C) respectively. These are illustrated in figure 15.

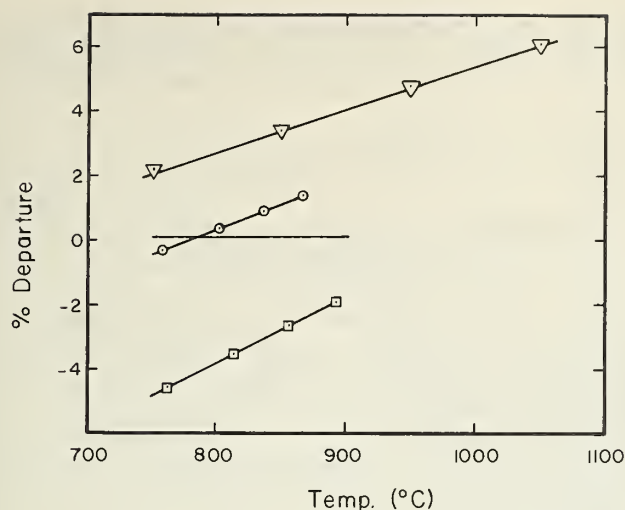


FIGURE 15. Comparison of percent departures of the data for NaBr.
 — Sokolova and Voskresenskaya (1962) [13]
 ▽ Jaeger (1917) [46]
 ○ Bertozzi (1965) [45]
 □ Bloom, Davis and James (1960) [1]

Some of the experimental aspects of the investigation of Sokolova and Voskresenskaya are discussed on p. 58. The uncertainty is estimated to be ± 0.5 percent.

Potassium Bromide

[Classification: Group A; see table 33, p. 85 for numerical values]

Two different experimental techniques have been used to measure the surface tension of molten KBr by four groups; the maximum bubble pressure method [1, 36, 46] and the Wilhelmy slide plate method [45]. The results of Bloom, Davis, and James [1] are recommended as the "best" values in the range 750 to 950 °C. The departures of the values of other investigators are: Ellis [36], 1.8 to 3.2 percent (803 to 972 °C); Bertozzi [45], 2.9 to 3.0 percent (740 to 850 °C) and Jaeger [46], -1.0 to -0.8 percent (775 to 920 °C). These departures are illustrated in figure 16.

Some of the experimental aspects of the investigation of Bloom et al. are as follows: analytical reagent grade KBr was oven dried before use; dry nitrogen was used to bubble through the melt; the precautions outlined in section 3.2 for the maximum bubble pressure were taken into consideration.

The uncertainty is estimated to be ± 1.0 percent.

Rubidium Bromide and Cesium Bromide

[Classification: Group B; see tables 34 and 35, p. 85 for numerical values]

Two different techniques have been used to measure the surface tension of molten RbBr and CsBr by two groups; the Wilhelmy slide plate method [45] and the maximum bubble pressure method [46]. The results of Bertozzi [45] are recommended as the

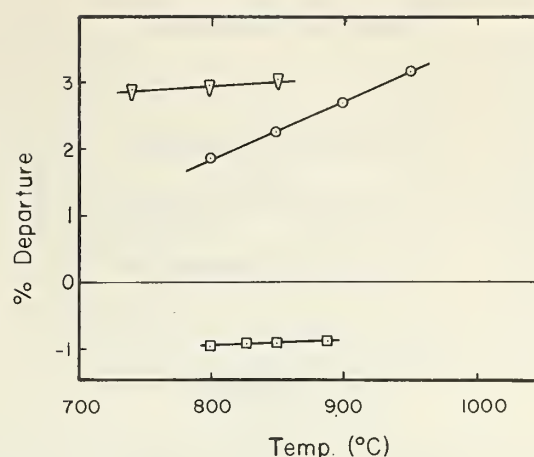


FIGURE 16. Comparison of percent departures of the data for KBr.
 — Bloom, Davis and James (1960) [1]
 ▽ Bertozzi (1965) [45]
 □ Jaeger (1917) [46]
 ○ Ellis (1959) [36]

"best" values for both salts. Jaeger's results show departures of 2.5 to 3.0 percent in the range 720 to 830 °C for RbBr and -0.5 to -1.0 percent in the range 666 to 750 °C for CsBr. The departures are shown in figure 17 (a, b).

The uncertainties for these two salts are estimated to be ± 0.6 percent.

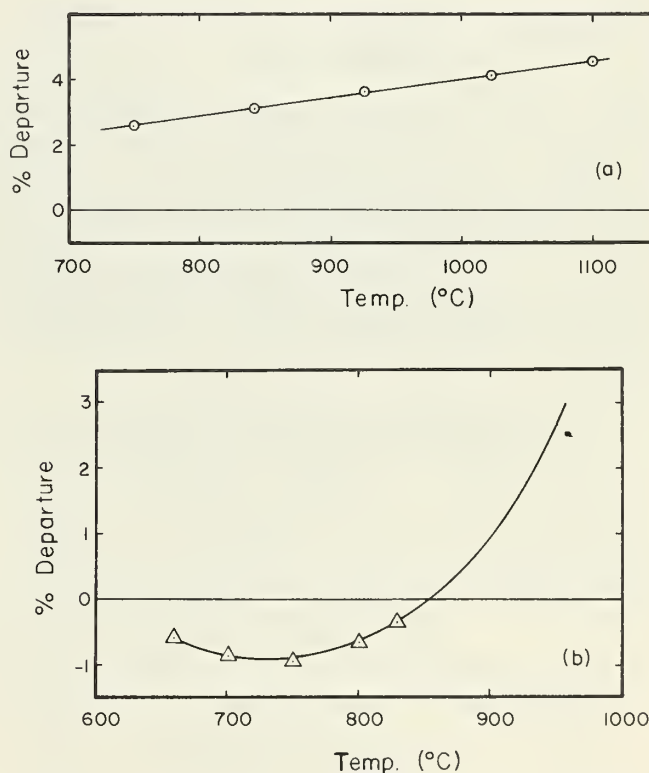


FIGURE 17. Comparison of percent departures of the data for RbBr and CsBr.

- a. RbBr
 — Bertozzi (1965) [45]
 ○ Jaeger (1917) [46]
 b. CsBr
 — Bertozzi (1965) [45]
 △ Jaeger (1917) [46]

Calcium Bromide

(see under CdCl_2 , p. 61)

Strontium Bromide

(see under CaI_2 , p. 65)

Barium Bromide

(see under CaI_2 , p. 65)

Zinc Bromide

(see under ZnCl_2 , p. 60)

Cadmium Bromide

(see under CdCl_2 , p. 61)

Mercuric Bromide

(see under HgCl_2 , p. 61)

Bismuth Bromide

(see under BiCl_3 , p. 62)

Sodium Iodide

[Classification: Group A; see table 43, p. 87 for numerical values]

The maximum bubble pressure technique has been used by three groups [1, 37, 46] to measure the surface tension of molten NaI . The results of Ellis [37] (28 points, 755 to 885 °C) are recommended as the "best" values. The departures of the values of Bloom, Davis, and James [1] and Jaeger [46] are -4.5 percent and -0.5 to 4.0 percent respectively in the range 760 to 820 °C. These are illustrated in figure 18.

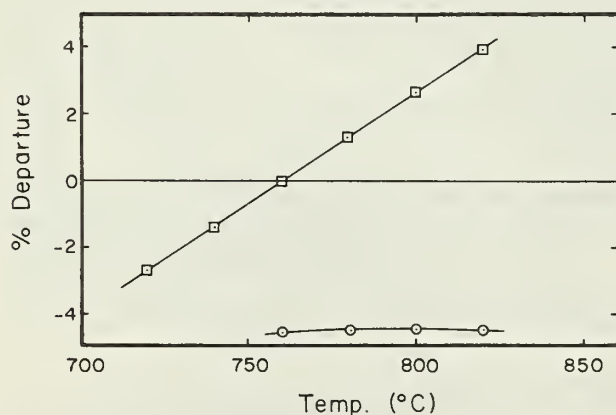


FIGURE 18. Comparison of percent departures of the data for NaI .

— Ellis (1961) [37]
□ Jaeger (1917) [46]
○ Bloom, Davis and James (1960) [1]

Some of the experimental aspects of Ellis' investigation are discussed on p. 55. The uncertainty for this salt is estimated to be ± 0.2 percent.

Potassium Iodide

[Classification: Group B; see table 44, p. 88 for numerical values]

The surface tension of molten KI has been measured by Jaeger [46] and Bloom, Davis, and James [1] (maximum bubble pressure method). The values of Bloom et al. in the range 700 to 900 °C are recommended as the "best" values ($s=0.2$ dyne cm^{-1}). The percent departure of Jaeger's results from those of Bloom, Davis, and James is illustrated in figure 19.

Some of the experimental details of the investigation of Bloom et al. are as follows: analytical reagent grade KI was oven dried before use; dry nitrogen was used to bubble through the melt; the precautions outlined in section 3.2 for the maximum bubble pressure were taken into consideration.

The uncertainty is estimated to be ± 0.5 percent.

Rubidium Iodide and Cesium Iodide

[Classification: Group B; see tables 45 and 46, p. 88 for numerical values]

The surface tensions of molten RbI and CsI have been determined by Jaeger [46] (maximum bubble pressure technique). The data for both RbI (8 points, 673 to 1016 °C) and CsI (8 points, 653 to 1030 °C) are better represented by quadratic equations ($s=0.1$ dyne cm^{-1} and $s=0.2$ dyne cm^{-1} respectively).

Some of the experimental aspects of Jaeger's investigation are discussed on p. 57. An accuracy estimate is not possible owing to limited information.

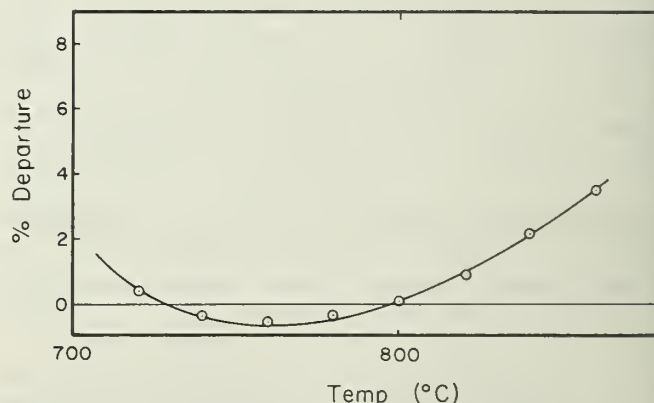


FIGURE 19. Comparison of percent departure of the data for KI .
— Bloom, Davis and James (1960) [1]
○ Jaeger (1917) [46]

Calcium Iodide, Strontium Chloride, Strontium Bromide, Strontium Iodide, and Barium Bromide

[Classification: Group B; see tables 47, 21, 38, 48, and 49, pp. 89, 82, 86, 89, and 89 respectively for numerical values]

The surface tensions of these five alkaline earth-metal halides have been measured by Ellis [34] (maximum bubble pressure technique).

The precautions outlined in section 3.2 for the maximum bubble pressure technique were taken into consideration. The surface tension assembly was in a vacuum type dry box. The compounds were prepared by thermal dehydration of the corresponding reagent grade hydrates under vacuum. A pressure of 0.3 mm mercury was maintained and temperatures up to 300 °C were used. The drying periods were 48 to 72 hr during which time heat was applied gradually. Both $\text{CaI}_2 \cdot n\text{H}_2\text{O}$ and $\text{SrBr}_2 \cdot 6\text{H}_2\text{O}$ were mixed with an excess of the corresponding ammonium halide and ball milled prior to vacuum drying. Strontium iodide was synthesized by the reaction of HI and SrCO_3 and dehydrating the crystallized product.

The uncertainty of the surface tension data for these five salts is estimated to be ± 1.0 percent.

Strontium Iodide

(see under CaI_2 , p. 65)

Barium Iodide

(see under CdCl_2 , p. 61)

Boron Trioxide

[Classification: Group B; see table 50, p. 90 for numerical values]

Two different techniques have been used to measure the surface tension of molten B_2O_3 : the maximum pull on cylinder technique [33] and the pendant drop technique [30]. The results of Shartsis and Canga [33] are recommended as the "best" values; the precision for the data is estimated to be $s = 0.04$ dyne cm^{-1} . Both investigations showed a positive temperature coefficient. Fajans [94] has discussed some anomalous temperature coefficients for surface tension and other physical properties for B_2O_3 . The departure of Kingery's values from those of Shartsis and Canga varies from -5 percent to $+5$ percent in the range 800 to 1200 °C. This is illustrated in figure 20.

Some of the experimental features of Shartsis and Canga are as follows: the oxide was prepared by thermal dehydration of boric acid; the temperature was controlled to ± 5 °C during the measurement; a sensitive optical lever was incorporated into the analytical balance to increase the sensitivity of

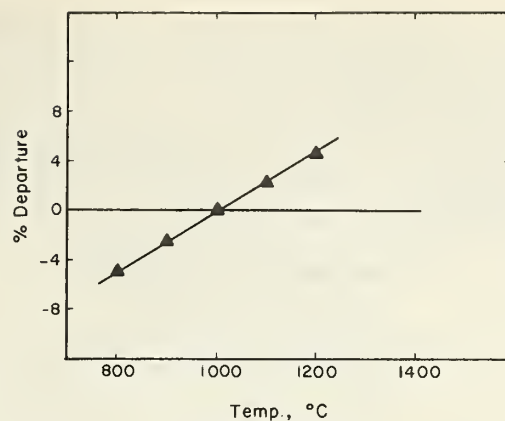


FIGURE 20. Comparison of percent departures of the data for B_2O_3 .

— Shartsis and Canga (1949) [33]
△ Kingery (1959) [30]

measuring the maximum pull exerted on the cylinder (Pt-20% Rh); measurements were taken at 100 °C intervals.

The uncertainty is estimated to be ± 4.0 percent.

Aluminum Oxide, Silicon Dioxide, and Germanium Dioxide

[Classification: Group C; see tables 49, 50, and 51, pp. 89 and 90 for numerical values]

The surface tensions of molten Al_2O_3 , SiO_2 and GeO_2 have been measured by Kingery [30] (pendant drop technique). In the case of Al_2O_3 , only one determination was made at 2050 ± 15 °C ($\gamma = 690$ dyne cm^{-1}). For SiO_2 and GeO_2 , the temperature coefficients of surface tension were determined; these values are positive, showing an unusual temperature dependence of the surface tension property in these single-component liquids.

Some of the experimental details of Kingery's investigation are as follows: samples of Al_2O_3 were formed by coating the tip of a molybdenum rod with a suspension of the melt and melting in an atmosphere of purified helium; with SiO_2 and GeO_2 , samples were formed by dipping a platinum rod in the corresponding oxide melt (in a platinum crucible) to gather a satisfactory gob; all materials were of analytical reagent-grade purity and were used without further purification; owing to clouding of the furnace windows, a significant error was introduced in the temperature measurement.

The uncertainty for the surface tension values is estimated to be no better than ± 7.0 percent.

Lead Oxide

[Classification: Group C; see table 51, p. 90 for numerical values]

The surface tension of PbO has been measured by Shartsis, Spinner, and Smock [91] (maximum pull on cylinder). The two values reported (132.0

dyne cm^{-1} at 900°C and 134.8 dyne cm^{-1} at 1000°C) indicate a positive temperature coefficient in this range of temperature.

Some of the experimental aspects of the investigation of Shartsis, Spinner, and Smock [91] are discussed on p. 65. An accuracy estimate is not possible owing to insufficient information.

Phosphorous Trioxide

[Classification: Group B; see table 54, p. 91 for numerical values]

The surface tensions for this compound have been measured by Schenck, Mihr, and Banthien [5]. The data (4 points, 30 to 110°C) have been used to generate a linear equation and the precision is $s = \pm 0.2$ dyne cm^{-1} .

An accuracy estimate is not possible owing to insufficient information.

Phosphorus Pentoxide

[Classification: Group C; see table 55, p. 91 for numerical values]

Surface tension data for "liquid P_2O_5 " in the temperature range of 100 to 300°C , have been reported by Kingery [30]. Comparison with the melting point [69] for anhydrous P_2O_5 , indicates that the samples used by Kingery were not one-component systems, but consisted possibly of a mixture of phosphorus oxides and/or were not anhydrous P_2O_5 .

Ferrous Oxide

[Classification: Group C; see table 51, p. 90 for numerical values]

The surface tension of FeO has been measured by Kozakevitch [90] (maximum pull on cylinder technique). The data (5 points) cover a very narrow temperature range (1415 to 1423°C); also the Fe_2O_3 impurity in the oxide was as much as 5 wt percent. It was estimated by the author that an error of 0.5 percent in composition may result in an error of 1 to 2 percent in the surface tension value. No attempt to generate an equation is made; instead a mean value of 585 dyne cm^{-1} is reported. This value is in reasonable agreement with the one reported elsewhere [87].

Cuprous Sulfide

(see under CuCl , p. 59)

Thallous Sulfide

[Classification: Group C; see table 56, p. 91 for numerical values]

The surface tension of Tl_2S has been determined by Lazarev and Abdusalyamova [85] (maximum

bubble pressure technique) in the range 500 to 700°C . The experimental data (5 points) give the following linear equation: $\gamma = 231.4 - 0.0356t$ ($s = \pm 0.4$ dyne cm^{-1}).

An accuracy estimate is not possible owing to insufficient information.

Lithium Metaborate, Sodium Metaborate, and Potassium Metaborate

[Classification: Group B; see tables 57, 58, and 59 p. 92 for numerical values]

The surface tensions of these three high melting salts have been determined by Jaeger [46] (maximum bubble pressure technique). The experimental data of Jaeger for LiBO_2 (14 points, 880 to 1520°C), NaBO_2 (10 points, 1015 to 1441°C) and KBO_2 (4 points, 992 to 1142°C) have been used to generate the corresponding least squares equations.

The experimental aspects and the accuracy estimates of Jaeger's investigation are discussed on p. 73. Decomposition of LiBO_2 into Li_2O at 1200°C was observed by the author.

Lithium Carbonate

[Classification: Group B; see table 60, p. 92 for numerical values]

Two different methods have been used to measure the surface tension of Li_2CO_3 by two groups: the pin detachment method [49] and the maximum bubble pressure method [76]. The values of Janz and Lorenz [49] are recommended as the "best" values in the range 750 to 850°C . The results of Moiseev and Stepanov [76] show departures of 0.3 to 0.6 in the same temperature range. The departure is illustrated in figure 21.

Some of the experimental details of the investigation of Janz and Lorenz are as follows: Li_2CO_3 , reagent grade quality, was dried to constant weight under an atmosphere of CO_2 at 600°C and stored in a desiccator over P_2O_5 until required; surface

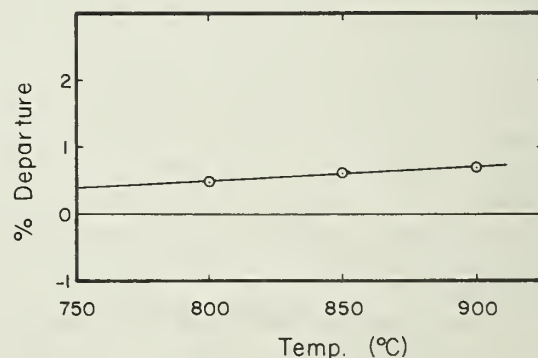


FIGURE 21. Comparison of percent departures of the data for Li_2CO_3 .
— Janz and Lorenz (1961) [49]
○ Moiseev and Stepanov (1964) [76]

tension measurements were made in an atmosphere of CO_2 at pressures in large excess to the dissociation partial pressure of the carbonate; since dissociation to oxide would lead to irreproducibility, the measurements were made in thermal cycles at temperatures randomly selected, first higher, then lower, then higher and so on, to detect possible changes in the values of the surface tension.

The uncertainty is estimated to be ± 0.3 percent or better.

Sodium Carbonate and Potassium Carbonate

[Classification: Group B; see tables 61 and 62 p. 93 for numerical values]

The surface tensions of these two molten carbonates have been determined by Janz and Lorenz [49] (pin detachment method). The linear equation expresses the data (10 points, 870 to 1010 $^{\circ}\text{C}$) for Na_2CO_3 with a precision, $s = 0.1$ dyne cm^{-1} , and the quadratic equation expresses the data for K_2CO_3 (14 points, 910 to 1010 $^{\circ}\text{C}$) with precision, $s = 0.2$ dyne cm^{-1} .

Some of the experimental aspects of the investigation of Janz and Lorenz are discussed on p. 66. The uncertainty is estimated to be ± 0.3 percent or better.

Lithium Nitrate

[Classification: Group B; see table 63, p. 93 for numerical values]

Two different techniques have been used to measure the surface tension of molten LiNO_3 by three groups; the maximum bubble pressure method [19, 46] and the Wilhelmy slide plate technique [26]. The values of Bertozzi and Sternheim [26] are recommended as the "best" values in the temperature range 300 to 500 $^{\circ}\text{C}$. The results of Jaeger [46] and Addison and Coldrey [19] show departures of 1.5 to 0.3 percent and -0.3 to $+0.2$ percent respectively in the same temperature range; these departures are shown in figure 22.

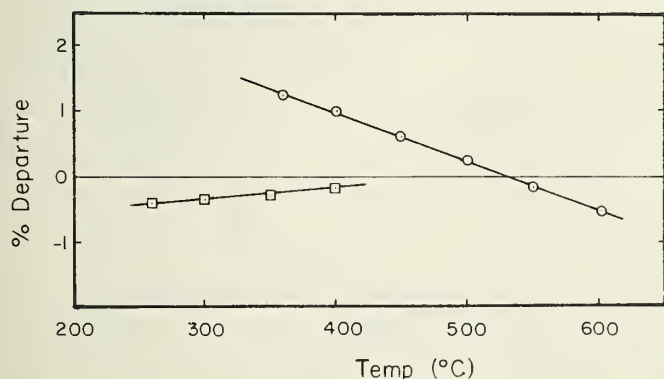


FIGURE 22. Comparison of percent departures of the data for LiNO_3 .

- Bertozzi and Sternheim (1946) [26]
- Jaeger (1917) [46]
- Addison and Coldrey (1961) [19]

Some of the experimental details of the investigation of Bertozzi and Sternheim are as follows: a platinum plate (edge length 15 mm and thickness 0.1 mm) was used. The temperature was measured a few mm above the surface of the melt and was accurate to ± 1 $^{\circ}\text{C}$. B. D. H. salts of analytical purity were dried and used without further purification.

The uncertainty is estimated to be ± 0.5 percent.

Sodium Nitrate

[Classification: Group A; see table 64, p. 93 for numerical values]

Two different techniques have been used to measure the surface tension of molten NaNO_3 by six groups; the maximum bubble pressure method [1, 18, 19, 41, 46], and the Wilhelmy slide plate method [26]. The results of Dahl and Duke [18] (22 points, 320 to 600 $^{\circ}\text{C}$) are recommended as the "best" values. The departure of the values of other investigators are: Bloom, Davis, and James [1], -2 to 1 percent; Addison and Coldrey [19], -2 to -1 percent; Semenchenko and Shikhobalova [41], -0.5 to 2.5 percent; Bertozzi and Sternheim [26], -0.6 to -0.4 percent and Jaeger [46], 0.9 to 1.3 percent. The percent departures are shown in figure 23.

The experimental aspects of the investigation of Dahl and Duke [18] are discussed on p. 61. The uncertainty is estimated to be ± 0.5 percent.

Potassium Nitrate

[Classification: Group A; see table 65, p. 94 for numerical values]

Three different techniques have been used to measure the surface tension of molten KNO_3 by six groups; the maximum bubble pressure method [1, 18, 19, 46], the Wilhelmy slide plate technique [26] and the pin method [48]. The values of Janz and

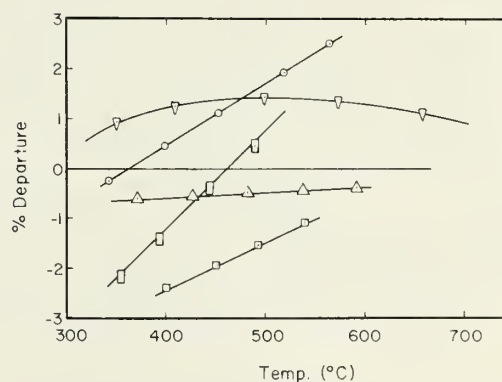


FIGURE 23. Comparison of percent departure of the data for NaNO_3 .

- Dahl and Duke (1958) [18]
- Semenchenko and Shikhobalova (1947) [41]
- ▽ Jaeger (1917) [46]
- Bloom, Davis and James (1960) [1]
- △ Bertozzi and Sternheim (1964) [26]
- Addison and Coldrey (1961) [19]

Lorenz [48] are recommended as the "best" values ($s = 0.1 \text{ dyne cm}^{-1}$) in the range 345 to 465 °C. The departures of the values of the other investigators from those of Janz and Lorenz are: Bloom, Davis, and James [1], -1.6 to -0.3 percent; Addison and Coldrey [19], 0.7 to -0.5 percent; Bertozzi and Sternheim [26], 1.1 to 0.5 percent; Dahl and Duke [18], 2 percent and Jaeger [46], 2.2 percent. The percent departures are shown in figure 24.

The experimental aspects of the investigation of Janz and Lorenz [48] are discussed on p. 66. The uncertainty is estimated to be ± 0.5 percent.

Rubidium Nitrate

[Classification: Group B; see table 66, p. 94 for numerical values]

Two different techniques have been used to measure the surface tension of molten RbNO_3 by two groups; the maximum bubble pressure method [46] and the Wilhelmy slide plate technique [26]. The values of Bertozzi and Sternheim [26] are recommended as the "best" values in the range 330 to 600 °C. The percent departure of Jaeger's values from those of Bertozzi and Sternheim varies from -0.3 to -3.8 in the same temperature range; this is shown in figure 25.

Some of the experimental details of the investigation of Bertozzi and Sternheim are discussed on p. 67. The uncertainty for this salt is estimated to be ± 0.5 percent.

Cesium Nitrate

[Classification: Group B; see table 67, p. 94 for numerical values]

Two different techniques have been used to measure the surface tension of molten CsNO_3 by three groups; the maximum bubble pressure

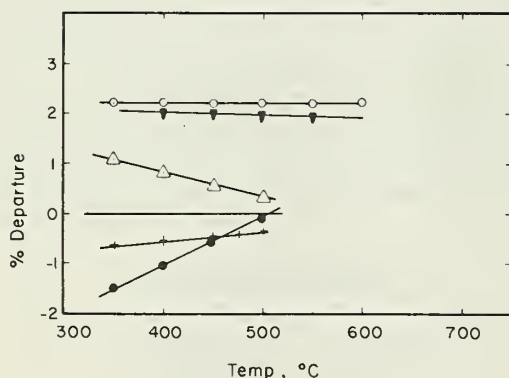


FIGURE 24. Comparison of percent departures of the data for KNO_3 .

- Janz and Lorenz (1960) [48]
- Jaeger (1917) [46]
- ▼ Dahl and Duke (1958) [18]
- △ Bertozzi and Sternheim (1964) [26]
- + Addison and Coldrey (1961) [19]
- Bloom, Davis and James (1960) [1]

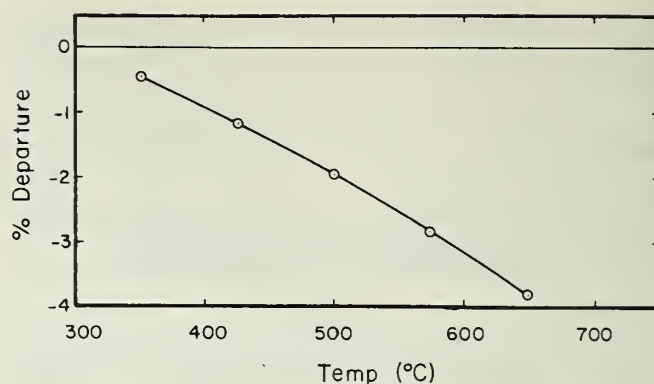


FIGURE 25. Comparison of the percent departures of the data for RbNO_3 .

- Bertozzi and Sternheim (1964) [26]
- Jaeger (1917) [46]

method [19, 46], and the Wilhelmy slide plate technique [26]. The values of Bertozzi and Sternheim [26] are recommended as the "best" values in the range 420 to 600 °C. Compared to the results of Bertozzi and Sternheim the values of Addison and Coldrey [19] show departures of 1.0 to 2.5 percent in this range, while those of Jaeger [46], show departures of 1.5 to -1.0 percent for the same range. The departures are illustrated in figure 26.

Some of the experimental details of the investigation of Bertozzi and Sternheim [26] are discussed on p. 67. The uncertainty for this salt is estimated to be ± 0.5 percent.

Silver Nitrate

[Classification: Group B; see table 68, p. 94 for numerical values]

Two different techniques have been used to measure the surface tension of molten AgNO_3 by four groups; the maximum bubble pressure method [1, 18, 19] and the Wilhelmy slide plate method [26]. The values of Dahl and Duke [18] are recommended as the "best" values in the temperature range 222 to 352 °C. Compared to the data of Dahl

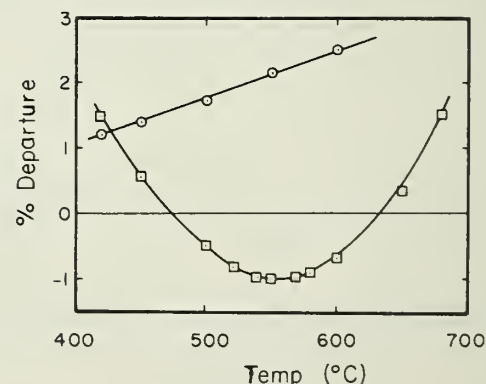


FIGURE 26. Comparison of percent departures of the data for CsNO_3 .

- Bertozzi and Sternheim (1964) [26]
- Addison and Coldrey (1961) [19]
- Jaeger (1917) [46]

and Duke, the values of Bloom, Davis, and James [1], Addison and Coldrey [19] and Bertozzi and Sternheim [26] show departures of -0.9 to 0.05 percent, 1.4 to -0.2 percent and 0.1 to -0.4 percent respectively in the same temperature range. These departures are illustrated in figure 27.

The experimental aspects of the investigation of Dahl and Duke are discussed on p. 61. The thermal decomposition of AgNO_3 has been studied by Peltier and Duval [77] using thermogravimetric technique. Results showed that AgNO_3 (m.p. 210°C) is thermally stable up to 473°C , above which decomposition into NO_2 , O_2 and metallic Ag occurs. At 608°C , decomposition is complete and pure metallic silver remains. All the surface tension measurements were carried out at temperatures well below 473°C and thus the stability of melt was established.

The uncertainty for this salt is estimated to be ± 1.0 percent.

Thallium Nitrate

[Classification: Group B; see table 69, p. 95 for numerical values]

The surface tension of molten TlNO_3 has been measured by Jaeger [46] and Addison and Coldrey [19] (maximum bubble pressure technique) in the temperature ranges 210 to 430°C and 226 to 458°C , respectively. The values of Addison and Coldrey are recommended as the "best" values. Compared to the data of Addison and Coldrey, the results of Jaeger show departure of 25 to 28 percent in the temperature range 226 to 460°C . This comparison is illustrated in figure 28.

Some of the experimental aspects of the investigation of Addison and Coldrey [19] are discussed on p. 70. The thermal decomposition of TlNO_3 has been studied by Wendlandt [72] using thermogravimetric technique. Results showed that TlNO_3

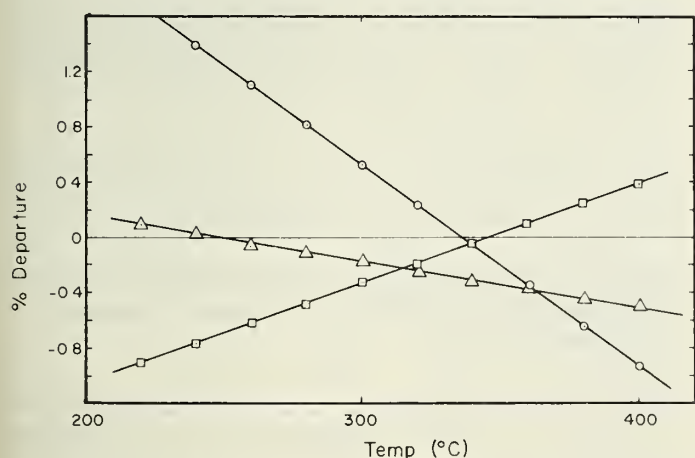


FIGURE 27. Comparison of percent departures of the data for AgNO_3 .

- Dahl and Duke (1958) [18]
- Addison and Coldrey (1961) [19]
- △ Bertozzi and Sternheim (1964) [26]
- Bloom, Davis and James (1960) [1]

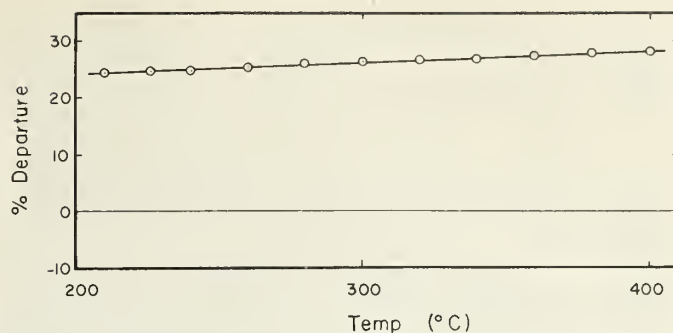


FIGURE 28. Comparison of percent departures of the data for TlNO_3 .

- Addison and Coldrey (1961) [19]
- Jaeger (1917) [46]

(m.p. 207°C) is thermally stable up to 265°C , above which the anhydrous salt begins to lose oxides of nitrogen. Between 460 and 505°C , the thermogravimetric curve exhibits a horizontal weight level (the composition data did not correspond to oxides of thallium). At 505°C , further weight losses occurred and decomposition was complete at 725°C . Thus, it should be noted that the two surface tension investigations were carried out in and above the stability range of TlNO_3 and the results should be viewed with some reservations.

The uncertainty for this salt is estimated to be ± 12 percent.

Ammonium Nitrate

[Classification: Group C; see table 70, p. 95 for numerical values]

The surface tension of molten NH_4NO_3 has been measured by Addison and Coldrey [19] (maximum bubble pressure technique) in the temperature range 170 to 220°C .

The decomposition of molten NH_4NO_3 in the range 180 to 280°C was studied by Guiochon and Jacque [75] using thermogravimetric technique. Results showed that the loss in weight of NH_4NO_3 with time in this temperature range is attributed to two phenomena: evaporation and decomposition; the latter is a first order process with the rate constant k given by $k = k_0 e^{-E/RT}$, where $k_0 = 10^{11.5}$ and $E = 36,500 \pm 1,800$ cal. Condensation of the salt vapor and of water vapor (a decomposition product) was also observed.

The surface tension values, thus represent, in part, that of decomposed melt and should be viewed with reservations. An estimate of accuracy is not possible due to insufficient information.

Calcium Nitrate, Strontium Nitrate, and Barium Nitrate

[Classification: Group C; see table 71, p. 91 for numerical values]

The surface tensions of molten $\text{Ca}(\text{NO}_3)_2$, and $\text{Sr}(\text{NO}_3)_2$ and $\text{Ba}(\text{NO}_3)_2$ have been determined by

Addison and Coldrey [19] (maximum bubble pressure technique). For $\text{Ca}(\text{NO}_3)_2$ and $\text{Sr}(\text{NO}_3)_2$ the authors reported only one data point for each salt (101.5 ± 0.4 dyne cm^{-1} at 560°C and 128.4 ± 0.5 dyne cm^{-1} at 615°C respectively). The data for $\text{Ba}(\text{NO}_3)_2$ (11 points, 600 to 660°C) are better represented by a linear equation ($\gamma = 143.7 - 0.015t$, $s = 0.6$ dyne cm^{-1}).

Some of the experimental details of the investigations of Addison and Coldrey, are as follows: argon (purity, 99.98%), further purified by passage through Linde molecular sieve (grade 4S), was used as the bubbling gas; supermax glass vessels and capillaries were used; analytical reagent grade salts, dried at 110°C for several hours, were used without further purification.

The stabilities of the melts investigated are summarized as follows:

	$\text{Ca}(\text{NO}_3)_2$	$\text{Sr}(\text{NO}_3)_2$	$\text{Ba}(\text{NO}_3)_2$
	$^\circ\text{C}$	$^\circ\text{C}$	$^\circ\text{C}$
Clear, pale amber liquid, gas evolution negligible.....	550	605	595
Small gas bubbles perceptible in melt.....	560	615	630
Gas evolution sufficient to interfere with surface tension measurement.....	575	635	675

Accuracy estimates are not possible for these salts owing to insufficient information.

Sodium Nitrite

[Classification: Group B; see table 72, p. 95 for numerical values]

The surface tension of molten NaNO_2 has been determined by three groups [1, 19, 23] (maximum bubble pressure method). The values of Addison and Coldrey [19] are recommended as the "best" values in the range 291 to 384°C . Compared to the values of Addison and Coldrey, the results of Bloom, Davis, and James [1] and Frame, Rhodes, and Ubbelohde [23] show departures of -1.0 to -0.1 percent and 2.6 to 0.2 percent, respectively, in the same temperature range. The departures are illustrated in figure 29.

The experimental aspects of the investigations of Addison and Coldrey [19] are discussed on p. . NaNO_2 has been shown to be stable below 620°C by Freeman [78] using a thermogravimetric technique. At 620°C , in the presence of O_2 , NaNO_2 undergoes partial oxidation and reaches a maximum weight gain at 740°C . At 780°C , rapid decomposition occurs, and further increase of temperature results in the formation of Na_2O (at 920°C).

The uncertainty for this salt is estimated to be ± 1.0 percent.

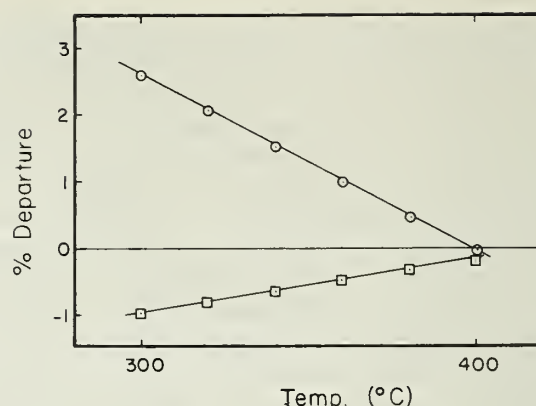


FIGURE 29. Comparison of percent departures of the data for NaNO_2 .

— Addison and Coldrey (1961) [19]

○ Frame, Rhodes and Ubbelohde (1959) [23]

△ Bloom, Davis and James (1960) [1]

Potassium Nitrite

[Classification: Group B, see table 73, p. 96 for numerical values]

The surface tension of molten KNO_2 has been determined by Addison and Coldrey [19], in the range 450 to 501°C (maximum bubble pressure method). The data (7 points, 4 of which were obtained during the heating cycle and the other 3 during subsequent cooling of the melt) are better represented by a linear equation with a precision, $s = 0.3$ dyne cm^{-1} .

Some of the experimental aspects of the investigation of the authors [19] are discussed on p. 70. The uncertainty is estimated to be ± 1.0 percent.

Lithium Silicate

[Classification: Group B; see table 74, p. 96 for numerical values]

The surface tension of Li_2SiO_3 has been determined by Jaeger [46] (maximum bubble pressure technique). The results (6 points, 1254 to 1601°C) are better represented by a quadratic equation with a precision, $s = 1.0$ dyne cm^{-1} .

The experimental aspects of Jaeger's investigation are discussed on p. 57. An accuracy estimate is not possible due to insufficient information.

Magnesium Metasilicate, Calcium Metasilicate, Manganese Metasilicate, and Manganese Orthosilicate

[Classification: Group C; see tables 75, 76, 77, and 78, pp. 96 and 97 respectively for numerical values]

The method of maximum pull on cylinder has been used by King [58] to measure the surface tensions of these four silicates. The surface tension-temperature equations used to generate the tabu-

lated values were obtained from the given temperature coefficients and the respective surface tension values at 1570 °C. It is to be noted that the coefficients are positive for these salts indicating an unusual behavior of temperature dependence for surface tension.

Some of the experimental aspects of King's investigation are as follows: correction factors applicable to the cylinder were determined using liquids of known surface tension; all four silicates were synthesized by grinding the respective oxides with SiO₂ and melting under nitrogen in graphite crucibles using induction heating; the melts were then cooled rapidly, ground, and ignited in oxygen before use for the surface tension measurements; iron crucibles were used for the manganese silicates to prevent reduction.

The pure oxides were obtained from the following materials; SiO₂, from rock quartz, ground and acid washed; MnO, prepared from manganese oxalate by heating in hydrogen and nitrogen (purity, 97.5 to 98.5%); CaO, obtained by ignition of A. R. calcium carbonate; and MgO, pure, fused magnesia.

An accuracy estimate is not possible owing to insufficient information.

Lithium Metaphosphate,* Cesium Metaphosphate, Strontium Metaphosphate, and Barium Metaphosphate

[Classification: Group C (except LiPO₃, Group B); see tables 79, 82, 84, and 85, pp. 97, 98, and 99 respectively for numerical values]

The surface tensions of molten LiPO₃, CsPO₃, Sr(PO₃)₂, and Ba(PO₃)₂ have been determined by Sokolova and Voskresenskaya [9] (maximum bubble pressure technique). The data for these salts are represented as follows: LiPO₃, 775 to 1072 °C, $\gamma = 206.1 - 0.0222t$ ($s = 1.0$ dyne cm⁻¹); CsPO₃, 737 to 1041 °C, $\gamma = 153.3 - 0.0487t$ ($s = 0.4$ dyne cm⁻¹); Sr(PO₃)₂, 1030 to 1082 °C, $\gamma = 233.7 - 0.00527t$ ($s = 0.5$ dyne cm⁻¹); Ba(PO₃)₂, 902 to 1075 °C, $\gamma = 239.9 - 0.0177t$ ($s = 0.5$ dyne cm⁻¹).

The experimental aspects of Sokolova's investigation are discussed on p. 58. The compounds were prepared by thermal decomposition of the corresponding dihydrogenphosphates; the latter were first obtained by the action of H₃PO₄ on carbonates of the alkali-metals and hydroxides of the alkaline earth-metals. (Analysis of the dihydrogenphosphates by their various constituents yielded the following results: Cs₂O/P₂O₅ = 1.00; SrO in Sr(H₂PO₄)₂ 36.4% (theoretical, 36.79%), and Ba in Ba(H₂PO₄)₂, 46.0% (theoretical, 46.28%).)

The uncertainty of the surface tension data for these four salts is estimated to be ± 1.0 percent.

Sodium Metaphosphate

[Classification: Group A; see table 80, p. 97 for numerical values]

Three different techniques have been used to measure the surface tension of NaPO₃ by five groups; the ring method [28, 88], the maximum pull on cylinder method [27b] and the maximum bubble pressure method [9, 46]. The results of Owens and Mayer [88] are recommended as the "best" values in the range 660 to 830 °C. The departures of the values of the other investigators are illustrated in figure 30.

Some of the experimental aspects of the investigation of Owens and Mayer [88] are as follows: NaPO₃ was prepared by thermal dehydration of reagent-grade NaH₂PO₄ at 520 °C for 1 week; analysis of the product by the zinc oxide method indicated a water content of less than 0.2 wt percent; a Du Nuoy tensiometer and a 6-cm platinum-iridium ring were used and the appropriate corrections [66] were applied for the surface tension calculations.

The uncertainty is estimated to be ± 0.1 percent.

Potassium Metaphosphate

[Classification: Group A; see table 81, p. 98 for numerical values]

Two different techniques have been used to measure the surface tension of molten KPO₃ by three groups; the maximum bubble pressure method [9, 46] and the maximum pull on cylinder method

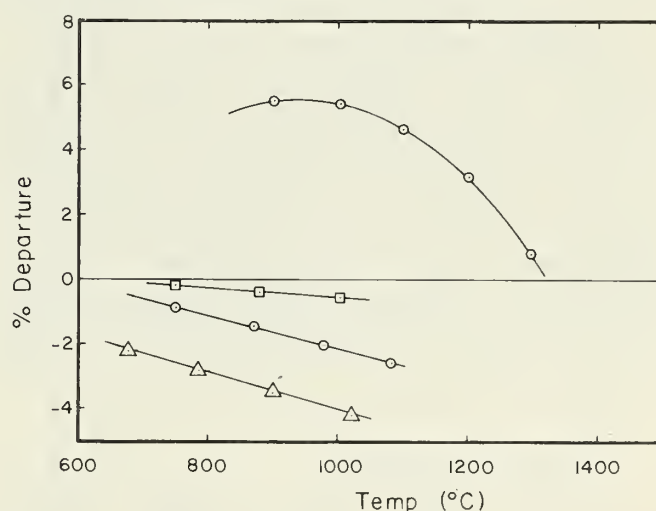


FIGURE 30. Comparison of percent departures of the data for NaPO₂.*

- Owens and Mayer (1964) [88]
- Jaeger (1917) [46]
- Callis, VanWazer and Metcalf (1955) [28]
- Bradbury and Maddocks (1959) [27b]
- △ Sokolova and Boskresenskaya (1963) [9]

*Recent surface tension results of Nijhar [17] (7 points, 745.5 to 1147.8 °C, $\gamma = 211.70 \pm 0.42 - 0.02413 \pm 0.00044t$, maximum pull on cylinder) showed departures of 3 to 2 percent from Sokolova's values in the same temperature range.

*Recent surface tension results of Nijhar [17] (4 points, 808.4 to 1153.0 °C, $\gamma = 223.71 \pm 0.14 - 0.04882 \pm 0.00014t$, maximum pull on cylinder) showed departures of -2 to -3 percent from Owen's values for the same temperature range.

[27a]. The values of Sokolova and Voskresenskaya [9] are recommended as the "best" values in the range 859 to 1082 °C. In the same range, the results of Williams, Bradbury, and Maddocks [27a] show departure of -4.9 to -4.7 percent while those of Jaeger [46] show departure of 7.6 to 8.1 percent. These are illustrated in figure 31.

The experimental aspects of the investigation of Sokolova and Voskresenskaya are discussed on p. 58. KPO_3 was prepared by thermal decomposition of the dihydrogenphosphate (Analysis of P_2O_5 content in KPO_3 yielded a value of 60.20 percent (theoretical, 60.11%)).

Cesium Metaphosphate

(see under LiPO_3 , p. 71)

Calcium Metaphosphate

[Classification: Group B; see table 83, p. 98 for numerical values]

The surface tension of molten $\text{Ca}(\text{PO}_3)_2$ has been measured by Sokolova and Voskresenskaya [9] (7 points, 1007 to 1110 °C, maximum bubble pressure) and by Bradbury and Maddocks [27b] (5 points, 1010 to 1110 °C, maximum pull on cylinder). The authors reported their data only in the form of equations; Sokolova, $\gamma = 240.6 - 0.0108t$ ($s = 0.8$ dyne cm^{-1}) and Bradbury, $\gamma = 249.0 - 0.020t$ (s , not given).

On the basis of other studies of Sokolova and Voskresenskaya (e.g., NaCl) their results are recommended as the "best" values. The percent departure

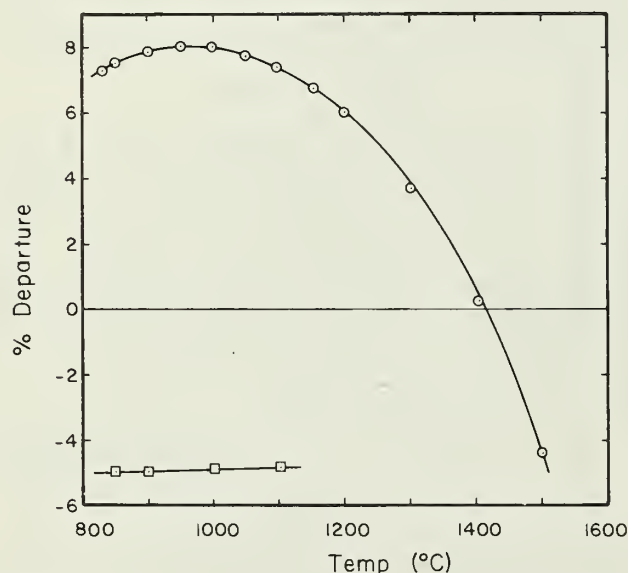


FIGURE 31. Comparison of percent departures of the data for KPO_3 .*

— Sokolova and Voskresenskaya (1963) [9]
 □ Williams, Bradbury and Maddocks (1959) [27a]
 ○ Jaeger (1917) [46]

*Recent surface tension results of Nijhar [17] (7 points, 853.5 to 1156.6 °C, $\gamma = 204.25 \pm 0.33 - 0.06357 \pm 0.00034t$, maximum pull on cylinder) showed departures of 3 to 2 percent from the values of Sokolova for the same temperature range.

of the values of Bradbury and Maddocks [27b] varies from -0.4 to -0.8 percent in the same temperature range and is shown in figure 32.

The experimental aspects of Sokolova's work are discussed on p. 58. $\text{Ca}(\text{PO}_3)_2$ was prepared by thermal dehydration of $\text{Ca}(\text{H}_2\text{PO}_4)_2$.

Strontium Metaphosphate

(see under LiPO_3 , p. 71)

Barium Metaphosphate

(see under LiPO_3 , p. 71)

Lithium Sulfate

[Classification: Group A; see table 86, p. 99 for numerical values]

The surface tension of molten Li_2SO_4 has been measured by Jaeger [46] and Semenchenko and Shikhobalova [4] (maximum bubble pressure method). The results of Jaeger (17 points, 860 to 1214 °C) are recommended as the "best" values. Compared to Jaeger's data, the results of Semenchenko and Shikhobalova show departure of 0.4 to 1.6 percent in the range 900 to 1100 °C. This comparison is illustrated in figure 33.

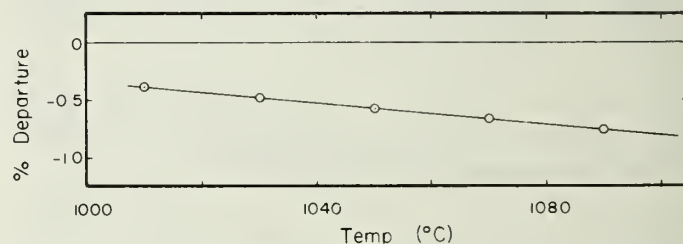


FIGURE 32. Comparison of percent departures of the data for $\text{Ca}(\text{PO}_3)_2$.*

— Sokolova and Voskresenskaya (1963) [9]
 ○ Bradbury and Maddocks (1959) [27b]

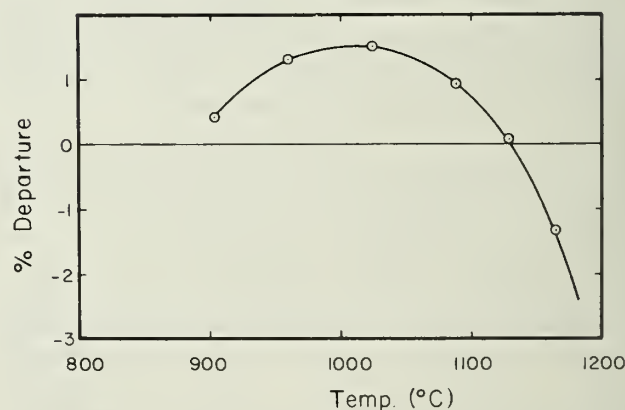


FIGURE 33. Comparison of percent departure of the data for Li_2SO_4 .

— Jaeger (1917) [46]
 ○ Semenchenko and Shikhobalova (1947) [4]

*Recent surface tension results of Nijhar [17] (9 points, 990.6 to 1154.8 °C, $\gamma = 259.18 \pm 1.70 - 0.02622 \pm 0.00156t$, maximum pull on cylinder) showed departures of 3 to 1 percent from the values of Sokolova for the same temperature range.

Some of the experimental aspects of Jaeger's surface tension work are discussed on p. 57. The thermal stability of Li_2SO_4 has been summarized by Stern and Weise [73]. Decomposition of Li_2SO_4 begins to be noticeable not far above its melting point (859 °C), the Li_2O product apparently dissolving in Li_2SO_4 while some volatilization of Li_2SO_4 occurs. No measurements of the decomposition pressures have been made.

The uncertainty of the surface tension data is estimated to ± 1.0 percent.

Sodium Sulfate

[Classification: Group B; see table 87, p. 99 for numerical values]

The surface tension of molten Na_2SO_4 has been determined by Jaeger [46] (maximum bubble pressure technique). The data (5 points, 900 to 1077 °C) are better represented by a quadratic equation ($\gamma = 476.5 - 0.532t + 2.43 \times 10^{-4}t^2$, $s = 1.1$ dyne cm^{-1}).

The thermal stability of Na_2SO_4 has been summarized by Stern and Weise [73]. Thermogravimetric analysis of Na_2SO_4 (m.p. 859 °C) showed that the salt is stable up to 900 °C. At higher temperatures there is a weight loss (0.04% at 1000 °C; 1.051 at 1200 °C) and analysis of the residue indicated that loss in weight is due to both decomposition (because of alkaline properties) and volatilization. This decomposition of Na_2SO_4 above 1000 °C may partially account for the deviation from linear behavior of surface tension with temperature.

Some of the experimental aspects of Jaeger's investigation are as follows: Platinum capillaries of radii 0.04935 to 0.05025 cm were used. Nitrogen, the bubbling gas, obtained by heating aqueous solutions of NaNO_2 and NH_4Cl , was purified by passing respectively through alkaline-pyrogallol solution, concentrated H_2SO_4 and P_2O_5 ; it was preheated to the melt temperature before passing through the capillary system; no details were given for the preparation and purification of the salt.

An accuracy estimate is not possible owing to insufficient information. It should be noted that most of Jaeger's data are 2 to 8 percent higher than those redetermined from more recent studies, and that for certain compounds the differences are significantly larger, e.g., NaF , 10 percent; $\text{K}_2\text{Cr}_2\text{O}_7$, 10 to 20 percent; TlNO_3 , 25 to 28 percent.

Potassium Sulfate

[Classification: Group A; see table 88, p. 99 for numerical values]

The surface tension of molten K_2SO_4 has been measured by three groups [6, 13, 46] (maximum bubble pressure technique). The results of Neithamer and Peake [6] (14 points 1099 to 1121 °C) are recommended as the "best" values. Compared to

the data of Neithamer and Peake, the results of Jaeger [46] and Sokolova and Voskresenskaya [13] show departures of 1.5 to 3.0 percent and -4.0 to -4.5 percent respectively in the same temperature range. This comparison is illustrated in figure 34.

Some of the experimental aspects of the investigation of Neithamer and Peake are as follows: purified nitrogen was used as the bubbling gas; the tips of the platinum-alloy capillaries were checked periodically; all other necessary precautions as outlined in section 3.2 for the maximum bubble pressure method were taken.

The thermal stability of K_2SO_4 (m.p. 1069 °C) has been summarized by Stern and Weise [73]. Thermogravimetric analysis showed that K_2SO_4 is stable up to 900 °C. At 1000 °C, a slight loss in weight was observed (attributed to sublimation). At higher temperature there is a weight loss (e.g., 3.6% at 1200 °C); subsequent analysis of the residue (no alkaline reaction or change in percentage composition) confirmed that all weight loss was attributed to volatilization and none to decomposition.

The uncertainty of the surface tension data for this salt is estimated to be ± 0.5 percent.

Rubidium Sulfate and Cesium Sulfate

[Classification: Group B; see tables 89 and 90, p. 100 for numerical values]

The surface tensions of these two alkali metal sulfates have been measured by Jaeger [46] (maximum bubble pressure technique). The data for Rb_2SO_4 (11 points, 1085 to 1545 °C) and Cs_2SO_4 (11 points, 1036 to 1530 °C) are better represented by quadratic equations ($s = 0.3$ dyne cm^{-1} and $s = 0.4$ dyne cm^{-1} , respectively).

The experimental aspects and the accuracy estimates of Jaeger's surface tension work are discussed on p. 73. The thermal stabilities of these two alkali sulfates have been summarized by Stern and Weise [73]. Thermogravimetric analysis of the salts showed that Rb_2SO_4 (m.p. 1074 °C) is stable up to 900 °C while Cs_2SO_4 (m.p. 1019 °C) is stable up to 800 °C. At higher temperatures there were weight losses (0.3% at 1000 °C and 6.3% at 1200 °C) for Rb_2SO_4 ; 0.2% at 900 °C, 0.87% at 1000 °C, and 13.9% at 1200 °C for Cs_2SO_4) which were confirmed by analy-

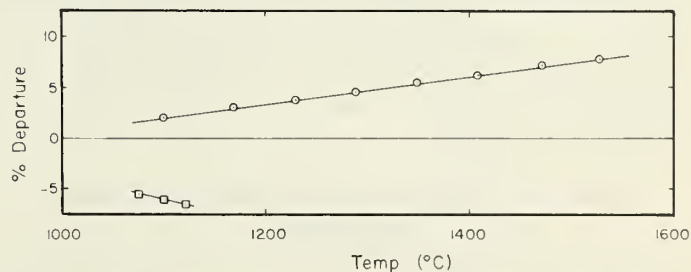


FIGURE 34. Comparison of percent departures of the data for K_2SO_4 .

- Neithamer and Peake (1961) [6]
- Jaeger (1917) [46]
- Sokolova and Voskresenskaya (1962) [13]

sis to be due to volatilization and not due to decomposition (absence of alkaline properties in the residue).

Sodium Molybdate and Potassium Molybdate

[Classification: Group B; see tables 91 and 92, p. 101 for numerical values]

The surface tensions of these two alkali molybdates have been determined by Jaeger [46] (maximum bubble pressure technique). The data for both Na_2MoO_4 (14 points, 698 to 1212 °C) and K_2MoO_4 (12 points, 930 to 1522 °C) are better represented by quadratic equations ($s=0.6$ dyne cm^{-1} and $s=0.4$ dyne cm^{-1} , respectively).

The experimental aspects and the accuracy estimates of Jaeger's surface tension work are discussed on p. 73.

Lead Molybdate and Bismuth Molybdate

[Classification: Group B; see tables 93 and 94, pp. 101 and 102 respectively for numerical values]

The surface tensions of these two molten molybdates have been determined by Morris, McNair and Koops [24] (pin method). The data for PbMoO_4 (4 points, 1093 to 1124 °C) and $\text{Bi}_2(\text{MoO}_4)_3$ (5 points, 680 to 760 °C) are represented respectively by a linear equation ($s=\pm 0.9$ dyne cm^{-1}) and a quadratic equation ($s=\pm 0.6$ dyne cm^{-1}).

Spectroscopic examinations [24] of the anhydrous salts revealed that both salts were of analytical reagent quality. Accuracy estimates of the surface tension data for these two salts are not possible due to insufficient information.

Sodium Tungstate and Potassium Tungstate

[Classification: Group B; see tables 95 and 96, p. 102 for numerical values]

The surface tensions of these two alkali tungstates have been determined by Jaeger [46] (maximum bubble pressure technique). The data for both Na_2WO_4 (20 points, 710 to 1595 °C) and K_2WO_4 (15 points, 925 to 1520 °C) are better represented by quadratic equations with precisions ($s=0.7$ dyne cm^{-1} and $s=0.6$ dyne cm^{-1} respectively).

The experimental aspects and the uncertainty estimates of Jaeger's surface tension work are discussed on p. 73.

Potassium Thiocyanate and Potassium Chlorate

[Classification: Group C; see table 97, p. 102 for numerical values]

The surface tensions of molten KCNS and KClO_3 have been determined by Frame, Rhodes and

Ubbelohde [23] (maximum bubble pressure technique). For KCNS, the freshly prepared melt showed a temperature dependence of -1.36 dyne cm^{-1} deg^{-1} ; after a certain time (period of time was unspecified) the value changed to 0.14 dyne cm^{-1} deg^{-1} . The two surface tension-temperature equations for KCNS accordingly are: $\gamma=339.5-1.36t$ (freshly prepared melt); $\gamma=126.0-0.14t$ (aged melt). Both equations yield the same value ($\gamma=101.5$ dyne cm^{-1}) at the melting point (175 °C). KClO_3 decomposes with the formation of KCl ; after a period of 4 days as much as 2 percent KCl was formed. The large variation of surface tensions with temperature and also with the age of the melt was partly attributed to decomposition.

Some of the experimental details of the investigation of Frame et al. are as follows: KCNS and KClO_3 (A.R. grade) were used without further purification. Nitrogen (O_2 content <1 p.p.m.; B.O.C. "white spot") dried in a liquid oxygen trap was used as the bubbling gas for KCNS melt. Oxygen (B.O.C. cylinder gas) dried in a similar manner, was used for KClO_3 . The bubbling rates were comparatively low (2 to 8 min per bubble). The gases were preheated to the temperatures of the melts by passing through a preheater immersed in a nitrate-nitrite bath, thermostatically controlled by a thyatron bridge circuit to ± 0.05 °C.

The uncertainty for both salts is estimated to be ± 2.0 percent.

Potassium Dichromate

[Classification: Group B; see table 98, p. 103, for numerical values]

The surface tension of molten $\text{K}_2\text{Cr}_2\text{O}_7$ has been determined by Jaeger [46] and Frame, Rhodes, and Ubbelohde [23] (maximum bubble pressure technique) in the temperature ranges 420 to 535 °C, and 400 to 440 °C, respectively. The results of Frame et al. are recommended as the "best" values. The values of Jaeger show departures of 9 to 16 percent in the range 400 to 440 °C. This comparison is illustrated in figure 35.

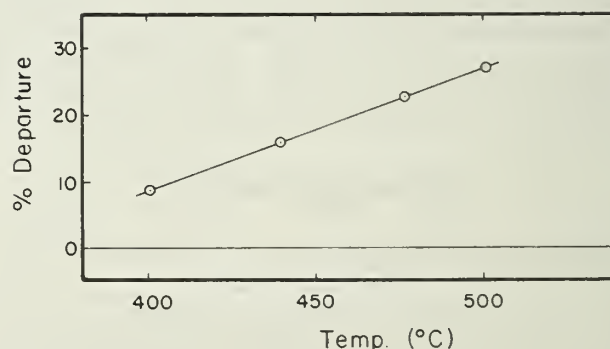


FIGURE 35. Comparison of percent departure of the data for $\text{K}_2\text{Cr}_2\text{O}_7$.
— Frame, Rhodes and Ubbelohde (1959) [23]
○ Jaeger (1917) [46]

The experimental aspects of the investigation of Frame et al. are discussed on p. 74. $K_2C_2O_7$ (A.R. grade), twice recrystallized from conductivity water, was air-dried at 180 °C for 48 hr, followed by thermal shock drying.

The uncertainty is estimated to be ± 2.0 percent.

Lithium Chlorate

[Classification: Group B; see table 99, p. 103 for numerical values]

The surface tension of molten $LiClO_3$ has been determined by Campbell and Williams [68] (capillary rise technique). The results (6 points, 132 to 162° C) are represented by a linear equation

($s = 0.1$ dyne cm^{-1}). Lithium chlorate is extremely hygroscopic; the authors have taken due precautions in preparing and handling the salt.

An accuracy estimate is not possible owing to insufficient information.

Sodium Chlorate

[Classification: Group B; see table 100, p. 103, for numerical values]

The surface tension of molten $NaClO_3$ has been determined by Campbell and van Der Kouwe [21] (capillary technique). The results (6 points, 265 to 290 °C) can best be represented by a linear equation ($s = 0.4$ dyne cm^{-1}). No estimate of accuracy was attempted owing to insufficient information.

List of Tables

	Table	Page
FLUORIDES		
LiF	3 Lithium fluoride.....	78
NaF	4 Sodium fluoride.....	78
KF	5 Potassium fluoride.....	78
RbF	6 Rubidium fluoride.....	78
CsF	7 Cesium fluoride.....	79
ThF ₄	8 Thorium tetrafluoride.....	79
UF ₄	9 Uranium tetrafluoride.....	79
UF ₆	10 Uranium hexafluoride.....	79
Na ₃ AlF ₆	11 Cryolite.....	79
CHLORIDES		
LiCl	12 Lithium chloride.....	80
NaCl	13 Sodium chloride.....	80
KCl	14 Potassium chloride.....	80
RbCl	15 Rubidium chloride.....	80
CsCl	16 Cesium chloride.....	81
CuCl	17 Cuprous chloride.....	81
AgCl	18 Silver chloride.....	81
MgCl ₂	19 Magnesium chloride.....	81
CaCl ₂	20 Calcium chloride.....	82
SrCl ₂	21 Strontium chloride.....	82
BaCl ₂	22 Barium chloride.....	82
ZnCl ₂	23 Zinc chloride.....	82
CdCl ₂	24 Cadmium chloride.....	83
SnCl ₂	25 Stannous chloride.....	83
HgCl ₂	26 Mercuric chloride.....	83
PbCl ₂	27 Lead chloride.....	83
AlCl ₃	28 Aluminium chloride.....	84
GaCl ₃	29 Gallium chloride.....	84
GaCl ₃ · 2C ₅ H ₁₀ NH	30 Gallium trichloride, piperidine complex (1:2).....	84
GaCl ₃ · C ₅ H ₁₀ NH	30 Gallium trichloride, piperidine complex (1:1).....	84
GaCl ₃ · C ₅ H ₅ N	30 Gallium trichloride, pyridine complex (1:1).....	84
BiCl ₃	31 Bismuth trichloride.....	84
BROMIDES		
NaBr	32 Sodium bromide.....	85
KBr	33 Potassium bromide.....	85
RbBr	34 Rubidium bromide.....	85
CsBr	35 Cesium bromide.....	85
AgBr	36 Silver bromide.....	86
CaBr ₂	37 Calcium bromide.....	86
SrBr ₂	38 Strontium bromide.....	86
BaBr ₂	39 Barium bromide.....	86
ZnBr ₂	40 Zinc bromide.....	87
CdBr ₂	41 Cadmium bromide.....	87
HgBr ₂	26 Mercuric bromide.....	83
BiBr ₃	42 Bismuth tribromide.....	87

IODIDES

NaI	43	Sodium iodide.....	87
KI	44	Potassium iodide.....	88
RbI	45	Rubidium iodide.....	88
CsI	46	Cesium iodide.....	88
CaI ₂	47	Calcium iodide.....	89
SrI ₂	48	Strontium iodide.....	89
BaI ₂	49	Barium iodide.....	89

OXIDES

B ₂ O ₃	50	Boron trioxide.....	90
Al ₂ O ₃	51	Aluminum oxide.....	90
SiO ₂	52	Silicon dioxide.....	90
GeO ₂	53	Germanium dioxide.....	91
PbO	51	Lead oxide.....	90
P ₂ O ₃	54	Phosphorus trioxide.....	91
P ₂ O ₅	55	Phosphorus pentoxide.....	91
FeO	51	Ferrous oxide.....	90

SULFIDES

Cu ₂ S	17	Cuprous sulfide.....	81
Tl ₂ S	56	Thallium sulfide.....	91

METABORATES

LiBO ₂	57	Lithium metaborate.....	92
NaBO ₂	58	Sodium metaborate.....	92
KBO ₂	59	Potassium metaborate.....	92

CARBONATES

Li ₂ CO ₃	60	Lithium carbonate.....	93
Na ₂ CO ₃	61	Sodium carbonate.....	93
K ₂ CO ₃	62	Potassium carbonate.....	93

NITRATES

LiNO ₃	63	Lithium nitrate.....	93
NaNO ₃	64	Sodium nitrate.....	93
KNO ₃	65	Potassium nitrate.....	94
RbNO ₃	66	Rubidium nitrate.....	94
CsNO ₃	67	Cesium nitrate.....	94
AgNO ₃	68	Silver nitrate.....	94
TlNO ₃	69	Thallium nitrate.....	95
NH ₄ NO ₃	70	Ammonium nitrate.....	95
Ca(NO ₃) ₂	71	Calcium nitrate.....	95
Sr(NO ₃) ₂	71	Strontium nitrate.....	95
Ba(NO ₃) ₂	71	Barium nitrate.....	95

NITRITES

NaNO ₂	72	Sodium nitrite.....	95
KNO ₂	73	Potassium nitrite.....	96

SILICATES

Li ₂ SiO ₃	74	Lithium silicate.....	96
MgSiO ₃	75	Magnesium metasilicate.....	96
CaSiO ₃	76	Calcium metasilicate.....	96
MnSiO ₃	77	Manganese metasilicate.....	97
Mn ₂ SiO ₄	78	Manganese orthosilicate.....	97

METAPHOSPHATES

LiPO ₃	79	Lithium metaphosphate.....	97
NaPO ₃	80	Sodium metaphosphate.....	97
KPO ₃	81	Potassium metaphosphate.....	98
CsPO ₃	82	Cesium metaphosphate.....	98
Ca(PO ₃) ₂	83	Calcium metaphosphate.....	98
Sr(PO ₃) ₂	84	Strontium metaphosphate.....	98
Ba(PO ₃) ₂	85	Barium metaphosphate.....	99

SULFATES

Li_2SO_4	86	Lithium sulfate.....	99
Na_2SO_4	87	Sodium sulfate.....	99
K_2SO_4	88	Potassium sulfate.....	99
Rb_2SO_4	89	Rubidium sulfate.....	100
Cs_2SO_4	90	Cesium sulfate.....	100

MOLYBDATES

Na_2MoO_4	91	Sodium molybdate.....	101
K_2MoO_4	92	Potassium molybdate.....	101
PbMoO_4	93	Lead molybdate.....	101
$\text{Bi}_2(\text{MoO}_4)_3$	94	Bismuth molybdate.....	102

TUNGSTATES

Na_2WO_4	95	Sodium tungstate.....	102
K_2WO_4	96	Potassium tungstate.....	102

MISCELLANEOUS

KCNS	97	Potassium thiocyanate.....	102
KClO_3	97	Potassium chlorate.....	102
$\text{K}_2\text{Cr}_2\text{O}_7$	98	Potassium dichromate.....	103
LiClO_3	99	Lithium chlorate.....	103
NaClO_3	100	Sodium chlorate.....	103

6. Numerical Values of Surface Tension

TABLE 3. *Lithium fluoride, LiF*
mp 845 °C

[Classification: Group A; for discussion see p. 55.]
 $\gamma = 319.5 - 0.0988t$ ($s = 0.7$ dyne cm⁻¹)

°C	γ	°C	γ
880	232.6	1080	212.8
900	230.6	1100	210.8
920	228.6	1120	208.8
940	226.6	1140	206.9
960	224.7	1160	204.9
980	222.7	1180	202.9
1000	220.7	1200	200.9
1020	218.7	1220	199.0
1040	216.8	1240	197.0
1060	214.8	1260	195.0

Reference: γ , [37, 46].
Melting Point: [69].

TABLE 4. *Sodium fluoride, NaF*
mp 980 °C

[Classification: Group A; for discussion see p. 56.]
 $\gamma = 267.2 - 0.082t$

°C	γ
1000	185.2
1010	184.4
1020	183.6
1030	182.7
1040	181.9
1050	181.1
1060	180.3
1070	179.5
1080	178.6

Reference: γ , [32, 37, 46].
Melting Point: [69].

TABLE 5. *Potassium fluoride, KF*
mp 856 °C

[Classification: Group B; for discussion see p. 57.]
 $\gamma = 176.2 - 0.0108t - 0.333 \times 10^{-4}t^2$ ($s = 0.3$ dyne cm⁻¹)

°C	γ	°C	γ	°C	γ
920	138.1	1060	127.3	1200	115.3
940	136.6	1080	125.7	1220	113.5
960	135.1	1100	124.0	1240	111.6
980	133.6	1120	122.3	1260	109.7
1000	132.1	1140	120.6	1280	107.8
1020	130.5	1160	118.9	1300	105.9
1040	129.0	1180	117.1

Reference: γ , [46].
Melting Point: [69].

TABLE 6. *Rubidium fluoride, RbF*
mp 775 °C

[Classification: Group A; for discussion see p. 57.]
 $\gamma = 187.6 - 0.0782t$ ($s = 1.7$ dyne cm⁻¹)

°C	γ	°C	γ	°C	γ
800	125.0	870	119.6	940	114.1
810	124.3	880	118.8	950	113.3
820	123.5	890	118.0	960	112.5
830	122.7	900	117.2	970	111.8
840	121.9	910	116.4	980	111.0
850	121.1	920	115.7	990	110.2
860	120.4	930	114.9	1000	109.4

Reference: γ , [37, 46].
Melting Point: [69].

TABLE 7. *Cesium fluoride*, CsF

mp 681 °C

[Classification: Group A; for discussion see p. 57.]

$$\gamma = 162.5 - 0.0808t \quad (s = 0.7 \text{ dyne cm}^{-1})$$

°C	γ	°C	γ	°C	γ
720	104.3	810	97.1	900	89.8
730	103.5	820	96.2	910	89.0
740	102.7	830	95.4	920	88.2
750	101.9	840	94.6	930	87.4
760	101.1	850	93.8	940	86.5
770	100.3	860	93.0	950	85.7
780	99.5	870	92.2	960	84.9
790	98.7	880	91.4	970	84.1
800	97.9	890	90.6	980	83.3

Reference: γ , [37, 46]

Melting Point: [69].

TABLE 8. *Thorium tetrafluoride*, ThF₄

mp 1110 °C

[Classification: Group C; for discussion see p. 57.]

$$\gamma = 416.9 - 0.161t \quad (s = 2.5 \text{ dyne cm}^{-1})$$

°C	γ	°C	γ
1160	230.2	1420	188.3
1180	227.0	1440	185.1
1200	223.8	1460	181.9
1220	220.5	1480	178.7
1240	217.3	1500	175.5
1260	214.1	1520	172.2
1280	210.9	1540	169.0
1300	207.7	1560	165.8
1320	204.4	1580	162.6
1340	201.2	1600	159.4
1360	198.0	1620	156.1
1380	194.8	1640	152.9
1400	191.6	1660	149.7

Reference: γ , [70].

Melting Point: [70].

TABLE 9. *Uranium tetrafluoride*, UF₄

mp 1036 °C

[Classification: Group C; for discussion see p. 57.]

$$\gamma = 394.5 - 0.192t \quad (s = 2.5 \text{ dyne cm}^{-1})$$

°C	γ	°C	γ	°C	γ
1060	191.0	1180	167.9	1300	144.9
1080	187.1	1200	164.1	1320	141.1
1100	183.3	1220	160.3	1340	137.2
1120	179.5	1240	156.4	1360	133.4
1140	175.6	1260	152.6	1380	129.5
1160	171.8	1280	148.7	1400	125.7
				1420	121.9

Reference: γ , [70].

Melting Point: [70].

TABLE 10. *Uranium hexafluoride*, UF₆

mp 64 °C

[Classification: Group C; for discussion see p. 57.]

°C	γ^*
65	17.66 ± 0.51
72.5	16.48 ± 0.06

Reference: γ , [50].

Melting Point: [69].

*The two tabulated values are the experimental points.

TABLE 11. *Cryolite*, Na₃AlF₆

mp 1000 °C

[Classification: Group C; for discussion see p. 57.]

$$\gamma = 262.0 - 0.128t \quad (s = 1.9 \text{ dyne cm}^{-1})$$

°C	γ
1000	134.0
1010	132.7
1020	131.4
1030	130.2
1040	128.9
1050	127.6
1060	126.3
1070	125.0
1080	123.8

Reference: γ , [32].

Melting Point: [69].

TABLE 12. *Lithium chloride*, LiCl
mp 610 °C

[Classification: Group A; for discussion see p. 57.]
 $\gamma = 164.5 - 0.0583t$ ($s = 0.3$ dyne cm⁻¹)

°C	γ	°C	γ	°C	γ
620	128.4	710	123.1	800	117.9
630	127.8	720	122.5	810	117.3
640	127.2	730	121.9	820	116.7
650	126.6	740	121.4	830	116.1
660	126.0	750	120.8	840	115.5
670	125.4	760	120.2	850	114.9
680	124.9	770	119.6	860	114.4
690	124.3	780	119.0	870	113.8
700	123.7	790	118.4

Reference: γ , [37, 46].

Melting Point: [69].

TABLE 13. *Sodium chloride*, NaCl
mp 800 °C

[Classification: Group A; for discussion see p. 57.]
 $\gamma = 171.5 - 0.0719t$ ($s = 0.2$ dyne cm⁻¹)

°C	γ	°C	γ
810	113.3	890	107.5
820	112.5	900	106.8
830	111.8	910	106.1
840	111.1	920	105.4
850	110.4	930	104.6
860	109.7	940	103.9
870	109.0	950	103.2
880	108.2	960	102.5
.....	970	101.8

Reference: γ , [1, 4, 7, 13, 10, 45, 46, 60].

Melting Point: [69].

TABLE 14. *Potassium chloride*, KCl
mp 770 °C

[Classification: Group A; for discussion see p. 58.]
 $\gamma = 160.4 - 0.0770t$ ($s = 0.4$ dyne cm⁻¹)

°C	γ	°C	γ
780	100.3	880	92.6
790	99.6	890	91.9
800	98.8	900	91.1
810	98.0	910	90.3
820	97.3	920	89.6
830	96.5	930	88.8
840	95.7	940	88.0
850	95.0	950	87.3
860	94.2	960	86.5
870	93.4	970	85.7

Reference: γ , [1, 4, 6, 10, 12, 29, 40, 45, 46, 60, 31a].

Melting Point: [69].

TABLE 15. *Rubidium chloride*, RbCl mp 715 °C
[Classification: Group A; for discussion see p. 58.]
 $\gamma = 162.2 - 0.0904t + 0.0239 \times 10^{-4}t^2$ ($s = 0.2$ dyne cm⁻¹)

°C	γ	°C	γ	°C	γ	°C	γ
760	94.9	860	86.2	960	77.6	1060	69.1
770	94.0	870	85.4	970	76.8	1070	68.2
780	93.1	880	84.5	980	75.9	1080	67.4
790	92.3	890	83.6	990	75.0	1090	66.5
800	91.4	900	82.8	1000	74.2	1100	65.7
810	90.5	910	81.9	1010	73.3	1110	64.8
820	89.7	920	81.1	1020	72.5	1120	64.0
830	88.8	930	80.2	1030	71.6	1130	63.1
840	88.0	940	79.3	1040	70.8	1140	62.3
850	87.1	950	78.5	1050	69.9	1150	61.4

Reference: γ , [4, 45, 46].

Melting Point: [69].

TABLE 16. *Cesium chloride, CsCl* mp 645 °C
 [Classification: Group A; for discussion see p. 58.]
 $\gamma = 112.5 - 0.00932t - 0.391 \times 10^{-4}t^2$ ($s = 0.4$ dyne cm⁻¹)

°C	γ	°C	γ	°C	γ
660	89.3	800	80.0	940	69.2
680	88.1	820	78.6	960	67.5
700	86.8	840	77.1	980	65.8
720	85.5	860	75.6	1000	64.1
740	84.2	880	74.0	1020	62.3
760	82.8	900	72.4	1040	60.5
780	81.4	920	70.8	1060	58.7
				1080	56.8

Reference: γ , [4, 29, 45, 46].

Melting Point: [69].

TABLE 17. *Cuprous chloride and cuprous sulfide*
Cuprous chloride, CuCl* mp 430 °C
 [Classification: Group C; for discussion see p. 59.]

°C	γ
450	92

Cuprous sulfide, Cu₂S* mp 1127 °C
 [Classification: Group C; for discussion see p. 59.]

°C	γ
1150	410

*Reference: γ , [92].

Melting Point: [69].

TABLE 18. *Silver chloride, AgCl*
 mp 455 °C

[Classification: Group C; for discussion see p. 59.]
 $\gamma = 202.2 - 0.052t$ ($s = 0.8$ dyne cm⁻¹)

°C	γ	°C	γ	°C	γ
460	178.3	540	174.1	620	170.0
470	177.8	550	173.6	630	169.4
480	177.2	560	173.1	640	168.9
490	176.7	570	172.6	650	168.4
500	176.2	580	172.0	660	167.9
510	175.7	590	171.5	670	167.4
520	175.2	600	171.0	680	166.8
530	174.6	610	170.5	690	166.3
				700	165.8

Reference: γ , [14].

Melting Point: [69].

TABLE 19. *Magnesium chloride, MgCl₂*

mp 714 °C

[Classification: Group C; for discussion see p. 59.]

$\gamma = 74.0 - 0.010t$

°C	γ	°C	γ
720	66.8	830	65.7
730	66.7	840	65.6
740	66.6	850	65.5
750	66.5	860	65.4
760	66.4	870	65.3
770	66.3	880	65.2
780	66.2	890	65.1
790	66.1	900	65.0
800	66.0	910	64.9
810	65.9	920	64.8
820	65.8	930	64.7

Reference: γ , [40, 60, 10].

Melting Point: [69].

TABLE 20. *Calcium chloride*, CaCl_2

mp 782 °C

[Classification: Group A; for discussion see p. 60.]

$$\gamma = 203.9 - 0.0728t \quad (s = 0.4 \text{ dyne cm}^{-1})$$

°C	γ	°C	γ
770	147.8	850	142.0
780	147.1	860	141.3
790	146.4	870	140.6
800	145.7	880	139.8
810	144.9	890	139.1
820	144.2	900	138.4
830	143.5	910	137.7
840	142.8	920	136.9

Reference: γ , [7, 29, 37].

Melting Point: [69].

TABLE 21. *Strontium chloride*, SrCl_2

mp 875 °C

[Classification: Group B; for discussion see p. 60.]

$$\gamma = 215.9 - 0.0541t \quad (s = 1.0 \text{ dyne cm}^{-1})$$

°C	γ	°C	γ
880	168.4	970	163.5
890	167.8	980	163.0
900	167.3	990	162.4
910	166.8	1000	161.9
920	166.2	1010	161.4
930	165.7	1020	160.8
940	165.1	1030	160.3
950	164.6	1040	159.7
960	164.1

Reference: γ , [34].

Melting Point: [69].

TABLE 22. *Barium chloride*, BaCl_2

mp 962 °C

[Classification: Group A; for discussion see p. 60.]

$$\gamma = 241.6 - 0.0790t \quad (s = 0.3 \text{ dyne cm}^{-1})$$

°C	γ
970	165.0
980	164.2
990	163.4
1000	162.6
1010	161.8
1020	161.0
1030	160.2
1040	159.4

Reference: γ , [12, 13].

Melting Point: [69].

TABLE 23. *Zinc chloride*, ZnCl_2 mp 283 °C

[Classification: Group C; for discussion see p. 60.]

$$\gamma = 54.4 - 0.00199t \quad (300\text{--}550^\circ\text{C}) \quad (s = 1.1 \text{ dyne cm}^{-1})$$

$$\gamma = 63.6 - 0.0190t \quad (550\text{--}700^\circ\text{C}) \quad (s = 0.6 \text{ dyne cm}^{-1})$$

°C	γ	°C	γ	°C	γ
300	53.80	420	53.56	550	53.2
310	53.78	430	53.54	560	53.0
320	53.76	440	53.52	570	52.8
330	53.74	450	53.50	580	52.6
340	53.72	460	53.48	590	52.4
350	53.70	470	53.46	600	52.2
360	53.68	480	53.44	610	52.0
370	53.66	490	53.42	620	51.8
380	53.64	500	53.40	630	51.6
390	53.62	510	53.39	640	51.4
400	53.60	520	53.37	650	51.2
410	53.58	530	53.35	660	51.0
.....	540	53.33	670	50.8
.....	680	50.6
.....	690	50.4
.....	700	50.2

Reference: γ [39].

Melting Point: [69].

TABLE 24. *Cadmium chloride*, CdCl_2 mp 568 °C
 [Classification: Group B; for discussion see p. 61.]
 $\gamma = 74.15 + 0.0459t - 0.492 \times 10^{-4} t^2$ ($s = 0.3$ dyne cm^{-1})

°C	γ	°C	γ	°C	γ
580	84.22	690	82.40	810	79.05
590	84.10	700	82.17	820	78.71
600	83.98	710	81.94	830	78.35
610	83.84	720	81.69	840	77.99
620	83.70	730	81.44	850	77.62
630	83.54	740	81.17	860	77.24
640	83.37	750	80.90	870	76.84
650	83.20	760	80.62	880	76.44
660	83.01	770	80.32	890	76.03
670	82.82	780	80.02	900	75.61
680	82.61	790	79.71	910	75.18
		800	79.38	920	74.74

Reference: γ [35].
 Melting Point: [69].

TABLE 25. *Stannous chloride*, SnCl_2
 mp 245 °C
 [Classification: Group A; for discussion see p. 61.]
 $\gamma = 128.0 - 0.0984t$ ($s = 2.7$ dyne cm^{-1})

°C	γ	°C	γ	°C	γ
280	100.6	350	93.7	420	86.8
290	99.6	360	92.7	430	85.9
300	98.6	370	91.7	440	84.9
310	97.6	380	90.8	450	83.9
320	96.6	390	89.8	460	82.9
330	95.7	400	88.8	470	81.9
340	94.7	410	87.8	480	81.0

Reference: γ , [35, 46].
 Melting Point: [69].

TABLE 26. *Mercuric chloride and mercuric bromide*
Mercuric chloride, HgCl_2^* mp 277 °C
 [Classification: Group C; for discussion see p. 61.]

°C	γ
293	56.1

Mercuric bromide HgBr_2^* mp 241 °C
 [Classification: Group C; for discussion see p. 61.]

°C	γ
241	64.5
276	59.8

*Reference: γ , [59].
 Melting Point: [69].

TABLE 27. *Lead chloride*, PbCl_2
 mp 498 °C
 [Classification: Group B; for discussion see p. 61.]
 $\gamma = 199.8 - 0.124t$ ($s = 0.7$ dyne cm^{-1})

°C	γ
520	135.3
530	134.1
540	132.8
550	131.6
560	130.4
570	129.1
580	127.9

Reference: γ , [1, 31, 10].
 Melting Point: [69].

TABLE 28. *Aluminum chloride*, AlCl_3

mp 192.5 °C

[Classification: Group B; for discussion see p. 62.]

$$\gamma = 23.20 - 0.0704t \quad (s = 0.2 \text{ dyne cm}^{-1})$$

°C	γ	°C	γ
200	9.12	260	4.90
210	8.42	270	4.19
220	7.71	280	3.49
230	7.01	290	2.78
240	6.30	300	2.08
250	5.6	310	1.38
.....	320	0.67

Reference: γ , [61].

Melting Point: [69].

TABLE 29. *Gallium chloride*, GaCl_3

mp 77.9 °C

[Classification: Group A; for discussion see p. 62.]

$$\gamma = 34.97 - 0.0997t \quad (s = 0.1 \text{ dyne cm}^{-1})$$

°C	γ
80	26.99
90	25.99
100	25.00
110	24.00
120	23.01
130	22.01
140	21.01

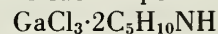
Reference: γ , [44, 61].

Melting Point: [69].

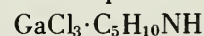
TABLE 30.

[Classification: Group C; for discussion see p. 62.]

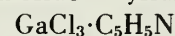
A. Gallium trichloride—Piperidine complex (1:2)

mp 112 °C $\gamma = 46.0 - 0.16t$ ($s = 0.2 \text{ dyne cm}^{-1}$)

B. Gallium trichloride—Piperidine complex (1:1)

mp 134 °C $\gamma = 45.5 - 0.084t$ ($s = 0.5 \text{ dyne cm}^{-1}$)

C. Gallium trichloride—Pyridine complex (1:1)

mp 126 °C $\gamma = 50.3 - 0.097t$ ($s = 0.5 \text{ dyne cm}^{-1}$)

°C	γ_A	γ_B	γ_C
120	25.9
130	24.3	37.7
140	22.6	33.6	36.7
150	21.0	32.8	35.8
160	19.3	31.9	34.8

Reference: γ , [43, 42].

Melting Point: [43, 42].

TABLE 31. *Bismuth trichloride*, BiCl_3

mp 232 °C

[Classification: Group B; for discussion see p. 62.]

$$\gamma = 114.0 - 0.210t + 1.243 \times 10^{-4}t^2 \quad (s = 0.1 \text{ dyne cm}^{-1})$$

°C	γ
270	66.36
280	64.95
290	63.55
300	62.19
310	60.85
320	59.53
330	58.24
340	56.97
350	55.73
360	54.51
370	53.32
380	52.15

Reference: γ , [46].

Melting Point: [69].

TABLE 32. *Sodium bromide*, NaBr mp 750 °C
[Classification: Group A; for discussion see p. 62.]
 $\gamma = 164.8 - 0.0809t$ ($s = 0.8$ dyne cm⁻¹)

°C	γ	°C	γ
760	103.3	840	96.8
770	102.5	850	96.0
780	101.7	860	95.2
790	100.9	870	94.4
800	100.1	880	93.6
810	99.3	890	92.8
820	98.5	900	92.0
830	97.7

Reference: γ [1, 13, 45, 46].
Melting Point: [69].

TABLE 33. *Potassium bromide*, KBr mp 735 °C
[Classification: Group A; for discussion see p. 63.]
 $\gamma = 142.2 - 0.072t$ ($s = 0.2$ dyne cm⁻¹)

°C	γ	°C	γ
750	88.2	850	81.0
760	87.5	860	80.3
770	86.8	870	79.6
780	86.0	880	78.8
790	85.3	890	78.1
800	84.6	900	77.4
810	83.9	910	76.7
820	83.2	920	76.0
830	82.4	930	75.2
840	81.7	940	74.5
.....	950	73.8

Reference: γ [1, 36, 45, 46].
Melting Point: [69].

TABLE 34. *Rubidium bromide*, RbBr mp 680 °C
[Classification: Group B; for discussion see p. 63.]
 $\gamma = 138.0 - 0.0720t$ ($s = 0.2$ dyne cm⁻¹)

°C	γ	°C	γ
720	86.2	780	81.8
730	85.4	790	81.1
740	84.7	800	80.4
750	84.0	810	79.7
760	83.3	820	78.9
770	82.6	830	78.2

Reference: γ [45, 46].
Melting Point: [69].

TABLE 35. *Cesium bromide*, CsBr
mp 636 °C
[Classification: Group B; for discussion see p. 63.]
 $\gamma = 127.1 - 0.068t$ ($s = 0.1$ dyne cm⁻¹)

°C	γ	°C	γ
660	82.22	760	75.42
670	81.54	770	74.74
680	80.86	780	74.06
690	80.18	790	73.38
700	79.50	800	72.70
710	78.82	810	72.02
720	78.14	820	71.34
730	77.46	830	70.66
740	76.78
750	76.10

Reference: γ [45, 46].
Melting Point: [69].

TABLE 36. *Silver bromide*, AgBr

mp 430 °C

[Classification: Group C; for discussion see p. 59.]

$$\gamma = 164.5 - 0.025t \quad (s = 0.7 \text{ dyne cm}^{-1})$$

°C	γ
460	153.0
470	152.8
480	152.5
490	152.3
500	152.0
510	151.8
520	151.5
530	151.3
540	151.0
550	150.8
560	150.5
570	150.3
580	150.0
590	149.8
600	149.5
610	149.3
620	149.0

Reference: γ [14].

Melting Point: [69].

TABLE 37. *Calcium bromide*, CaBr₂

mp 730 °C

[Classification: Group B; for discussion see p. 61.]

$$\gamma = 153.1 - 0.0459t \quad (s = 0.3 \text{ dyne cm}^{-1})$$

°C	γ
770	117.8
780	117.3
790	116.8
800	116.4
810	115.9

Reference: γ [35].

Melting Point: [69].

TABLE 38. *Strontium Bromide*, SrBr₂

mp 643 °C

[Classification: Group B; for discussion see p. 64.]

$$\gamma = 178.0 - 0.0439t \quad (s = 1.5 \text{ dyne cm}^{-1})$$

°C	γ	°C	γ	°C	γ
680	148.2	790	143.3	900	138.5
690	147.7	800	142.9	910	138.1
700	147.3	810	142.4	920	137.6
710	146.8	820	142.0	930	137.2
720	146.4	830	141.6	940	136.7
730	145.9	840	141.1	950	136.3
740	145.5	850	140.7	960	135.9
750	145.1	860	140.3	970	135.4
760	144.6	870	139.8	980	134.9
770	144.2	880	139.4	990	134.5
780	143.8	890	138.9	1000	134.1
.....	1010	133.7

Reference: γ . [34].

Melting Point: [69].

TABLE 39. *Barium bromide*, BaBr₂

mp 850 °C

[Classification: Group B; for discussion see p. 64.]

$$\gamma = 207.6 - 0.0644t \quad (s = 1.2 \text{ dyne cm}^{-1})$$

°C	γ
870	151.6
880	150.9
890	150.3
900	149.6
910	149.0
920	148.4
930	147.7
940	147.1
950	146.4
960	145.8
970	145.1
980	144.5
990	143.8
1000	143.2
1010	142.6

Reference: γ . [34].

Melting Point: [69].

TABLE 40. *Zinc bromide*, ZnBr_2
mp 394 °C

[Classification: Group C; for discussion see p. 64.]
 $\gamma = 58.1 - 0.0172t$ (500–600 °C) ($s = 0.7$ dyne cm^{-1})
 $\gamma = 100.5 - 0.0895t$ (600–670 °C) ($s = 0.08$ dyne cm^{-1})

°C	γ	°C	γ
500	49.50	610	45.9
510	49.33	620	45.0
520	49.16	630	44.1
530	48.98	640	43.2
540	48.81	650	42.3
550	48.64	660	41.4
560	48.47	670	40.5
570	48.30
580	48.12
590	47.95
600	47.78

Reference: γ , [39].
 Melting Point: [69].

TABLE 41. *Cadmium bromide*, CdBr_2
mp 568 °C

[Classification: Group B; for discussion see p. 64.]
 $\gamma = 16.12 + 0.167t - 0.143 \times 10^{-3}t^2$ ($s = 1.0$ dyne cm^{-1})

°C	γ	°C	γ
630	64.57	710	62.60
640	64.43	720	62.23
650	64.25	730	61.83
660	64.05	740	61.39
670	63.82	750	60.93
680	63.56	760	60.44
690	63.27	770	59.93
700	62.95	780	59.38

Reference: γ , [37].
 Melting Point: [69].

TABLE 42. *Bismuth tribromide*, BiBr_3
mp 218 °C

[Classification: Group B; for discussion see p. 64.]
 $\gamma = 90.18 - 0.0871t - 0.284 \times 10^{-4}t^2$ ($s = 0.1$ dyne cm^{-1})

°C	γ	°C	γ
250	66.63	350	56.22
260	65.61	360	55.14
270	64.59	370	54.07
280	63.57	380	52.98
290	62.53	390	51.89
300	61.49	400	50.80
310	60.45	410	49.70
320	59.40	420	48.59
330	58.34	430	47.48
340	57.28	440	46.36

Reference: γ , [46].
 Melting Point: [69].

TABLE 43. *Sodium iodide*, NaI
mp 662 °C

[Classification: Group A; for discussion see p. 64.]
 $\gamma = 433.7 - 0.793t + 0.437 \times 10^{-3}t^2$ ($s = 1.0$ dyne cm^{-1})

°C	γ
760	83.4
770	82.2
780	81.0
790	80.0
800	79.0
810	78.1
820	77.3
830	76.6
840	75.9
850	75.4
860	74.9

Reference: γ , [1, 37, 46].
 Melting Point: [69].

TABLE 44. *Potassium iodide, KI*
mp 685 °C

[Classification: Group B; for discussion see p. 64.]
 $\gamma = 138.7 - 0.087t$ ($s = 0.2$ dyne cm⁻¹)

°C	γ	°C	γ	°C	γ
700	77.8	770	71.7	840	65.6
710	76.9	780	70.8	850	64.8
720	76.1	790	70.0	860	63.9
730	75.2	800	69.1	870	63.0
740	74.3	810	68.2	880	62.1
750	73.5	820	67.4	890	61.3
760	72.6	830	66.5	900	60.4

Reference: γ , [1, 46].

Melting Point: [69].

TABLE 45. *Rubidium iodide, RbI*
mp 640 °C

[Classification: Group B; for discussion see p. 64.]
 $\gamma = 140.2 - 0.103t + 0.193 \times 10^{-4}t^2$ ($s = 0.1$ dyne cm⁻¹)

°C	γ	°C	γ	°C	γ
670	79.85	790	70.88	910	62.45
680	79.08	800	70.15	920	61.78
690	78.32	810	69.43	930	61.10
700	77.56	820	68.72	940	60.43
710	76.80	830	68.00	950	59.77
720	76.05	840	67.30	960	59.11
730	75.30	850	66.59	970	58.45
740	74.55	860	65.89	980	57.79
750	73.81	870	65.19	990	57.15
760	73.07	880	64.51	1000	56.50
770	72.33	890	63.82	1010	55.86
780	71.60	900	63.13	1020	55.22

Reference: γ [46].

Melting Point: [69].

TABLE 46. *Cesium iodide, CsI*
mp 621 °C

[Classification: Group B; for discussion see p. 64.]
 $\gamma = 125.4 - 0.0946t + 0.219 \times 10^{-4}t^2$ ($s = 0.2$ dyne cm⁻¹)

°C	γ	°C	γ	°C	γ	°C	γ
650	73.16	750	66.77	850	60.81	950	55.30
660	72.50	760	66.15	860	60.24	960	54.77
670	71.85	770	65.54	870	59.67	970	54.24
680	71.19	780	64.94	880	59.11	980	53.73
690	70.55	790	64.33	890	58.55	990	53.21
700	69.91	800	63.74	900	57.99	1000	52.70
710	69.27	810	63.14	910	57.44	1010	52.19
720	68.64	820	62.55	920	56.90	1020	51.69
730	68.01	830	61.97	930	56.36	1030	51.19
740	67.39	840	61.39	940	55.83

Reference: γ [46].

Melting Point: [69].

TABLE 47. *Calcium iodide*, CaI_2

mp 575 °C

[Classification: Group B; for discussion see p. 65.]

$$\gamma = 98.63 - 0.0173t \quad (s = 1.5 \text{ dyne cm}^{-1})$$

°C	γ	°C	γ
800	84.79	930	82.54
810	84.62	940	82.37
820	84.44	950	82.20
830	84.27	960	82.02
840	84.10	970	81.85
850	83.93	980	81.68
860	83.75	990	81.50
870	83.58	1000	81.33
880	83.41	1010	81.16
890	83.23	1020	80.98
900	83.06	1030	80.81
910	82.89	1040	80.64
920	82.71	1050	80.47

Reference: γ , [34].

Melting Point: [69].

TABLE 49. *Barium iodide*, BaI_2

mp 740 °C

[Classification: Group B; for discussion see p. 65.]

$$\gamma = 165.7 - 0.0420t \quad (s = 0.4 \text{ dyne cm}^{-1})$$

°C	γ	°C	γ
830	130.8	900	127.9
840	130.4	910	127.5
850	130.0	920	127.1
860	129.6	930	126.6
870	129.2	940	126.2
880	128.7	950	125.8
890	128.3	960	125.4

Reference: γ , [35].

Melting Point: [69].

TABLE 48. *Strontium iodide*, SrI_2

mp 515 °C

[Classification: Group B; for discussion see p. 65]

$$\gamma = 114.6 + 0.0144t - 0.334 \times 10^{-4}t^2 \quad (s = 0.9 \text{ dyne cm}^{-1})$$

°C	γ	°C	γ	°C	γ	°C	γ
580	111.7	680	108.9	780	105.5	890	101.0
590	111.5	690	108.6	790	105.1	900	100.5
600	111.2	700	108.3	800	104.7	910	100.0
610	110.9	710	108.0	810	104.3	920	99.6
620	110.7	720	107.7	820	104.0	930	99.1
630	110.4	730	107.3	830	103.5	940	98.6
640	110.1	740	107.0	840	103.1	950	98.1
650	109.9	750	106.6	850	102.7	960	97.6
660	109.6	760	106.3	860	102.3	970	97.1
670	109.3	770	105.9	870	101.9	980	96.6
				880	101.4	990	96.1

Reference: γ , [34].

Melting Point: [69].

TABLE 50. *Boron trioxide, B₂O₃*

mp 450 °C

[Classification: Group B; for discussion see p. 65.]

$$\gamma = 47.57 + 0.0354t \quad (s = 0.04 \text{ dyne cm}^{-1})$$

°C	γ	°C	γ	°C	γ
700	72.35	940	80.85	1180	89.34
720	73.06	960	81.55	1200	90.05
740	73.77	980	82.26	1220	90.76
760	74.47	1000	82.97	1240	91.47
780	75.18	1020	83.68	1260	92.17
800	75.89	1040	84.39	1280	92.88
820	76.60	1060	85.09	1300	93.59
840	77.30	1080	85.80	1320	94.30
860	78.01	1100	86.51	1340	95.01
880	78.72	1120	87.22	1360	95.71
900	79.43	1140	87.93	1380	96.42
920	80.14	1160	88.63	1400	97.13

Reference: γ , [30, 33].

Melting Point: [69].

TABLE 51. *Aluminum oxide, lead oxide, and ferrous oxide***Aluminum oxide, Al₂O₃** mp 2040 °C

[Classification: Group C; for discussion see p. 65.]

°C	γ
2050 ± 15	690.0

Reference: γ , [30].

Melting Point: [69].

Lead oxide, PbO mp 886 °C

[Classification: Group C; for discussion see p. 65.]

°C	γ
900	132.0
1000	134.8

Reference: γ , [91].

Melting Point: [69].

Ferrous oxide, FeO mp 1368 °C

[Classification: Group C; for discussion see p. 66.]

°C	γ
1415–1423	585. (mean value)

Reference: γ , [90, 87].

Melting Point: [69].

TABLE 52. *Silicon dioxide, SiO₂*

mp 1470 °C

[Classification: Group C; for discussion see p. 65.]

$$\gamma = 251.7 + 0.031t \quad (s = 6.0 \text{ dyne cm}^{-1})$$

°C	γ	°C	γ	°C	γ
1500	298.2	1610	301.6	1710	304.7
1510	298.5	1620	301.9	1720	305.0
1520	298.8	1630	302.2	1730	305.3
1530	299.1	1640	302.5	1740	305.6
1540	299.4	1650	302.9	1750	305.9
1550	299.8	1660	303.2	1760	306.3
1560	300.0	1670	303.5	1770	306.6
1570	300.3	1680	303.8	1780	306.9
1580	300.7	1690	304.1	1790	307.2
1590	301.0	1700	304.4	1800	307.5
1600	301.3

Reference: γ , [30].

Melting Point: [69].

TABLE 53. *Germanium dioxide*, GeO_2
mp 1116 °C

[Classification: Group C; for discussion see p. 65.]

$$\gamma = 185.6 + 0.056t \quad (s = 5.0 \text{ dyne cm}^{-1})$$

°C	γ	°C	γ
1200	252.8	1310	259.0
1210	253.4	1320	259.5
1220	253.9	1330	260.1
1230	254.5	1340	260.6
1240	255.0	1350	261.2
1250	255.6	1360	261.8
1260	256.2	1370	262.3
1270	256.7	1380	262.9
1280	257.3	1390	263.4
1290	257.8	1400	264.0
1300	258.4

Reference: γ , [30].

Melting Point: [69].

TABLE 55. *Phosphorus pentoxide*, P_2O_5
mp 569 °C

[Classification: Group C; for discussion see p. 66.]

$$\gamma = 62.1 - 0.021t \quad (s = 1.8 \text{ dyne cm}^{-1})$$

°C	γ	°C	γ
100	60.0	210	57.7
110	59.8	220	57.5
120	59.6	230	57.3
130	59.4	240	57.1
140	59.2	250	56.9
150	59.0	260	56.6
160	58.7	270	56.4
170	58.5	280	56.2
180	58.3	290	56.0
190	58.1	300	55.8
200	57.9

Reference: γ , [30].

Melting Point: [69].

TABLE 54. *Phosphorus trioxide*, P_2O_3
mp 23.8 °C

[Classification: Group B; for discussion see p. 66.]

$$\gamma = 40.4 - 0.116t \quad (s = 0.2 \text{ dyne cm}^{-1})$$

°C	γ
30	37.0
40	35.8
50	34.7
60	33.5
70	32.3
80	31.2
90	30.0
100	28.9
110	27.7

Reference: γ , [5].

Melting Point: [69].

TABLE 56. *Thallium sulfide*, Tl_2S
mp 448 °C

[Classification: Group B; for discussion see p. 66.]

$$\gamma = 231.4 - 0.0356t \quad (s = 0.4 \text{ dyne cm}^{-1})$$

°C	γ	°C	γ	°C	γ
500	213.6	570	211.1	640	208.6
510	213.2	580	210.8	650	208.3
520	212.9	590	210.4	660	207.9
530	212.5	600	210.0	670	207.6
540	212.2	610	209.7	680	207.2
550	211.8	620	209.3	690	206.8
560	211.5	630	209.0	700	206.5

Reference: γ , [85].

Melting Point: [69].

TABLE 57. *Lithium metaborate*, LiBO_2
mp 845 °C

[Classification: Group B; for discussion see p. 66.]
 $\gamma = 197.7 + 0.174t - 1.16 \times 10^{-4}t^2$ ($s = 1.0$ dyne cm^{-1})

°C	γ	°C	γ	°C	γ
880	261.0	1100	248.7	1320	225.3
900	260.3	1120	247.1	1340	222.6
920	259.6	1140	245.3	1360	219.8
940	258.8	1160	243.5	1380	216.9
960	257.8	1180	241.5	1400	213.9
980	256.8	1200	239.5	1420	210.9
1000	255.7	1220	237.3	1440	207.7
1020	254.5	1240	235.1	1460	204.5
1040	253.2	1260	232.8	1480	201.1
1060	251.8	1280	230.4	1500	197.7
1080	250.3	1300	227.9	1520	194.2

Reference: γ , [46].
Melting Point: [69].

TABLE 58. *Sodium metaborate*, NaBO_2
mp 966 °C

[Classification: Group B; for discussion see p. 66.]
 $\gamma = 359.6 - 0.163t$ ($s = 1.0$ dyne cm^{-1})

°C	γ	°C	γ	°C	γ
1020	193.3	1160	170.5	1300	147.7
1040	190.1	1180	167.3	1320	144.4
1060	186.8	1200	164.0	1340	141.2
1080	183.6	1220	160.7	1360	137.9
1100	180.3	1240	157.5	1380	134.7
1120	177.0	1260	154.2	1400	131.4
1140	173.8	1280	151.0	1420	128.1

Reference: γ , [46].
Melting Point: [69].

TABLE 59. *Potassium metaborate*, KBO_2
mp 947 °C

[Classification: Group B; for discussion see p. 66.]
 $\gamma = 948.2 - 1.3998t + 5.727 \times 10^{-4}t^2$ ($s = 0.6$ dyne cm^{-1})

°C	γ	°C	γ
990	123.8	1070	106.2
1000	121.2	1080	104.5
1010	118.7	1090	102.9
1020	116.3	1100	101.5
1030	114.1	1110	100.1
1040	111.9	1120	98.9
1050	109.9	1130	97.8
1060	108.0	1140	96.8

Reference: γ , [46].
Melting Point: [69].

TABLE 60. *Lithium carbonate*, Li_2CO_3
mp 618 °C

[Classification: Group A; for discussion see p. 66.]
 $\gamma = 273.5 - 0.0406t$ ($s = 0.5$ dyne cm^{-1})

°C	γ
750	243.1
760	242.6
770	242.2
780	241.8
790	241.4
800	241.0
810	240.6
820	240.2
830	239.8
840	239.4
850	239.0

Reference: γ , [49, 76].
Melting Point: [69].

TABLE 61. *Sodium carbonate*, Na_2CO_3
mp 854 °C

[Classification: Group B; for discussion see p. 67.]

$$\gamma = 254.8 - 0.0502t \quad (s = 0.1 \text{ dyne cm}^{-1})$$

°C	γ	°C	γ
870	211.1	940	207.6
880	210.6	950	207.1
890	210.1	960	206.6
900	209.6	970	206.1
910	209.1	980	205.6
920	208.6	990	205.1
930	208.1	1000	204.6
.....	1010	204.1

Reference: γ , [49].

Melting Point: [69].

TABLE 63. *Lithium nitrate*, LiNO_3
mp 254 °C

[Classification: Group B; for discussion see p. 67.]

$$\gamma = 129.9 - 0.055t \quad (s = 0.5 \text{ dyne cm}^{-1})$$

°C	γ	°C	γ	°C	γ
300	113.4	370	109.6	440	105.7
310	112.9	380	109.0	450	105.2
320	112.3	390	108.5	460	104.6
330	111.8	400	107.9	470	104.1
340	111.2	410	107.4	480	103.5
350	110.7	420	106.8	490	103.0
360	110.1	430	106.3	500	102.4

Reference: γ , [19, 26, 46].

Melting Point: [69].

TABLE 62. *Potassium carbonate*, K_2CO_3
mp 896 °C

[Classification: Group B; for discussion see p. 67.]

$$\gamma = 283.2 - 0.183t + 0.625 \times 10^{-4}t^2 \quad (s = 0.2 \text{ dyne cm}^{-1})$$

°C	γ
910	168.4
920	167.7
930	167.1
940	166.4
950	165.8
960	165.1
970	164.5
980	163.9
990	163.3
1000	162.7
1010	162.1

Reference: γ , [49].

Melting Point: [69].

TABLE 64. *Sodium nitrate*, NaNO_3
mp 310 °C

[Classification: Group A; for discussion see p. 67.]

$$\gamma = 138.8 - 0.0613t \quad (s = 0.3 \text{ dyne cm}^{-1})$$

°C	γ	°C	γ	°C	γ
320	119.2	420	113.1	520	106.9
330	118.6	430	112.4	530	106.3
340	118.0	440	111.8	540	105.7
350	117.4	450	111.2	550	105.1
360	116.7	460	110.6	560	104.5
370	116.1	470	110.0	570	103.9
380	115.5	480	109.4	580	103.3
390	114.9	490	108.8	590	102.6
400	114.3	500	108.2	600	102.0
410	113.7	510	107.5

Reference: γ , [1, 18, 19, 26, 41, 46].

Melting Point: [69].

TABLE 65. *Potassium nitrate*, KNO_3

mp 337 °C

[Classification: Group A; for discussion see p. 67.]

$$\gamma = 136.5 - 0.0750t \quad (s = 0.1 \text{ dyne cm}^{-1})$$

°C	γ	°C	γ
340	111.0	420	105.0
350	110.3	430	104.3
360	109.5	440	103.5
370	108.8	450	102.8
380	108.0	460	102.0
390	107.3	470	101.3
400	106.5	480	100.5
410	105.8	490	99.8
.....	500	99.0

Reference: γ , [1, 18, 19, 26, 46, 48].

Melting Point: [69].

TABLE 67. *Cesium nitrate*, CsNO_3

mp 414 °C

[Classification: Group B; for discussion see p. 68.]

$$\gamma = 122.1 - 0.074t \quad (s = 0.4 \text{ dyne cm}^{-1})$$

°C	γ	°C	γ
420	91.0	520	83.6
430	90.3	530	82.9
440	89.5	540	82.1
450	88.8	550	81.4
460	88.1	560	80.7
470	87.3	570	79.9
480	86.6	580	79.2
490	85.8	590	78.4
500	85.1	600	77.7
510	84.4

Reference: γ , [19, 26, 46].

Melting Point: [69].

TABLE 66. *Rubidium nitrate*, RbNO_3

mp 316 °C

[Classification: Group B; for discussion see p. 68.]

$$\gamma = 134.3 - 0.083t \quad (s = 0.4 \text{ dyne cm}^{-1})$$

°C	γ	°C	γ	°C	γ
330	106.9	430	98.6	530	90.3
340	106.1	440	97.8	540	89.5
350	105.3	450	96.9	550	88.7
360	104.4	460	96.1	560	87.8
370	103.6	470	95.3	570	87.0
380	102.8	480	94.5	580	86.2
390	101.9	490	93.6	590	85.3
400	101.1	500	92.8	600	84.5
410	100.3	510	92.0
420	99.4	520	91.1

Reference: γ , [26, 46].

Melting Point: [69].

TABLE 68. *Silver nitrate*, AgNO_3

mp 210 °C

[Classification: Group B; for discussion see p. 68.]

$$\gamma = 162.5 - 0.0613t \quad (s = 0.7 \text{ dyne cm}^{-1})$$

°C	γ	°C	γ
220	149.0	290	144.7
230	148.4	300	144.1
240	147.8	310	143.5
250	147.2	320	142.9
260	146.6	330	142.3
280	146.0	340	141.7
.....	350	141.1

Reference: γ , [1, 18, 19, 26].

Melting Point: [69].

TABLE 69. *Thallium nitrate*, TlNO_3
mp 207 °C

[Classification: Group B; for discussion see p. 69.]
 $\gamma = 110.9 - 0.078t$ ($s = 0.4$ dyne cm^{-1})

°C	γ	°C	γ	°C	γ
210	94.5	300	87.5	390	80.5
220	93.7	310	86.7	400	79.7
230	93.0	320	85.9	410	78.9
240	92.2	330	85.2	420	78.1
250	91.4	340	84.4	430	77.4
260	90.6	350	83.6	440	76.6
270	89.8	360	82.8	450	75.8
280	89.1	370	82.0	460	75.0
290	88.3	380	81.3

Reference: γ , [19, 46].
Melting point: [69].

TABLE 70. *Ammonium nitrate*, NH_4NO_3
mp 169.6 °C

[Classification: Group C; for discussion see p. 69.]
 $\gamma = 119.7 - 0.105t$ ($s = 0.5$ dyne cm^{-1})

°C	γ
170	101.9
180	100.8
190	99.8
200	98.7
210	97.7
220	96.6

Reference: γ , [19, 74].
Melting Point: [69].

TABLE 71. *Calcium nitrate, strontium nitrate, and barium nitrate*

Calcium nitrate, $\text{Ca}(\text{NO}_3)_2^*$ mp 551 °C

[Classification: Group C; for discussion see p. 69.]
 $\gamma = 101.5 \pm 0.5$ at 560 °C

Strontium nitrate, $\text{Sr}(\text{NO}_3)_2^*$ mp 605 °C

[Classification: Group C; for discussion see p. 69.]
 $\gamma = 128.4 \pm 0.5$ at 615 °C

Barium nitrate, $\text{Ba}(\text{NO}_3)_2^*$ mp 595 °C

[Classification: Group C; for discussion see p. 69.]
 $\gamma = 143.7 - 0.015t$ ($s = 0.6$ dyne cm^{-1})

°C	γ
600	134.7
610	134.6
620	134.4
630	134.3
640	134.1
650	134.0
660	133.8

*Reference: γ , [19].
Melting Point: [69].

TABLE 72. *Sodium nitrite*, NaNO_2
mp 281 °C

[Classification: Group B; for discussion see p. 70.]
 $\gamma = 131.4 - 0.0378t$ ($s = 0.4$ dyne cm^{-1})

°C	γ	°C	γ	°C	γ
280	120.8	360	117.8	440	114.8
290	120.4	370	117.4	450	114.4
300	120.0	380	117.0	460	114.0
310	119.7	390	116.7	470	113.6
320	119.3	400	116.3	480	113.2
330	118.9	410	115.9	490	112.9
340	118.6	420	115.5	500	112.6
350	118.2	430	115.2

Reference: γ , [1, 19, 23].
Melting Point: [69].

TABLE 73. *Potassium nitrite*, KNO_2
mp 419 °C

[Classification: Group B; for discussion see p. 70.]

$$\gamma = 134.6 - 0.0623t \quad (s = 0.3 \text{ dyne cm}^{-1})$$

°C	γ
450	106.6
460	105.9
470	105.3
480	104.7
490	104.0
500	103.5

Reference: γ , [19].

Melting Point: [69].

TABLE 74. *Lithium silicate*, Li_2SiO_3
mp 1188 °C

[Classification: Group B; for discussion see p. 70.]

$$\gamma = 819.9 - 0.572t + 1.73 \times 10^{-4}t^2 \quad (s = 1.0 \text{ dyne cm}^{-1})$$

°C	γ	°C	γ	°C	γ
1250	375.2	1370	361.0	1490	351.7
1260	373.8	1380	360.0	1500	351.2
1270	372.5	1390	359.1	1510	350.6
1280	371.2	1400	358.2	1520	350.2
1290	369.9	1410	357.3	1530	349.7
1300	368.7	1420	356.5	1540	349.3
1310	367.5	1430	355.7	1550	348.9
1320	366.3	1440	355.0	1560	348.6
1330	365.2	1450	354.2	1570	348.3
1340	364.1	1460	353.6	1580	348.0
1350	363.0	1470	352.9	1590	347.8
1360	362.0	1480	352.3	1600	347.6

Reference: γ , [46].

Melting Point: [69].

TABLE 75. *Magnesium metasilicate*, MgSiO_3
mp 1525 °C

[Classification: Group C; for discussion see p. 70.]

$$\gamma = 224.1 + 0.098t$$

°C	γ
1540	375.1
1550	376.0
1560	377.0
1570	378.0
1580	379.0
1590	380.0
1600	381.0
1610	381.9
1620	382.9

Reference: γ , [58].

Melting Point: [69].

TABLE 76. *Calcium metasilicate*, CaSiO_3
mp 1530 °C

[Classification: Group C; for discussion see p. 70.]

$$\gamma = 367 + 0.021t$$

°C	γ
1530	399.2
1540	399.4
1550	399.6
1560	399.8
1570	400.0
1580	400.2
1590	400.4
1600	400.6
1610	400.8
1620	401.1

Reference: γ , [58].

Melting Point: [69].

TABLE 77. *Manganese metasilicate*, MnSiO_3
mp 1272 °C

[Classification: Group C; for discussion see p. 70.]

$$\gamma = 280 + 0.086t$$

°C	γ
1450	404.7
1460	405.5
1470	406.4
1480	407.3
1490	408.1
1500	409.0
1510	409.8
1520	410.7
1530	411.6
1540	412.2
1550	413.3
1560	414.1
1570	415.0
1580	415.9

Reference: γ , [58].

Melting Point: [69].

TABLE 78. *Manganese orthosilicate*, Mn_2SiO_4
mp 1290 °C

[Classification: Group C; for discussion see p. 70.]

$$\gamma = 468.4 + 0.015t$$

°C	γ
1410	489.6
1430	489.9
1450	490.2
1470	490.5
1490	490.8
1510	491.1
1530	491.4
1550	491.7
1570	492.0
1590	492.3

Reference: γ , [58].

Melting Point: [69].

TABLE 79. *Lithium metaphosphate*, LiPO_3
mp 675 ± 4 °C

[Classification: Group B; for discussion see p. 71.]

$$\gamma = 206.1 - 0.0222t \quad (s = 1.0 \text{ dyne cm}^{-1})$$

°C	γ	°C	γ	°C	γ
750	189.5	860	187.0	970	184.6
760	189.2	870	186.8	980	184.3
770	189.0	880	186.6	990	184.1
780	188.8	890	186.3	1000	183.9
790	188.6	900	186.1	1010	183.7
800	188.3	910	185.9	1020	183.5
810	188.1	920	185.7	1030	183.2
820	187.9	930	185.5	1040	183.0
830	187.7	940	185.2	1050	182.8
840	187.5	950	185.0	1060	182.6
850	187.2	960	184.8	1070	182.4

Reference: γ , [9].

Melting Point: [69].

TABLE 80. *Sodium metaphosphate*, NaPO_3
mp 625 °C

[Classification: Group A; for discussion see p. 71.]

$$\gamma = 217.8 - 0.0398t \quad (s = 0.2 \text{ dyne cm}^{-1})$$

°C	γ	°C	γ	°C	γ
660	191.6	770	187.2	880	182.7
670	191.2	780	186.8	890	182.3
680	190.8	790	186.4	900	181.9
690	190.4	800	185.9	910	181.5
700	190.0	810	185.5	920	181.1
710	189.6	820	185.1	930	180.7
720	189.2	830	184.7	940	180.2
730	188.8	840	184.3	950	179.8
740	188.4	850	183.9	960	179.4
750	188.0	860	183.5	970	179.0
760	187.6	870	183.1	980	178.6

Reference: γ , [9, 27, 28, 46, 88].

Melting Point: [69].

TABLE 81. *Potassium metaphosphate*, KPO_3

mp 817 °C

[Classification: Group A; for discussion see p. 71.]

$$\gamma = 193.2 - 0.0556t \quad (s = 0.3 \text{ dyne cm}^{-1})$$

°C	γ	°C	γ	°C	γ
860	145.4	1080	133.2	1300	120.9
880	144.3	1100	132.0	1320	119.8
900	143.2	1120	130.9	1340	118.7
920	142.1	1140	129.8	1360	117.6
940	140.9	1160	128.7	1380	116.5
960	139.8	1180	127.6	1400	115.4
980	138.7	1200	126.5	1420	114.3
1000	137.6	1220	125.4	1440	113.1
1020	136.5	1240	124.3	1460	112.0
1040	135.4	1260	123.1	1480	110.9
1060	134.3	1280	122.0	1500	109.8

Reference: γ , [27, 46, 9].

Melting Point: [69].

TABLE 82. *Cesium metaphosphate*, CsPO_3 mp 724 ± 3 °C

[Classification: Group C; for discussion see p. 72.]

$$\gamma = 153.3 - 0.0487t \quad (s = 0.4 \text{ dyne cm}^{-1})$$

°C	γ	°C	γ	°C	γ
740	117.3	850	111.9	950	107.0
750	116.8	860	111.4	960	106.5
760	116.3	870	110.9	970	106.0
770	115.8	880	110.4	980	105.6
780	115.3	890	109.9	990	105.1
790	114.8	900	109.5	1000	104.6
800	114.3	910	109.0	1010	104.1
810	113.8	920	108.5	1020	103.6
820	113.3	930	108.0	1030	103.1
830	112.9	940	107.5	1040	102.7
840	112.4

Reference: γ , [9].

Melting Point: [69].

TABLE 83. *Calcium metaphosphate*, $\text{Ca}(\text{PO}_3)_2$

mp 975 °C

[Classification: Group B; for discussion see p. 72.]

$$\gamma = 240.6 - 0.0108t \quad (s = 0.8 \text{ dyne cm}^{-1})$$

°C	γ
1010	229.7
1020	229.6
1030	229.5
1040	229.4
1050	229.3
1060	229.2
1070	229.0
1080	228.9
1090	228.8
1100	228.7
1110	228.6

Reference: γ , [9, 27].

Melting Point: [69].

TABLE 84. *Strontium metaphosphate*, $\text{Sr}(\text{PO}_3)_2$ mp 1010 ± 5 °C

[Classification: Group C; for discussion see p. 72.]

$$\gamma = 233.7 - 0.00527t \quad (s = 0.5 \text{ dyne cm}^{-1})$$

°C	γ
1030	228.27
1040	228.22
1050	228.17
1060	228.11
1070	228.06
1080	228.01

Reference: γ , [9].

Melting Point: [69].

TABLE 85. *Barium metaphosphate*, $\text{Ba}(\text{PO}_3)_2$ mp $868 \pm 5^\circ\text{C}$

[Classification: Group C; for discussion see p. 72.]

$$\gamma = 239.9 - 0.0177t \quad (s = 0.5 \text{ dyne cm}^{-1})$$

$^\circ\text{C}$	γ	$^\circ\text{C}$	γ
900	224.0	1000	222.2
910	223.8	1010	222.0
920	223.6	1020	221.9
930	223.4	1030	221.7
940	223.3	1040	221.5
950	223.1	1050	221.3
960	222.9	1060	221.1
970	222.7	1070	220.9
980	222.6	1080	220.8
990	222.4

Reference: γ , [9].

Melting Point: [69].

TABLE 86. *Lithium sulfate*, Li_2SO_4 mp 859°C

[Classification: Group A; for discussion see p. 72.]

$$\gamma = 282.6 - 0.0672t \quad (s = 0.1 \text{ dyne cm}^{-1})$$

$^\circ\text{C}$	γ	$^\circ\text{C}$	γ	$^\circ\text{C}$	γ
860	224.8	950	218.8	1040	212.7
870	224.1	960	218.1	1050	212.0
880	223.5	970	217.4	1060	211.4
890	222.8	980	216.7	1070	210.7
900	222.1	990	216.1	1080	210.0
910	221.5	1000	215.4	1090	209.4
920	220.8	1010	214.7	1100	208.7
930	220.1	1020	214.1
940	219.4	1030	213.4

Reference: γ , [4, 46].

Melting Point: [69].

TABLE 87. *Sodium sulfate*, Na_2SO_4 mp 884°C

[Classification: Group B; for discussion see p. 73.]

$$\gamma = 476.5 - 0.532t + 2.43 \times 10^{-4}t^2 \quad (s = 1.1 \text{ dyne cm}^{-1})$$

$^\circ\text{C}$	γ	$^\circ\text{C}$	γ
900	194.5	1000	187.5
910	193.6	1010	187.1
920	192.7	1020	186.7
930	191.9	1030	186.3
940	191.1	1040	186.1
950	190.4	1050	185.8
960	189.7	1060	185.6
970	189.1	1070	185.5
980	188.5	1080	185.4
990	187.9

Reference: γ , [46].

Melting Point: [69].

TABLE 88. *Potassium sulfate*, K_2SO_4 mp 1069°C

[Classification: Group A; for discussion see p. 73.]

$$\gamma = 224.3 - 0.0765t \quad (s = 0.1 \text{ dyne cm}^{-1})$$

$^\circ\text{C}$	γ
1080	141.7
1090	140.9
1100	140.2
1110	139.4
1120	138.6

Reference: γ , [6, 13, 46].

Melting Point: [69].

TABLE 89. *Rubidium sulfate*, Rb_2SO_4

mp 1074 °C

[Classification: Group B; for discussion see p. 73.]

$$\gamma = 286.1 - 0.207t + 0.596 \times 10^{-4}t^2 \quad (s = 0.3 \text{ dyne cm}^{-1})$$

°C	γ	°C	γ	°C	γ	°C	γ	°C	γ
1080	132.1	1180	124.8	1280	118.8	1380	113.9	1480	110.3
1090	131.3	1190	124.2	1290	118.3	1390	113.5	1490	110.0
1100	130.5	1200	123.5	1300	117.7	1400	113.1	1500	109.7
1110	129.8	1210	122.9	1310	117.2	1410	112.7	1510	109.4
1120	129.0	1220	122.3	1320	116.7	1420	112.3	1520	109.2
1130	128.3	1230	121.7	1330	116.2	1430	112.0	1530	108.9
1140	127.6	1240	121.1	1340	115.7	1440	111.6	1540	108.7
1150	126.9	1250	120.5	1350	115.3	1450	111.3	1550	108.4
1160	126.2	1260	119.9	1360	114.8	1460	110.9
1170	125.5	1270	119.3	1370	114.4	1470	110.6

Reference: γ , [46].

Melting Point: [69].

TABLE 90. *Cesium sulfate*, Cs_2SO_4

mp 1019 °C

[Classification: Group B; for discussion see p. 73.]

$$\gamma = 244.3 - 0.179t + 0.483 \times 10^{-4}t^2 \quad (s = 0.4 \text{ dyne cm}^{-1})$$

°C	γ	°C	γ	°C	γ	°C	γ	°C	γ
1040	110.4	1140	103.0	1240	96.6	1340	91.2	1440	86.7
1050	109.6	1150	102.3	1250	96.0	1350	90.7	1450	86.3
1060	108.8	1160	101.7	1260	95.4	1360	90.2	1460	85.9
1070	108.1	1170	101.0	1270	94.9	1370	89.7	1470	85.5
1080	107.3	1180	100.3	1280	94.3	1380	89.3	1480	85.2
1090	106.6	1190	99.7	1290	93.8	1390	88.8	1490	84.8
1100	105.8	1200	99.1	1300	93.2	1400	88.4	1500	84.5
1110	105.1	1210	98.4	1310	92.7	1410	87.9	1510	84.1
1120	104.4	1220	97.8	1320	92.2	1420	87.5	1520	83.8
1130	103.7	1230	97.2	1330	91.7	1430	87.1	1530	83.5

Reference: γ , [46].

Melting Point: [69].

TABLE 91. *Sodium molybdate*, Na_2MoO_4

mp 687 °C

[Classification: Group B; for discussion see p. 74.]

$$\gamma = 309.5 - 0.172t + 0.498 \times 10^{-4}t^2 \quad (s = 0.6 \text{ dyne cm}^{-1})$$

°C	γ	°C	γ	°C	γ	°C	γ
700	213.5	830	201.1	960	190.3	1090	181.2
710	213.5	840	200.2	970	189.5	1100	180.6
720	211.5	850	199.3	980	188.8	1110	179.9
730	210.5	860	198.4	990	188.0	1120	179.3
740	209.5	870	197.6	1000	187.3	1130	178.7
750	208.5	880	196.7	1010	186.6	1140	178.1
760	207.5	890	195.9	1020	185.9	1150	177.6
770	206.6	900	195.0	1030	185.2	1160	177.0
780	205.6	910	194.2	1040	184.5	1170	176.4
790	204.7	920	193.4	1050	183.8	1180	175.9
800	203.8	930	192.6	1060	183.1	1190	175.3
810	202.9	940	191.8	1070	182.5	1200	174.8
820	202.0	950	191.0	1080	181.8	1210	174.3

Reference: γ , [46].

Melting Point: [69].

TABLE 92. *Potassium molybdate*, K_2MoO_4

mp 926 °C

[Classification: Group B; for discussion see p. 74.]

$$\gamma = 182.3 - 0.0158t - 0.199 \times 10^{-4}t^2 \quad (s = 0.4 \text{ dyne cm}^{-1})$$

°C	γ	°C	γ	°C	γ
940	149.9	1140	138.4	1340	125.4
960	148.8	1160	137.2	1360	124.0
980	147.7	1180	136.0	1380	122.6
1000	146.6	1200	134.7	1400	121.2
1020	145.5	1220	133.4	1420	119.7
1040	144.3	1240	132.1	1440	118.3
1060	143.2	1260	130.8	1460	116.8
1080	142.0	1280	129.5	1480	115.3
1100	140.8	1300	128.1	1500	113.8
1120	139.6	1320	126.8	1520	112.3

Reference: γ , [46].

Melting Point: [69].

TABLE 93. *Lead molybdate*, PbMoO_4

mp 1065 °C

[Classification: Group B; for discussion see p. 74.]

$$\gamma = 236.0 - 0.064t \quad (s = 0.9 \text{ dyne cm}^{-1})$$

°C	γ
1090	166.2
1100	165.6
1110	165.0
1120	164.3
1130	163.7

Reference: γ , [24].

Melting Point: [69].

TABLE 94. *Bismuth molybdate*, $\text{Bi}_2(\text{MoO}_4)_3$
mp 643 °C

[Classification: Group B; for discussion see p. 74.]
 $\gamma = -207.2 + 1.110t - 0.834 \times 10^{-3}t^2$ ($s = 0.6$ dyne cm^{-1})

°C	γ
680	162.0
690	161.6
700	161.1
710	160.5
720	159.7
730	158.7
740	157.5
750	156.2
760	154.7

Reference: γ , [24].
 Melting Point: [24].

TABLE 96. *Potassium tungstate*, K_2WO_4
mp 930 °C

[Classification: Group B; for discussion see p. 74.]
 $\gamma = 283.6 - 0.160t + 0.283 \times 10^{-4}t^2$ ($s = 0.6$ dyne cm^{-1})

°C	γ	°C	γ	°C	γ
940	158.2	1140	138.0	1340	120.0
960	156.1	1160	136.1	1360	118.3
980	154.0	1180	134.2	1380	116.7
1000	151.9	1200	132.4	1400	115.1
1020	149.8	1220	130.5	1420	113.5
1040	147.8	1240	128.7	1440	111.9
1060	145.8	1260	126.9	1460	110.3
1080	143.8	1280	125.2	1480	108.8
1100	141.8	1300	123.4	1500	107.3
1120	139.9	1320	121.7	1520	105.8

Reference: γ , [46].
 Melting Point: [69].

TABLE 95. *Sodium tungstate*, Na_2WO_4
mp 698 °C

[Classification: Group B; for discussion see p. 74.]
 $\gamma = 248.1 - 0.0602t - 0.0414 \times 10^{-4}t^2$ ($s = 0.6$ dyne cm^{-1})

°C	γ	°C	γ
750	200.6	1200	169.9
800	197.3	1250	166.4
850	193.9	1300	162.8
900	190.6	1350	159.3
950	187.2	1400	155.7
1000	183.8	1450	152.1
1050	180.3	1500	148.5
1100	176.9	1550	144.8
1150	173.4	1600	141.2

Reference: γ , [46].
 Melting Point: [69].

TABLE 97. *Potassium thiocyanate and potassium chlorate*
Potassium thiocyanate, KCNS* mp 175 °C

[Classification: Group C; for discussion see p. 74.]
 $\gamma = 339.5 - 1.36t$ (fresh melt) ($s = 0.5$ dyne cm^{-1})
 $\gamma = 126.0 - 0.14t$ (aged melt) ($s = 0.5$ dyne cm^{-1})

°C	γ (fresh melt)	γ (aged melt)
175	101.5	101.5
185	88.9	100.1
195	98.7
205	97.3

Potassium chlorate, KClO_3^* mp 368 °C
 [Classification: Group C; for discussion see p. 74.]
 $\gamma = 228.0 - 0.40t$ ($s = 0.5$ dyne cm^{-1})

°C	γ
370	80.0
380	76.0

*Reference: γ , [23].
 Melting Point: [23].

TABLE 98. *Potassium dichromate*, $K_2Cr_2O_7$

mp 398 °C

[Classification: Group B; for discussion see p. 74.]

$$\gamma = 236.2 - 0.27t \quad (s = 0.5 \text{ dyne cm}^{-1})$$

°C	γ
400	128.2
410	125.5
420	122.8
430	120.1
440	117.4

Reference: γ , [23, 46].

Melting Point: [69].

TABLE 99. *Lithium chlorate*, $LiClO_3$

mp 127.8 °C

[Classification: Group B; for discussion see p. 75.]

$$\gamma = 96.71 - 0.0692t \quad (s = 0.1 \text{ dyne cm}^{-1})$$

°C	γ
130	87.71
140	87.02
150	86.33
160	85.64
170	84.95

Reference: γ , [68].

Melting Point: [68].

TABLE 100. *Sodium chlorate*, $NaClO_3$

mp 255 °C

[Classification: Group B; for discussion see p. 75.]

$$\gamma = 110.27 - 0.0738t \quad (s = 0.4 \text{ dyne cm}^{-1})$$

°C	γ
260	91.08
270	90.34
280	89.61
290	88.87

Reference: γ , [21].

Melting Point: [69].

7. Cumulative Table of Temperature Dependent Equations

TABLE 101. Surface Tensions of Single-Salt Melts ^{a, b}

Salt	mp °C	Best equation	Range (°C)	s (dyne cm ⁻¹)	Uncertainty (%)	Ref.
Fluorides						
LiF	845	$\gamma = 319.5 - 0.0988t$	868-1260	0.7	± 3.0	[37]
NaF	980	$\gamma = 267.2 - 0.082t$	1000-1080	± 8.0	[32]
KF	856	$\gamma = 176.2 - 0.0108t - 0.333 \times 10^{-4}t^2$	912-1310	0.3	[46]
RbF	775	$\gamma = 187.6 - 0.0782t$	795-945	1.7	± 1.0	[37]
CsF	681	$\gamma = 162.5 - 0.0808t$	775-980	0.7	± 1.0	[37]
ThF ₄	1110	$\gamma = 416.9 - 0.161t$	1147-1667	2.5	± 3.0	[70]
UF ₄	1036	$\gamma = 394.5 - 0.192t$	1047-1427	2.5	± 3.0	[70]
UF ₆	64	$\gamma = 17.66 \pm 0.51$	65	[50]
		$\gamma = 16.48 \pm 0.06$	72.5	[50]
N _{a3} AlF ₆	1000	$\gamma = 262.0 - 0.128t$	1000-1080	*1.9	[32]
Chlorides						
LiCl	610	$\gamma = 164.5 - 0.0583t$	645-865	0.3	± 3.0	[37]
NaCl	800	$\gamma = 171.5 - 0.0719t$	806-966	0.2	± 0.1	[13]
KCl	770	$\gamma = 160.4 - 0.0770t$	780-970	0.4	± 0.5	[31a]
RbCl	715	$\gamma = 162.2 - 0.0904t + 0.0239 \times 10^{-4}t^2$	750-1150	0.2	± 0.1	[46]
CsCl	645	$\gamma = 112.5 - 0.00932t - 0.391 \times 10^{-4}t^2$	663-1080	0.4	± 0.2	[46]
CuCl	430	$\gamma = 92$	450	[92]
AgCl	455	$\gamma = 202.2 - 0.052t$	460-700	*0.8	(± 1.0)	[14]
MgCl ₂	714	$\gamma = 74.0 - 0.010t$	720-920	± 0.8	[60]
CaCl ₂	782	$\gamma = 203.9 - 0.0728t$	840-915	0.4	± 0.5	[37]
SrCl ₂	875	$\gamma = 215.9 - 0.0541t$	884-1034	1.0	± 1.0	[34]
BaCl ₂	962	$\gamma = 241.6 - 0.0790t$	981-1041	0.3	± 1.0	[12]
ZnCl ₂	283	$\gamma = 54.4 - 0.00199t$	300-550	1.1	± 3.0	[39]
		$\gamma = 63.6 - 0.0190t$	550-700	0.6	± 1.5	[39]
CdCl ₂	568	$\gamma = 74.15 + 0.0459t - 0.492 \times 10^{-4}t^2$	580-921	0.3	± 1.0	[35]
SnCl ₂	245	$\gamma = 128.0 - 0.0984t$	283-456	2.7	± 1.0	[35]
HgCl ₂	277	$\gamma = 56.1$	293	[59]

PbCl ₂	498	$\gamma = 199.8 - 0.124t$	518-572	0.7	± 1.0	[31]
AlCl ₃	192.5	$\gamma = 23.20 - 0.0704t$	200-319	0.2	[61]
GaCl ₃	77.9	$\gamma = 34.97 - 0.0997t$	71-140	0.1	± 3.0	[44]
GaCl ₃ · 2C ₅ H ₁₀ NH	112	$\gamma = 46.0 - 0.167t$	110-155	0.2	[43]
GaCl ₃ · C ₅ H ₁₀ NH	134	$\gamma = 45.5 - 0.084t$	125-160	0.5	[43]
GaCl ₃ · C ₅ H ₅ N	126	$\gamma = 50.3 - 0.097t$	125-160	0.5	[42]
BiCl ₃	232	$\gamma = 114.0 - 0.210t + 1.243 \times 10^{-4}t^2$	271-382	0.1	[46]

Bromides

NaBr	750	$\gamma = 164.8 - 0.0809t$	755-905	0.8	± 0.5	[13]
KBr	735	$\gamma = 142.2 - 0.072t$	750-950	0.2	± 1.0	[1]
RbBr	680	$\gamma = 138.0 - 0.0720t$	720-830	0.2	± 0.6	[45]
CsBr	636	$\gamma = 127.1 - 0.068t$	660-830	0.1	± 0.6	[45]
AgBr	430	$\gamma = 164.5 - 0.025t$	460-620	0.7	± 1.0	[14]
CaBr ₂	730	$\gamma = 153.1 - 0.0459t$	774-809	0.3	± 1.0	[35]
SrBr ₂	643	$\gamma = 178.0 - 0.0439t$	657-1011	1.5	± 1.0	[34]
BaBr ₂	850	$\gamma = 207.6 - 0.0644t$	865-1009	1.2	± 1.0	[34]
ZnBr ₂	394	$\gamma = 58.1 - 0.0172t$	500-600	0.7	± 3.0	[39]
		$\gamma = 100.5 - 0.0895t$	600-670	0.08	± 1.5	[39]
CdBr ₂	568	$\gamma = 16.12 + 0.167t - 0.143 \times 10^{-3}t^2$	635-775	1.0	± 1.0	[37]
HgBr ₂	241	$\gamma = 64.5$	241	[59]
		$\gamma = 59.8$	276	[59]
BiBr ₃	218	$\gamma = 90.18 - 0.871t - 0.284 \times 10^{-4}t^2$	250-442	0.1	[46]

Iodides

NaI	662	$\gamma = 433.7 - 0.793t + 0.437 \times 10^{-3}t^2$	755-885	1.0	± 2.0	[37]
KI	685	$\gamma = 138.7 - 0.087t$	700-900	*0.2	± 1.5	[1]
RbI	640	$\gamma = 140.2 - 0.103t + 0.193 \times 10^{-4}t^2$	673-1016	0.1	[46]
CsI	621	$\gamma = 125.4 - 0.0946t + 0.219 \times 10^{-4}t^2$	653-1030	0.2	[46]
CaI ₂	575	$\gamma = 98.63 - 0.0173t$	795-1052	1.5	± 1.0	[34]
SrI ₂	515	$\gamma = 114.6 + 0.0144t - 0.334 \times 10^{-4}t^2$	577-987	0.9	± 1.0	[34]
BaI ₂	740	$\gamma = 165.7 - 0.0420t$	826-958	0.4	± 1.0	[35]

Oxides

B ₂ O ₃	450	$\gamma = 47.57 + 0.0354t$	700-1400	0.04	± 4.0	[33]
Al ₂ O ₃	2040	$\gamma = 690.0$	2050 \pm 15	± 7.0	[30]

See footnotes at the end of the table, p. 108.

7. Cumulative Table of Temperature Dependent Equations

TABLE 101. *Surface Tensions of Single-Salt Melts* ^{a, b} — Continued

Salt	mp °C	Best equation	Range (°C)	s(dyne cm ⁻¹)	Uncertainty (%)	Ref.
Oxides — Continued						
SiO ₂	1470	$\gamma = 251.7 + 0.031t$	1500–1800	*6.0	± 7.0	[30]
GeO ₂	1116	$\gamma = 185.6 + 0.056t$	1200–1400	*5.0	± 7.0	[30]
PbO	886	$\gamma = 132.0$	900	± 2.0	[91]
		$\gamma = 134.8$	1000	± 2.0	[91]
P ₂ O ₃	23.8	$\gamma = 40.4 - 0.116t$	31–110	0.2	[5]
P ₂ O ₅	569	$\gamma = 62.1 - 0.021t$	100–300	1.8	[30]
FeO	1368	$\gamma = 585. \text{ (mean value)}$	1415–1423	[90]
Sulfides						
Cu ₂ S	1127	$\gamma = 410$	1130	[92]
Tl ₂ S	448	$\gamma = 231.4 - 0.0356t$	500–700	0.4	[85]
Metaborates						
LiBO ₂	845	$\gamma = 197.7 + 0.174t - 1.16 \times 10^{-4}t^2$	880–1520	1.0	[46]
NaBO ₂	966	$\gamma = 359.6 - 0.163t$	1015–1441	1.0	[46]
KBO ₂	947	$\gamma = 948.2 - 1.398t + 5.727 \times 10^{-4}t^2$	992–1142	0.6	[46]
Carbonates						
Li ₂ CO ₃	618	$\gamma = 273.5 - 0.0406t$	750–850	0.5	± 0.3	[49]
Na ₂ CO ₃	854	$\gamma = 254.8 - 0.0502t$	870–1005	0.1	± 0.3	[49]
K ₂ CO ₃	896	$\gamma = 283.2 - 0.183t + 0.625 \times 10^{-4}t^2$	905–1010	0.2	± 0.3	[49]
Nitrates						
LiNO ₃	254	$\gamma = 129.9 - 0.055t$	300–500	0.5	± 0.5	[26]
NaNO ₃	310	$\gamma = 138.8 - 0.0613t$	316–596	0.3	± 0.5	[18]
KNO ₃	337	$\gamma = 136.5 - 0.0750t$	345–500	0.1	± 0.5	[48]
RbNO ₃	316	$\gamma = 134.3 - 0.083t$	330–600	*0.4	± 0.5	[26]

Nitrites

CsNO ₃	414	$\gamma = 122.1 - 0.074t$	420-600	*0.4	± 0.5	[26]
AgNO ₃	210	$\gamma = 162.5 - 0.0613t$	222-352	0.7	± 1.0	[18]
TiNO ₃	207	$\gamma = 110.9 - 0.078t$	226-458	*0.4	± 12.0	[19]
NH ₄ NO ₃	169.6	$\gamma = 119.7 - 0.105t$	170-220	*0.5	[19]
Ca(NO ₃) ₂	551	$\gamma = 101.5 \pm 0.5$	560	[19]
Sr(NO ₃) ₂	605	$\gamma = 128.4 \pm 0.5$	615	[19]
Ba(NO ₃) ₂	595.5	$\gamma = 143.7 - 0.015t$	600-660	0.6	[19]

Silicates

NaNO ₂	281	$\gamma = 131.4 - 0.0378t$	291-384	*0.4	(± 1.0)	[19]
KNO ₂	419	$\gamma = 134.6 - 0.0623t$	445-501	*0.3	(± 1.0)	[19]

Metaphosphates

Li ₂ SiO ₃	1188	$\gamma = 819.9 - 0.572t + 1.73 \times 10^{-4}t^2$	1254-1601	1.0	[46]
MgSiO ₃	1525	$\gamma = 224.1 + 0.098t$	1540-1620	[58]
CaSiO ₃	1530	$\gamma = 367 + 0.021t$	1530-1620	[58]
MnSiO ₃	1272	$\gamma = 280 + 0.086t$	1450-1580	[58]
Mn ₂ SiO ₄	1290	$\gamma = 468.4 + 0.015t$	1400-1600	[58]

LiPO ₃	675 \pm 4	$\gamma = 206.1 - 0.0222t$	755-1072	1.0	(± 1.0)	[9]
NaPO ₃	625	$\gamma = 217.8 - 0.0398t$	732-977	0.2	± 0.1	[88]
KPO ₃	817	$\gamma = 193.2 - 0.0556t$	859-1500	0.3	± 1.0	[9]
CsPO ₃	724 \pm 3	$\gamma = 153.3 - 0.0487t$	737-1041	0.4	(± 1.0)	[9]
Ca(PO ₃) ₂	975	$\gamma = 240.6 - 0.0108t$	1007-1110	0.8	± 0.5	[9]
Sr(PO ₃) ₂	1010 \pm 5	$\gamma = 233.7 - 0.00527t$	1030-1082	0.5	(± 1.0)	[9]
Ba(PO ₃) ₂	868 \pm 5	$\gamma = 239.9 - 0.0177t$	902-1075	0.5	(± 1.0)	[9]

Sulfates

Li ₂ SO ₄	859	$\gamma = 282.6 - 0.0672t$	860-1100	0.1	± 1.0	[46]
Na ₂ SO ₄	884	$\gamma = 476.5 - 0.532t + 2.43 \times 10^{-4}t^2$	900-1077	1.1	[46]
K ₂ SO ₄	1069	$\gamma = 224.3 - 0.0765t$	1099-1121	0.1	± 0.5	[6]
Rb ₂ SO ₄	1074	$\gamma = 286.1 - 0.207t + 0.596 \times 10^{-4}t^2$	1086-1545	0.3	[46]
Cs ₂ SO ₄	1019	$\gamma = 244.3 - 0.179t + 0.483 \times 10^{-4}t^2$	1036-1530	0.4	[46]

See footnotes at the end of the table, p. 108.

7. Cumulative Table of Temperature Dependent Equations

TABLE 101. *Surface Tensions of Single-Salt Melts*^{a, b} — Continued

Salt	mp °C	Best equation	Range (°C)	s(dyne cm ⁻¹)	Uncertainty (%)	Ref.
Molybdates						
Na ₂ MoO ₄	687	$\gamma = 309.5 - 0.172t + 0.498 \times 10^{-4}t^2$	698–1212	0.6	[46]
K ₂ MoO ₄	926	$\gamma = 182.3 - 0.0158t - 0.199 \times 10^{-4}t^2$	930–1533	0.4	[46]
PbMoO ₄	1065	$\gamma = 236.0 - 0.064t$	1093–1124	0.9	[24]
Bi ₂ (MoO ₄) ₃	643	$\gamma = -207.2 + 1.110t - 0.834 \times 10^{-3}t^2$	680–760	0.6	[24]
Tungstates						
Na ₂ WO ₄	698	$\gamma = 248.1 - 0.0602t - 0.0414 \times 10^{-4}t^2$	710–1595	0.6	[46]
K ₂ WO ₄	930	$\gamma = 283.6 - 0.160t + 0.283 \times 10^{-4}t^2$	925–1520	0.6	[46]
Miscellaneous						
KCNS	175	$\gamma = 339.5 - 1.36t$ (fresh melt)	175–185	*0.5	(±2.0)	[23]
KClO ₃	368	$\gamma = 126.0 - 0.14t$ (aged melt)	175–205	*0.5	(±2.0)	[23]
K ₂ Cr ₂ O ₇	398	$\gamma = 228.0 - 0.40t$	368–378	0.5	±2.0	[23]
LiClO ₃	127.8	$\gamma = 236.2 - 0.27t$	400–440	0.5	±2.0	[23]
NaClO ₃	255	$\gamma = 96.71 - 0.0692t$	130–160	0.1	[68]
		$\gamma = 110.27 - 0.0738t$	265–290	0.4	[21]

^a The precisions marked with asterisks (*) are approximate.

^b The uncertainties in parentheses, being based on minimal information, are more qualitative than the unbracketed values.

8. References

[References marked with asterisks have data for molten salt mixtures.]

- *[1] Bloom, H., Davis, F. G., and James, D. W., *Trans. Faraday Soc.*, **56**, 1179 (1960).
- [2] Ellis, R. B., and Wilcox, W. S., *Prog. Rep. U.S.A.E.C., Contract No. AT-(40-1)-2073, Tpl0-7622*, pp. 128-36 (1962).
- [3] Sokolova, O. K., *Izv. Akas. Nauk. S.S.S.R., Met.; Gorn. Delo* **4**, 59 (1963).
- *[4] Semenchenko, K., and Shikhobalova, L. P., *J. Phys. Chem. (U.S.S.R.)*, **21**, 707 (1947).
- [5] Schenck, R., Mihr, F., and Banthien, H., *Ber. der Deut. Chem. Ges.* **39**, 1506 (1906); *International Critical Tables (E. W. Washburn, Ed.)*, (McGraw-Hill Book Company, Inc., New York, 1926).
- *[6] Neithamer, R. W., and Peake, J. S., *J. Chem. Eng. Data*, **6**, 197 (1961).
- *[7] Lantratov, M. F., *Zhur. Prik. Khim.*, **34**, L249 (1961).
- [8] Sokolova, I. D., and Sokolova, V. A., *Rus. J. Phys. Chem.*, **34**, 944 (1960).
- [9] Sokolova, I. D., and Voskresenskaya, N. K., *Zhur. Neorg. Khim.* **8**, 2625 (1963).
- [10] Barzakovskii, V. P., *Zhur. Fiz. Khim.*, **13**, 1117 (1940).
- [11] Ellis, R. B., Smith, J. E., and Baker, E. B., *J. Phys. Chem.*, **62**, 766 (1958).
- *[12] Peake, J. S., and Bothwell, M. R., *J. Am. Chem. Soc.*, **76**, 2656 (1954).
- *[13] Sokolova, I. D., and Voskresenskaya, N. K., *Russ. J. Phys. Chem.*, **36**, 502 (1962).
- *[14] Boardman, N. K., Palmer, A. R., and Heymann, E. *Trans. Faraday Soc.*, **51**, 277 (1955).
- *[15] Ellis, R. B., Smith, J. E., Wilcox, W. S., and Crook, E. H., *J. Phys. Chem.*, **65**, 1186 (1961).
- [16] Greenwood, N. N., and Worrall, I. J., *J. Chem. Soc.*, 1680 (1958).
- [17] Nijhar, R. S., M. S. Thesis, University of Bradford, U.K. (1967).
- *[18] Dahl, J. L., and Duke, F. R., *J. Phys. Chem.*, **62**, 1142 (1958).
- [19] Addison, C. C., and Coldrey, J. M., *J. Chem. Soc.*, 468 (1961).
- [20] Semenchenko, K., and Shikhobalova, L. P., *J. Phys. Chem. (U.S.S.R.)* **21**, 613 (1947); (*C.A.* **41**, 6778f).
- *[21] Campbell, A. N., and van Der Kouwe, E. T., *Can. J. Chem.* **46**, 1279 (1968).
- [22] NBS Technical News Bulletin, October, 1963.
- [23] Frame, J. P., Rhodes, E., and Ubbelohde, A. R., *Trans. Faraday Soc.*, **55**, 2039 (1959).
- *[24] Morris, K. B., McNair, N., and Koops, G., *J. Chem. Eng. Data*, **7**, No. 2, 244 (1962).
- [25] Motylewski S., *Z. anorg. u. allgem. Chem.* **38**, 410 (1904).
- *[26] Bertozzi, G., and Sternheim, G., *J. Phys. Chem.*, **68**, 2908 (1964).
- [27a] Williams, D. J., Bradbury, B. T., and Maddocks, W. R., *J. Soc. Glass Technol.*, **43**, 3087 (1959).
- [27b] Bradbury, B. T., and Maddocks, W. R., *J. Soc. Glass Technol.* **42**, 325T (1959).
- *[28] Callis, C. F., Van Wazer, J. R., and Metcalf, J. S., *J. Am. Chem. Soc.*, **11**, 1468 (1955).
- *[29] Lehman, D. S., Ph. D. Thesis, Indiana University, U.S.A. (1959).
- [30] Kingery, W. D., *J. Am. Ceram. Soc.*, **42** (1), 6 (1959).
- *[31] Dahl, J. L., and Duke, F. R., *J. Phys. Chem.*, **62**, 1498 (1958).
- [31a] Dahl, J. L., and Duke, F. R., *Prog. Rep. U.S.A.E.C. Contract No. W-7405-Eng-82* (1957).
- *[32] Bloom, H., and Burrows, B. W., *Proceedings of the 1st Australian Electrochemistry Conference* 882 (1963).
- *[33] Shartsis, L., and Canga, R., *J. Res. NBS* **43**, No. 3, 221 (1949), RP2023.
- [34] Ellis, R. B., *Prog. Rep. U.S.A.E.C., Contract No. AT-(40-1)-2073, II* (1958).
- *[35] Ellis, R. B., *Prog. Rep. U.S.A.E.C., Contract No. AT-(40-1)-2073, III* (1958).
- *[36] Ellis, R. B., *Prog. Rep. U.S.A.E.C., Contract No. AT-(40-1)-2073* (1959).
- *[37] Ellis, R. B., *Prog. Rep. U.S.A.E.C., Contract No. AT-(40-1)-2073* (1961).
- [38] Ellis, R. B., *Prog. Rep. U.S.A.E.C., Contract No. AT-(40-1)-2073* (1962).
- [39] Ellis, R. B., *Prog. Rep. U.S.A.E.C., Contract No. AT-(40-1)-2073* (1963).
- *[40] Reding, J. D., *J. Chem. Eng. Data*, **11** (2), 239 (1966).
- *[41] Semenchenko, K., and Shikhobalova, L. P., *Zhur. Fiz. Khim.*, **21**, 613 (1947).
- [42] Greenwood, N. N., and Wade, K., *J. Chem. Soc.* 1663 (1958).
- [43] Greenwood, N. N., and Wade, K., *J. Chem. Soc.* 1671 (1958).
- [44] Greenwood, N. N., and Wade, K., *J. Inorg. and Nucl. Chem.* **3**, 349 (1957).
- [45] Bertozzi, G., *J. Phys. Chem.* **69**, 2606 (1965).
- [46] Jaeger, F. M., *Z. anorg. u. allgem. Chem.*, **101**, 1 (1917).
- [47] Rogers, M. T., and Garver, E. E., *J. Phys. Chem.* **62**, 952 (1958).
- [48] Janz, G. J., and Lorenz, M. R., *Rev. Sci. Instr.*, **31**, 18 (1960).
- *[49] Janz, G. J., and Lorenz, M. R., *J. Electrochem. Soc.* **108**, 1052 (1961).
- [50] Priest, H. F., *U.S.A.E.C. TID 5290*, **2**, 722 (1958).
- [51] Harkins, W. D., *Physical Methods of Organic Chemistry (A. Weissberger, Ed.)*, Part 1, 2nd ed., pp. 403-405, Interscience Publishers Inc., New York, N.Y. (1949).
- [52a] Sugden, S., *J. Chem. Soc. (London)* **121**, 858 (1922).
- [52] Sugden, S., *J. Chem. Soc. (London)* **119**, 1483 (1921).
- [53] Richards, T. W., and Carver, E. K., *J. Am. Chem. Soc.*, **43**, 827 (1921).
- [54] Dorsey, N. E., *NBS Sci. Paper* 540, p. 579 (1926).
- [55] Cantor, M., *Ann. Phys.*, **7**, 698 (1902).
- [56] Adamson, A. N., *Physical Chemistry of Surfaces*, Interscience Publishers Inc., New York, New York (1960).
- [57] Ruysen, R., *Rec. Trav. Chim.*, **65**, 580 (1946).
- [58] King, T. B., *J. Soc. Glass Technol.*, **36**, 241 (1951).
- [59] Prideaux, E. B. R., and Jarratt, J. R., *J. Chem. Soc.*, 1203 (1938).
- [60] Desyatnikov, O. G., *J. Appl. Chem., U.S.S.R.*, **29**, 945 (1956).
- [61] Nisel'son, L. A., and Sokolova, T. D., *Russ. J. Inorg. Chem.*, **10** (7), 827 (1965).
- [62] Bashforth, F., and Adams, S. C., *An Attempt to Test the Theories of Capillarity*, Cambridge Univ. Press, London (1833).
- [63] Kozakevitch, P., in *Physical Measurements at High Temperatures*, J. O'M. Bockris, J. L. White and J. D. Mackenzie, Ed., Academic Press, New York, Chap. 9 (1959).
- [64] Harkins, W. D., and Brown, F. E., *J. Am. Chem. Soc.*, **41**, 499 (1919).
- [65] Harkins, W. D., Young, T. F., and Cheng, L. H., *Science*, **64**, 333 (1926).
- [66] Harkins, W. D., and Jordan, H. F., *J. Am. Chem. Soc.*, **52**, 1751 (1930).
- [67] Moiseev, G. K., Stepanov, G. K., *Transactions (Trudy) No. 6* (1965) *Inst. Electrochem., Urals. Acad. Sci., Eng. Trans.*, Vol. 41 (1966). Consultants Bureau, New York (1966).
- [68] Campbell, A. N., and Williams, D. F., *Can. J. Chem.*, **42**, 1779 (1964).
- [69] *Selected Values of Chemical Thermodynamic Properties*, NBS Circular 500, United States Government Printing Office, Washington, D.C. (1952).
- [70] Kirshenbaum, A. D., and Cahill, J. A., *J. Phys. Chem.*, **70**, 3037 (1966).
- [71] Freud, B. B., and Harkins, W. D., *J. Phys. Chem.*, **33**, 1217 (1929).
- [72] Wendlandt, W. W., *Texas J. Sci.*, **10**, 392 (1958).
- [73] Stern, K. H., and Weise, E. L., *High Temp. Properties and Decomposition of Inorganic Salts, Part 1. Sulfates*.

NSRDS-NBS 7, U.S. Gov't Printing Office, Washington, D.C., October 1966.

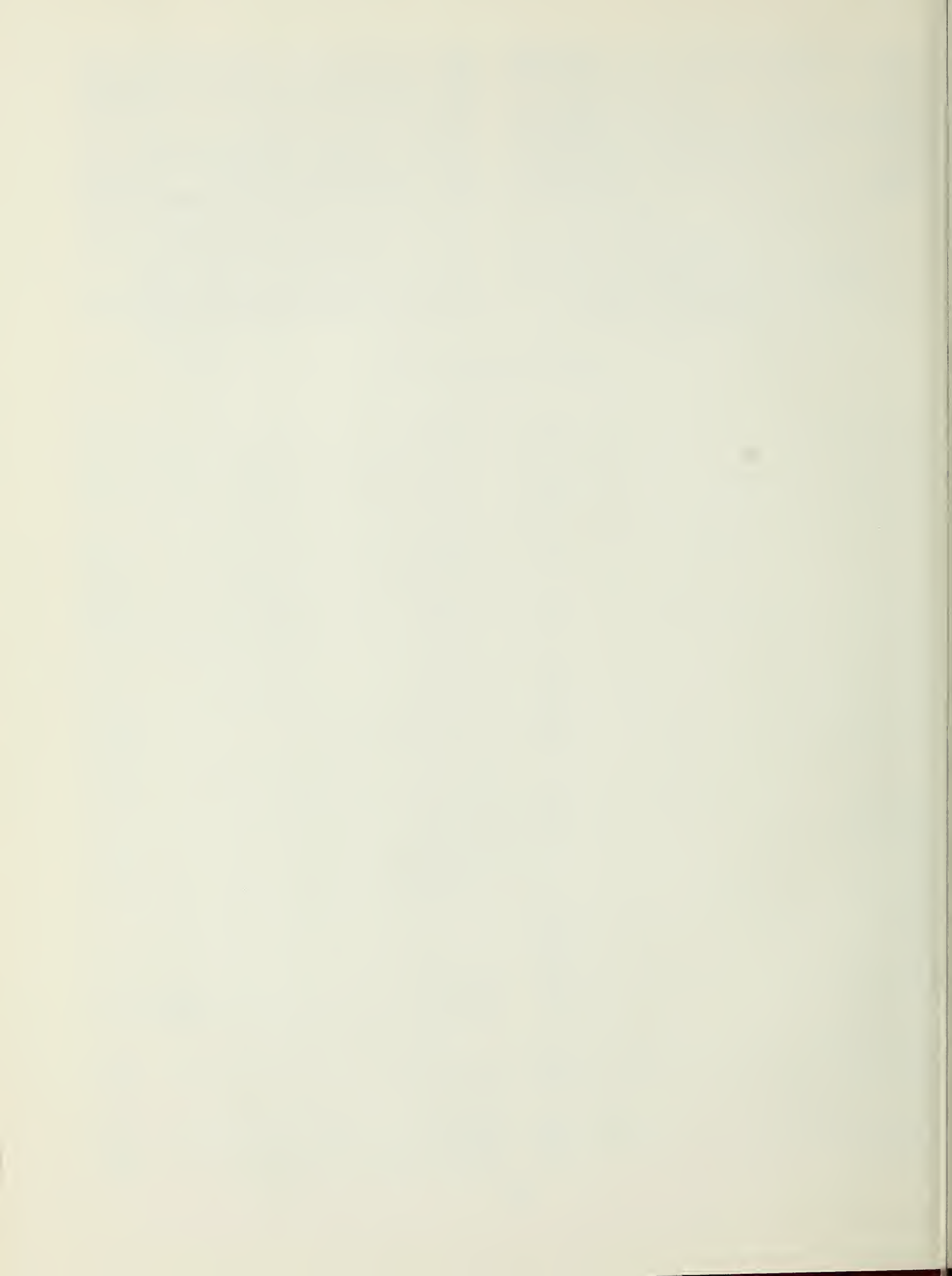
- [74] Reh binder, P., Z. Phys. Chem., **121**, 103 (1926).
 [75] Guiochon, G., and Jacque, L., Compt. Rend. **244**, 771 (1957).
 * [76] Moiseev, G. K., and Stepanov, G. K. (Reports of the Institute of Electrochemistry), Akad. Nauk. SSSR. Urals 'SK Fil. (Sverdlovsk) No. 5, 69 (1964).
 [77] Peltier, S., and Duval, C., Compt. Rend. **226**, 1727 (1948).
 [78] Freeman, E. S., J. Phys. Chem., **60**, 1487 (1956).
 [79] Macdougall, F. H., Science, **62**, 290 (1925).
 [80] Freud, B. B., and Freud, H. Z., J. Am. Chem. Soc., **52**, 1772 (1930).
 [81] Simon, M., Ann. Chim. Phys. **33**, 5 (1851).
 [82] Hoffman, M., Pressure as a Function of the Shapes of Liquid Surfaces, M.S. Thesis, University of Chicago (1926).
 [83] Tripp, H. P., Maximum Bubble Pressure for Measurement of Surface Tension, Ph. D. Thesis, Univ. of Chicago (1934).
 [84] Wilhelmy, L., Ann. Physik, **119**, 177 (1863).
 [85] Lazarev, V. B., and Abdusalyamova, M. N., Izv. Akad. Nauk. S.S.S.R. Ser. Khim. **6**, 1104 (1964).
 [86] Andreas, J. M., Hauser, E. A., Tucker, W. B., J. Phys. Chem., **42**, 1001 (1938).
 [87] Popel, S. I., and Esin, O. A., Fiz. Khim. Osnovy Proizv. Stali., Akad. Nauk. SSSR, Inst. Met., Conf. 24-29 January, 1955, pp. 497-504 (Moscow, 1957).
 [88] Owens, B. B., and Mayer, S. W., J. Am. Ceram. Soc. **47**, 347 (1964).
 [89] Bondarenko, N. V., and Strelets, K. L., Zhur. Prik. Khim. **35**, 1271 (1962).
 [90] Kozakevitch, P., Rev. de Metall. **46**, 505, 572 (1949).
 * [91] Shartsis, L., Spinner, S., and Smock, A. W., J. Res. Natl. Bur. Stand., **40**, 60 (1948).
 * [92] Boni, R. E., and Derge, G., J. Metal., **8** (1), 53 (1956).
 * [93] Kirslis, S. S., and Blankenship, F. F., Oak Ridge National Laboratory, Oak Ridge, Tennessee 37831, private communication to G. J. Janz (1968).
 [94] Fajans, K., J. Am. Chem. Soc., **74**, 2761 (1952).

9. Compound Index

	Page		Page
AgBr.....	59, 86, 105	K ₂ CO ₃	67, 93, 106
AgCl.....	59, 81, 104	K ₂ Cr ₂ O ₇	74, 75, 103, 108
AgI.....	59	KF.....	57, 78, 104
AgNO ₃	68, 69, 94, 107	KI.....	64, 88, 105
AlCl ₃	62, 84, 105	K ₂ MoO ₄	74, 101, 108
Al ₂ O ₃	54, 55, 65, 90, 105	KNO ₂	70, 96, 107
B ₂ O ₃	54, 65, 90, 105	KNO ₃	67, 68, 94, 106
BaBr ₂	64, 65, 86, 105	KPO ₃	71, 98, 107
BaCl ₂	60, 82, 104	K ₂ SO ₄	73, 99, 107
BaI ₂	61, 89, 105	K ₂ WO ₄	74, 102, 108
Ba(NO ₃) ₂	69, 70, 95, 107	LiBO ₂	66, 92, 106
Ba(PO ₃) ₂	71, 99, 107	LiCl.....	55, 80, 104
BiBr ₃	62, 87, 105	LiClO ₃	75, 103, 104
BiCl ₃	62, 84, 105	Li ₂ CO ₃	66, 92, 106
Bi ₂ (MoO ₄) ₃	74, 102, 108	LiF.....	55, 78, 104
CaBr ₂	61, 86, 105	LiNO ₃	67, 93, 106
CaCl ₂	60, 82, 104	LiPO ₃	71, 97, 107
CaI ₂	65, 89, 105	Li ₂ SO ₄	72, 73, 99, 107
Ca(NO ₃) ₂	69, 95, 107	Li ₂ SiO ₃	70, 96, 107
Ca(PO ₃) ₂	55, 72, 98, 107	MgCl ₂	55, 59, 81, 104
CaSiO ₃	70, 71, 96, 107	MgSiO ₃	70, 71, 96, 107
CdBr ₂	61, 87, 105	MnSiO ₃	70, 71, 97, 107
CdCl ₂	61, 83, 104	MnSiO ₄	70, 71, 97, 107
CsBr.....	63, 85, 105	Na ₃ AlF ₆	57, 79, 104
CsCl.....	58, 59, 81, 104	NaBO ₂	66, 92, 106
CsF.....	55, 79, 104	NaBr.....	62, 85, 105
CsI.....	64, 88, 105	NaCl.....	57, 58, 80, 104
CsNO ₃	68, 94, 107	NaClO ₃	75, 102, 103, 108
CsPO ₃	71, 98, 107	Na ₂ CO ₃	67, 93, 106
Cs ₂ SO ₄	73, 100, 107	NaF.....	56, 57, 78, 104
CuCl.....	55, 59, 81, 104	NaI.....	64, 87, 105
Cu ₂ S.....	55, 59, 81, 106	Na ₂ MoO ₄	74, 101, 108
FeO.....	55, 66, 90, 106	NaNO ₂	70, 95, 107
GaCl ₃	52, 62, 84, 105	NaNO ₃	67, 93, 106
GaCl ₃ · C ₅ H ₅ N.....	62, 84, 105	NaPO ₃	52, 71, 97, 107
GaCl ₃ · C ₅ H ₁₀ NH.....	62, 84, 105	Na ₂ SO ₄	73, 99, 107
GaCl ₃ · 2C ₅ H ₁₀ NH.....	62, 84, 105	Na ₂ WO ₄	74, 102, 108
GeO ₂	54, 65, 91, 106	NH ₄ NO ₃	69, 95, 107
HgBr ₂	55, 61, 83, 105	P ₂ O ₃	66, 91, 106
HgCl ₂	55, 61, 83, 104	P ₂ O ₅	52, 54, 66, 91, 106
KBO ₂	66, 92, 106	PbCl ₂	61, 83, 105
KBr.....	63, 85, 105	PbMoO ₄	74, 101, 108
KCl.....	58, 80, 104	PbO.....	55, 65, 90, 106
KClO ₃	74, 102, 108	RbBr.....	63, 85, 105
KCNS.....	74, 102, 108	RbCl.....	58, 80, 104
		RbF.....	55, 78, 104
		RbI.....	64, 88, 105

	Page
RbNO ₃	68, 94, 106
Rb ₂ SO ₄	73, 100, 107
SiO ₂	54, 65, 90, 106
SnCl ₂	61, 83, 104
SrBr ₂	64, 65, 86, 105
SrCl ₂	65, 82, 104
SrI ₂	65, 89, 105
Sr(NO ₃) ₂	69, 70, 95, 107
Sr(PO ₃) ₂	71, 98, 107

	Page
ThF ₄	57, 79, 104
TlNO ₃	69, 95, 107
Tl ₂ S.....	66, 91, 106
UF ₄	57, 79, 104
UF ₆	52, 55, 57, 79, 104
ZnBr ₂	60, 87, 105
ZnCl ₂	51, 52, 53, 60, 82, 104



NATIONAL BUREAU OF STANDARDS

The National Bureau of Standards¹ was established by an act of Congress March 3, 1901. Today, in addition to serving as the Nation's central measurement laboratory, the Bureau is a principal focal point in the Federal Government for assuring maximum application of the physical and engineering sciences to the advancement of technology in industry and commerce. To this end the Bureau conducts research and provides central national services in four broad program areas. These are: (1) basic measurements and standards, (2) materials measurements and standards, (3) technological measurements and standards, and (4) transfer of technology.

The Bureau comprises the Institute for Basic Standards, the Institute for Materials Research, the Institute for Applied Technology, the Center for Radiation Research, the Center for Computer Sciences and Technology, and the Office for Information Programs.

THE INSTITUTE FOR BASIC STANDARDS provides the central basis within the United States of a complete and consistent system of physical measurement; coordinates that system with measurement systems of other nations; and furnishes essential services leading to accurate and uniform physical measurements throughout the Nation's scientific community, industry, and commerce. The Institute consists of an Office of Measurement Services and the following technical divisions:

Applied Mathematics—Electricity—Metrology—Mechanics—Heat—Atomic and Molecular Physics—Radio Physics²—Radio Engineering²—Time and Frequency²—Astrophysics²—Cryogenics.²

THE INSTITUTE FOR MATERIALS RESEARCH conducts materials research leading to improved methods of measurement standards, and data on the properties of well-characterized materials needed by industry, commerce, educational institutions, and Government; develops, produces, and distributes standard reference materials; relates the physical and chemical properties of materials to their behavior and their interaction with their environments; and provides advisory and research services to other Government agencies. The Institute consists of an Office of Standard Reference Materials and the following divisions:

Analytical Chemistry—Polymers—Metallurgy—Inorganic Materials—Physical Chemistry.

THE INSTITUTE FOR APPLIED TECHNOLOGY provides technical services to promote the use of available technology and to facilitate technological innovation in industry and Government; cooperates with public and private organizations in the development of technological standards, and test methodologies; and provides advisory and research services for Federal, state, and local government agencies. The Institute consists of the following technical divisions and offices:

Engineering Standards—Weights and Measures—Invention and Innovation—Vehicle Systems Research—Product Evaluation—Building Research—Instrument Shops—Measurement Engineering—Electronic Technology—Technical Analysis.

THE CENTER FOR RADIATION RESEARCH engages in research, measurement, and application of radiation to the solution of Bureau mission problems and the problems of other agencies and institutions. The Center consists of the following divisions:

Reactor Radiation—Linac Radiation—Nuclear Radiation—Applied Radiation.

THE CENTER FOR COMPUTER SCIENCES AND TECHNOLOGY conducts research and provides technical services designed to aid Government agencies in the selection, acquisition, and effective use of automatic data processing equipment; and serves as the principal focus for the development of Federal standards for automatic data processing equipment, techniques, and computer languages. The Center consists of the following offices and divisions:

Information Processing Standards—Computer Information—Computer Services—Systems Development—Information Processing Technology.

THE OFFICE FOR INFORMATION PROGRAMS promotes optimum dissemination and accessibility of scientific information generated within NBS and other agencies of the Federal government; promotes the development of the National Standard Reference Data System and a system of information analysis centers dealing with the broader aspects of the National Measurement System, and provides appropriate services to ensure that the NBS staff has optimum accessibility to the scientific information of the world. The Office consists of the following organizational units:

Office of Standard Reference Data—Clearinghouse for Federal Scientific and Technical Information³—Office of Technical Information and Publications—Library—Office of Public Information—Office of International Relations.

¹ Headquarters and Laboratories at Gaithersburg, Maryland, unless otherwise noted; mailing address Washington, D.C. 20234.

² Located at Boulder, Colorado 80302.

³ Located at 5285 Port Royal Road, Springfield, Virginia 22151.

NBS TECHNICAL PUBLICATIONS

PERIODICALS

JOURNAL OF RESEARCH reports National Bureau of Standards research and development in physics, mathematics, chemistry, and engineering. Comprehensive scientific papers give complete details of the work, including laboratory data, experimental procedures, and theoretical and mathematical analyses. Illustrated with photographs, drawings, and charts.

Published in three sections, available separately:

● Physics and Chemistry

Papers of interest primarily to scientists working in these fields. This section covers a broad range of physical and chemical research, with major emphasis on standards of physical measurement, fundamental constants, and properties of matter. Issued six times a year. Annual subscription: Domestic, \$9.50; foreign, \$11.75*.

● Mathematical Sciences

Studies and compilations designed mainly for the mathematician and theoretical physicist. Topics in mathematical statistics, theory of experiment design, numerical analysis, theoretical physics and chemistry, logical design and programming of computers and computer systems. Short numerical tables. Issued quarterly. Annual subscription: Domestic, \$5.00; foreign, \$6.25*.

● Engineering and Instrumentation

Reporting results of interest chiefly to the engineer and the applied scientist. This section includes many of the new developments in instrumentation resulting from the Bureau's work in physical measurement, data processing, and development of test methods. It will also cover some of the work in acoustics, applied mechanics, building research, and cryogenic engineering. Issued quarterly. Annual subscription: Domestic, \$5.00; foreign, \$6.25*.

TECHNICAL NEWS BULLETIN

The best single source of information concerning the Bureau's research, developmental, cooperative and publication activities, this monthly publication is designed for the industry-oriented individual whose daily work involves intimate contact with science and technology—for *engineers, chemists, physicists, research managers, product-development managers, and company executives*. Annual subscription: Domestic, \$3.00; foreign, \$4.00*.

* Difference in price is due to extra cost of foreign mailing.

Order NBS publications from:

Superintendent of Documents
Government Printing Office
Washington, D.C. 20402

NONPERIODICALS

Applied Mathematics Series. Mathematical tables, manuals, and studies.

Building Science Series. Research results, test methods, and performance criteria of building materials, components, systems, and structures.

Handbooks. Recommended codes of engineering and industrial practice (including safety codes) developed in cooperation with interested industries, professional organizations, and regulatory bodies.

Special Publications. Proceedings of NBS conferences, bibliographies, annual reports, wall charts, pamphlets, etc.

Monographs. Major contributions to the technical literature on various subjects related to the Bureau's scientific and technical activities.

National Standard Reference Data Series. NSRDS provides quantitative data on the physical and chemical properties of materials, compiled from the world's literature and critically evaluated.

Product Standards. Provide requirements for sizes, types, quality and methods for testing various industrial products. These standards are developed cooperatively with interested Government and industry groups and provide the basis for common understanding of product characteristics for both buyers and sellers. Their use is voluntary.

Technical Notes. This series consists of communications and reports (covering both other agency and NBS-sponsored work) of limited or transitory interest.

Federal Information Processing Standards Publications. This series is the official publication within the Federal Government for information on standards adopted and promulgated under the Public Law 89-306, and Bureau of the Budget Circular A-86 entitled, Standardization of Data Elements and Codes in Data Systems.

CLEARINGHOUSE

The Clearinghouse for Federal Scientific and Technical Information, operated by NBS, supplies unclassified information related to Government-generated science and technology in defense, space, atomic energy, and other national programs. For further information on Clearinghouse services, write:

Clearinghouse
U.S. Department of Commerce
Springfield, Virginia 22151

Publications in the National Standard Reference Data Series National Bureau of Standards

You may use this listing as your order form by checking the proper box of the publication(s) you desire or by providing the full identification of the publication you wish to purchase. The full letter symbols with each publications number and full title of the publication and author must be given in your order, e.g. NSRDS-NBS-17, Tables of Molecular Vibrational Frequencies, Part 3, by T. Shimanouchi.

Pay for publications by check, money order, or Superintendent of Documents coupons or deposit account. Make checks and money orders payable to Superintendent of Documents. Foreign remit-

tances should be made either by international money order or draft on an American bank. Postage stamps are not acceptable.

No charge is made for postage to destinations in the United States and possessions, Canada, Mexico, and certain Central and South American countries. To other countries, payments for documents must cover postage. Therefore, one-fourth of the price of the publication should be added for postage.

Send your order together with remittance to Superintendent of Documents, Government Printing Office, Washington, D.C. 20402.

- ☐ NSRD-NBS 1, **National Standard Reference Data System—Plan of Operation**, by E. L. Brady and M. B. Wallenstein, 1964 (15 cents).
- ☐ NSRDS-NBS 2, **Thermal Properties of Aqueous Uni-univalent Electrolytes**, by V. B. Parker, 1965 (45 cents).
- ☐ NSRDS-NBS 3, Sec. 1, **Selected Tables of Atomic Spectra, Atomic Energy Levels and Multiplet Tables, Si II, Si III, Si IV**, by C. E. Moore, 1965 (35 cents).
- ☐ NSRDS-NBS 3, Sec. 2, **Selected Tables of Atomic Spectra, Atomic Energy Levels and Multiplet Tables, Si I**, by C. E. Moore, 1967 (20 cents).
- ☐ NSRDC-NBS 4, **Atomic Transition Probabilities, Volume 1, Hydrogen Through Neon**, by W. L. Wiese, M. W. Smith and B. M. Glennon, 1966 (\$2.50).
- ☐ NSRDS-NBS 5, **The Band Spectrum of Carbon Monoxide**, by P. H. Krupenie, 1966 (70 cents).
- ☐ NSRDS-NBS 6, **Tables of Molecular Vibrational Frequencies, Part 1**, by T. Shimanouchi, 1967 (40 cents).
- ☐ NSRDS-NBS 7, **High Temperature Properties and Decomposition of Inorganic Salts, Part 1, Sulfates**, by K. H. Stern and E. L. Weise, 1966 (35 cents).
- ☐ NSRDS-NBS 8, **Thermal Conductivity of Selected Materials**, by R. W. Powell, C. Y. Ho, and P. E. Liley, 1966 (\$1).
- ☐ NSRDS-NBS 9, **Bimolecular Gas Phase Reactions (rate coefficients)**, by A. F. Trotman-Dickenson and G. S. Milne, 1967 (\$2).
- ☐ NSRDS-NBS 10, **Selected Values of Electric Dipole Moments for Molecules in the Gas Phase**, by R. D. Nelson, Jr., D. R. Lide, Jr., and A. A. Maryott, 1967 (40 cents).
- ☐ NSRDS-NBS 11, **Tables of Molecular Vibrational Frequencies, Part 2**, by T. Shimanouchi, 1967 (30 cents).
- ☐ NSRDS-NBS 12, **Tables for the Rigid Asymmetric Roto: Transformation Coefficients from Symmetric to Asymmetric Bases and Expectation Values of P_z^2 , P_z^4 , and P_z^6** , by R. H. Schwendeman, 1968 (60 cents).
- ☐ NSRDS-NBS 13, **Hydrogenation of Ethylene on Metallic Catalysts**, by J. Horiuti and K. Miyahara, 1968 (\$1.00).
- ☐ NSRDS-NBS 14, **X-Ray Wavelengths and X-Ray Atomic Energy Levels**, by J. A. Bearden, 1967 (40 cents).
- ☐ NSRDS-NBS 15, **Molten Salts, Vol. 1, Electrical Conductance, Density, and Viscosity Data**, by G. Janz, F. W. Dampier, G. R. Lakshminarayanan, P. K. Lorenz, and R. P. T. Tomkins, 1968 (\$3).
- ☐ NSRDS-NBS 16, **Thermal Conductivity of Selected Materials, Part 2**, by C. Y. Ho, R. W. Powell, and P. E. Liley, 1968 (\$2).
- ☐ NSRDS-NBS 17, **Tables of Molecular Vibration Frequencies, Part 3**, by T. Shimanouchi, 1968 (30 cents).
- ☐ NSRDS-NBS 18, **Critical Analysis of the Heat-Capacity Data of the Literature and Evaluation of Thermodynamic Properties of Copper, Silver, and Gold From 0 to 300 K**, by G. T. Furukawa, W. G. Saba, and M. L. Reilly, 1968 (40 cents).
- ☐ NSRDS-NBS 19, **Thermodynamic Properties of Ammonia as an Ideal Gas**, by L. Haar, 1968 (20 cents).
- ☐ NSRDS-NBS 20, **Gas Phase Reaction Kinetics of Neutral Oxygen Species**, by H. S. Johnson, 1968 (45 cents).
- ☐ NSRDS-NBS 21, **Kinetic Data on Gas Phase Unimolecular Reactions**, by S. W. Benson and H. E. O'Neal, (In press).
- ☐ NSRDS-NBS 22, **Atomic Transition Probabilities, Vol. II, Sodium Through Calcium, A Critical Data Compilation**, by W. L. Wiese, M. W. Smith, and B. M. Miles, (In press).
- ☐ NSRDS-NBS 23, **Partial Grottrian Diagrams of Astrophysical Interest**, by C. E. Moore and P. W. Merrill, 1968 (55 cents).
- ☐ NSRDS-NBS 24, **Theoretical Mean Activity Coefficients of Strong Electrolytes in Aqueous Solutions from 0 to 100° C**, by Walter J. Hamer, 1968 (\$4.25).
- ☐ NSRDS-NBS 25, **Electron Impact Excitation of Atoms**, by B. L. Moiseiwitsch and S. J. Smith, 1968 (\$2).
- ☐ NSRDS-NBS 26, **Ionization Potentials, Appearance Potentials, and Heats of Formation of Positive Ions**, by J. L. Franklin, J. G. Dillard, H. M. Rosenstock, J. T. Herron, K. Draxl, and F. H. Field, (\$4).
- ☐ NSRDS-NBS 27, **Thermodynamic Properties of Argon from the Triple Point to 300 K at Pressures to 1000 Atmospheres**, by A. L. Gosman, R. D. McCarty, and J. G. Hust, (\$1.25).





